

Copyright

by

Michael Ethan Cloos

2014

**The Thesis Committee for Michael Ethan Cloos
Certifies that this is the approved version of the following thesis:**

**Detrital Zircon U-Pb and (U-Th)/He Geo-Thermochronometry
and Submarine Turbidite Fan Development in the Mio-Pliocene
Gulf of California, Fish Creek-Vallecito Basin, Southern
California**

**APPROVED BY
SUPERVISING COMMITTEE:**

Supervisor:

Ronald J. Steel

Co-Supervisor:

Daniel Stockli

Cornel Olariu

**Detrital Zircon U-Pb and (U-Th)/He Geo-Thermochronometry
and Submarine Turbidite Fan Development in the Mio-Pliocene
Gulf of California, Fish Creek-Vallecito Basin, Southern
California**

by

Michael Ethan Cloos, B.S.

Thesis

Presented to the Faculty of the Graduate School of
The University of Texas at Austin
in Partial Fulfillment
of the Requirements
for the Degree of

Master of Science in Geological Sciences

The University of Texas at Austin

August 2014

Dedication

To my parents, Rhonda and Mark, and my sister, Marlee.

Acknowledgements

I'd like to first of all thank my committee members Ron Steel, Danny Stockli, and Cornel Olariu for the advice and expertise they provided throughout this project. It's hard to believe it was just two years ago I was with Ron and Cornel out in Anza-Borrego Desert State Park getting my first glimpse of the amazing stratigraphy. Danny's expertise on western US geology and geo-thermochronology has helped take this project to another level.

Thanks to Lyn Murray for being a helpful contact at Anza-Borrego Desert State Park headquarters as well as assisting with sample collection permitting. I appreciate the insightful stories on the paleontology, geology, and history of the area. I am also thankful for the helpful conversations I had with George Jefferson, Lowell Lindsay, and Arnie Mroz.

Thanks to Marty Grove for helpful input on my detrital zircon results and for getting me in contact with David Kimbrough so that a sample of mineral separate from the modern Colorado River could be analyzed in this study. Thanks also to Dennis Kerr who provided good discussion on the Fish Creek-Vallecito Basin at GSA 2013.

Many thanks to the Stockli research group for getting me going on the intense process of obtaining those zircon helium ages. Without the help of seasoned laboratory veterans Spencer Seman, Tim Shin, Edgardo Pujols, Josh Burrus, Adam Goldsmith, Sol Cooperdock and Mike Prior I would still be second guessing myself on leak checks on the

helium lines. Thanks also to Des Patterson who I could count on when things went awry on Line A or C and for keeping the helium lines running smooth and also Lisa Stockli for help with LA-ICP-MS. And of course thank you to the rest of the Stockli group who were always available to help out.

I appreciate the input I received from the Steel Group on the sedimentological aspect of my project, either at Double-Dave's, in the office, or in the deserts of California. I am especially grateful for the excellent Jacob's staff work provided by Eugen Tudor, who endured freezing temperatures in the name of data collection, and also Bud Davis, and David Conwell. I also appreciate assistance in the field from Josh Dixon and Jeremy Slaugenwhite. Thanks also to Sarah Bateman for help in the field as well as being supportive during the thesis writing process.

Finally I would like to thank my family including my mother Rhonda, father Mark, and sister Marlee. I've enjoyed being back in Austin and only a few miles down the road from a home cooked meal. I know Marlee would think this section to be incomplete without a thank you also to the family dogs, Sammie and Toby, who provided a welcome distraction on visits home. A special thank you also to my dad who provided much support along the way, and who sparked an interest in science from a young age.

Abstract

Detrital Zircon U-Pb and (U-Th)/He Geo-Thermochronometry and Submarine Turbidite Fan Development in the Mio-Pliocene Gulf of California, Fish Creek-Vallecito Basin, Southern California

Michael Ethan Cloos, MS Geo Sci

The University of Texas at Austin, 2014

Supervisors: Ronald J. Steel and Daniel
Stockli

ABSTRACT

The Fish Creek-Vallecito Basin exposes an archive of sediment related to early rifting of the Gulf of California beginning at 8.0 Ma followed by Colorado River delta progradation from 5.3-3.0 Ma. Mio-Pliocene deposits from the Fish Creek-Vallecito Basin of southern California and a sample from the modern Colorado River delta were analyzed through detrital zircon U-Pb (n=1996) and (U-Th)/He (n=280) double-dating in order to better constrain sediment provenance, hinterland exhumation, and Colorado River evolution. Coupling this dataset with outcrop study of the first Colorado River-sourced

turbidites into the basin at 5.3 Ma, allows for evolution of the Colorado River system to be viewed from a source-to-sink perspective.

Detrital zircon U-Pb and (U-Th)/He (ZHe) ages obtained in this study suggest earliest derivation of sediment was from the Peninsular Ranges followed by more distant sediment sourcing from the Colorado River. Initial Colorado River-sourced deposits show Yavapai-Mazatzal U-Pb ages with Laramide ZHe ages suggesting that the river was sourcing from Laramide basement cored uplifts at the onset of deposition into the Gulf of California, supporting a top-down model of river evolution. An increased percentage of Grenville U-Pb age grains as well as a wider range of ZHe ages associated with western US basement-derived zircon from a modern Colorado River delta sample indicate erosion into older stratigraphic units through time which is consistent with deep erosion on the Colorado Plateau since ~6 Ma.

Vertically measured sedimentology logs through the Wind Caves Member, the first Colorado River-sourced unit deposited, were used to determine slope and basin floor architecture as the Colorado River and delta dispersed subaqueous sediment gravity flows into the marine Gulf. Measured sections arrayed along depositional strike show a 4.5 km wide pod of sand-rich turbidites that were delivered through a broad Fish Creek exit point from the paleo-Colorado shelf. The vertical sedimentation trend is one showing thick bedded, amalgamated channelized and sheet-like sandstones initially, shifting to thinner-bedded sheets and more isolated channels higher in the increasingly muddy section. The facies variability up section is interpreted as a change from a submarine basin floor fan to a lower slope environment as the Colorado River prograded its delta into the Gulf.

Table of Contents

List of Tables	xii
List of Figures.....	xiii
Chapter 1: Introduction.....	1
Chapter 2: Detrital Zircon U-Pb and (U-Th)/He Geo-Thermochronometry of the Mio-Pliocene Gulf of California, Fish Creek-Vallecito Basin, Southern California	4
Introduction	4
Colorado River	6
Modern Colorado River Overview	6
Models of Colorado River Evolution	8
Mio-Pliocene Colorado River Deposits in the Fish Creek-Vallecito Basin .	12
Geologic Background of the Colorado River Drainage Area.....	18
Rocky Mountains.....	19
Colorado Plateau.....	19
Basin and Range	21
Cordilleran Arc	21
Previous Geo-Thermochronometry of the Colorado River Drainage Area.....	23
Methods	24
Detrital Zircon U-Pb and (U-Th)/He Double-Dating	24
Zircon U-Pb Dating Methods	25
Zircon (U-Th)/He Dating Methods.....	25
Data Display	26
Results	27
Elephant Trees Formation	29
Latrania Formation, Lycium Mbr. and Lower Wind Caves Mbr.	30
Latrania Formation, Wind Caves Member	32
Deguynos Formation	33

Arroyo Diablo Formation	35
Olla Formation.....	37
Modern Colorado River Deltaic Sand	38
Crystalline Sources for Pliocene Colorado River-Sourced Detrital Zircon .	49
Pre-Colorado River Sediment Provenance	53
Pliocene Integration of the Colorado River Into the Gulf of California.....	54
Evolution of Detrital Zircon U-Pb and (U-Th)/He Ages.....	55
Maximum Depositional Ages.....	56
Discussion.....	57
Implications for Colorado River Evolution	57
Comparison to Other Studies and Utility of Double-Dating	62
Conclusion	66
Chapter 3: Submarine Turbidite Fan Development in the Mio-Pliocene Gulf of California, Fish Creek-Vallecito Basin, Southern California	69
Introduction.....	66
Geologic Background.....	71
Tectonic Setting.....	71
Stratigraphic Setting	73
Depositional System.....	76
Latrania Formation	76
Colorado River Drainage Area	78
Methods	80
Outcrop Dataset	80
Results	81
Facies Associations.....	87
Thick Bedded, Structureless sandstone (Lithofacies A).....	87
Amalgamated, Normally Graded Sandstone (Lithofacies B).....	90
Non-Amalgamated, Normally Graded Sandstone (Lithofacies C).....	92
Heterolithic Interbedded Sandstone and Silty Mudstone (Lithofacies D)....	94

Silty Mudstone and Claystone (Lithofacies E).....	94
Facies Variation.....	96
Architectural Elements	97
Fan Complex: Basin Floor Channels Feeding Thick Sheet sandstone Fan Lobes	98
Slope Deposits: Slope Channeled Sandstone Beds and Lobes Within a Low Net/Gross Succession	104
Discussion.....	108
Transition From Basin Floor to Slope Deposition.....	112
Conclusion	113
Appendix A: Sample Location Table	115
Appendix B: Sample Photographs.....	116
Appendix C: U-Pb Data Table.....	119
Appendix D: (U-Th)/He Data Table.....	184
Appendix E: Measured Section Illustrations	194
References	207
Vita	216

List of Tables

- Table 2-1: Percentages of detrital zircon grains from each U-Pb population from early Paleozoic-Eocene stratigraphic units on the Colorado plateau compared to ages obtained from Pliocene and recent Colorado River-sourced samples analyzed in this study.64
- Table 3-1: Average sandstone bed thickness from NW to SE. Also shown are average paleocurrents taken from measured sections.....83

List of Figures

Figure 2-1: Geologic map of Colorado River drainage area	7
Figure 2-2: Schematic diagram showing Colorado River integration through headward erosion	10
Figure 2-3: Schematic diagram showing Colorado River top-down integration	11
Figure 2-1: Satellite image showing location of the Fish Creek-Vallecito Basin	12
Figure 2-5: Fish Creek-Vallecito Basin tectonic setting	13
Figure 2-6: Stratigraphic column of the Fish Creek-Vallecito Basin with magnetostratigraphic ages	15
Figure 2-7: Photographs of lithologies encountered in the Fish Creek-Vallecito Basin	16
Figure 2-8: Geologic map of lithostratigraphic units in the Fish Creek-Vallecito Basin	17
Figure 2-9: Detrital zircon U-Pb and ZHe results for L-Suite sandstones	31
Figure 2-10: U-Pb age distributions of C-Suite (Colorado River-sourced) sandstones	41
Figure 2-11: U-Pb and ZHe age plot of double-dated grains from Pliocene C-Suite samples.	31
Figure 2-12: U-Pb and ZHe age plot of double-dated grains from Pliocene C-Suite samples and grains from the modern Colorado River delta sample .	42
Figure 2-13: ZHe ages for the 285-900 Ma U-Pb age population for samples from the Latrania and Deguynos formations.....	43
Figure 2-14: ZHe ages for the 900-1300 Ma U-Pb age population by formation.	44
Figure 2-15: ZHe ages for the 1300-1535 Ma U-Pb age population by formation.	45

Figure 2-16: ZHe ages for the 1535-1810 Ma U-Pb age population by formation 46

Figure 2-17: ZHe ages for the >1810 Ma U-Pb age population for the Latrania and Deguynos Formations..... 47

Figure 2-18: ZHe for each U-Pb age population from combined Pliocene samples. 48

Figure 2-19: Map showing major crystalline provinces in southern North America from which zircon are primarily derived from. 50

Figure 2-20: Timing of sediment sourcing from crystalline provinces based on crystallization and cooling histories of individual detrital zircon grains. 53

Figure 2-21: Model for Colorado River evolution based on detrital zircon U-Pb and ZHe results from this study. Model shows 1) Late Miocene local drainage sourcing 59

Figure 2-22: Detrital zircon U-Pb age distributions from Early Paleozoic to Eocene stratigraphic units on the Colorado Plateau..... 63

Figure 2-23: Detrital zircon ZHe age distributions of Permian-Jurassic units from the Canyonlands, Utah.. 65

Figure 3-1: Satellite image showing location of the Fish Creek-Vallecito Basin 72

Figure 3-2: Stratigraphic column showing units encountered in the study area within the Fish Creek-Vallecito Basin..... 75

Figure 3-3: Satellite image highlighting the outcrop extent of the Wind Caves Member 78

Figure 3-4: Locations of vertical measured sections taken throughout the outcrop extent of the Wind Caves Member. 83

Figure 3-5: Photograph of Outcrop A (Lower Wind Caves Member) showing locations of samples from L-Suite and C-Suite sandstones analyzed for U-Pb ages85-86

Figure 3-6: Lithofacies A: Thick bedded, structureless sandstones 89

Figure 3-7: Lithofacies B: Amalgamated, normally graded sandstone 91

Figure 3-8: Lithofacies C: Non-amalgamated, normally graded sandstone 93

Figure 3-9: Lithofacies D: Heterolithic interbedded sandstone and silty mudstone, and Lithofacies E: Silty Mudstone 95

Figure 3-10: Photograph of Outcrop B showing thick bedded, structureless sandstones and amalgamated, normally graded sandstones of the lower Wind Caves Member100-101

Figure 3-11: Photograph of Outcrop C showing thick bedded, sheetlike sandstones cut by small channels of the lower Wind Caves Member102-103

Figure 3-12: Photograph of Outcrop D showing thin bedded, nonamalgamated sandstones of the upper Wind Caves Member106-107

Figure 3-13: Photograph of outcrop E showing discontinuous sandstone bedding of the upper Wind Caves Member. Also shown is a photograph of discontinuous sandstones within the Mud Hills Member 108

Figure 3-14: Correlation diagram of vertical measured sections taken throughout Wind
Caves Member outcrops 111

Figure 3-15: Concept diagram for the environmental relationship between
lithostratigraphic units in the Fish Creek-Vallecito Basin..... 113

Chapter 1

Introduction

The Colorado River has been an integral contributor to the landscape evolution of western North America. This system currently originates at high elevations in the Rocky Mountains and flows through the Colorado Plateau, Basin and Range, and into the Gulf of California (Hunt, 1956). The Gulf of California, an inlet to the Pacific Ocean which is relatively narrow in expanse compared to the 640,000 km² drained by the Colorado River, acts as the repository for an archive of the river's sediment deposited since 5.3 Ma (Dorsey et al., 2011). Evidence for the vast amount of sediment transported from the Colorado River drainage area is seen by erosional features on the Colorado Plateau such as the sandstone arches in Moab, the incised meanders of the San Juan River, and the Grand Canyon in Arizona. How the Colorado River evolved and began depositing sediment into the Gulf of California is of foremost interest to this study.

The Fish Creek-Vallecito Basin within Anza-Borrego Desert State Park of southern California offers the opportunity to study sediment deposited into the Miocene to Pleistocene Gulf of California. This sediment records a ~7 million year story of deposition into the Gulf as slip along the San Andreas fault created local detachment faulting and basin development, first accumulating locally derived sediment followed by Colorado River delta progradation beginning at 5.3 Ma. Northwestern translation and uplift of the basin in the last ~1.0 Ma have brought these units above sea level and exposed them in a tilted succession (Dorsey et al., 2012). Analysis of these sediments for

this study has been conducted using two methodologies, 1) detrital zircon U-Pb and (U-Th)/He double-dating of Mio-Pliocene sediments, and 2) detailed outcrop study of the first Colorado River-sourced turbidite sediments, known as the Wind Caves Member of the Latrania Formation.

Chapter II addresses the question of sedimentary provenance, hinterland exhumation, and Colorado River evolution through detrital zircon U-Pb and (U-Th)/He double-dating. This method allows for both the crystallization age and cooling age (to 180 degrees C) to be obtained from individual zircon grains. Previous studies (Kimbrough et al., 2011, 2014) have shown detrital zircon U-Pb age distributions to be relatively steady throughout the Pliocene Colorado River-sourced units in the Fish Creek-Vallecito Basin. Low-temperature thermochronometry of grains with known U-Pb ages allows for cooling age evolution to be discriminated from individual U-Pb age populations analyzed from Mio-Pliocene units in the Fish Creek-Vallecito Basin and modern Colorado River delta . The U-Pb age and (U-Th)/He age represent crystallization and thermal history, respectively, of their drainage hinterland and can therefore be used to constrain source area. Due to the diverse areas sourced by the Colorado River, these ages provide clues as to where the river was sourcing from during the Pliocene and how this sourcing has changed through time up to the modern river. These data also have implications for how the Colorado River extended and evolved upstream and became integrated into the Gulf of California.

Chapter III examines deposition of the first Colorado River-sourced sediment into the Gulf through outcrop study of the Wind Caves Member. This unit consists of subaqueous sediment gravity flows which accumulated on top of locally, catastrophically emplaced sediment (mass transport deposits). The Wind Caves Member is the foundation of the progradational prism of deepwater to deltaic shelf sequence deposited by the Colorado River in the Pliocene. Outcrop study at bed-level resolution will be used to model early deposition into the Gulf as the Colorado River constructed its embryonic shelf and slope into the Pliocene Gulf.

This study offers a look into both evolution of the Colorado River drainage area upstream and downstream as it built its delta into the Pliocene Gulf of California. Investigation of Mio-Pliocene sediments through detrital zircon U-Pb and (U-Th)/He double-dating analyzes changes in sedimentary provenance and hinterland exhumation through Miocene pre-Colorado River, Pliocene Colorado River, and modern Colorado River sediment. An outcrop sedimentary study provides the paleogeographic details of a tomographically irregular seascape onto which Colorado River-sourced turbidite sands were emplaced as submarine fan lobes, emanating southwards from a Fish Cree shelf exit point into the Gulf. These studies are tied together through a source to sink perspective of Colorado River evolution which will help to understand how large river systems develop.

Chapter 2

Detrital Zircon U-Pb and (U-Th)/He Geo/Thermochronometry of the Mio-Pliocene Gulf of California, Fish Creek-Vallecito Basin, Southern California

INTRODUCTION

River systems are long-term recorders of the tectonic and climatic conditions of the areas which they drain. Far-travelled rivers have the ability to transport sediment from a large hinterland and funnel it into smaller marine basins upon reaching base level. As a result, sediment from a huge area becomes confined into a relatively compact stratigraphic package. Provenance can be narrowed and drainage evolution can be gleaned by comparing characteristics of sediments, such as mineral age and grain composition to lithological characteristics of possible source terranes. This has been long practiced through petrographic methods and more recently through detrital mineral geochronometry and thermochronometry (Rahl et al., 2003; Weltje and Von Eynatten, 2004).

The Colorado River provides an excellent case study of a fluvial system transporting sediment from a large drainage area into a small basin. This system currently connects the Rocky Mountains to the Gulf of California via a fluvial system draining much of the western US. Evolution of the Colorado River system has been a subject of interest to researchers for more than a century (Hunt, 1956). Timing of when this river became an integrated system allowing flow off of the Rocky Mountains onto the Colorado Plateau, through the Basin and Range, and into the Gulf of California has been constrained to the Mio-Pliocene, although mechanisms for how the drainage exited the

plateau are still debated (Lucchitta, 1972; Meek and Douglass, 2001). The Colorado River drains approximately 640,000 km² of southwestern North America, transporting sediment from an the arid western US landscape. Fluvial transport of sediment by the Colorado River system into the GOC was established in the earliest Pliocene (Dorsey et al., 2011; Ingersoll et al. 2013). During the late Miocene the newly opened GOC had been a depocenter for sediment transported by local fluvial systems (Winker 1987, Dorsey et al. 2007, 2011). The Mio-Pliocene Fish Creek-Vallecito Basin of southern California offers the best exposure of pre and post Colorado River sedimentation into the GOC with a conformable section of stratigraphic units.

Previous investigations into the provenance of sediment in the Fish Creek-Vallecito Basin have involved petrography as well as detrital zircon U-Pb and detrital muscovite Ar/Ar (Winker, 1987; Dorsey et al., 2011; Kimbrough et al. 2011, 2014; Cisneros et al., 2011). Synthesis of these results with magnetostratigraphic dating have placed introduction of Colorado River sediment into the basin at 5.3 Ma (Johnson, 1983; Winker, 1987; Dorsey et al., 2011; Kimbrough et al., 2011, 2014). Kimbrough et al.'s (2011, 2014) zircon U-Pb studies of Colorado River sourced sediment in the Fish Creek-Vallecito Basin show a relatively steady signal throughout the Pliocene units. The Colorado Plateau contains a vast quantity of sediment accumulated throughout the Phanerozoic as well as basement cored uplifts primarily of Laramide age. The spatial arrangement of geologic units of known ages and thermal histories allows for models to be assessed of how Colorado River drainage evolved during the Pliocene. These models include drainage enlargement through headward erosion in which the river system

expands upstream and top-down integration in which the river fills and spills into topographically lower basins before reaching base level (Lucchitta, 1972, 1989; Meek and Douglass, 2001).

This study analyzes the archive of sediment eroded from the western US terranes and deposited by Mio-Pliocene pre-Colorado River and Colorado River systems in the Gulf of California through detrital zircon U-Pb and (U-Th)/He double-dating. Combination of geochronometric as well as low-temperature thermochronometric methods allows for study of sediment provenance as well as inferences to be made about tectonism and landscape evolution of the Colorado River drainage area.

COLORADO RIVER

Modern Colorado River Overview

The main trunk of the Colorado River system is fed by six tributaries which drain 78% of the total drainage basin area (Andrews, 1991). These tributaries are shown in Figure 2-1 and include the Green, Grand, San Juan, Little Colorado, Virgin, and Gila Rivers. Contributions of water and sediment are not evenly delivered from inputs within the drainage area (Howard 1947; Irons et al. 1965; Andrews 1991). 75% of river flow is delivered from snowmelt high in the Rocky Mountains while 69% of sediment is discharged by the central Colorado Plateau around southeastern Utah, northeastern Arizona, and northwestern New Mexico. This area predominately exposes more easily erodible sedimentary rocks of Paleozoic, Mesozoic, and Cenozoic age.

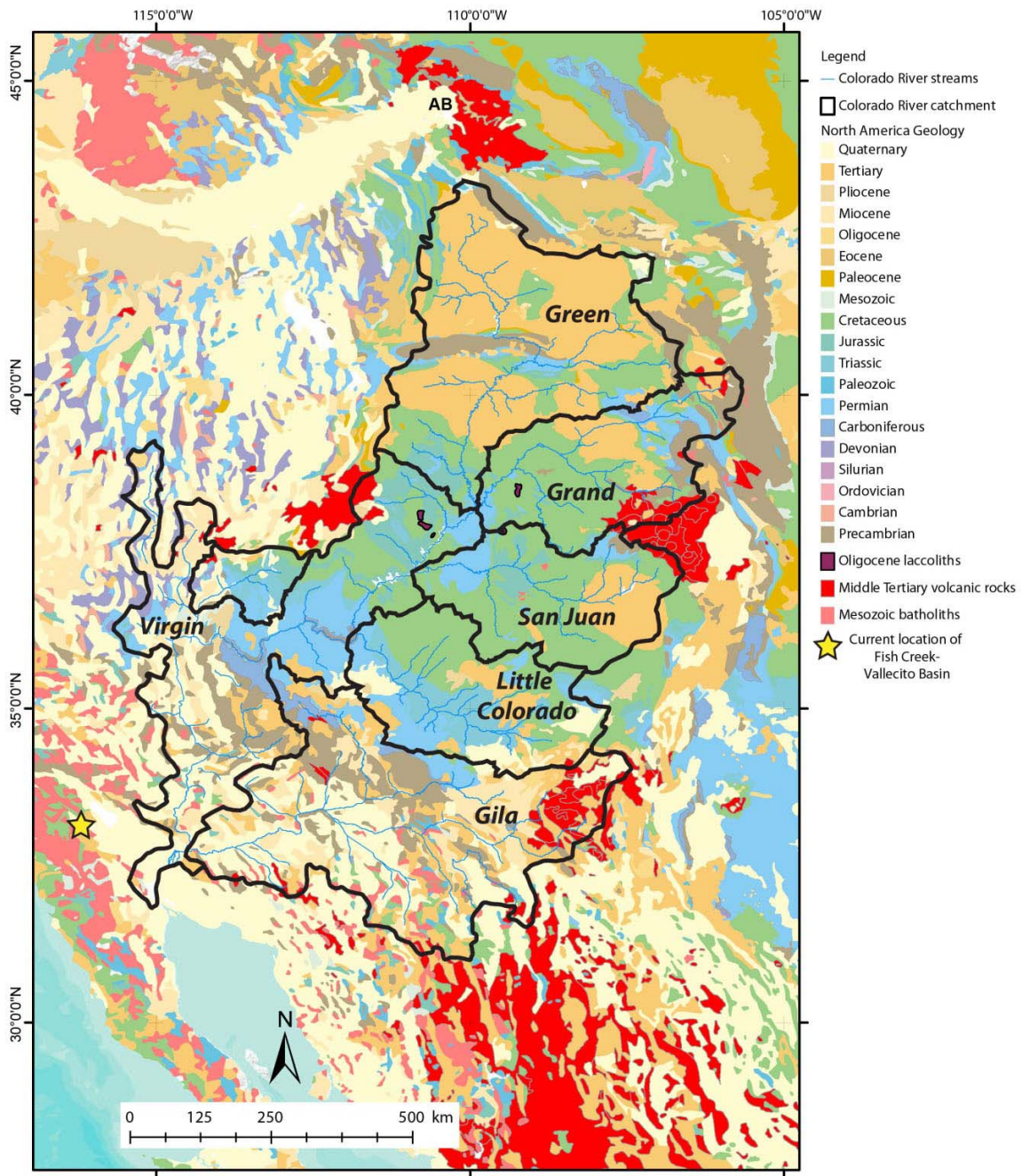


Figure 2-1. Map showing ages of lithologies presently exposed within the Colorado River drainage area. Major tributaries are outlined. (modified from Kimbrough, 2014)

Models of Colorado River Evolution

Drainage integration of much of the Colorado River system on the Colorado Plateau above the Kaibab upwarp has been constrained to the Miocene (Lucchitta, 1989). Pre-Miocene integrated drainage is unlikely due to an arid climate as evidenced by Oligocene erg deposits such as the Chuska erg covering much of the area (Dickinson, 2013). Integrated, west flowing drainage is believed to have begun by Miocene time as Basin and Range related faulting along the Grand Wash Fault lowered the area southwest of the Colorado Plateau (Faulds et al. 2001).

Mechanisms for how the Colorado Plateau exited the Colorado Plateau and ultimately flowed into the Gulf of California are still debated. These mechanisms include a headward erosion model expanding the river's reach upstream (Lucchitta, 1972) and a top-down integration model in which the upper Colorado River exited the Colorado Plateau and subsequently filled and spilled successively lower basins (Meek and Douglass, 2001). Headward erosion, shown in Figure 2-2, involves northward propagation of a river across the Kaibab uplift on the Colorado Plateau and capture of the upper Colorado River drainage system. Interpretation of the Mio-Pliocene Bouse Formation, located south of the Kaibab upwarp, as marine or lacustrine has implications for whether headward erosion or top down river integration was the main culprit for incorporation of the Colorado River into the Gulf. Lucchitta et al. (2001) postulates that the marine fossils found within the Bouse Formation are a clear indication of its marine origin as headward eroding streams were inundated by water from the Gulf. Spencer and Patchett (1997) argue that Bouse Sr-isotope ratios are similar to that of the modern river

and that marine fossils were likely avian-transported. This supports the idea that the Bouse Formation was deposited under lacustrine conditions and filled by the Colorado River during filling and spilling events (Spencer and Pearthree, 2001). From a sedimentary provenance perspective, deposits into the Mio-Pliocene Gulf of California by a headward eroding Colorado River should initially show characteristics of sourcing from the Basin and Range and southern Colorado Plateau followed by a change in provenance to the northern plateau as the upper drainage becomes captured. A top-down integrating Colorado River, shown in Figure 2-3, should show evidence of sourcing from the northern portions of the plateau and Rocky Mountains as flow originating in the far reach of the drainage area would fill and spill progressively lower basins.

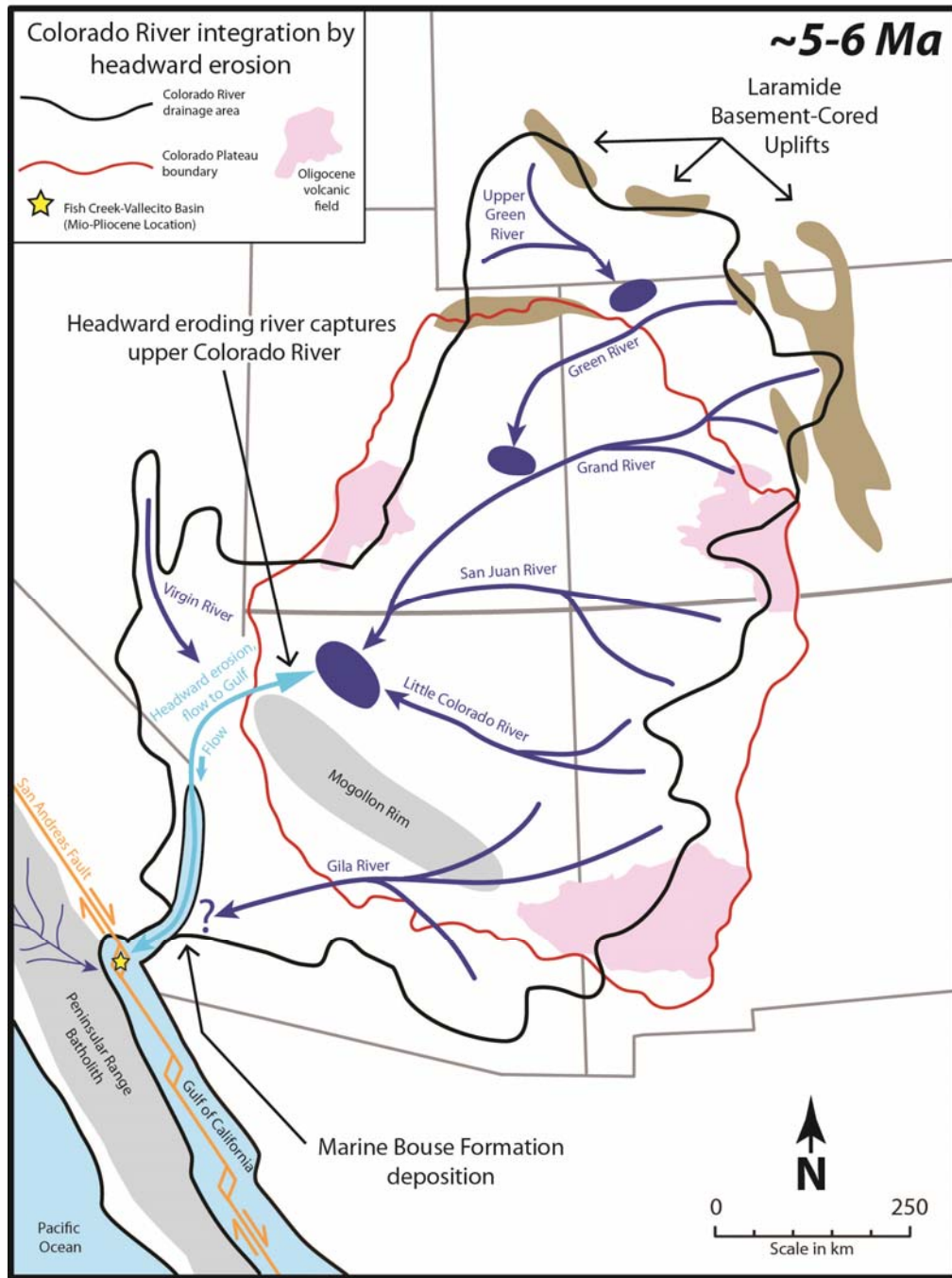


Figure 2-2. Colorado River integration through headward erosion. Lucchitta (1972) proposed a headward eroding river extending from the Gulf of California captured a well-integrated upper Colorado River.

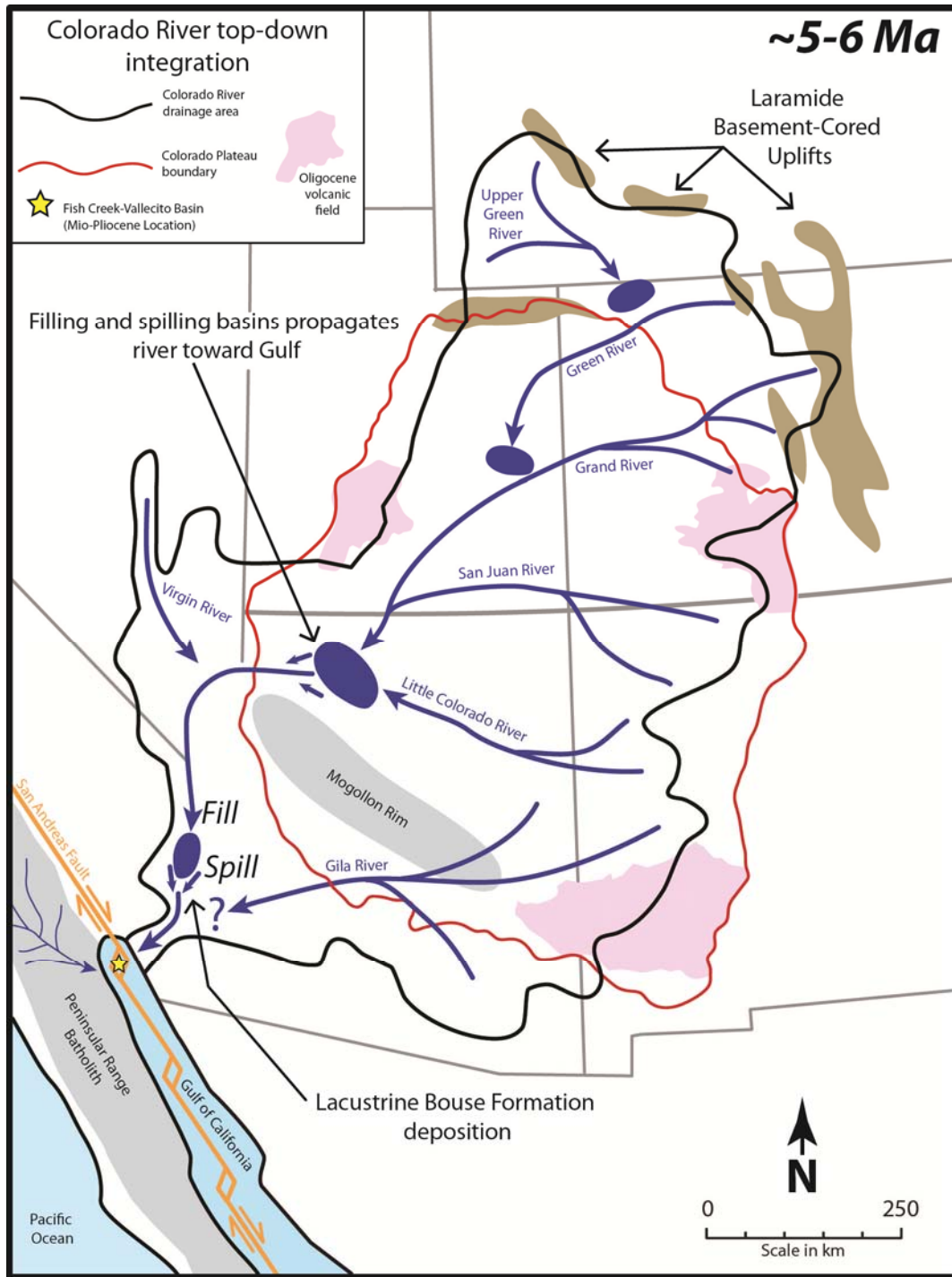


Figure 2-3. Colorado River integration into the Gulf of California top-down river migration. Meek and Douglass (2001) suggest that the Colorado River was integrated into the Gulf of California by successively filling and spilling into lower basins.

Mio-Pliocene Colorado River Deposits in the Fish Creek-Vallecito Basin

An archive of sediment deposited into the Miocene-Pleistocene Gulf of California is preserved and partially exposed in the Fish Creek-Vallecito Basin of southern California. The study area is shown in Figure 2-4.

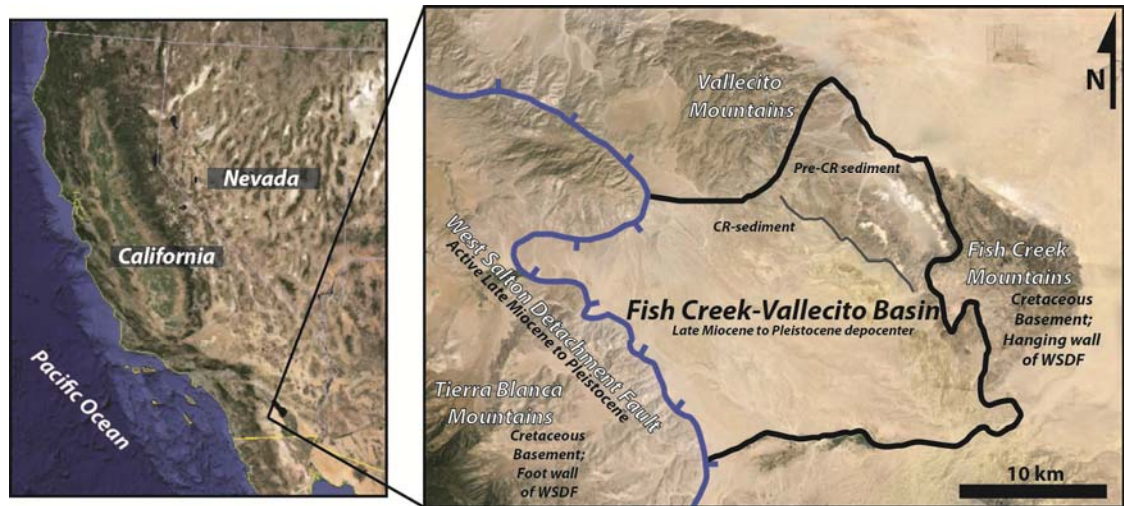


Figure 2-4. Satellite image showing field area with major features highlighted.

This study analyzed sediment of Mio-Pliocene age deposited from local fluvial systems during early rifting as well the earliest Colorado River-sourced sediments deposited into the Gulf. This archive contains a record of tectonics and landscape evolution of the Colorado River drainage area. The Fish Creek-Vallecito is a sub-basin within the western Salton Trough of the southern California/northern Mexico Gulf Extensional Province (Johnson, 1983; Winker, 1987). Sediments accumulated in the basin as dextral slip along the San Andreas Fault caused late Miocene local detachment faulting along the West Salton Detachment Fault with accumulation of sediment on the

upper plate of the detachment (Axen and Fletcher, 1998; Shirvell et al. 2009). The tectonic evolution of the Gulf of California is displayed in Figure 2-5.

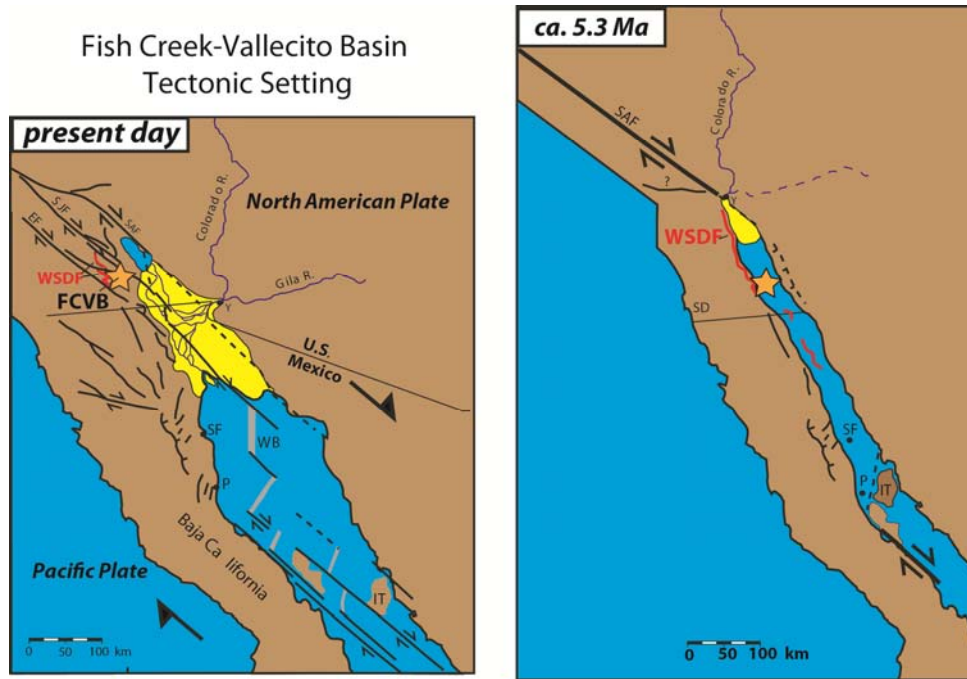


Figure 2-5. Present day tectonic setting of the Gulf of California (right) and reconstruction of the Gulf at the onset of Colorado River delta progradation at 5.3 Ma. Star shows location of Fish Creek-Vallecito Basin in the present day and at 5.3 Ma. (Modified from Dorsey et al., 2007)

Figure 2-6 shows stratigraphic units in the Fish Creek-Vallecito Basin with their corresponding ages dated through magnetostratigraphic methods. Deposition into the basin occurred from 8.0-1.0 Ma (Johnson, 1983; Dorsey, 2007, 2011). Local deposition occurred from ~8.0 Ma to 5.3 Ma followed by integration of the Colorado River and delta progradation from 5.3 to ~3.0 Ma. From ~3.0-1.0 Ma local sediments again began to accumulate as the Colorado River abandoned the area. Figure 2-7 shows units encountered in the field area. Samples were taken from each of these units with locations

marked in Figure 2-8. Tectonic reorganization between the Pacific and North American plates along the San Andreas Fault initiating the Elsinore Fault inverted the basin since ~1.0 Ma and exposed the Mio-Pliocene stratigraphy (Dorsey et al. 2012).

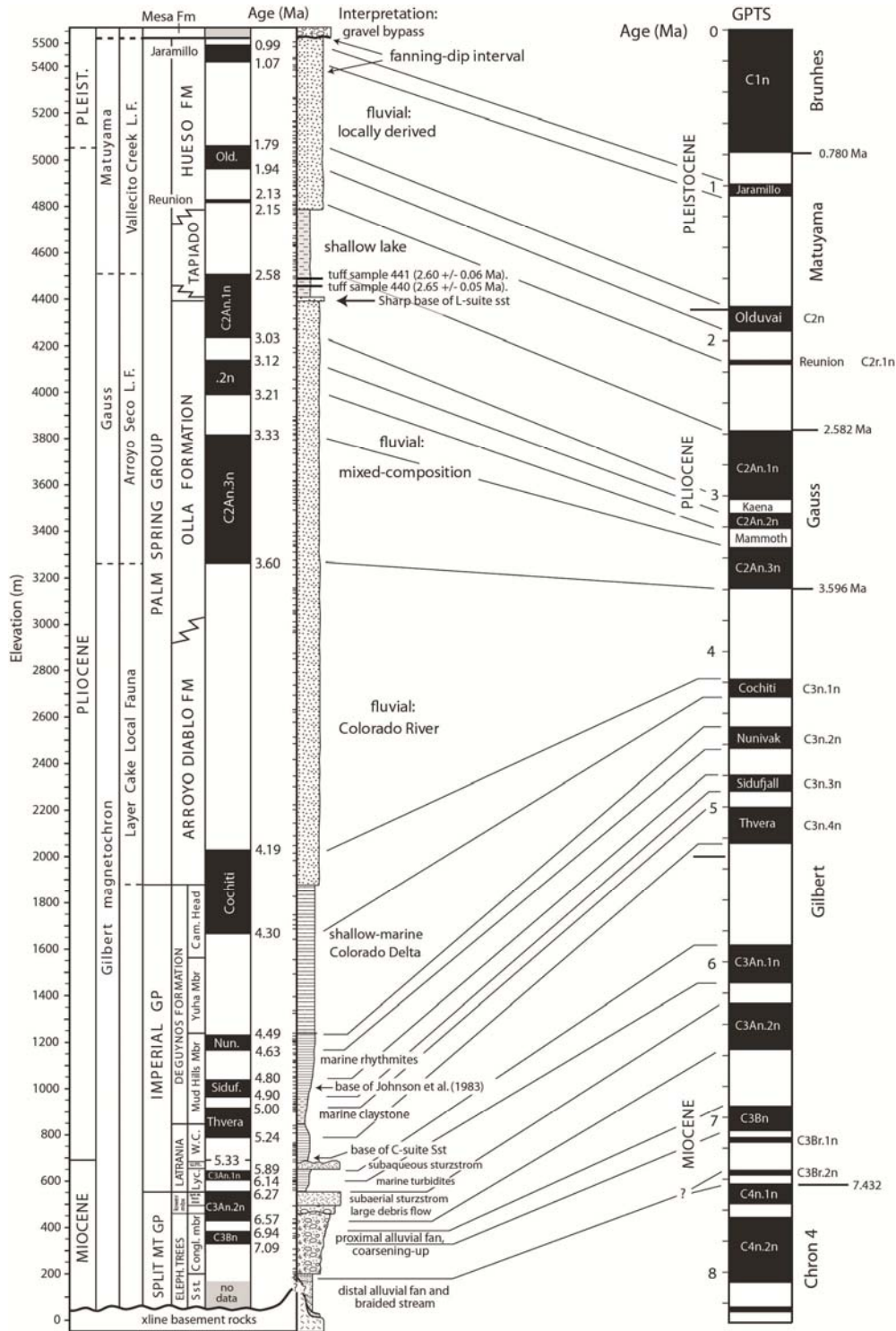
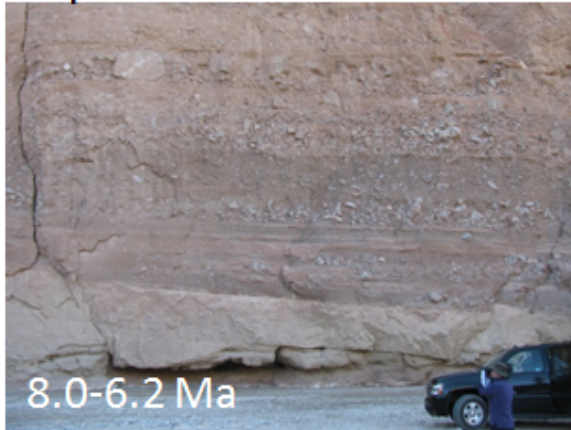
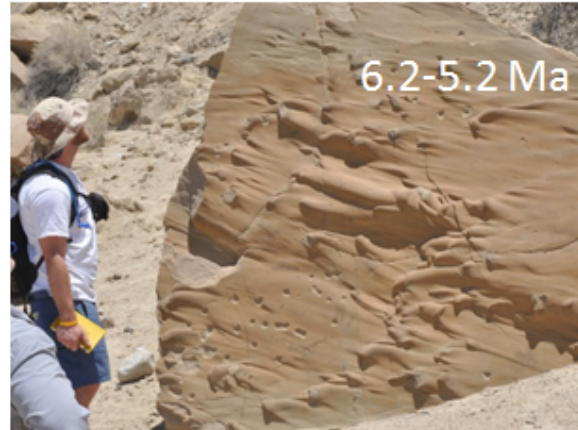


Figure 2-6. Stratigraphic column showing units exposed within the Fish Creek-Vallecito Basin and surrounding areas. Units were precisely dated through magnetostratigraphy by Johnson (1983) and Dorsey et al., 2007, 2011).

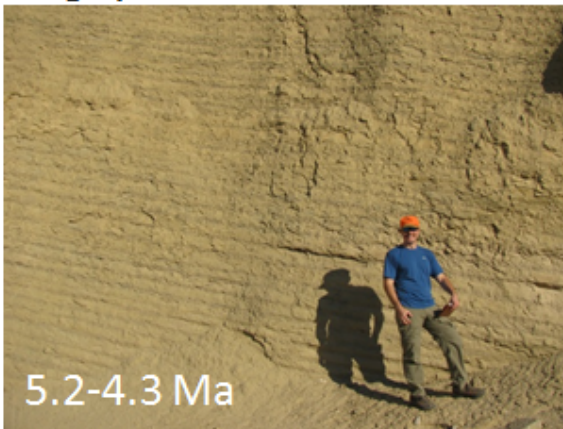
Elephant Trees Fm.



Latrania Fm.



Deguynos Fm.



Arroyo Diablo Fm.



Figure 2-7. Lithologies exposed within the area sampled in the Fish Creek-Vallecito Basin. These included conglomerates and sandstones deposited as alluvial fans in the Elephant Trees Fm., sandy marine turbidites of the Latrania Fm., silty mudstones and sandstones of the deltaic Deguynos Fm., and cross bedded sandstones of the Arroyo Diablo Fm.

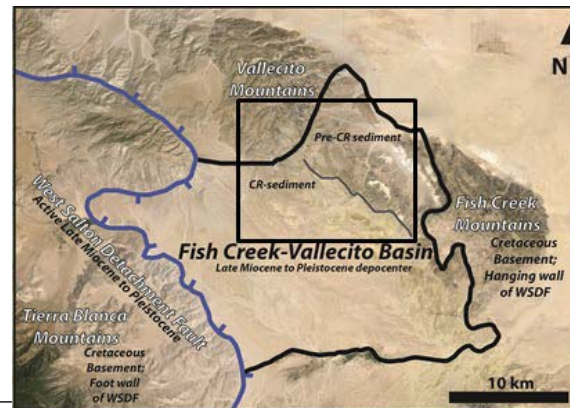
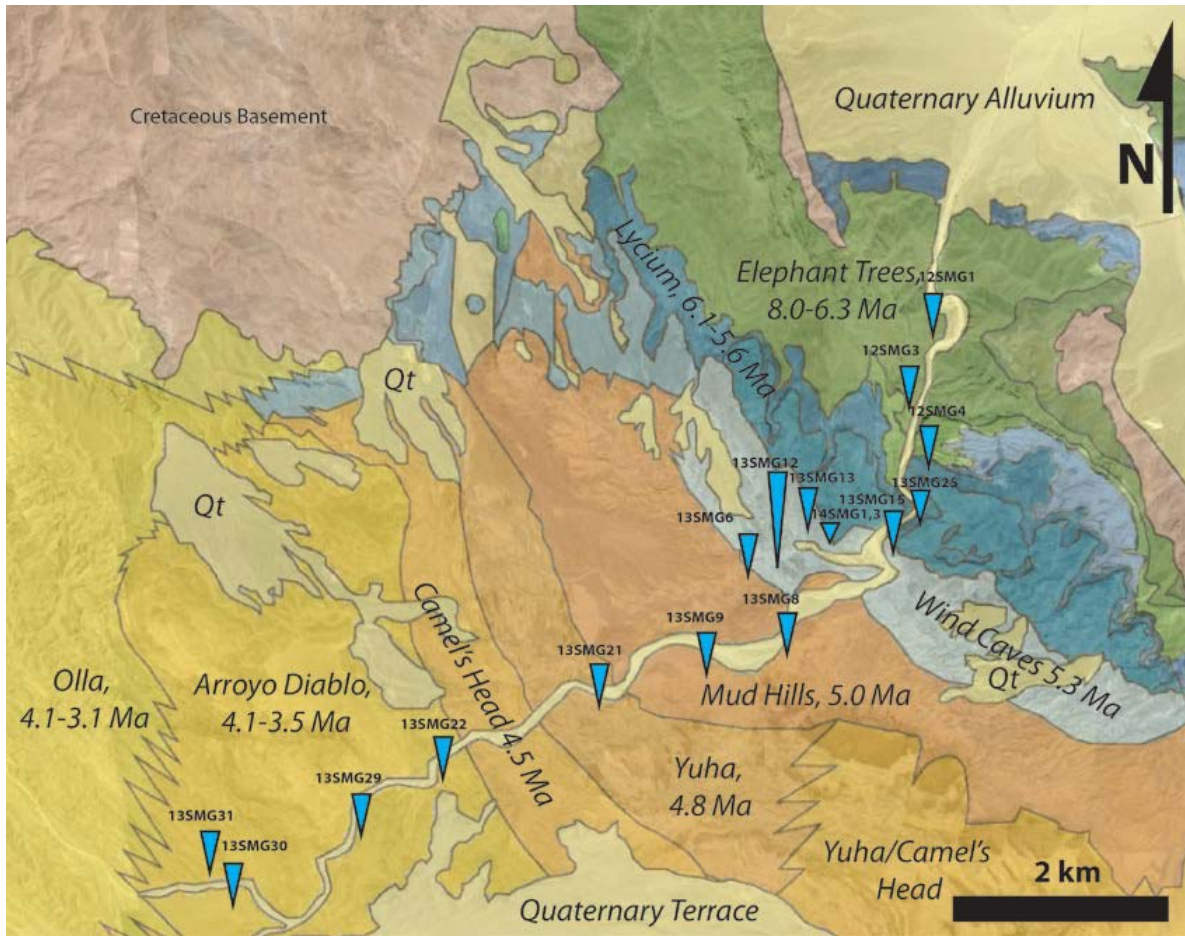


Figure 2-8. Map of lithostratigraphic units within the study area with sample locations marked. Areal photo shows outline of mapped area. (Modified from Winker, 1987)

The switch in sediment source has previously been documented through thin-section petrography and detrital zircon U-Pb (Winker 1987, Kimbrough et al. 2011, 2014). Thin-section petrography has shown deltaic sediments of the Fish Creek-Vallecito Basin to contain Cretaceous foraminifera derived from sedimentary units of the Colorado Plateau, primarily the Mancos shale (Merriam and Bandy 1965; Lucchita 1972; Buising 1990).

GEOLOGIC BACKGROUND OF THE COLORADO RIVER DRAINAGE AREA

The Colorado River drainage area runs through diverse crystalline terranes with distinct thermal histories. The crystalline terranes are exposed within basement-cored uplifts of mainly Laramide age but are largely buried by kilometers of stratigraphy deposited in the Colorado Plateau area throughout the Phanerozoic prior uplift and erosion by through going drainage. Upon exiting the Colorado Plateau, the Colorado River passes through the extensional Basin and Range Province before reaching the Gulf of California. Abundant volcanism since the Eocene as well as detritus from exhumed Cretaceous batholiths to the west is also a notable contributor of sediment. Recorded within zircon eroded from these terranes are the crystallization and exhumation (from 6 km depth) histories allowing provenance to be constrained at a higher resolution.

Rocky Mountains

The Southern Rocky Mountains of Wyoming, Colorado, Utah, and New Mexico make up the northern and eastern extent of the Colorado River catchment area. As mentioned earlier, 78% of river flow into the modern Colorado River system originates as snowmelt from the Rocky Mountains. The Rocky Mountains contain basement-cored uplifts of the Late Cretaceous to Eocene Laramide orogeny exposed at altitudes up to 4 km. The eastern extent of these uplifts is the result of flat slab subduction of the Farallon Plate under the North American Plate. (Dickinson and Snyder, 1978)

Colorado Plateau

The Colorado Plateau makes up about half of the Colorado River drainage area and covers ~340,000 km² of the western US and is contained within portions of Utah, Arizona, New Mexico, and Colorado (Hunt, 1956). The plateau is a broad, highstanding region residing at ~2 km and containing relatively little deformation (Pederson, 2002). Deformation that is present on the plateau consists of monoclines and uplifts of Laramide age. Uplift of the Colorado Plateau has been attributed to Laramide crustal thickening as well as epeirogenic uplift mechanisms resulting from anomalous mantle conditions (Pederson 2002, Karlstrom et al., 2012).

The high elevation of the Colorado Plateau has exposed Phanerozoic sediments to heavy erosion from the Late Cretaceous through Cenozoic. Early sediments were deposited in the Plateau region in a predominately passive margin interrupted by pulses of tectonic events in the Paleozoic. The episodic Appalachian orogenies created high topography to the east, shedding sediment into large-scale fluvial and eolian systems which deposited sediment into the western passive margin (Gehrels, 1995; Rahl, 2003).

Periods of western US tectonism occurred from the Devonian through the Permian with the Antler and Ancestral Rockies orogenic events interrupting passive margin sedimentation (Kluth, 1981). Mesozoic sedimentation occurred in an active margin setting as subduction along the western margin of the North American continent tectonically consolidated the region by the Late Jurassic, with continued subduction generating thin skinned deformation during the ~180-110 Ma Nevadan and Sevier orogenies. (Decelles, 2004). Flat-slab subduction during Laramide mountain building created basement involved uplifts ~1000 km from the Late Cretaceous to Eocene shoreline generating a series of monoclines and uplifts on the Colorado Plateau as well as the uplifts of the Rocky Mountains. Evidence for confinement of fluvial systems to the Colorado Plateau region is supported by detrital zircon evidence from Southern California showing no extraregional sediments being deposited from the Late Cretaceous until the Pliocene (Ingersoll et al., 2013). Fluvio-lacustrine and eolian deposits, notably the Chuska erg make up the Cenozoic stratigraphy but are largely eroded (Dickinson et al., 2010). Laccolith emplacement also occurred on the plateau during Laramide tectonism with volcanism continuing into the Oligocene. While much denuded, these laccoliths may have been prominent topographic features on the Colorado Plateau surrounded by >50 km volcanoclastic aprons (Dickinson, 2013). Erosion on the Colorado Plateau has primarily occurred since the Miocene in conjunction with the opening of the Gulf of California. Deep erosion of over 2.5 km has occurred in the central Colorado Plateau around the junction of where the Green River joins the main trunk of the Colorado River (Hoffman, 2009). Debate also surrounds timing of erosion into Paleozoic

stratigraphy in the Grand Canyon, with estimates ranging from 70 Ma (Wernicke, 2011; Flowers and Farley, 2012) to Miocene (Lee et al, 2011; Cather et al. 2012).

Basin and Range

The southern Basin and Range province is a highly extended terrane making up a large portion of the Colorado River drainage area southwest of the Colorado Plateau. Basin and Range extension is attributed to all extension that has occurred in the western US from the Eocene to recent (Wernicke et al., 1987; Parsons, 1995). Extension occurred in two phases with initial high extension of terranes by low-angle normal faulting creating local core complexes followed by a later stage of broader extension manifested by widespread high angle block faulting (Parsons, 1995). Estimates of extension average around 50 to 100% with as little as 10% in some areas and as much as 300% in others (Hamilton, and Myers, 1966; Zoback et al., 1981; Wernicke, 1987; Parsons, 1995). This widespread extension has caused exhumation of basement rock to low crustal levels (Foster and John, 1999).

Cordilleran Arc

Abundant magmatism occurred along the western North American continent as subduction ensued from Late Triassic through Late Cretaceous. Large batholiths were emplaced along this active margin and are exposed over >4000 km from the Peninsular Range Batholith in southern California and northern Mexico to the Idaho Batholith of northern Idaho and Western Montana (DeCelles, 2004). As subduction ceased in Late Cretaceous/Eocene a series of Basin and Range extensional events overprinted the structure of the Arc.

Igneous and Metamorphic Sources of Detrital Zircon

The terranes mentioned in the preceding paragraphs represent the main physiographic provinces from which the Colorado River flows through and derives sediment. While these provinces are composed of diverse lithologies, weathering and erosion of crystalline basement underlying these provinces provided sediment to stratigraphic units preserved upstream of the Colorado River sink as well as supplying sediment to the modern Colorado River through weathering and erosion of basement uplifts. These “crystalline provinces” composed of igneous and metamorphic rock are distinguished from each other based on geochronology of minerals within the crystalline rock. Much of this crystalline basement was accreted in the Precambrian (Whitmeyer and Karlstrom, 2007). The following is a summary of basement crystalline provinces summarized from Dickinson and Gehrels (2010), Gehrels et al., (2014); and Kimbrough et al. (2014): 1. Archean craton and early Proterozoic accretionary terranes (>1810 Ma); 3. Yavapai-Mazatzal Provinces (1535-1810 Ma); 4. Granite-Rhyolite Province (1300-1535 Ma); 5. Grenville Belt (900-1300 Ma); 6. Appalachian/Ouachita Orogen (285-725 Ma); 6. Cordilleran Arc, Ignimbrite Flare-Up, and Basin and Range (285- ~5 Ma). While it is possible for zircon falling into one of these age groups to be derived from a smaller igneous terrane, the ones mentioned above represent the most likely primary source areas.

PREVIOUS GEO-THERMOCHRONOMETRY OF THE COLORADO RIVER

DRAINAGE AREA

Detrital zircon U-Pb age distributions of Pliocene Colorado River sediments from the Fish Creek-Vallecito Basin show a very consistent age signal throughout the 5.3-3.0

Ma section (Kimbrough, 2011, 2014). As a result, distinguishing changes in sedimentary provenance is difficult as the same U-Pb age can be derived from basement uplifts as well as recycled from sedimentary stratigraphy of various age. Colorado Plateau stratigraphy of Lower Paleozoic to Early Cretaceous age show over half of grains in each unit to be derived from >900 Ma crust of the Grenville, Yavapai-Mazatzal, and Archean crust which makes up most of the southern North American basement (Dickinson and Gehrels, 2010; Gehrels et al., 2011). As a result, recycling sediment from stratigraphic units of different ages would yield similar proportions of U-Pb ages in downstream deposits.

Low-temperature thermochronometry involving zircon fission track (ZFT) apatite fission-track (AFT) and apatite (U-Th)/He (AHe) thermochronology has been used extensively to characterize thermal history on the Colorado Plateau (Dumitru et al., 1994; Hoffman, 2009). AFT and AHe has documented a “bull’s eye” of >2.5 km of erosion where the Green and Grand Rivers join the trunk of the Colorado River indicating a large amount of erosion has occurred on the central Colorado Plateau since ~6 Ma. AHe data from the Canyonlands show this area to have had greatest exhumation on the Colorado Plateau since ~6 Ma, however Jurassic and older ZHe from the same samples show that these units were not buried deeply.

METHODS

Detrital Zircon U-Pb and (U-Th)/He Double-Dating

Detrital zircon U-Pb and (U-Th)/He (ZHe) double dating allow for provenance determinations to be made at a higher resolution by using crystallization and cooling age

(to ~180 C as proxies for sediment source (Rahl, 2003). Obtaining both a crystallization age and cooling age is extremely useful in areas with terranes of varied crystallization and thermal histories (Reiners et al. 2005; Campbell et al., 2005). (U-Th/He) age records time since exhumation in zircon derived from active orogens as accelerated erosion and faulting which can cause rapid exhumation at a rate of 0.5-5.0 km/m.y. (Ring et al. 1999). This can bring a zircon from a depth of 6-9 km (~180 C assuming 20-30 C geothermal gradient) to the surface in ~1-18 m.y. (Rahl, 2003). This is useful when discriminating sedimentary provenance in basins which contain sediment derived from uplifts with the same crystalline basement but different exhumation histories or distinguishing between erosion from crystalline terranes and sedimentary stratigraphy (Reiners, 2005; Campbell, 2005). The Colorado River drainage area contains a southern portion influenced by Basin and Range extension, a central portion (Colorado Plateau) which contains thick sediments derived from orogenic events throughout the Phanerozoic, and flanked by the Rocky Mountains which contain basement cored uplifts of Laramide age. Whitmeyer and Karlstrom's (2007) model for Proterozoic growth of North America shows much of southern North America containing >900 Ma crystalline basement. While western US basement is abundant in >900 Ma crystalline basement, cooling ages for zircon of this age should be spatially variable allowing for provenance determinations to be made.

Zircon U-Pb Dating Methods

Crystallization ages were obtained by measuring concentrations of parent nuclides ^{238}U , ^{235}U , ^{232}Th , and their respective daughter isotopes ^{206}Pb , ^{207}Pb , and ^{208}Pb through laser ablation inductively coupled plasma mass spectrometry (LA-ICP-MS). LA-ICP-MS

was conducted on euhedral or rounded grains of zircon with short-axis diameters generally between 60 and 100 μm . Spot size for laser ablation analyses was either 20 or 30 μm with pit depths around 20 μm . Ablated material was carried by helium gas into an Element2 mass spectrometer. Prior to laser ablation, photographs were taken of sticky tape grain mounts in order for grains locations to be recorded and U-Pb ages to be accurately assigned to individual zircon. Raw data was reduced with Iolite software to obtain U-Pb ages. U-Pb ages reported are based on ratio of $^{206}\text{Pb}/^{238}\text{U}$ for zircon <800 Ma and are based on ratio of $^{206}\text{Pb}/^{207}\text{Pb}$ for zircon >800 Ma.

Zircon (U-Th)/He Dating Methods

Cooling histories (to ~ 180 C) were obtained by measuring concentrations of parent nuclides ^{238}U , ^{235}U , ^{232}Th , and ^{147}Sm to daughter ^4He through laser degassing, dissolution, and solution ICP-MS. Certain grains with U-Pb ages determined from LA-ICP-MS were later selected for (U-Th)/He analysis. Photographs of sticky tape mounts with labeled grains were used to find grains with known U-Pb ages ensuring that calculated (U-Th)/He (ZHe) ages were from the same grain. Grains were picked off of sticky tape, measured, and placed into Pt foil tubes which were lightly crimped shut with tweezers. Grains were selected based on U-Pb age distribution. Individual platinum-contained zircon aliquots were laser heated for 10 minutes at 1300 C for He gas extraction. Heating was repeated for each aliquot until subsequent re-extracts yielded $<1\%$ of total He. Extracted He was analyzed in an ultra-high vacuum (UHV) He line and spiked with ^3He standardized with a known volume of ^4He in order to determine unknown ^4He concentration by isotope dilution. This gas mixture was then cryogenically

purified by variable temperature release at 16-37K which separated He from other gases. A Blazers Prisma QMS-200 quadrupole mass spectrometer was then used for measuring $^3\text{He}/^4\text{He}$ ratios.

Degassed aliquots were then unwrapped from their Pt containers and dissolved for U, Th, and Sm concentration measurement. Zircons were placed individually in capsules and spiked with isotopically enriched ^{235}U , ^{230}Th , and ^{149}Sm . Capsules were then pressure heated at 180 C within Parr dissolution process, first with an HF-NO₃ solution for four days prior to drydown and 12 more hours of pressure heating with an HCl solution. Solution contained within capsules was then placed into larger vials for solution mass spectrometer analysis. NO₃ was again added to the solution followed by heating at 90 C for 45 minutes. 1000 microliters of 18 ohm MilliQ water was then added to each vial prior to analysis with a Thermo Scientific Element 2 HR-ICP-MS which measured isotopic abundances of ^{238}U , ^{235}U , ^{232}Th , ^{230}Th , ^{147}Sm .

Data Display

U-Pb and ZHe data are presented by showing relative distributions of ages generated by either method of analysis. Charts in this study show relative distributions of ages primarily through Kernel density estimators (KDE's) which will have a thick line with shading underneath. Probability density plots PDP's will have thin line, unshaded underneath for comparison. Histograms with predetermined bin widths (generally 50 Ma in this study) are also provided. A critical difference between KDE's and PDP's is the latter's use of analytical uncertainty to determine peak height rather than just the local

probability density (Vermeesh, 2012). As a result, young grains can generate high peaks due to low uncertainty. By using local probability density (KDE method), relative proportions of older grains can be visually compared to younger populations more accurately.

RESULTS

Seventeen fine to medium grained sandstones were collected in each stratigraphic unit from fresh exposures along Fish Creek Wash in the Fish Creek-Vallecito Basin. Pebbly sandstones were collected from two coarser-grained alluvial fan units of the Elephant Trees Formation. Sample CR05 was collected from sands of the modern Colorado River delta and was processed at San Diego State University before being sent as zircon mineral separate. Mineral separation of sandstone samples involved crushing using a steel mortar and pestle followed by sieving out >250 um fragments to remove cemented grains. Water table separation was performed using a Gemini water table followed by bromoform and methylene iodide heavy liquid density separation and magnetic separation using a Frantz magnetic mineral separator. These methods yielded a mineral separate with a high fraction of zircon in order to obtain both U-Pb and (U-Th)/He ages on single grains. LA-ICP-MS of detrital zircons yielded ~2000 near concordant (generally within ~10% concordance) to concordant analyses from 17 Mio-Pliocene sandstone samples collected from stratigraphic units in the Fish-Creek-Vallecito Basin and one from the modern Colorado River delta in northern Mexico. U-Pb age distributions fall into two main suites: 1. Miocene pre-Colorado River sandstones and uncommon Pliocene sandstones interbedded with Colorado River deposits with bimodal

Late Jurassic and Cretaceous U-Pb age peaks (“L-Suite” sandstones) and, 2. Pliocene and recent Colorado River sandstones and unconsolidated sands with U-Pb ages ranging from Pliocene to Archean (“C-Suite” sandstones). The classification into L- and C-Suite sandstones is after Winker (1987) These two sandstone suites can be distinguished in hand sample the by Miocene pre-Colorado River sandstones being generally medium to coarse grained and biotite-rich while Pliocene sandstones are very fine to medium grained with more well sorted grains. Zircon grains from non-Colorado River deposited sandstones also predominately subhedral to euhedral while Colorado River zircon grains are subrounded to rounded with minor amounts of euhedral grains. Field relations show that once the Colorado River inundates the basin, L-Suite sandstones become much less common and occurs primarily as thin interbeds within the basin-floor fan complex (Wind Caves Member, Latrania Formation), and the prograding delta sequence Deguynos Formation). With deposition of fluvial Colorado River sediment (Arroyo Diablo Formation), L-Suite sandstone beds become thicker and are more commonly interbedded with C-Suite sandstones.

280 out of the ~2000 U-Pb dated grains were “double-dated” in order to obtain (U-Th)/He (ZHe) ages. As mentioned before, the ZHe age records the time since the zircon was at ~180 C, representing the time at which the zircon was exhumed to a crustal depth of ~6 km under standard geothermal gradients. Grains analyzed for ZHe ages were generally between 60 and 90 microns and were rounded to euhedral. Most grains analyzed for U-Pb ages fell within this criteria and selection of grains for ZHe analysis was based on relative abundances of U-Pb ages. Analysis was done on grains from

Pliocene to Archean in age, however relatively few grains younger than 285 Ma were selected for ZHe analysis as the few double-dated grains revealed ZHe age to be equal to U-Pb age. This occurred in Colorado River-deposited samples in which 218/384 grains had U-Pb ages <50 Ma. Of the 11 grains dated from this population, the uncertainty of the ZHe age generally overlapped with that of the U-Pb age.

Discussion of results below will pool U-Pb results of multiple sandstone samples together when detrital zircon signature of samples is similar. Combining samples within stratigraphic units allows for better representation of U-Pb age populations and a more accurate evaluation of possible source areas providing zircon to the Colorado River system. U-Pb and ZHe age distributions are displayed in Figure 2-9 for L-Suite sandstones (non-Colorado River-sourced). Figures 2-10 to 2-18 summarize U-Pb and ZHe results for C-Suite (Colorado River-sourced) sandstones from samples collected from the Pliocene section as well as the modern Colorado River delta sample.

Elephant Trees Formation

Two pebbly, coarse sandstone samples were collected from the lowest exposed stratigraphic unit consisting of sandstones and gravel to boulder conglomerates deposited from ~8.1 to 6.8 Ma in an alluvial fan setting. 203 single-grain U-Pb ages were obtained from this sample ranging in age from 63.2 ± 1.4 Ma to 1700.9 ± 4.7 Ma. 95.5% of grains have U-Pb ages less than 125 Ma with a median age of 97.3 ± 2.2 Ma. 2.5% of grain ages are between 125 and 285 Ma and the remaining 2% of grains were Precambrian in age

between 1121 and 1700 Ma. One main peak occurred around 97 Ma while a subordinate peak occurred around 74 Ma.

19 of the 203 U-Pb dated grains from two samples were chosen for (U-Th)/He analysis. Grains from the entire U-Pb age range were chosen at random and yielded (U-Th)/He ages ranging from 39.8 Ma to 72.6 Ma with a median of 60.4 Ma.

Latrania Fomation, Lycium Mbr. and Lower Wind Caves Mbr.

Three medium to coarse grained samples were collected within the lower to middle Latrania Formation. The Latrania Formation consists of marine sandstones deposited by gravity flows which were interrupted by a subaqueous landslide deposit from ~6.2-5.2 Ma during initial marine incursion into the basin (Winker, 1987; Dorsey et al. 2011). 268 single grain U-Pb ages were obtained ranging in age from 80.61 ± 0.78 Ma to 1720 ± 21 Ma. 84.7% of grains yielded U-Pb ages less than 125 Ma with a median age of 94.3 ± 1.6 Ma while 12.7% of grains fell between 125 and 285 Ma with a median age of 162.3 ± 2.7 Ma. The remaining 2.6% of grains were between 472 ± 17 Ma and 1720 ± 21 Ma. Two peaks occurred with a dominant peak at 94 Ma and a subordinate peak at 160 Ma.

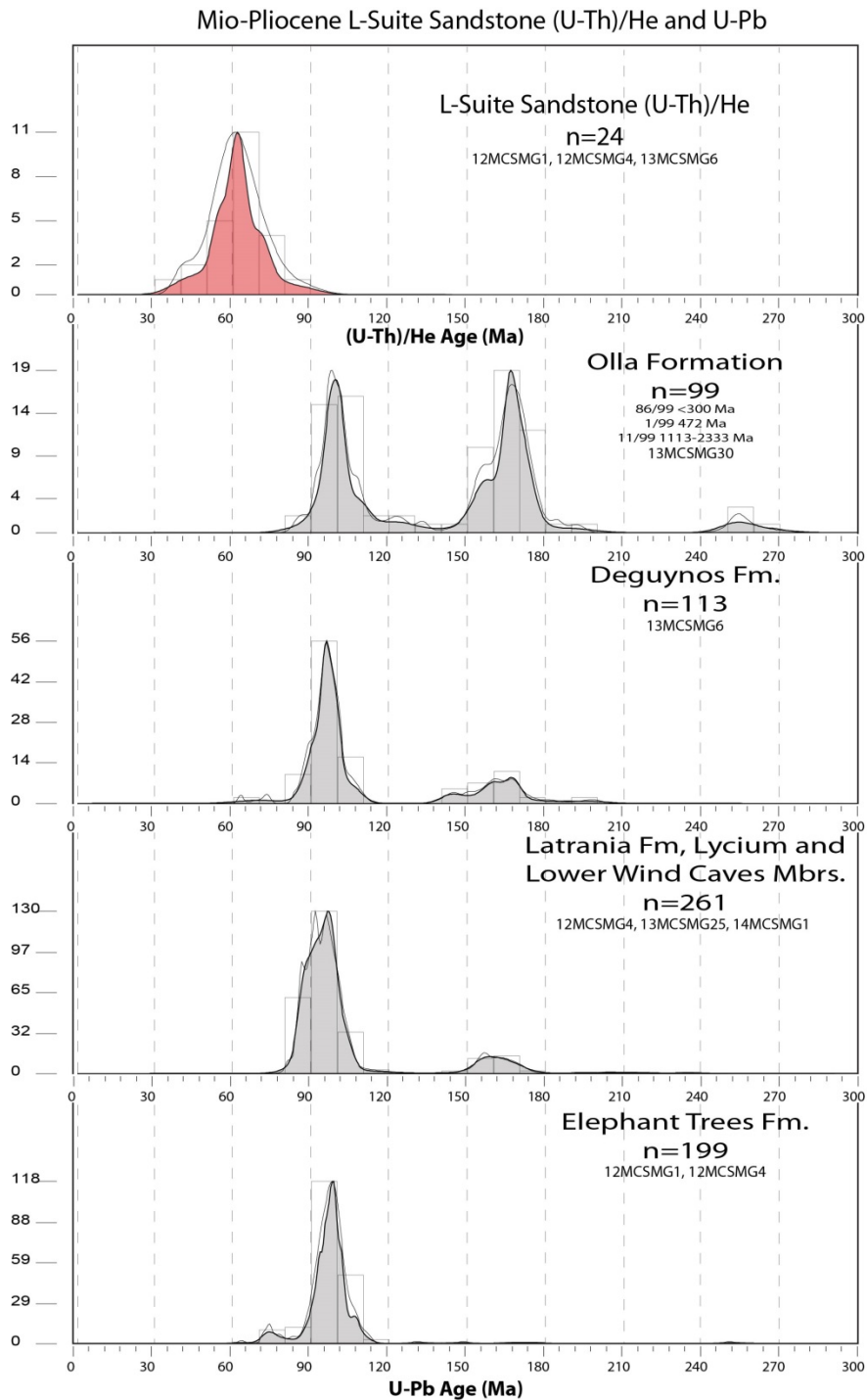


Figure 2-9. U-Pb age distributions of L-Suite sandstones by formation. ZHe age distribution plot at top combines samples taken from Elephant Trees, Latrania, and Deguynos Fm. As mentioned in the methods section, Kernel

density estimators (shaded) are primarily used to show age distributions. Probability density plots as well as histograms are also shown with thinner lines for comparison.

Latrania Formation, Wind Caves Member

Four fine to medium grained sandstones samples were collected from throughout the Wind Caves Member of the Latrania Formation. This unit was deposited from ~5.3-5.2 Ma primarily by turbidity currents as evidenced by outcrops showing abundant graded bedding and common flute and groove casts with heavy scouring. Thick bedded sandstones occurred near the base of the section with increases of mud accompanied by thinner bedded sandstones higher in the section. A change from primarily coarse, biotite rich sand to very fine to medium grained quartz rich sand occurs abruptly within the first few to tens of meters within the section. This discussion of results focuses on data from the latter sandstone which has U-Pb ages that are distinct from the age populations mentioned within the previous section.

375 single-grain U-Pb grain ages were obtained for the Wind Caves Member ranging from 4.29 ± 0.1 Ma to 2773 ± 11 . A dominant peak occurs around 28 Ma with smaller but prominent peaks at 1057 Ma, 1441 Ma, and 1685 Ma. 32.5% of grains have U-Pb ages <285 Ma with 86.1% of grains <125 Ma with a median age of 30.8 ± 1.1 Ma. 8.5% of grains have U-Pb ages between 285 and 900 Ma with a mean age of 475 ± 5.0 Ma. 13.3% of grains have U-Pb ages between 900 and 1300 with a median age of 1068.5 ± 24.5 Ma. 19.5% of grains had U-Pb ages between 1300 and 1535 with a median age of 1439.1 ± 8.2 Ma. 21.6% of grains had U-Pb ages between 1535 and 1810 Ma with a

median age of 1695 ± 13 Ma. Grains with U-Pb ages older than 1810 Ma accounted for 4.5% of all grains and had a median age of 1999 ± 25 Ma.

71 of the 375 grains were chosen for (U-Th)/He analysis. ZHe ages for 285-900 Ma U-Pb age grains (n=9) ranged from 91.2 ± 7.3 Ma to 329.1 ± 26.3 Ma with a median cooling age of 269.2 ± 21.5 Ma. A major peak for this population occurred at 323 Ma with a subordinate one at 249 Ma. ZHe ages for 900-1300 Ma U-Pb age population (n=18) ranged from 25.4 ± 2.0 Ma to 874.7 ± 70 Ma. A major peak for this population occurred around 230 Ma and 453 Ma. ZHe ages for the 1300-1535 Ma U-Pb age population (n=14) ranged from 13.6 ± 1.1 Ma to 269.6 ± 21.6 Ma. Major peaks for this population were around 66 Ma and 176 Ma. ZHe ages for the 1535-1810 U-Pb age population (n=15) ranged from 42.3 ± 3.4 Ma to 434.1 ± 34.7 M.. Two major peaks for this population occurred at 50 Ma, 89 Ma. and 149 Ma. ZHe ages for grains with ages >1810 Ma ranged from 58.4 ± 4.7 Ma to 390.6 ± 31.2 Ma. A major peak for this population occurred at 226 Ma with a shoulder off of this peak at 268 Ma.

Deguynos Formation

Five samples were collected from the Mud Hills, and Yuha Members while one was taken from the lowest Arroyo Diablo Formation, just above the Camel's Head member of the 5.1-4.4 Ma Deguynos Formation. Within the lowest stratigraphic unit, the Mud Hills Member, Lithologies vary from claystone/mudstone with minor bedded sandstones toward the base to "rhythmites" with interbedded siltstones and very fine to fine sandstones with bedding ~10-20 cm thick. Overlying the Mud Hills Member are the

Yuha and Camel's Head Members which outcrop as lenticular, thick bedded fine to medium sandstones. Oyster beds <1m thick are also commonly found in the upper Deguynos Formation. Throughout the Deguynos Member, thin bedded, coarse grained, biotite rich sandstones are also found. The Deguynos Formation is interpreted to represent a prograding deltaic sequence deposited in a tide-dominated environment.

One heavily bioturbated, coarse grained, biotite-rich sandstone was collected from a thin-bedded sandstone unit in the lower Mud Hills. This sample yielded 117 U-Pb ages ranging from 62.8 ± 1.1 Ma to 1350 ± 33 Ma. 72.7% of grains with U-Pb ages below 125 Ma with a median age of 95.8 ± 1.3 Ma. 23.9% of grains were between 125 Ma and 285 Ma with a median of 161.9 ± 2.9 Ma. The remaining 3.4% of grains had U-Pb ages which ranged from 770 ± 18 Ma to 1350 ± 33 Ma.

Of the 117 grains analyzed for U-Pb ages, 6 were chosen for ZHe analysis. Grains with U-Pb ages ranging from 97.1 ± 1.6 Ma to 156.9 ± 2.7 Ma yielded ZHe ages between 60.9 ± 4.9 Ma to 86.1 ± 6.9 Ma with a median ZHe age of 70.6 ± 5.6 Ma.

453 U-Pb single-grain ages were obtained with ages ranging from 3.84 ± 0.31 Ma to 2743 ± 15 Ma. Major peaks occurred at 27.4 Ma, 84 Ma, 400 Ma, 558 Ma, 1160 Ma, 1432 Ma, 1703 Ma, and 2720 Ma. 32.5% of grains had U-Pb ages <285 Ma with 85.7% of these grains <125 Ma. The median age for <125 Ma grains was 31.8 ± 1.1 Ma and 125-285 Ma grains was 206.4 ± 2 Ma. 13% of grains had U-Pb ages between 285 and 900 Ma with a median age of 466.9 ± 9.9 Ma. 12.1% of grains had U-Pb ages between 900 and 1300 Ma with a median U-Pb age of 1135 ± 16 Ma. 14.3% of grains had U-Pb ages

between 1300 and 1535 Ma with a median age of 1436 ± 11 Ma. 22.1% of grains had U-Pb ages between 1535 and 1810 Ma with a median age of 1708 ± 12 Ma. Grains with U-Pb ages >1810 Ma comprised the remaining 6% of single-grain ages and had a median age of 2155 ± 7.5 Ma.

75 of the 453 grains analyzed for U-Pb ages were chosen for ZHe analysis. Grains chosen for ZHe analysis from the 285-900 Ma U-Pb age population ($n=10$) had ZHe ages ranging from 159.3 ± 12.8 Ma to 374.9 ± 30.0 Ma with a median age of 274.8 ± 22.0 Ma. Two peaks for the 285-900 Ma U-Pb population occur at 255 Ma and 310 Ma. Grains chosen from the 900-1300 Ma U-Pb age population ($n=10$) had ZHe ages ranging from 30.2 ± 2.4 Ma to 738 ± 59 Ma. The two largest ZHe age peaks for the 900-1300 Ma population occurred at 83 Ma and 350 Ma. Grains chosen from the 1300-1535 Ma U-Pb population ($n=11$) had ZHe ages ranging from 38.3 ± 3.1 Ma to 410.3 ± 32.8 . ZHe age peaks for the 1300-1535 Ma U-Pb population occur at 51 Ma and 200 Ma. Grains chosen from the 1535-1810 U-Pb age population had ZHe ages ranging from 37.0 ± 3.0 Ma to 251.7 ± 20.1 . ZHe age peaks occur at 65 Ma and 148 Ma. Grains chosen from the >1810 U-Pb age population had ZHe ages between 49.6 ± 4.0 Ma and 982 ± 78.6 Ma. A main ZHe age peak occurs at 356 Ma with a shoulder at 305 Ma.

Arroyo Diablo Formation

Two samples were collected from the 4.2-3.5 Ma Arroyo Diablo Formation. Samples were fine to medium grained sandstones which showed abundant cross bedding. Sandstones were bedded and had a lenticular appearance in outcrop. Sandstones were

often associated with thick bedded gray and red siltstones. This unit was deposited in a fluvial environment as evidenced by the amalgamated, cross bedded sandstone with interfluvial overbank areas in which silt and clay deposition occurred. This unit interfingered with the Olla Formation (discussed in the next section) of the same age but can be distinguished by having a finer grained texture and a lack of biotite.

196 single-grain U-Pb ages were obtained from the two samples taken from Arroyo Diablo Formation outcrops. Single-grain U-Pb ages ranged from 16.73 ± 0.54 Ma to 2774 ± 7.2 Ma with major U-Pb age peaks at 33 Ma, 96 Ma, 163 Ma, 406 Ma, 1420 Ma, 1708 Ma, and a small age peak at 2676 Ma. 39.8% of grains has U-Pb ages < 285 Ma with 78.2% of these grains < 125 Ma. The < 125 Ma U-Pb population had a median age of 40.9 ± 1.3 Ma while the 125-285 Ma U-Pb age population had a median age of 208.7 ± 3.3 . 9.2% of grains had U-Pb ages between 285 and 900 Ma with a median age of 424.9 ± 5.3 Ma. 7.7% of grains had U-Pb ages between 900 and 1300 Ma with a median age of 1145 ± 24 Ma. 12.8% of grains had U-Pb ages between 1300 and 1535 Ma with a median age of 1426 ± 11 Ma. 25.5% of grains had U-Pb ages between 1535 and 1810 Ma with a median age of 1708 ± 16 Ma. Grains older than 1810 Ma made up the remaining 5.1% of single-grain U-Pb ages and had a median age of 2669 ± 8.0 Ma.

50 grains from the 196 U-Pb analyses were selected for ZHe analysis. Grains were mainly selected from the 900-3000 Ma U-Pb populations for ZHe analysis as the evolution of the ZHe signal for these populations was of particular interest. ZHe ages for populations < 900 Ma were generally > 200 Ma and did not show much evolution. As a

result, effort was focused on obtaining ZHe ages for the >900 Ma U-Pb populations. ZHe age distribution for the 900-1300 (n=7) Ma age population ranged from 283.1 ± 22.6 Ma to 717.7 ± 57.4 Ma. Prominent ZHe age peaks occurred at 285 Ma and 512 Ma. ZHe age distribution for the 1300-1535 Ma U-Pb population (n=13) ranged from 47.2 ± 3.8 Ma to 979 ± 78.3 Ma. ZHe age peaks included a dominant peak at 134 Ma and two subordinate age peaks at 205 Ma and 628 Ma. ZHe age distribution for the 1535-1810 Ma U-Pb age population (n=22) ranged from 44.6 ± 3.6 Ma to 664.6 ± 53.2 Ma with a single age peak occurred at 86 Ma. ZHe age distribution for the >1810 Ma age population (n=3) ranges from 62.7 ± 5.0 to 383.5 ± 30.7 .

Olla Formation

One sample was collected in the Olla Formation which, as mentioned above, interfingers with the Arroyo Diablo Formation and is distinguished from the Arroyo Diablo Formation by having a medium to coarse grained texture with abundant biotite much like the sandstones in the Pre-Colorado River deposited units and the coarse grained, biotite-rich sandstones interbedded with Colorado River fine sands in the Latrania and Deguyos Formations. Sandstone beds are thick, commonly cross bedded and are interpreted to be deposited in a fluvial environment.

99 single-grain U-Pb ages were obtained from the single sample collected from this formation. The Olla Formation has two dominant peaks at 99 Ma and 167 Ma. 37.4% of grains have U-Pb ages <125 Ma with a median age of 100.2 ± 3.3 Ma. 49.9% of grains are between 125 and 285 Ma with a median age of 167.1 ± 3.8 Ma. The remaining 13.1% of

grains range in age from 472.3 ± 9.2 Ma to 2333 ± 16 Ma. ZHe ages were not obtained for this sample.

Modern Colorado River Deltaic Sand

Modern Colorado River zircon mineral separates were provided by Professor David Kimbrough of San Diego State University. This sample was sourced from just north of the Gulf of California on the Colorado River delta plain in northern Mexico. 285 single-grain U-Pb ages were obtained from this sample with ages ranging from 16.4 ± 0.2 Ma to 3321 ± 12 Ma. Major U-Pb age peaks occurred at 152 Ma, 404 Ma, 538 Ma, 610 Ma, 1022 Ma, 1180 Ma, 1445 Ma, 1683 Ma, and 2705 Ma. In contrast to previous samples which contained ~30-40% <285 Ma U-Pb ages, the modern Colorado River deltaic sand had only 13% of grains with U-Pb ages <285 Ma. Of these, 37.8% of grains were <125 Ma with a median age of 70 ± 2.1 Ma. Grains with U-Pb ages between 125 and 285 Ma comprised 62.2% of the <285 Ma population with a median U-Pb age of 165.5 ± 2.6 Ma. The 285-900 U-Pb age population increased significantly from prior samples, making up 21.1% of total grain ages with a median U-Pb age of 454.4 ± 8.0 Ma. Grains in the 900-1300 Ma U-Pb age population made up 23.5% of total grain ages with a median U-Pb age of 1101 ± 35 Ma. Grains from the 1300-1535 Ma U-Pb age population made up 14.4% of total grain ages with a median U-Pb age of 1438 ± 22.5 Ma. Grains from the 1535-1810 Ma U-Pb age population made up 19.3% of total grain ages with a median U-Pb age of 1689 ± 30 Ma. Grains older than 1810 Ma made up the remaining 8.8% of total U-Pb grain ages with a median U-Pb age of 2412 ± 13 Ma.

60 grains of the 285 analyzed for U-Pb ages were selected for ZHe analysis. ZHe ages for the 285-900 Ma U-Pb age population (n=4) ranged from 252.5 ± 20.2 to 348.9 ± 27.9 with a peak ZHe age at 271 Ma. ZHe ages for the 900-1300 Ma U-Pb age population (n=8) ranged from 143.0 ± 11.4 to 461.7 ± 36.9 with a peak ZHe age at 363 Ma. Grains selected for ZHe analysis from the 1300-1535 Ma U-Pb age population (n=17) had ZHe ages ranging from 24.8 ± 1.5 Ma to 587.9 ± 38.3 Ma. ZHe age peaks occurred at 65 Ma, 187 Ma, and 260 Ma, with a major peak at 357 Ma. Grains selected for ZHe analysis from the 1535-1810 Ma U-Pb age population (n=23) ranged from 41.3 ± 2.8 Ma to 806.7 ± 48.4 Ma. ZHe age peaks for this population occurred at 49 Ma, 234 Ma, and 324 Ma with a major ZHe age peak at 140 Ma. ZHe ages for the >1810 Ma U-Pb age population (n=4) contained the oldest ZHe ages in this study and ranged from 385.2 ± 30.8 Ma to 1283.9 ± 102.7 Ma

Detrital Zircon U-Pb Results by Formation

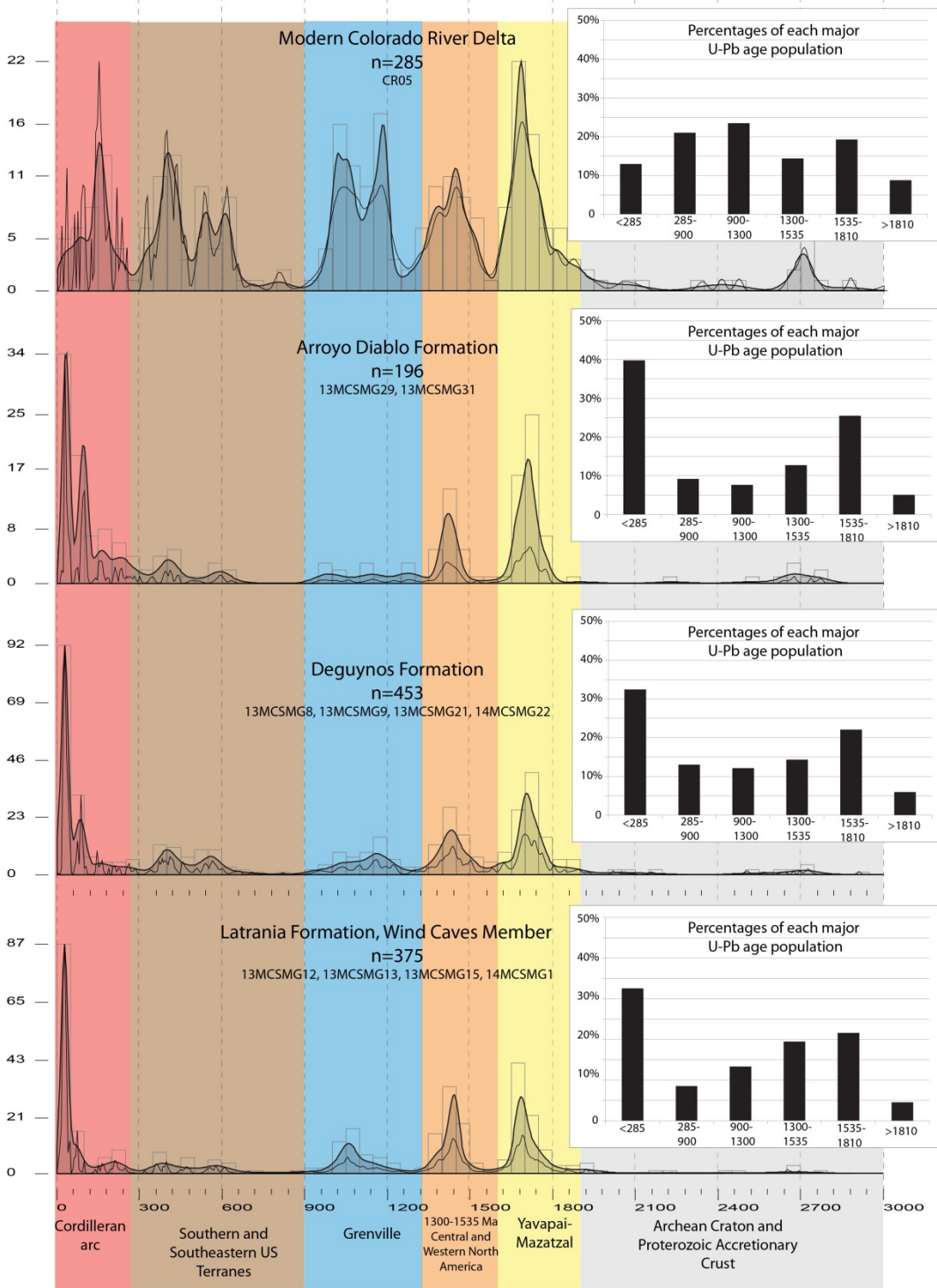


Figure 2-10. U-Pb age distributions of C-Suite (Colorado River-sourced) samples.

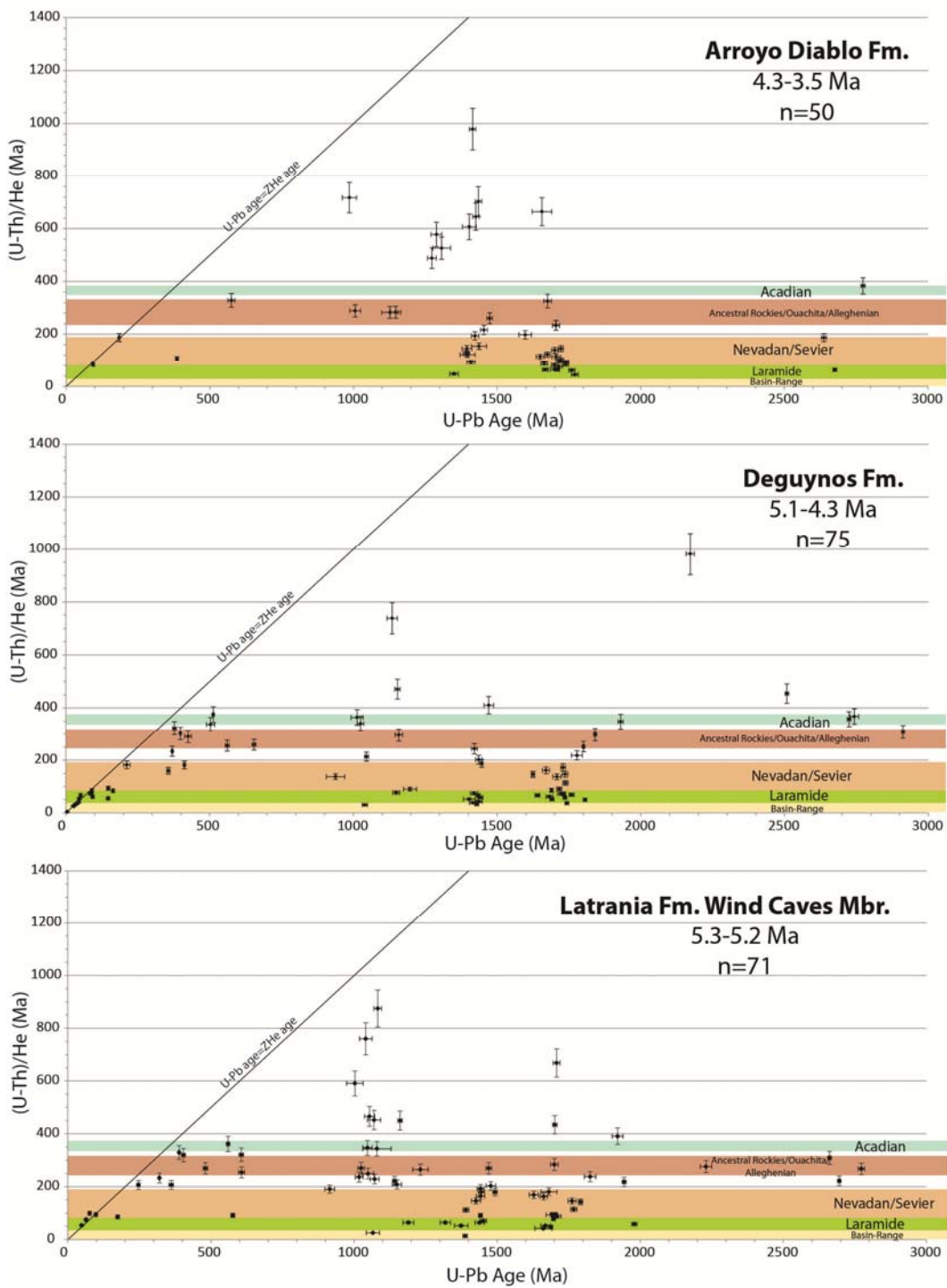


Figure 2-11. U-Pb and ZHe age plot of double-dated grains from Pliocene C-Suite samples.

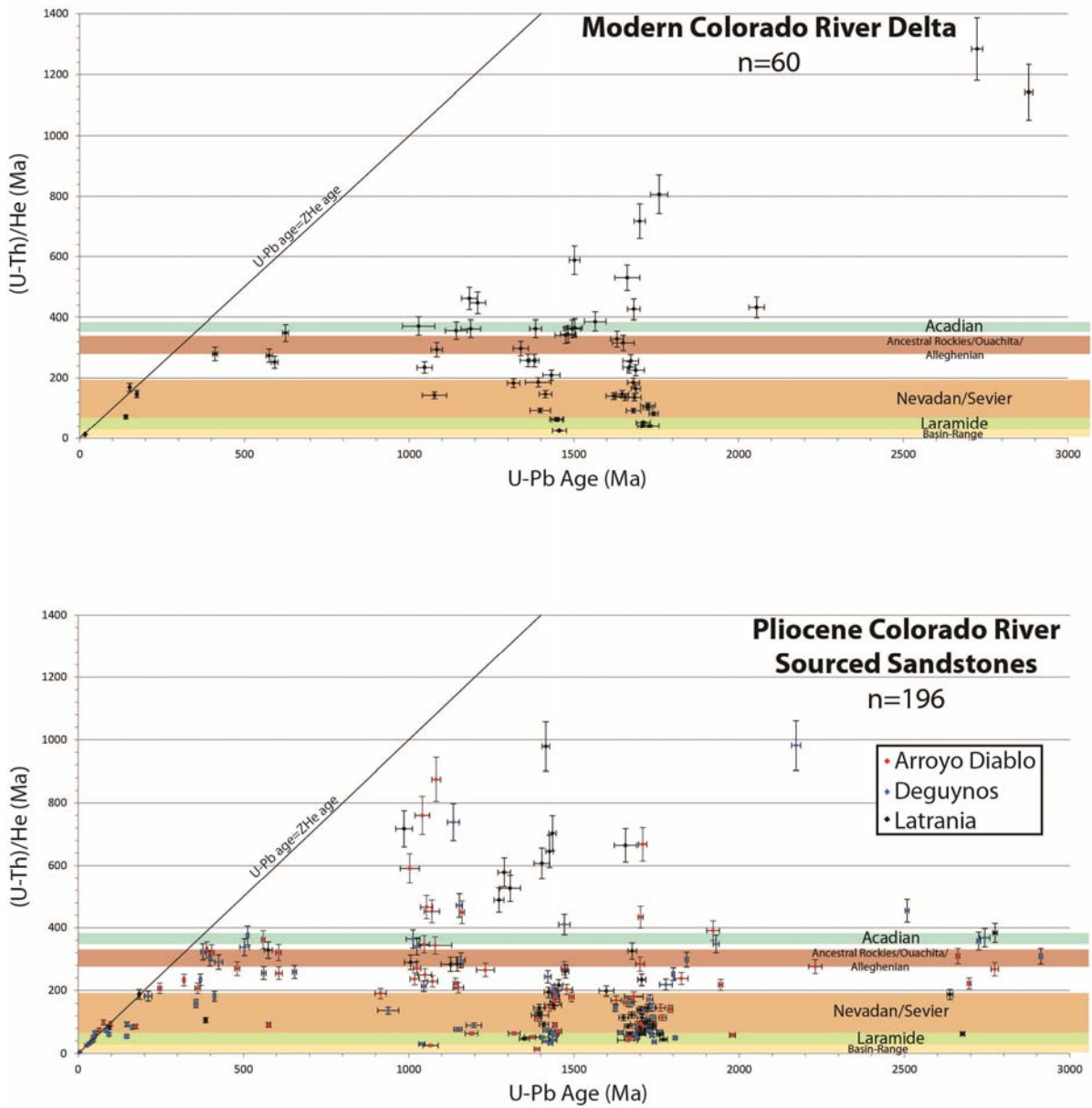


Figure 2-12. U-Pb and ZHe age plot of double-dated grains from Pliocene C-Suite samples (bottom) and grains from the modern Colorado River delta sample (top).

(U-Th)/He Age Distribution for 285-900 Ma U-Pb Population

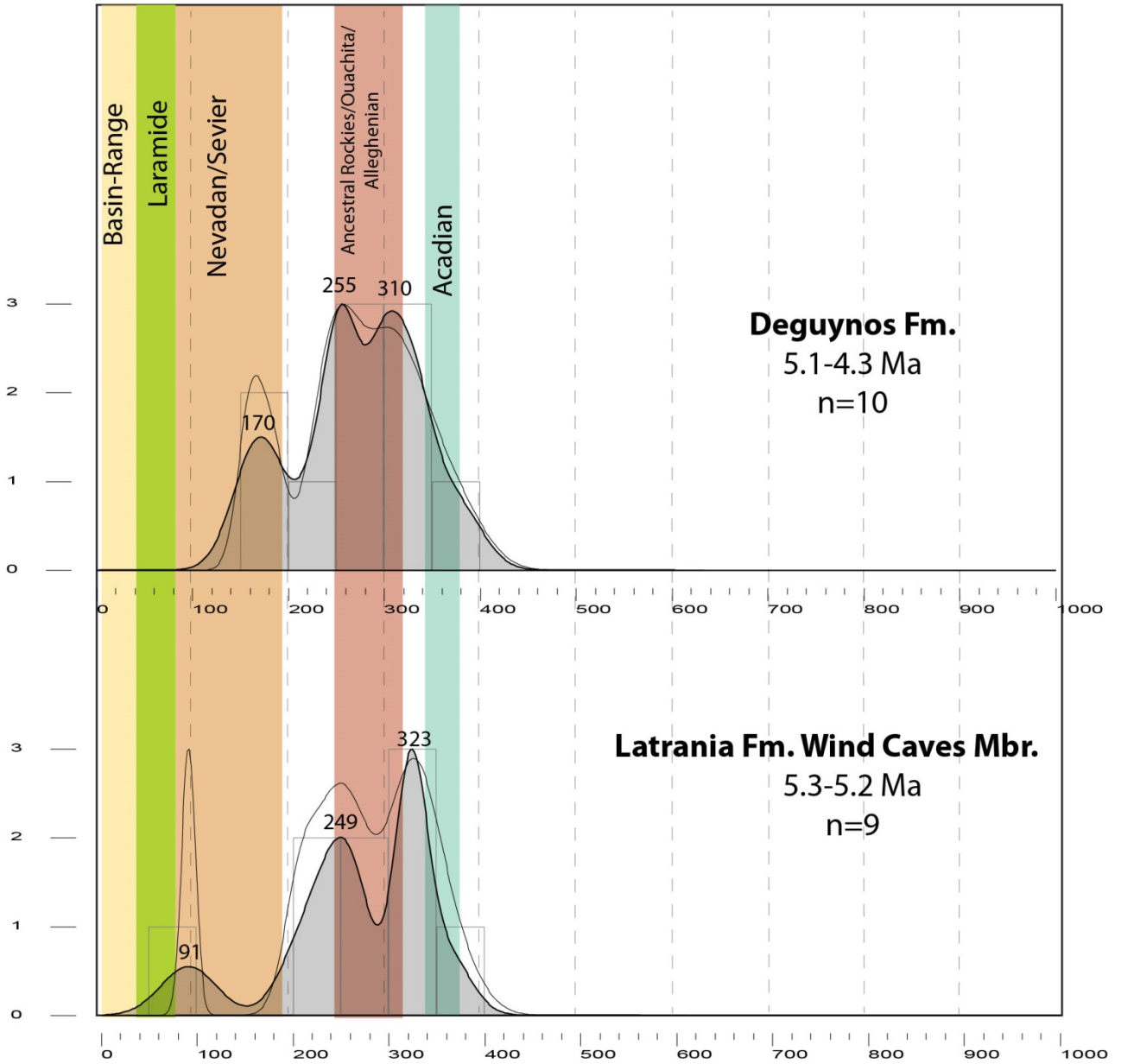


Figure 2-13. ZHe ages for the 285-900 Ma U-Pb age population for samples from the Latrania and Deguynos formations.

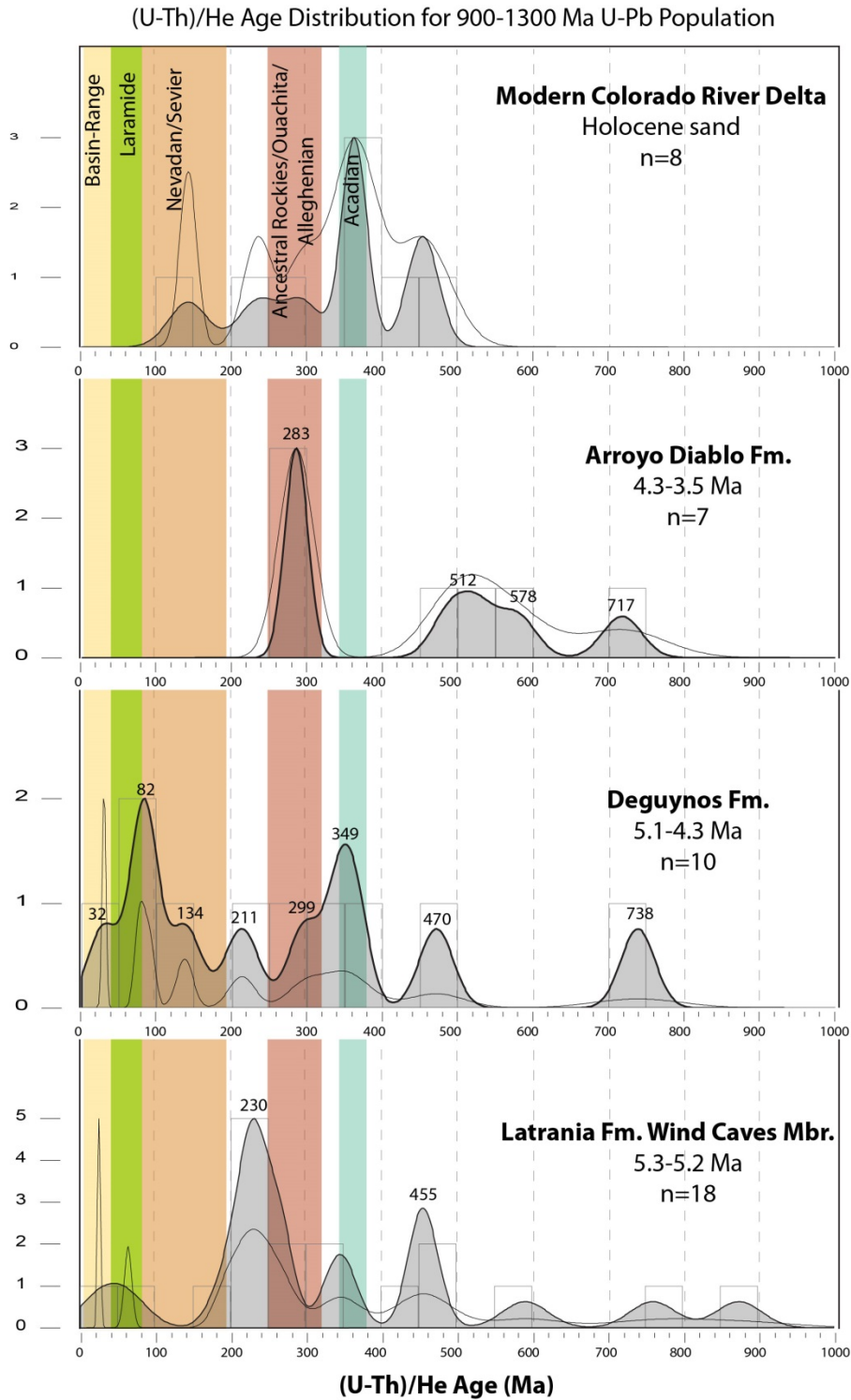


Figure 2-14. ZHe ages for the 900-1300 Ma U-Pb age population by formation.

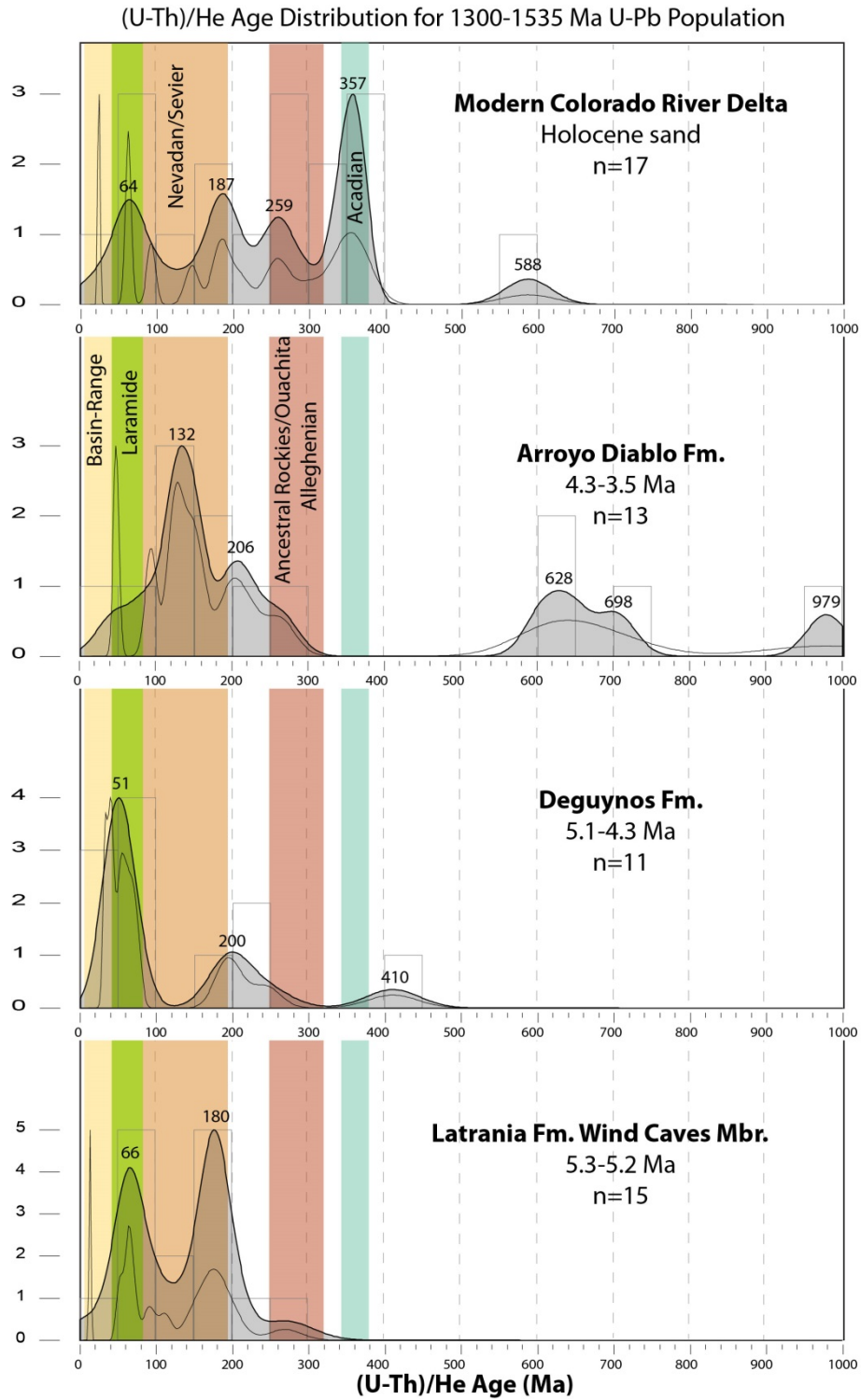


Figure 2-15. ZHe ages for the 1300-1535 Ma U-Pb age population by formation.

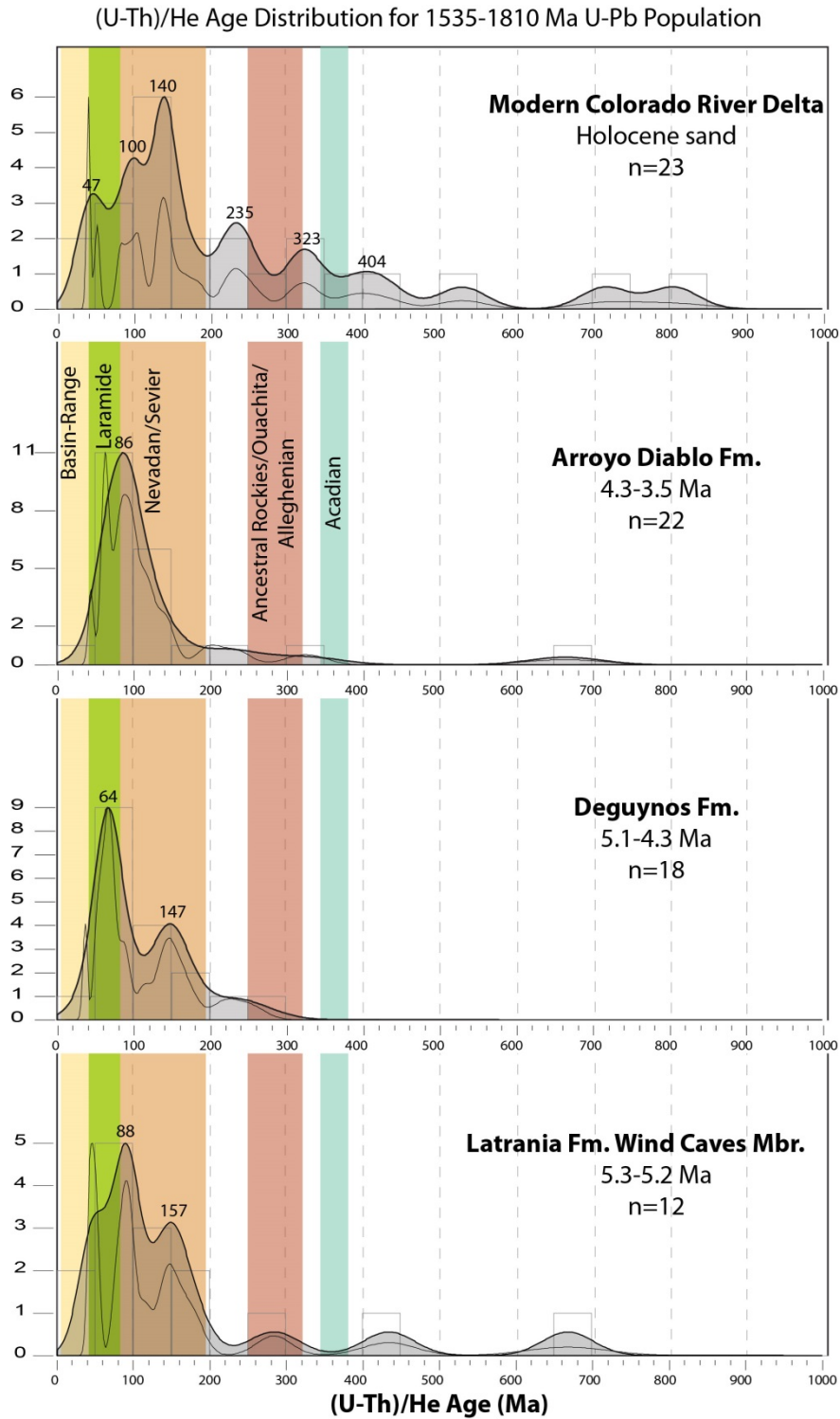


Figure 2-16. ZHe ages for the 1535-1810 Ma U-Pb age population by formation.

(U-Th)/He Age Distribution for >1810 Ma U-Pb Population

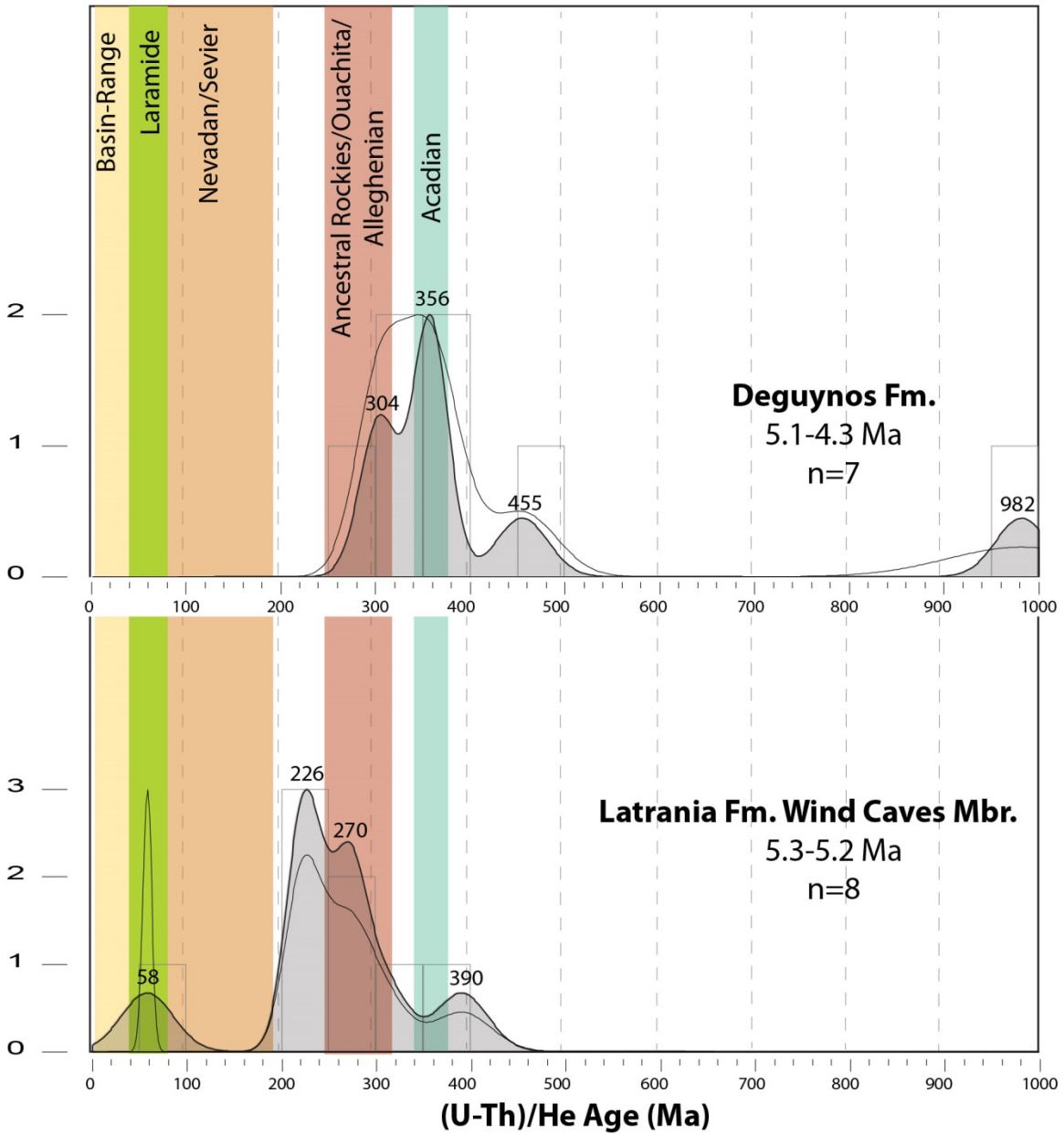


Figure 2-17. ZHe ages for the >1810 Ma U-Pb age population for the Latrania and Deguynos Formations.

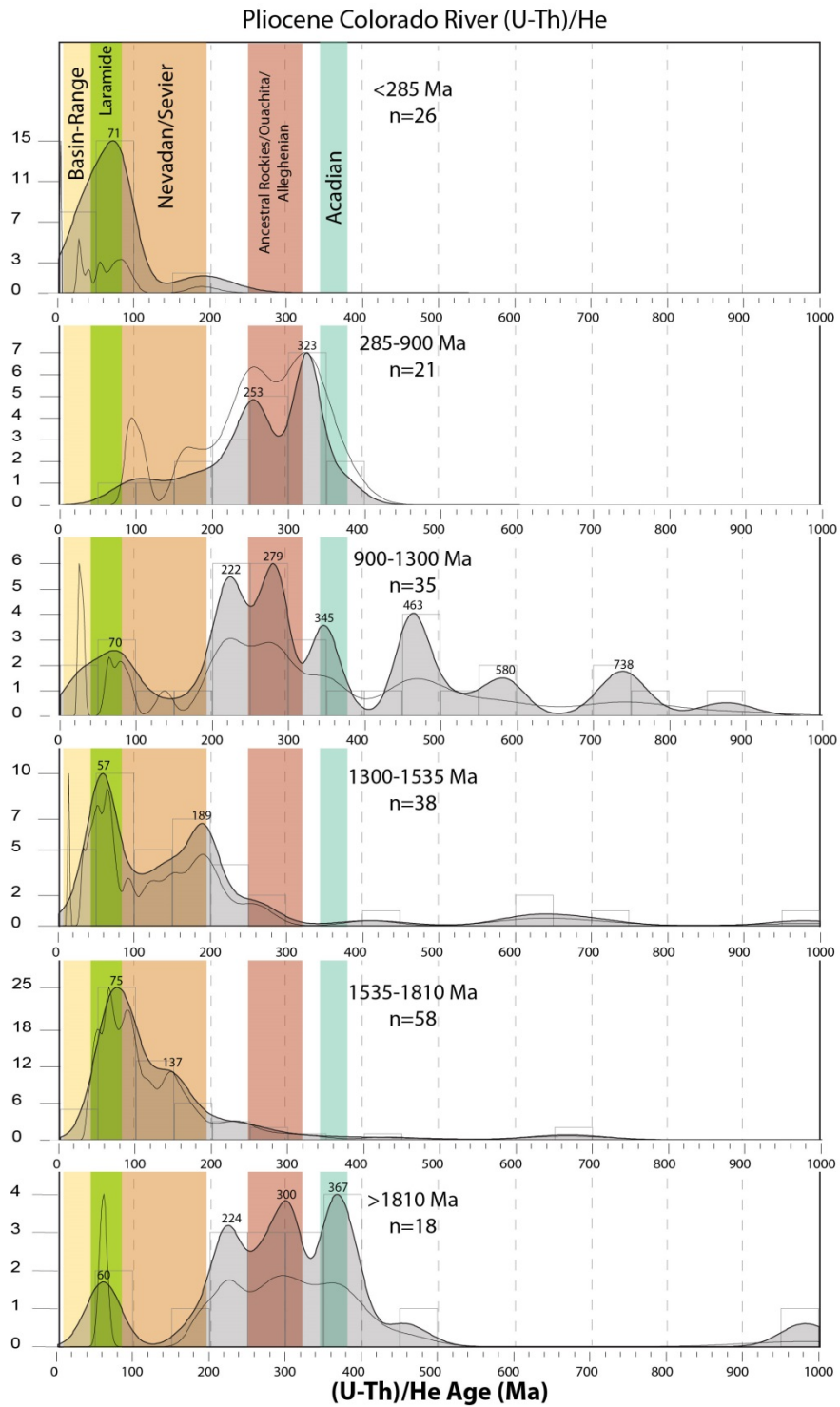


Figure 2-18. ZHe for each U-Pb age population from combined Pliocene samples.

Crystalline Sources for Pliocene Colorado River-Sourced Detrital Zircon

Provenance interpretations are made based on U-Pb ages of zircon grains compared to crystalline provinces of known age in southern North America as defined by Gehrels and Pecha (2014). The crystalline provinces are shown in Figure 2-19. U-Pb and (U-Th)/He double-dated grains can show when peak exhumation of these age provinces occurred and can be matched to potential source terranes with known exhumation histories (Rahl, 2003). Zircon deposited by the Colorado River into the Fish Creek-Vallecito Basin during the Pliocene were predominately eroded from basement uplifts of the Rocky Mountains and stratigraphy present on the Colorado Plateau which had been deposited from the latest Precambrian through the Phanerozoic. The resulting U-Pb and (U-Th)/He age spectrum reflects a broad array of potential source terranes throughout the North American continent.

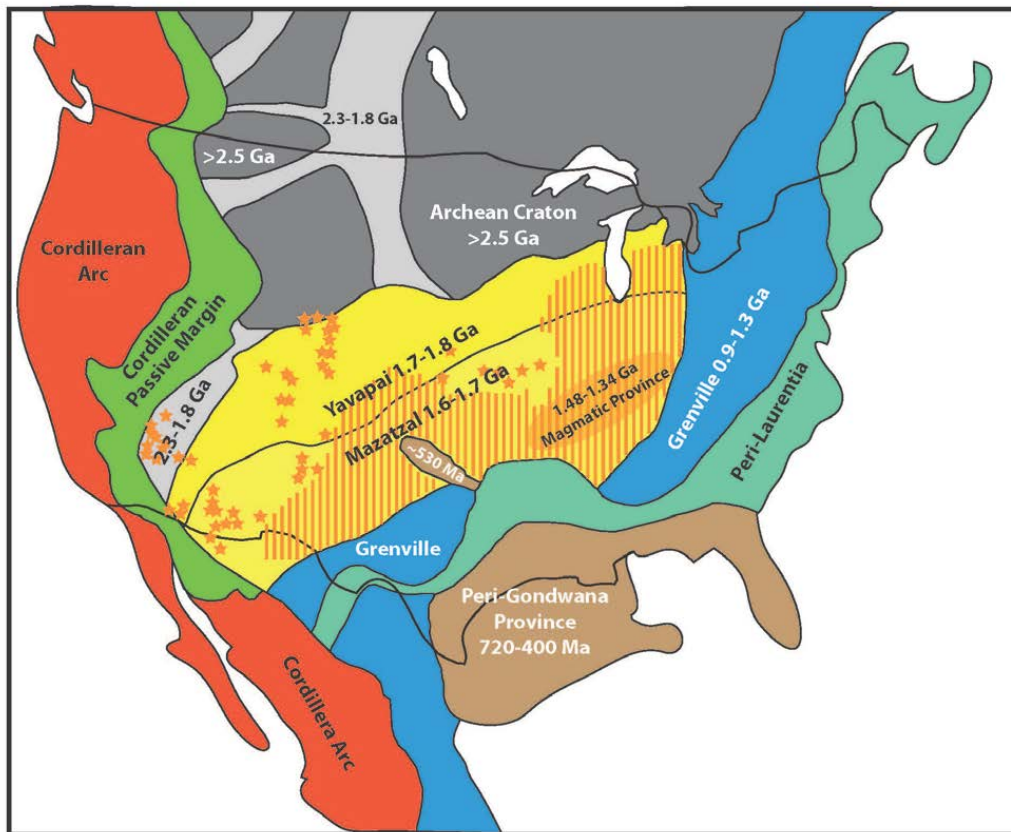


Figure 2-19. Map showing major crystalline provinces in southern North America from which zircon are primarily derived from. (Modified from Gehrels and Pecha, 2014).

As mentioned before, zircon U-Pb ages can be grouped into six categories: 1) >1810 Ma, 2) 1535-1810 Ma, 3) 1300-1535 Ma, 4) 900-1300 Ma, 5) 285-900 Ma, and 6) <285 Ma. For Pliocene samples from the Fish Creek-Vallecito Basin each of these age populations also have corresponding peak (U-Th)/He ages which are 1) 224 Ma, 300 Ma, and 367 Ma, 2) 75 Ma, 3) 57 Ma and 189 Ma, 4) 70 Ma, 222 Ma, and 279 Ma, and 463 Ma, 5) 253 Ma and 353 Ma, and 6) 71 Ma (most likely lower due to high amount of grains <50 Ma which were not double-dated). The following is a summary of crystalline sources for zircon from Pliocene stratigraphy in the Fish Creek-Vallecito Basin based on U-Pb age with the tectonic event which lead to exhumation, inferred from the (U-Th)/He (ZHe) age. This is schematically shown in Figure 2-20.

Crust older than 1810 Ma is made up of the Archean Wyoming, Superior and Proterozoic crustal accretion around Archean crust. A single ZHe age peak at 297 Ma suggests that peak exhumation of this terrane occurred during either the 320-270 Ma Ancestral Rockies Orogeny in the west or Alleghenian orogeny in the east. Due to the western location of the bulk of >1810 Ma crust it is most likely that zircon with U-Pb ages >1810 were exhumed during the Ancestral Rockies Orogeny (Kluth, 1981).

Crust formed between 1535-1810 Ma consists predominately of the 1800-1700 Ma Yavapai and 1700-1600 Ma Mazatzal province which makes up a large amount of North American mid-continent crust. ZHe ages associated with Yavapai-Mazatzal have a

single peak age of 76 Ma suggesting peak exhumation during early Laramide orogenesis (Dickinson, 2004).

1300-1535 Ma crust is commonly found within the 1.48-1.34 Ma Granite-Rhyolite Province of the Central and Western US. Crust of this age has peak ZHe ages of 55 Ma, 182 Ma and subordinate peak age at 643 Ma. This suggests peak exhumation during Laramide and possible early Nevadan orogenesis.

900-1300 Ma crust is found within the Grenville Province of eastern and southern North America. Peak associated ZHe ages are 65 Ma and 469 Ma with a dominant peak at 278 Ma. This suggests peak exhumation during Alleghenian orogenesis (Rast, 1989).

285-900 Ma crust is found in Eastern and southeastern North America. ZHe age peaks occur at 260 Ma and 317 Ma suggesting peak exhumation during Acadian and Alleghenian orogenesis (Rast, 1989).

<125 Ma grains make up 28-30% of grains in these samples with a major peak at 28 Ma for the Wind Caves Member and 33 Ma for the Arroyo Diablo Formation. Four grains with U-Pb ages from 25.9-41.8 Ma had ZHe ages within error of U-Pb age. These ages are correlative with the 40-23 Ma ignimbrite flare up.

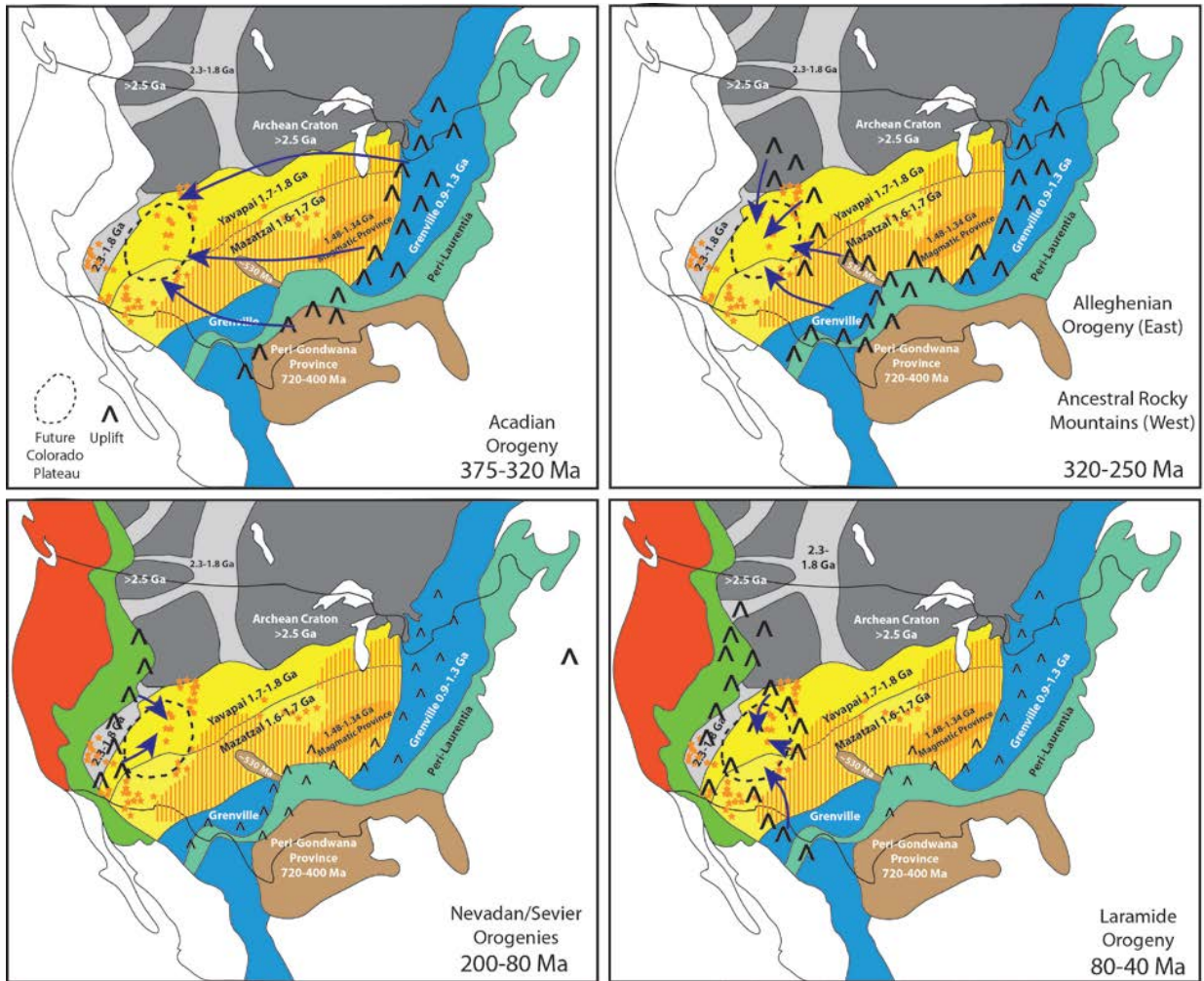


Figure 2-20. Timing of sediment sourcing from crystalline provinces based on crystallization and cooling histories of individual detrital zircon grains.

Pre-Colorado River Sediment Provenance

Pre-Colorado River sedimentation consisting of alluvial fans, subaqueous sediment gravity flows, and megabreccias is preserved within the 8.0-6.2 Ma Elephant Trees Formation and the Latrania Formation's Lycium Member. The sandstone samples taken from these units have between 85 and 95% of U-Pb ages falling between 70 and

125 Ma indicating a source area within the 80-140 Ma Peninsular Range Batholith (PRB) (Silver, 1998). Tonalites of the PRB make up the basement of the Fish Creek-Vallecito Basin and surrounding highlands. ZHe ages for the Elephant Trees Formation and Lycium Member (n=19) range from 86-40 Ma with a peak ZHe age of 60 Ma. This matches closely with PRB samples taken from just north of the area which have ZHe ages ranging from 79.9-34 Ma (Shirvell et al., 2009). These cooling ages likely correspond to Late Cretaceous to Early Tertiary unroofing related to flat-slab subduction while Eocene to early Oligocene cooling is related to late Laramide deformation (Dumitru, 1990; Grove et al., 2003; Axen et al. 2000). These sands were very likely sourced from nearby basement and transported by local streams based on the strong correlation between detrital zircon U-Pb and (U-Th)/He ages to crystallization and thermal history of the PRB.

Pliocene Integration of the Colorado River Into the Gulf of California

In the field, the first Colorado River-sourced sediment is marked by an abrupt transition from coarse grained, biotite rich sandstone to fine to medium grained sandstone lacking biotite. These two types of sandstones have been referred to as C-Suite for Colorado River deposited sandstones and L-Suite for sandstones deposited by local fluvial systems (Winker, 1987). In outcrop, the first C-Suite sandstone appears above a one to tens of meter thick silty mudstone interval which was correlative throughout the Wind Caves Member. Samples 14MCSMG3 and 14MCSMG1 were taken below and above this interval in a location where it was ~1 m thick. 51/53 grains analyzed for U-Pb

age from sample 14MCSMG3 were Cretaceous with the youngest grain at 80.4 ± 2.4 Ma. This age distribution was very similar to ages from samples taken from the Lycium Member of the Latrania Formation indicating that these two sandstone units have the same sediment source. Sample 14 MCSMG1 had 52 grains analyzed resulting in a Miocene to Archean age spread. Measured sections taken throughout the Wind Caves Member show that L-Suite sandstone beds become rare after appearance of the first C-Suite sandstone bed and are only seen as discrete beds within heterolithic sandstone and silty mudstone units. These units are interpreted as areas off axis of channels and lobes depositing C-Suite sandstone.

Evolution of Detrital Zircon U-Pb and (U-Th)/He Ages

Pliocene Colorado River sourced sandstones in the Fish Creek-Vallecito Basin have a fairly consistent U-Pb age signature throughout the ~5.3-3.5 Ma progradational sequence exposed. The main trends heading stratigraphically higher in the Pliocene section include slight increases in percentages of grains in 1535-1810 Ma and 125-285 Ma U-Pb age populations and a decrease in the 900-1300 Ma population. While U-Pb age evolution is subtle, ZHe age evolution of grains within the 900-1300 Ma, 1300-1535 Ma, and 1535-1810 Ma populations is more pronounced, generally showing older ZHe ages associated with U-Pb age populations going up section. This is true for the 1300-1535 Ma U-Pb population where the highest peak is Laramide in age and increases to pre-Laramide in Arroyo Diablo Formation samples. The 1300-1535 Ma U-Pb age population also features a wider range of ZHe grain ages upsection while the age range for the 1535-

1810 Ma population decreases upsection. For the 900-1300 Ma U-Pb population ZHe ages have a cluster around Acadian and Alleghenian ages, with youngest grain ages (Laramide, Basin and Range) within the Wind Caves Member and Deguynos Formation.

The U-Pb age spectra for Modern Colorado River deposits differs from the Pliocene by the vast decrease in <125 Ma grains (30-40% in Pliocene, ~5% in modern) and increase in 285-1300 Ma grains (~17-25% in Pliocene, ~45% in modern). Changes in other U-Pb age populations are subtle. ZHe ages for 1300-1535 and 1535-1810 Ma U-Pb populations in the modern sample show a wider spread of ages than those in the Pliocene, with highest peak ages older than Laramide.

Maximum Depositional Ages

Timing for integration of the Colorado River into the Gulf of California has been precisely dated at 5.33 Ma through magnetostratigraphy (Dorsey, 2007; 2011). For detrital zircon U-Pb age distributions the youngest zircon in a population can be used to infer maximum depositional age. In this study, stratigraphic ages have been previously well constrained and youngest U-Pb age can be used to test these age constraints. This study analyzed four grains from the Wind Caves Member with U-Pb ages <5.33 Ma with a nearly concordant grain within the Colorado River-deposited Wind Caves Member dated at 4.6 ± 0.1 Ma. Within the 5.2-4.3 Ma Deguynos Formation a concordant 3.84 ± 0.31 Ma grain was found in a sample from the rhythmite portion of the section. These data suggest that stratigraphic ages might be younger than previously reported. However, these ages also fit better with Alternative correlation-2 of Dorsey et al. (2011).

DISCUSSION

Implications for Colorado River Evolution

Pliocene sediment of Colorado River origin deposited in the Fish Creek-Vallecito Basin contain abundant zircon with U-Pb ages of 1300-1810 Ma indicating derivation from western US basement consisting of 1300-1500 Ma anorogenic igneous provinces and 1600-1800 Ma Yavapai-Mazatzal province (Dickinson and Gehrels, 2010). Samples from the Latrania Formation (Wind Caves Member), Deguynos Formation, and Arroyo Diablo Formation contain 30%, 53%, and 27% Laramide (40-80 Ma) ZHe ages within the 1300-1810 Ma U-Pb population. Combination of crystallization and cooling ages (to ~180 C) suggest sourcing of sediment from basement-cored uplifts on the northern and eastern margins of the Colorado River drainage area. Zircon with Oligocene U-Pb ages also make up a notable portion (~14-18%) and are derived from volcanic centers flanking the Colorado River drainage area. This suggests a drainage extent with similar northern and eastern reaches as that of the modern Colorado River.

Laramide basement uplift-derived zircon found within the first Colorado River-sourced deposits in the Fish Creek-Vallecito Basin suggest connection between the Gulf of California and Rocky Mountains via the Colorado River at 5.3 Ma. This contrasts with Lucchitta's (1972, 1989) conclusion that an upper Colorado River, which had become a mostly integrated system in the Miocene, was later captured by a headward-eroding river which cut across the Kaibab uplift and captured the upper drainage. Rather, this is more consistent with top-down river integration in which a filling and successive spilling of

the Colorado River into lower basins expanded the river system downstream (Meek and Douglass, 2001). Pre-Colorado River detrital zircon ages in the Fish Creek-Vallecito Basin also do not support headward erosion having caused capture of the upper Colorado River as U-Pb and ZHe ages of pre-Colorado River sourced sediment are consistent with derivation from the Peninsular Range Batholith rather than lithologies on or near the Colorado Plateau. Evolution of the Colorado River from Pliocene to recent is schematically shown in Figure 2-21.

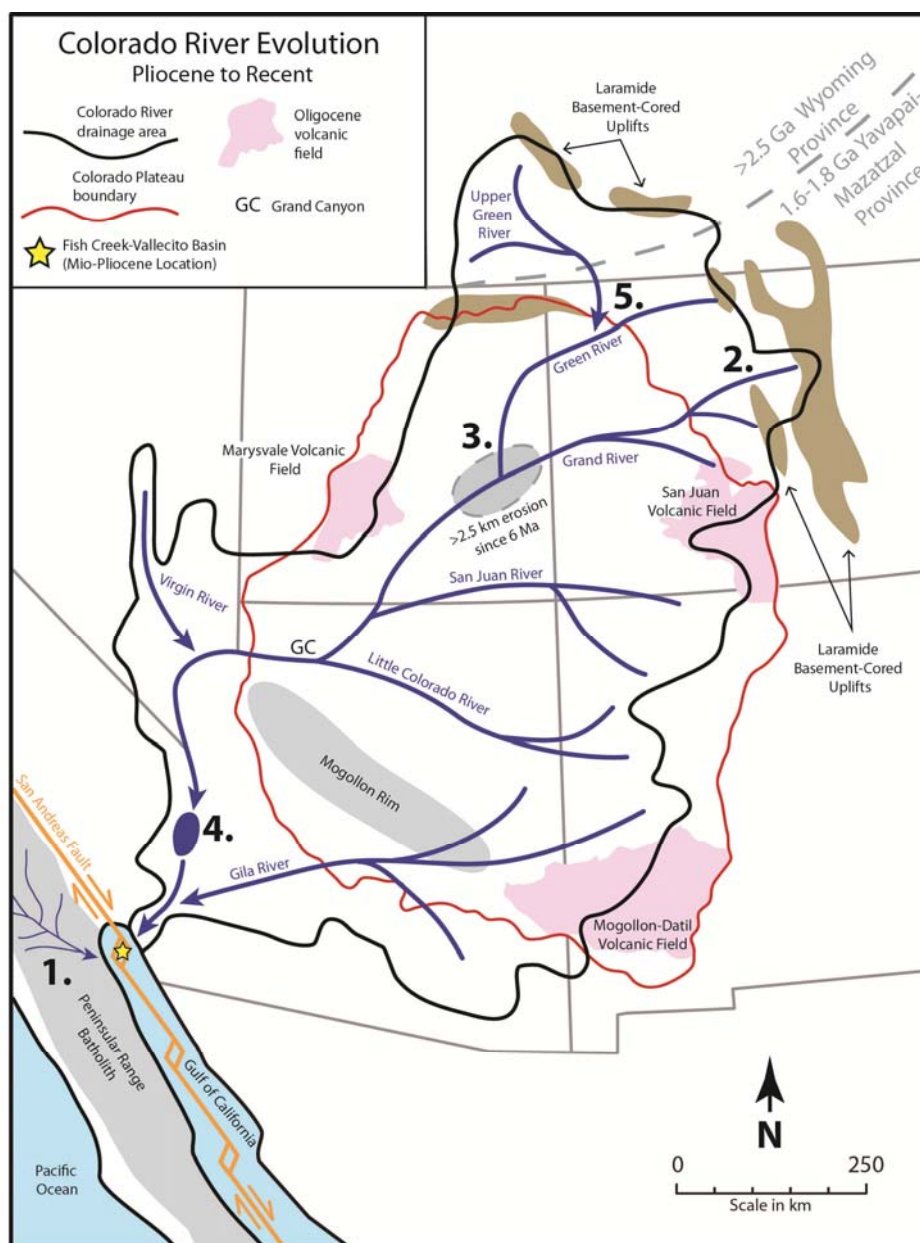


Figure 2-21. Model for Colorado River evolution based on detrital zircon U-Pb and ZHe results from this study. Model shows 1) Late Miocene local drainage sourcing sediment from the Peninsular Range Batholith prior to Colorado River integration. 2) Combination of 1300-1810 Ma grains with Laramide ZHe ages indicated grains were exhumed during Laramide orogenesis from western US bedrock giving solid evidence of Colorado River drainage extending to the Rocky Mountains at the onset of deposition into the Gulf of California. 3) River flow coming off of Laramide uplifts in Pliocene lead to

deep erosion of sedimentary stratigraphy since latest Miocene. Erosion into Mesozoic and Paleozoic stratigraphy rich in 285-1300 Ma U-Pb age grains explains why this population makes up a high percentage of grains in a sample from the modern Colorado River delta. 4) River flow was ponded in successively lower basins which became overfilled and spilled toward the Gulf. Little evolution in U-Pb age signal just prior to Colorado River deposition into Gulf and evidence of sourcing from Laramide uplifts suggests a well-integrated Colorado River initially deposited into Gulf of California. 5) Increase in Archean U-Pb age grains throughout Pliocene and a Laramide ZHe age associated with the population from an Arroyo Diablo Fm. sample suggest that the upper Green River began integrated into the Colorado River system after initial deposition into the Gulf.

Changes in Colorado River sediment sourcing are interpreted from slight variations in relative proportions of detrital zircon U-Pb age populations, with primary differences being a relative increase in 1535-1810 Ma grains, and relative decreases in the 900-1300 Ma and 1300-1535 Ma age populations. The large amount of 1535-1810 Ma grains in younger Pliocene units is also seen in Paleocene-Eocene stratigraphy on the Colorado Plateau from previous studies by Dickinson and Gehrels (2010) and Gehrels et al. (2011). The high proportion of 1535-1810 Ma grains in early Cenozoic Colorado Plateau stratigraphy were likely shed from Laramide uplifts into adjacent basins. The increased amounts of 1535-1810 Ma U-Pb ages and association with Laramide ZHe going up section in the Pliocene stratigraphy suggest possible increased erosion in northern portions of the Colorado River drainage area where the Colorado River taps into Laramide uplifts and Cenozoic stratigraphy deposited from sediment derived during early phases of Laramide orogenesis.

Contributions of sediment from Archean crust, likely the Wyoming Craton, increase in the Pliocene as seen by >2500 Ma U-Pb ages increases from 1% in the Wind Caves Member to 4% in the Arroyo Diablo Formation. This small increase could be evidence of capture of the Green River sometime after Wind Caves but before Arroyo Diablo deposition. Out of four double-dated Archean grains from the Arroyo Diablo Formation, one yielded a Laramide ZHe (62.7 ± 5.0 Ma) indicating possible derivation from a Laramide basement uplift within the catchment of the upper Green River. This suggests that some or all of the Green River may not have been integrated into the Colorado River system until later in the Pliocene. Prior to integration, the Green River above the Uinta Uplift may have flowed into lakes just north of the Colorado Plateau. A possible scenario is that the Green River south of the Uinta Uplift became integrated to the Colorado River system during either the late Miocene-early Pliocene with capture of the upper Green River having occurred later in the Pliocene.

The large increase in 285-1300 Ma U-Pb age grains in the modern Colorado River sample compared to the Pliocene sample are indicative of sediment recycling from stratigraphic units on the Colorado Plateau. 285-1300 Ma grains do not commonly have ZHe ages <200 Ma, indicating little exhumation during western US tectonic events since the beginning of the Mesozoic. Rather, ZHe ages fit better with primarily Appalachian orogeny exhumation, as was previously recognized by Rahl (2003) in which samples taken from the Navajo Sandstone had U-Pb ages of 550-600 Ma and 950-1200 Ma had ZHe ages of 225-500 Ma. Dickinson and Gehrels (2003) also concluded an Appalachian

source for 310-1315 Ma U-Pb age zircon and proposed a western directed fluvial and eolian cross continent course for sediment eroded from the Appalachian orogenic belt.

Comparison to Other Studies and Utility of Double-Dating

Detrital zircon U-Pb data compiled from Dickinson and Gehrels (2010) and Gehrels et al. (2011) of Early Paleozoic through Eocene stratigraphy on the Colorado Plateau shows evolution of the U-Pb age signature through time. Age distributions for this dataset are shown in Figure 2-21 and summarized in Table 2-1. 1300-1810 Ma grains were dominant U-Pb age peaks in Early Paleozoic and Paleocene to Eocene stratigraphy. Throughout the Late Paleozoic to Late Cretaceous 900-1300 Ma grains make up a significant portion of U-Pb ages with an increase in 1535-1810 Ma zircon in the Late Jurassic through Cretaceous. Increased erosion of Mesozoic and Paleozoic stratigraphy since the Pliocene would yield higher abundances of 285-1300 Ma grains. AHe data from Hoffman (2009) show erosion of up to 3 km of stratigraphy having occurred since 6 Ma in the Canyonlands region of the central Colorado Plateau. This age of erosion is nearly coincident with the 5.3 Ma age which Dorsey et al. (2011) reported for introduction of Colorado River sourced sediment into the Gulf of California. This deep erosion likely stripped away much of the Cenozoic and late Mesozoic stratigraphy from the Colorado Plateau. Mesozoic and Paleozoic stratigraphy is presently exposed in this area which

provides a rich source of 285-1300 Ma grains for the modern Colorado River.

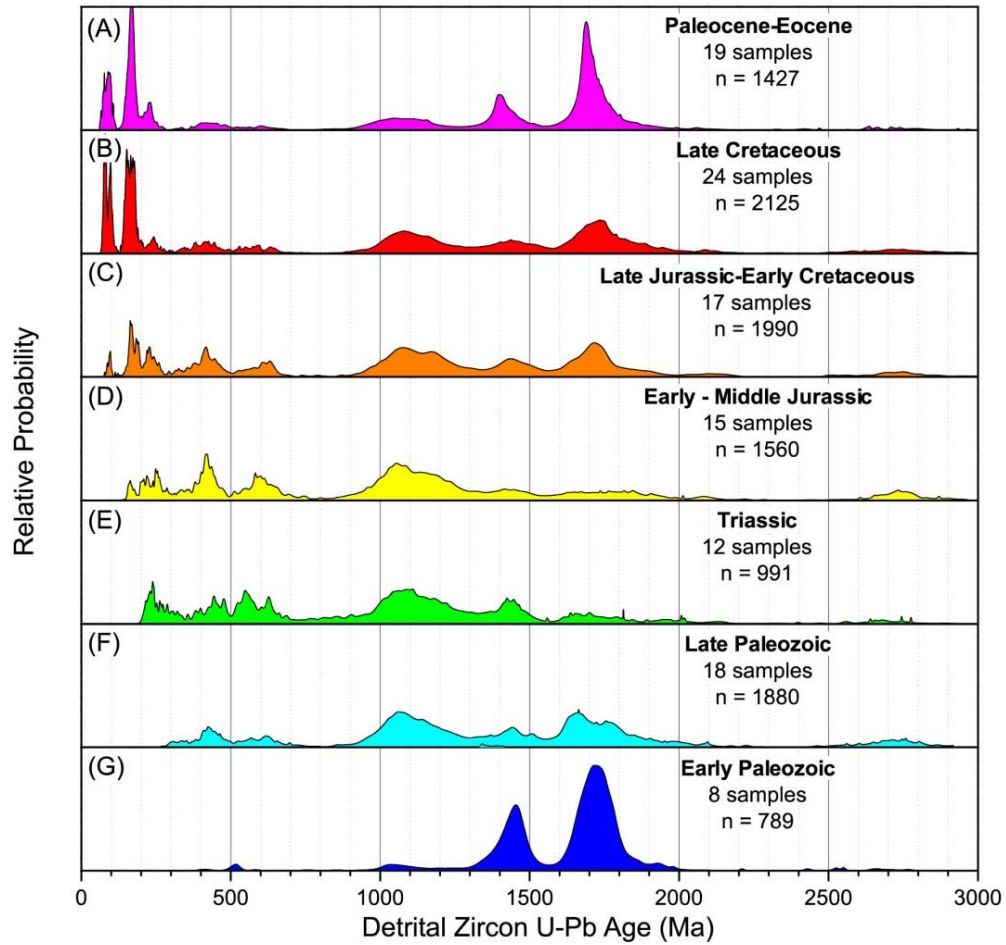


Figure 2-22. Detrital zircon U-Pb age distributions from Early Paleozoic to Eocene stratigraphic units on the Colorado Plateau. (From Dickinson and Gehrels, 2010; and Gehrels et al., 2011 as modified by Kimbrough et al., 2014)

Detrital Zircon Age Distributions of Colorado Plateau Strata (Dickinson and Gehrels, 2010; Gehrels et al., 2011)							Pliocene-Modern Colorado River				
Age Bin (Ma)	Lower Paleozoic Strata (n=789)	Upper Paleozoic Strata (n=1880)	Triassic Strata (n=1091)	Lower – Middle Jurassic Strata (n=1374)	Upper Jurassic-L. Cretaceo	Upper Cretaceous Strata (n=2125)	Early Cenozoic Strata (n=1427)	Latrania Fm. Wind Caves Member (n=375)	Deguynos Fm. (n=453)	Arroyo Diablo Formation (n=196)	Modern Colorado River Delta (n=285)
3-23 (%)	-	-	-	-	-	-	-	5.1	4.2	1.0	0.7
23-40 (%)	-	-	-	-	-	-	0.0	17.3	14.3	13.8	1.1
40-85 (%)	-	-	-	-	-	5.2	2.9	4.5	4.9	4.1	1.1
85-125 (%)	-	-	-	-	0.0	5.5	4.6	1.1	4.4	11.2	2.1
125-200 (%)	-	-	-	2.0	6.6	15.5	14.7	1.9	2.2	4.6	6.3
200-285 (%)	-	0.1	8.9	8.8	4.9	2.8	4.1	2.7	2.2	5.1	1.8
285-510 (%)	0.6	8.2	11.7	13.1	12.8	5.2	3.4	4.8	7.7	6.1	11.9
510-725 (%)	0.8	5.4	13.2	10.5	8.1	3.6	1.8	3.2	5.3	3.1	8.4
725-900 (%)	0.3	0.7	2.3	1.6	1.2	0.2	0.4	0.5	0.2	0.0	0.7
900-1300 (%)	4.6	32.1	28.3	35.7	32.5	19.9	11.9	13.3	12.1	7.7	23.5
1200-1535	28.0	12.4	15.3	7.6	11.3	9.5	13.7	19.5	14.1	12.8	14.4
1535-1810	57.7	24.7	10.2	8.1	10.7	20.0	35.4	21.6	22.1	25.5	19.3
1810-2015	6.1	6.6	3.2	4.2	4.3	6.1	3.7	2.4	2.2	0.5	3.2
>2015 Ma (%)	2.0	9.7	6.9	8.4	7.7	6.5	3.5	2.1	4.0	4.6	5.6

Table 2-1. Percentages of detrital zircon grains from each U-Pb population from early Paleozoic-Eocene stratigraphic units on the Colorado plateau from (Dickinson and Gehrels, 2010; and Gehrels et al. 2011) compared to ages obtained from Pliocene and recent Colorado River-sourced samples analyzed in this study.

ZHe data from Hoffman (2009, unpublished) of Permian through Jurassic stratigraphy from the Canyonlands (shown in Figure 2-23) allow for a comparison of detrital ZHe ages with depositional age. All samples show a several hundred million year spread of ZHe ages with the youngest age generally being near age of deposition. This high age spread was also seen in Pliocene and recent Colorado River-sourced sediment (this study) and suggests that much of the sediment from Canyonlands stratigraphy was recycled. The very high ZHe age spread of zircon with >900 Ma U-Pb ages can be attributed to sourcing much sediment from sedimentary stratigraphy on the Colorado Plateau.

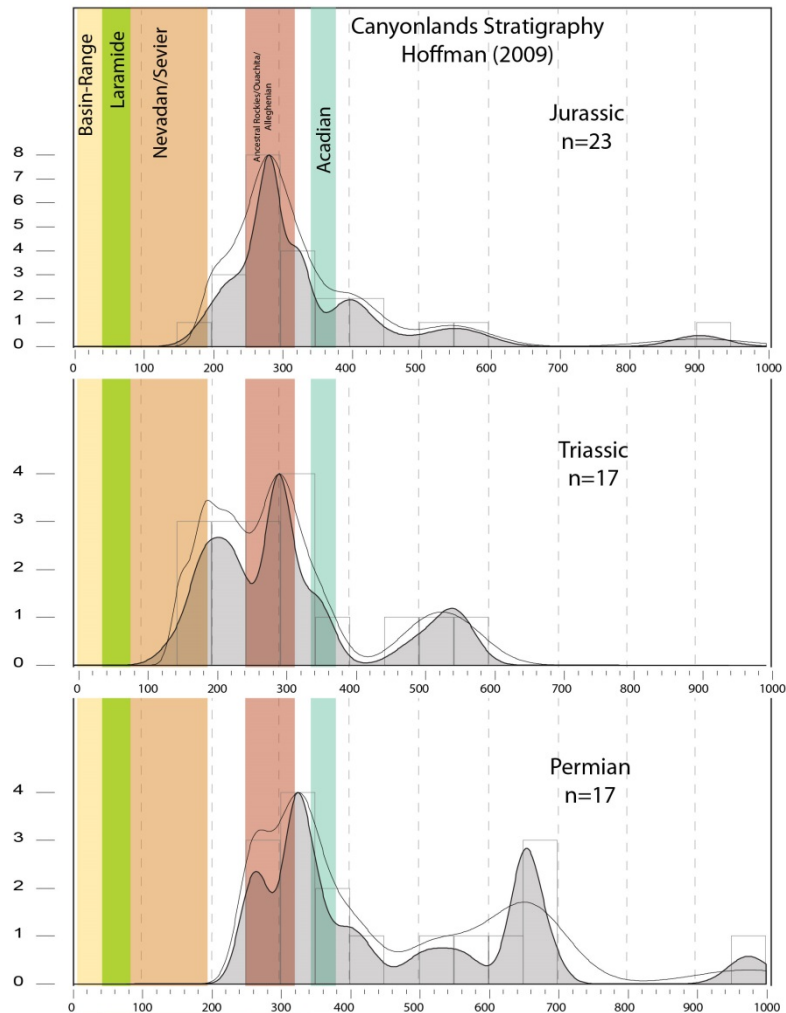


Figure 2-23. Detrital zircon ZHe age distributions of Permian-Jurassic units from the Canyonlands, Utah. (Hoffman, 2009 unpublished)

Campbell et al. (2005) noted the utility of U-Pb and ZHe double-dating in a detrital zircon study of Ganges and Indus River sediment. In that study, old ZHe ages relative to their respective U-Pb age indicated that 60% of Indus River and 70% of Ganges River zircon had been recycled. Only 18% of zircon from the Indus River and 2.5% from the Ganges could be linked to Himalayan sources through U-Pb dating as these grains had U-Pb ages younger than the onset of tectonism at 55 Ma. For this study,

detrital zircon U-Pb has been an efficient method for discriminating between local and regional sediment sourcing as early rift sediments show peak ages of 97 Ma, coincident with crystallization of the Peninsular Range Batholith which underlies and is exposed in much of southern California. The first Colorado River sediment has a notably increased age spread. However, this study, along with Kimbrough et al. (2011, 2014), has shown the Colorado River detrital zircon U-Pb age signature to be little evolved throughout Pliocene to recent Colorado River-sourced samples. However, detrital zircon U-Pb age distributions from the Colorado Plateau show zircon of Precambrian age can be found in stratigraphy of all ages. Due to the high amount of sedimentary stratigraphy, zircon of almost all U-Pb age populations can be found over most of the Colorado River drainage area. However, ZHe age is a powerful method to determine if sediment is coming from recent uplifts or recycled sediment. With the large amount of old ZHe ages in the study, along with AHe data from Hoffman (2009) suggesting sediments were never buried deep enough to reset ZHe age, these ages have the most utility for spatially resolving where sediment is coming from in large source areas where younger basement blocks are uplifted and exhumed through overlying sedimentary stratigraphy.

CONCLUSION

Detrital zircon U-Pb and (U-Th)/He double-dating more precisely resolves the provenance of sediment delivered by the Colorado River at the onset of deposition into the Gulf of California at 5.3 Ma and throughout the Pliocene. Prior to this study, evidence of sediment sourcing from the Rocky Mountains at the onset of Colorado River

deposition into the Gulf had not been demonstrated. Detrital zircon analyzed in this study with 1300-1810 Ma U-Pb ages and 40-80 Ma (U-Th)/He ages found within earliest Colorado River-sourced sediment imply derivation from basement-cored Laramide uplifts of the southern Rocky Mountains. These uplifts are currently the farthest northern and eastern extent of the Colorado River drainage and suggest the Pliocene Colorado River was similar in extent to the modern.

The steady U-Pb and ZHe signal of pre-Colorado River sediment, with consistent age peaks of 97 Ma and 60 Ma respectively, suggest sourcing from the Peninsular Range Batholith rather than from a headward-eroding river capturing an upper Colorado River drainage. Rather, the abrupt transition to a wide spectrum of U-Pb and ZHe ages within the first Colorado River sediment suggest rapid inundation by the Colorado River in the earliest Pliocene. This is consistent with a top-down river integration model which involved a well-integrated upper Colorado River system propagating downstream by filling and spilling lower basins until reaching the Gulf of California.

ZHe ages older than Laramide associated with the 1300-1810 Ma U-Pb age population suggest recycling of zircon from sedimentary stratigraphy on the Colorado Plateau previously sourced from uplifts related to Nevadan/Sevier and Ancestral Rockies tectonism. Zircon within the 900-1300 Ma U-Pb population commonly have ZHe ages between 250 and 400 Ma indicating exhumation during Appalachian orogenesis followed cross-continent fluvial and eolian sediment dispersal and later episodes of sediment recycling.

Modern Colorado River sediments contain greater amounts of zircon with 285-1300 Ma U-Pb ages and (U-Th)/He age clusters older than those for corresponding U-Pb age populations from Pliocene samples. This suggests that the modern system sources from predominately Mesozoic and older stratigraphy, which is consistent with deep erosion into Mesozoic and Paleozoic stratigraphy in the central Colorado Plateau since the Pliocene.

Abundances of grains with Archean U-Pb ages increase throughout the Pliocene indicating possible capture of the Green River occurring after initial Colorado River entrance into the Gulf. Further bolstering this conjecture is an Archean grain from the Arroyo Diablo Formation with a Laramide ZHe age, potentially indicative of direct sourcing from Laramide uplifts in the northernmost Colorado River drainage area which would be accessed by the upper Green River.

Zircon U-Pb and (U-Th)/He double-dating allows for improved provenance constraint when sourcing from geologically diverse terranes. ZHe can be used to obtain an exhumation age to 6 km depth, which is often synchronous with a tectonic event. U-Pb ages provide context for a ZHe age and can establish whether a grain is volcanic (U-Pb=ZHe), recycled from sedimentary stratigraphy, or from direct basement uplifts. Study of deposits from large river systems with little U-Pb age evolution through time can benefit significantly from double-dating as these large drainage areas often contain diverse thermal histories which can be elucidated through low-temperature thermochronometry of grains with known crystallization histories.

Chapter 3

Submarine Turbidite Fan Development in the Mio-Pliocene Gulf of California, Fish Creek-Vallecito Basin, Southern California

INTRODUCTION

Rift basins form in a variety of settings and the manner in which sedimentary sequences are deposited is quite variable. These rift basins are formed by extension of continental lithosphere through faulting and stretching creating depressions in which sediment accumulates (McKenzie, 1978, Ravnas and Steel, 1998). The depressions are often in the form of half-grabens in which sediment accumulates mainly on the hanging wall, though also with minor volumes derived from and banking against the footwall. The geometry and subsidence pattern of the rift as well as the volume and type of sediment supply influence the depositional style in which sediment ultimately accumulates. Study of siliciclastic stratigraphic packages deposited during rifting can yield clues as to the size, relief, and climate of the hinterland from which sediment is sourced as well as the rates of basin subsidence.

Large-scale stacking patterns of sediment infill into rift basin have been well studied, and show that sedimentary packages can accumulate in predictable manners based on subsidence rate and sediment supply (Ravnas and Steel, 1998). Study of the internal architecture of individual depositional units and the processes that form these in half graben basins demands more attention. Depositional complexity arises due to the dynamic morphology and environment in actively rifting basins. This complexity is a

result of basin floor topography, changes in sediment supply as drainages become captured, and active tectonism creating landscape instability. Outcrop study of stratigraphy in exhumed rift basins can reveal how depositional systems fill basins and how depositional style evolves through time in an active environment.

The Fish Creek-Vallecito Basin of southern California offers an excellent opportunity to study synrift deposition during Miocene-Pliocene opening of the Gulf of California (Winker, 1987; Winker and Kidwell, 1995; Dorsey et al. 2011). Lithologies exposed within the thick rift succession show a general grain-size trend of coarsening to fining to coarsening from 8.0 Ma to ~1.0 Ma as early rifting generated footwall uplifts that shed alluvial fans onto subsiding hanging walls. Marine flooding into the rift from the south (Pacific Ocean) ensued as the area was incorporated into the Gulf of California causing an abrupt deepening of the environment as evidenced by a transition from subaerial fan deposits to thick, deepwater subaqueous gravity flows. Periods of landscape instability are evidenced by basement derived boulders and mass-transport complexes inundating the marine environment from areas of high topography. At ~5.3 Ma capture of the Colorado River as an axial drainage marked the beginning of Colorado Delta progradation into the early Pliocene gulf.

This study focusses on the deposition of initial Colorado River-transported sediment deposited mainly as turbidites at ~5.3 Ma, known as the Wind Caves Member of the Latrania Formation. High-resolution facies analysis of these outcropping turbidites

allows an unravelling of the depositional architecture and basin paleogeography during early delta progradation by the Colorado River into the Gulf of California.

GEOLOGIC BACKGROUND

Tectonic Setting

The Fish Creek-Vallecito Basin exists as an exhumed Miocene through Pliocene depocenter within the broader Salton Trough region, a seismically active area currently and the furthest north extent of the Gulf Extensional Province (Gastil et al., 1975). The area of study consists of Mio-Pliocene sediment deposited by local systems during early rifting and later by the Pliocene Colorado River system. Basins in this region were generally created by local transtension due to transform motion between the Pacific and North American plates. These pull-apart basins are bounded by dextral strike-slip faults within the area. Basin depths found within these spreading centers are not as deep as within the Gulf of California itself, due rapid infill from both local and Colorado River fluvial input (Winker 1987). Since the initial basin filling during the late Miocene, the Fish Creek-Vallecito Basin has been uplifted and exhumed since ~1.0 Ma as transtension ceased in the Pleistocene followed by a period of wrench tectonism (Dorsey et al., 2012).

Previous studies have concluded that initial rifting in the Gulf Extensional Province occurred when subduction along southwestern Baja California ended at ~12 Ma (Shirvell et al. 2009). This extension was accommodated in the Salton Trough by the northeast dipping low-angle West Salton Detachment Fault (WSDF). This rift-related structure establishes the Western boundary of the Fish Creek-Vallecito Basin where the fault cuts the Peninsular Range Batholith. The Peninsular Range Batholith as well as the

Vallecito, Fish Creek, and Coyote Mountains created the basement margins of the study area as shown in Figure 3-1. This crystalline basement consists of granitic and metamorphic rock of Paleozoic and Mesozoic age. Middle to late Cretaceous magmatism resulting from subduction created much of this basement which originally formed as plutons intruding metamorphic and sedimentary rock. (DeCelles, 2004)

Since earliest onset of transtension in the study area at 8.0 ± 0.4 Ma, subsidence rates in the basin fluctuated until 0.95 Ma when the area began to uplift. Paleomagnetic data from Johnson (1983) and Dorsey (2011) suggests that the basin subsided at a rate of 0.46 mm/yr from 8.0 to 4.5 Ma, increasing to 2.1 mm/yr from 4.5 to 3.1 Ma from 4.5 to 3.1 Ma, and decreasing again to 0.40 mm/yr from 3.1 Ma prior to basin uplift and inversion at 0.95 Ma.

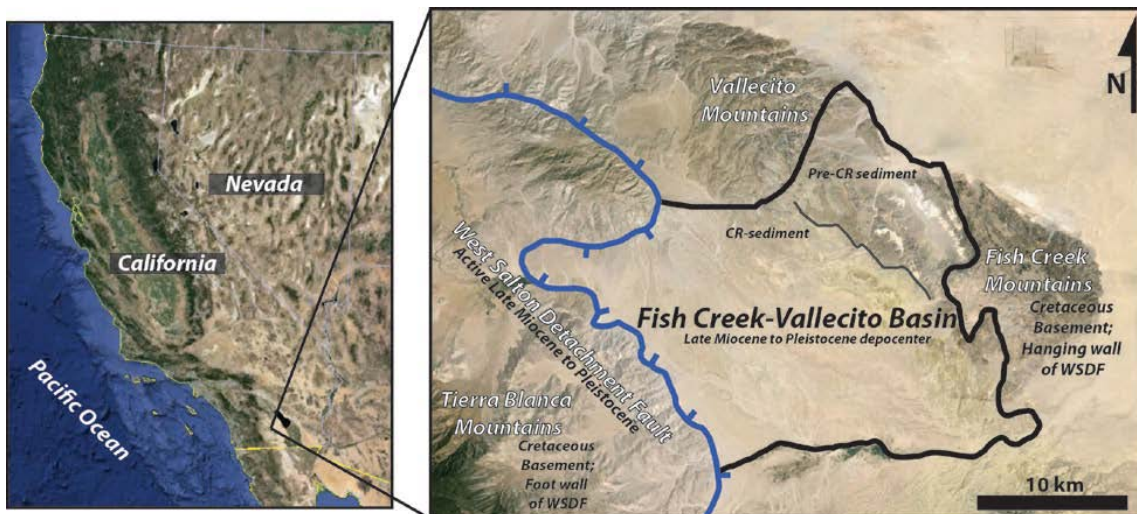


Figure 3-1. Google Earth image showing field area with major features highlighted.

Stratigraphic Setting

The section exposed within the Fish Creek-Vallecito Basin consists of three lithostratigraphic units formally assembled into groups and are summarized in Figure 3-2. Nomenclature for these groups is based on that used by Winker and Kidwell (1996) and revised by Dorsey et al. (2007). These groups include the Miocene Split Mountain Group, Mio-Pliocene Imperial Group, and Plio-Pleistocene Palm Spring Group.

The subdivision into groups is based on changes in lithology and depositional environment and is summarized in Figure 3-2. The Split Mountain Group contains the non-marine Elephant Trees Formation which consists of sandstones and conglomerates deposited as alluvial fans during early extension and subsidence accommodated along the low-angle West Salton Detachment Fault (Kerr, 1984; Winker, 1987; Dorsey et al. 2011). This unit is capped by the first of two long run out landslides, or sturzstroms. These sturzstrom deposits are interpreted as subaerial and subaqueous sturzstroms, respectively. These deposits are alternatively given the names first megabreccia and second megabreccia.

Following the Split Mountain Group is the marine Imperial Group. This group is divided into the Latrania and Deguynos formations. Lithologies within the Latrania Formation include early gypsum deposits of non-marine and marine origin as well as two sand-rich members deposited as submarine, sediment-gravity flows as the depositional environment deepened from ~6.2 Ma during integration of the area into the Gulf of California (Dorsey et al. 2011). These two lower and upper turbidite succession are divided by a long run out landslide deposit at ~5.3 Ma (subaqueous sturzstrom). The

lower and upper turbidites are termed the Lycium and Wind Caves members, respectively. Within the Wind Caves Member an important change in sediment source is recorded as the Colorado River began depositing much finer grained and better sorted sand (on and beyond a deepwater slope well in front of the delta itself) compared to the coarse, micaceous turbidite sands derived from local fluvial systems (Winker, 1987; Dorsey, 2011).

The overlying ~5.0 Ma-4.2 Ma Deguynos Formation records the basinward accretion of a long, muddy deepwater slope that would have downlapped onto the underlying Latrania Formation turbidites. Both the Latrania and lower Deguynos form a deepwater wedge driven basinwards by the high sediment supply of the Colorado River delta system that developed on the adjacent coeval shelf. The muddy deepwater slope deposits of the Mud Hills Member shallow upwards to sand-rich deposits of the Camel's Head Member. The upper Mud Hills (uppermost 1-200 m) and the sandy and carbonate rich Camel's Head Member represent the Colorado delta front proper (Winker, 1987). Continued progradation and shallowing of the depositional environment is recorded as deposits change from marine through brackish marine to non-marine fluvial deposits in the units of the overlying Palm Spring Group.

The last group exposed in the section studied is the ~4.2 Ma-2.8 Ma Palm Spring Group consisting of locally derived conglomerate flanking the basin margins to the north transitioning to local fluvial deposits of the Olla Formation. This local fluvial system interfingers with the Colorado River-deposited Arroyo Diablo Formation. Additional units of the Palm Springs Group not encountered in the study area are ~2.8 Ma-1.0 Ma

lacustrine Tapiado and fluvial Hueso formations. These formations make up basin fill after departure of the Colorado River system from the area.

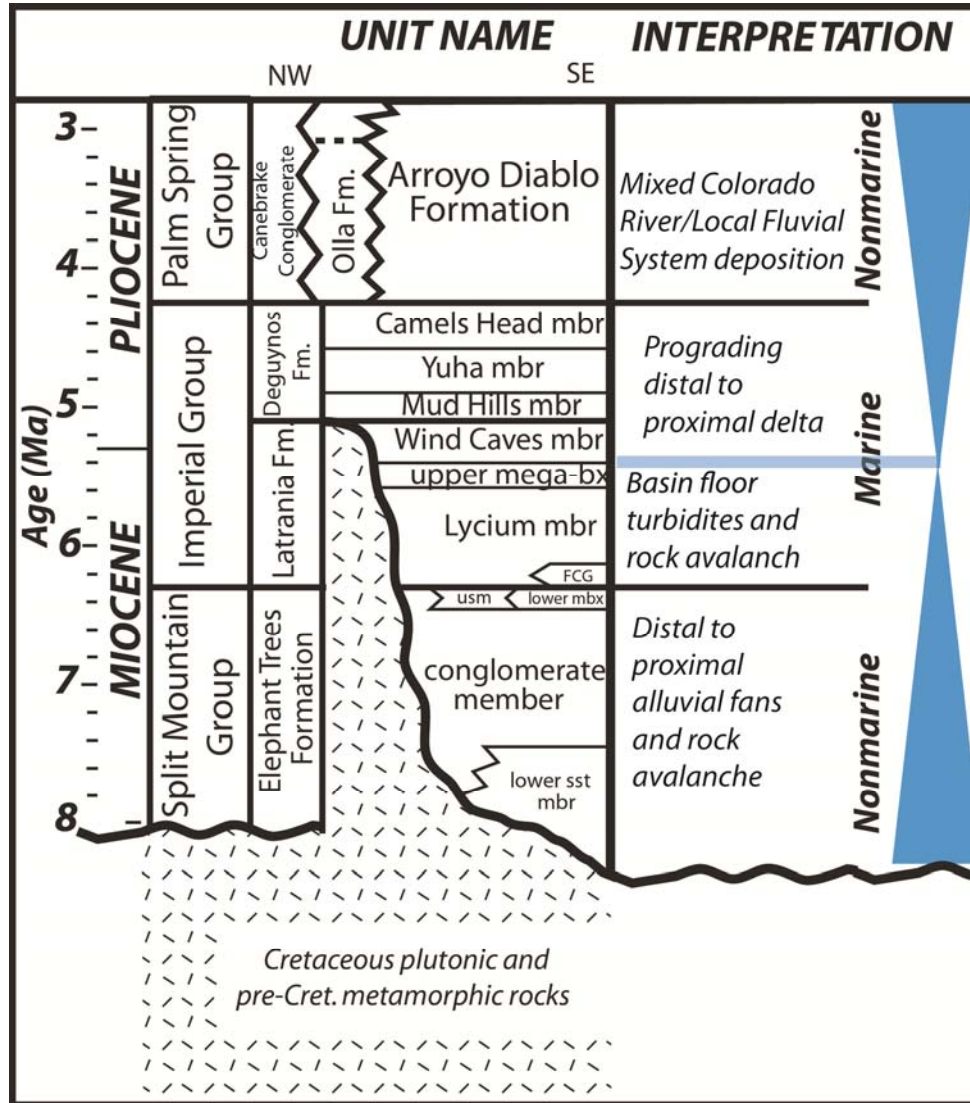


Figure 3-2. Stratigraphic units encountered in the study area within the Fish Creek-Vallecito Basin. Arrows indicate relative sea level during basin lowering followed by Colorado River delta progradation. (Modified from Dorsey et al., 2011)

Depositional System

Deposition of the units described above occurred in the Fish Creek Vallecito Basin from 8.0 ±0.4 Ma until around 0.95 Ma depositing about 5.5 km of sediment (Dorsey et al. 2011). The following ages and thicknesses are reproduced from the section measured by Dorsey et al. (2011).

Sedimentation from small, local, laterally derived alluvial fan and fluvial systems onto the hanging wall of the West Salton Detachment Fault occurred from 8.0 Ma until 5.3 Ma depositing approximately 700 m of red bed conglomerate and sandstones in the section. As the Colorado River became integrated into the basin, locally sourced drainage began to contribute a small fraction of the stratigraphy and is expressed as thin (observed beds were <20 cm) discrete beds of coarse-grained, biotite rich sandstone interbedded in areas dominated by low-energy sedimentation of silts and clays.

Colorado River drainage in the area dominated from 5.3 to ~3.0 Ma depositing ~3000 m of sediment as the Colorado River delta prograded into the basin. This spanned from deposits of the early Wind Caves deepwater turbidites as basin floor fans during initial deposition up to fluvial sediments from 4.5-3.0 Ma. Above this, mixed local drainage and Colorado River sediments are found in an ~800 m thick interval with overlying locally sourced sediment preserved in lacustrine and fluvial sediments ~1100 m thick Tapiado and Hueso Formations.

Latrania Formation

Within the Imperial Group, the 6.2 -5.2 Ma Latrania Formation is of foremost interest in this study. This unit contains sedimentary deposits sourced from local

basement initially and abruptly shifts to sediment transported by the Pliocene Colorado River and river delta within the Wind Caves Member. Thicknesses for the Latrania Formation are difficult to constrain as lateral variations occur in the exposed outcrops. Dorsey et al. (2011) reported a thickness for the Latrania Formation at ~300 m. This thickness is in agreement with unit thicknesses from Winker (1987) and Abbott et al. (2002). The unit consists of about 75 m of early sand-rich turbidite deposits within the Lycium Member, subaqueous sturzstrom of variable thickness with an average of 17 m (Abbot et al., 2002), followed by a 200 m succession of sandy to muddy beds deposited primarily by turbidity currents making up the Wind Caves Member.

The individual turbidite beds of the Lycium and Wind Caves members both show common normal and inverse-to-normal grading as well as basal tool marks and flutes indicative of sediment transport and deposition by turbidity currents (Winker, 1987). The deposition of the Lycium turbidites remains somewhat problematic as they cannot be derived directly from a coeval alluvial system, and there is currently no field evidence of an intermediate local shoreline or delta system. A turbidite succession of this thickness (75-100 m) requires a reasonable water depth and run-out distance to develop in front of a coastal source. Grains making up the Lycium member as well as the earliest Wind Caves member are generally coarse grained, angular, and biotite-rich. The majority of Wind Caves member grains, by contrast, are medium to fine grained, well rounded and sorted, and do not have abundant biotite. Emplacement of the intermediate, regionally extensive subaqueous sturzstrom makes these two turbidite units easy to distinguish in the field. Within the Wind Caves Member, locally-derived and Colorado River sediment

are easy to discriminate at the base of the section by not only by grain character but also by a mudstone layer identified to persist along the outcrop extent of the Wind Caves member. The outcrop extent is shown in Figure 3-3.

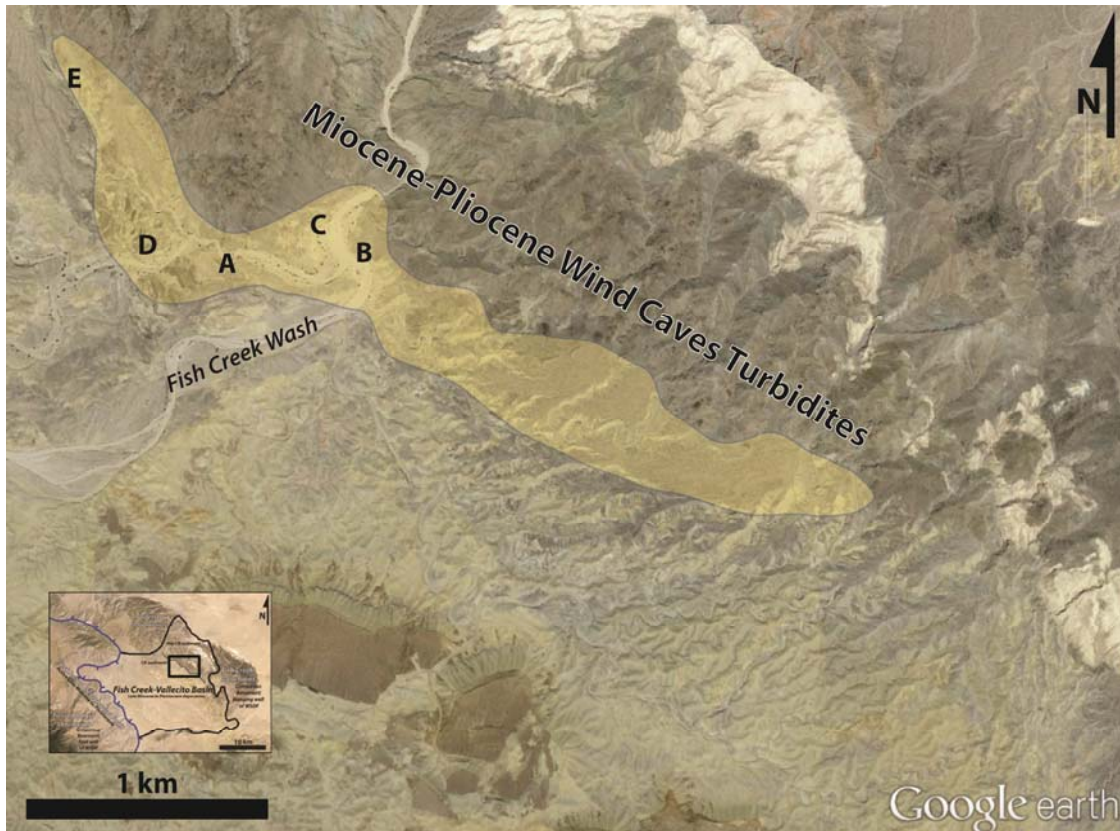


Figure 3-3. Satellite image highlighting the outcrop extent of the Wind Caves Member. This unit was deposited as subaqueous sediment gravity flows and is the first Colorado River-sourced sediment into the basin at 5.3 Ma.

Colorado River Drainage Area

The 640,000 km² area presently drained by the Colorado River covers a vast region of western North America (Hunt, 1956). This system sources sediment predominately from high relief terranes of the Colorado Plateau, which makes up more than half of the drainage basin area (Hunt 1956). Other provinces drained by the

Colorado River include portions of the Basin and Range and Southern and Central Rocky Mountains physiographic provinces. These regions are connected to the main trunk of the Colorado River through six main tributaries which encompass 78% of the drainage basins catchment area. These tributaries include the Green, San Juan, and Upper Colorado (also called Grand) Rivers which source from the northern portions of the basin. Southern portions of the Colorado River drainage basin are integrated into the main trunk via the Little Colorado, Virgin and Gila Rivers.

Diverse lithologies exist on the Colorado Plateau ranging between basement cored uplifts generated during Laramide orogenesis exposing Precambrian crystalline rock to thick stratigraphic successions deposited during the Phanerozoic. These successions accumulated during periods of tectonic quiescence during which deposition occurred primarily in a passive margin setting interrupted by periods of orogenesis during the Paleozoic Antler and Ancestral Rockies orogenies (Kluth, 1981). Mesozoic stratigraphy accumulated in a foreland basin setting as subduction generated the Sevier Highlands to the west followed by flat-slab subduction creating basement cored Laramide uplifts (Dickinson and Snyder, 1978; DeCelles, 2004). Cenozoic uplift of the Colorado Plateau has placed sediment originally deposited at sea level at a current elevation of ~2000 m (Pederson et al. 2002). Many easily erodible terranes exist on the Colorado Plateau due to the thick sedimentary rock stratigraphy, high relief, and through going drainage. The ease at which sediment is eroded from the Colorado Plateau contributes to the high sediment supply delivered by the Colorado River. This high sediment supply rapidly

filled the Fish Creek-Vallecito Basin from ~5.3-3.0 Ma, depositing an upward fining to coarsening upward sediment-overfilled basin.

METHODS

Outcrop Dataset

15 outcrop sections were logged measuring sedimentary detail of the Wind Caves Member of the Latrania Formation along a northwest to southeast transect within the Fish Creek-Vallecito Basin. Correlations between measured sections over the entire distance of the outcrops were sometimes difficult to establish exactly due to abrupt lateral variations in sandstone bed thickness, lack of regional flooding surfaces, small fault offsets, and cover on fine grained lithologies. Outcrops were primarily found along Fish Creek Wash and the smaller dry creeks feeding into the main wash. The majority of logged sections were taken in the central portion of the outcrop belt where erosion of gulleys into sandstone created good exposure of bedding geometries. Outcrops became less abundant away from the center of the Wind Caves member outcrop belt, probably reflecting the large-scale lens-like nature of the sandy Wind Caves unit along structural strike. Structural dip of the beds was generally 20 degrees to the SSE. As a result of the similarity of the structural and depositional dips, measurements down depositional dip were not possible for any significant distance (<20-100 m). Rather, the extensive exposure (~4.5 km) from NW to SE allowed for measurements to be taken roughly along depositional strike.

Measurements were taken to record bed thickness, lithology, grain size, sedimentary structures, and paleocurrent directions. The extent of the Wind Caves

Member as mapped by Winker (1987) includes both sandstone and mudstone lithologies, with the lower portion of the member being sand rich and the upper composed of a heterolithic succession of sand and mud interbeds as the Wind Caves Member grades upwards into the Mud Hills Member of the Deguynos Formation above. Measurements were taken on the sand rich lower portion of the succession as the majority of the upper finer grained portion was not well exposed. Outcrop photomosaics were also used to document lateral changes in bedding geometry. Distinctive bed types seen in the measured characteristics through the succession were grouped into facies that allowed for interpretations on processes and conditions under which the sediment was deposited. The main importance of the sedimentology outcrop dataset is that it will provide along-strike paleogeographic map with details including the NW-SE orientation and extent of the subaqueous landscape while the turbidite fan systems were developing for the Wind Caves system, as well as the significance of the time change up stratigraphic section.

RESULTS

Outcrops of exposed Wind Caves Member occur over ~6km lens-like lithosome with sandstones pinching out to the NW and SE. Lithologies present include graded and structureless sandstones, claystones and silty mudstones, as well as sandstone/mudstone heterolithic units. The 15 sections measured show a vertical and lateral trend of fining toward the NW and SE margins of the outcrop extent as well as vertically upsection. The section locations are displayed in Figure 3-4. Paleocurrent directions were recorded from flute and groove casts oriented obliquely to the outcrop belt, i.e. SW to S to SE as measurements were taken NW to SE and area summarized along with average sandstone

bed thicknesses in Table 3-1 Faulting, erosion of gulleys, and cover limited the vertical length of sections that could be measured. The longest continuous section (Section 14-1) is located in the middle of the outcrop extent along Fish Creek Wash and had a height of 88.5 m measured from the second Megabreccia which Winker (1987) defined as the base for the Wind Caves Member. Winker (1987) measured the Wind Caves succession to be up to 200 m thick from the second megabreccia to the top of the succession which was defined as the last 2 cm sandstone bed as the unit graded into the Mud Hills Member of the Deguynos Formation. Linkage of the Wind Caves Member sediment gravity flows directly into upstream sources cannot be mapped due to current structural tilting and erosion, however the turbidites are known to have come from the Colorado Delta which lay 10s of kilometers to the north as this time. The turbidite accumulation area was separated from the river and delta by a long (>5 km) muddy slope, similar to a min-continental slope at the edge of the developing Gulf.

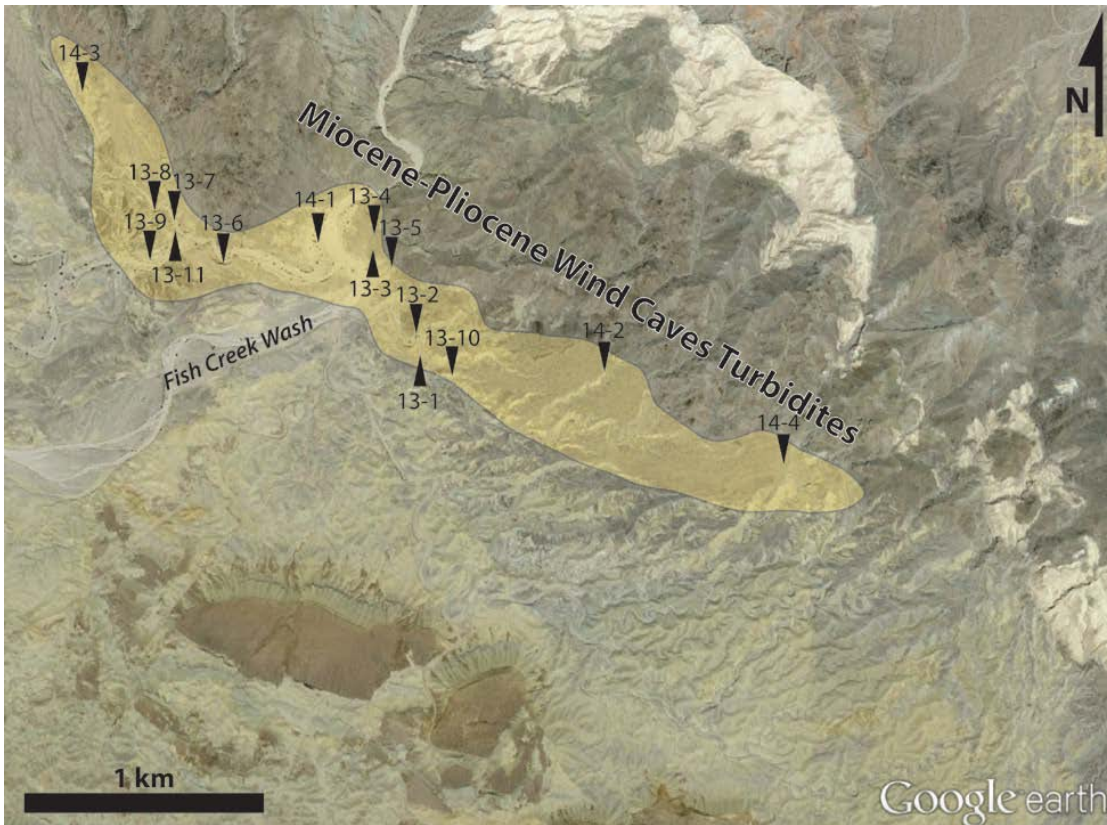


Figure 3-4. Locations of vertical measured sections taken throughout the outcrop extent of the Wind Caves Member.

Pliocene Colorado River avg sandstone bed thicknesses and Paleocurrents													
	NW											SE	
Section	13-8	13-9	13-7	13-6	14-1	13-4	13-3	13-5	13-2	13-1	13-10	14-2	14-4
Thickness (cm)	36.0	45.6	101.5	155.0	104.3	295.0	131.4	149.2	115.0	54.2	101.3	86.3	55.5
Avg Paleocurrent	168	210	249	210	218	-	225	176	150	167	175	159	127
# of measurements	2	10	2	14	12	-	7	4	2	6	1	7	5

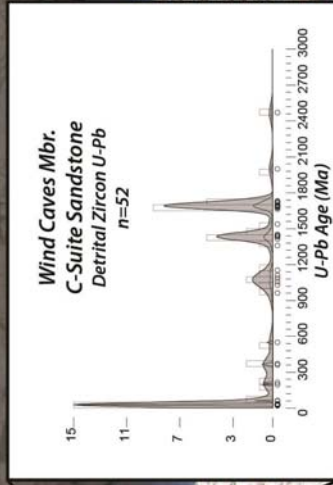
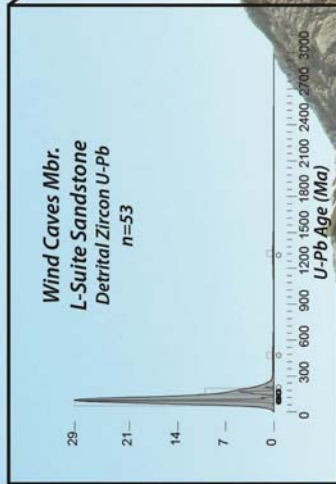
Table 3-1. Average sandstone bed thickness from NW to SE. Also shown are average paleocurrents taken from measured sections.

Sandstones of both “local” sourcing (L-Suite) and Colorado River sourcing (C-Suite) were documented by Winker (1987) and occur within the Wind Caves Member. L-Suite and C-Suite sandstone are differentiated in hand sample mainly by mineralogy and texture. L-Suite sandstones have medium to coarse grains with abundant biotite while C-

Suite sandstones are generally medium to fine grained and have abundant quartz. L-Suite sandstones occur just above the second megabreccia for up to tens of meters prior to the appearance of C-Suite sandstones. An interval of silty mudstone/cover ranging from ~1 m to tens of meters thick separates the lower L-Suite sandstones from the C-Suite sandstones which make up most of the sandstones within the Wind Caves sandstones. L-Suite sandstone beds are also found as thin beds (up to 20 cm) interbedded with silty mudstones higher in the section. Detrital zircon taken from the last thick bedded L-Suite sandstone and the first C-Suite sandstone show a distinct shift in U-Pb ages with the L-Suite bed dominated by Cretaceous age grains while the C-Suite bed contains grains of Miocene-Archean age. Zircon U-Pb ages (n=375) from four samples throughout the Wind Caves Member section show the age range to be Pliocene to Archean. This broad age range would be expected of a fluvial system sourcing from a large area encompassing diverse terranes, such as the Colorado Plateau. Erosion from a source area such as this would involve recycling of previously deposited sediment and give a wide spread of U-Pb ages in downstream deposits.

Figure 3-5. Outcrop A shows the Second Megabreccia/Wind Caves contact. Locally sourced (L-Suite sandstone) can be discriminated from Colorado River-sourced (C-Suite sandstone) by its coarser texture and common biotite. U-Pb age distributions show C-Suite sandstones to have a Miocene-Archean age spread. This larger age spread would be expected from deposits of a larger river system sourcing from more geologically diverse areas. Sandstone clast at top of megabreccia is ~2 m.

Outcrop A



Latrania Fm.
Lower Wind Caves Member
Thick bedded
C-Suite Sandstone

Silty Mudstone Interval

Latrania Fm.
Lower Wind Caves Member
L-Suite Sandstone

Base Wind Caves Member
Top Second Megabreccia

Facies Associations

Six lithofacies were identified from vertical sections measured throughout the Wind Caves Member and these tend to form larger scale architectural elements. Lithofacies (A through E) identified were linked to process-based interpretations of deposition. These lithofacies include Thick bedded, structureless sandstone (A); amalgamated, normally graded sandstone (B); non-amalgamated, normally graded sandstone (C); heterolithic interbedded sandstone and silty mudstone (D); and silty mudstone (E). Lithofacies identified are related to the turbidity current classification schemes of Bouma (1962), Lowe (1982), and Talling (2012) based on deposits from varied flow conditions. These facies can be used to characterize variation throughout the architectural elements within the Wind Caves Member both vertically and laterally.

Thick Bedded, Structureless Sandstone (Lithofacies A)

Thick bedded, structureless sandstone beds (>50 cm, up to 8 m) occur abundantly in sections measured in the central outcrops of the Wind Caves Member which occur along Fish Creek Wash. Figure 3-6 shows characteristics of this lithofacies. These sandstone beds are up to ~8 m thick and commonly form amalgamated intervals. Where individual beds (flows) can be seen (separated by silty mudstone) they reach a thickness of 3 m, generally averaging a thickness of ~1 m. While predominately structureless, these beds commonly exhibit grading from fine gravel at the base, with mostly medium to fine sandstone throughout the bed. The basal grading is similar to the S1 and S2 portion of Lowe (1982) model for high density turbidity current deposition. In these flows, a small portion of grains are carried by traction while the majority are deposited out of

suspension and appear similar to the S3 (structureless sandstone) interval. Mudstone rip up clasts are also common and occur along discrete horizons, giving evidence that these beds are deposited from high-density turbidity currents rather than liquefied debris flows (Talling, 2012). Scour marks in the form of flute and groove casts, a hallmark of turbidites, are also common. Lack of internal stratification is attributed to rapid fallout of suspended particles during deposition (Talling, 2012). Beds with this character were observed to persist laterally in outcrop over ~2 km with most frequent occurrence within measured section 14-1. Some of these beds also featured boulders up to a meter that were likely derived from the underlying megabreccia where it was high standing lateral to the turbidity flows. Due to the irregular topographic surface generated by the rapid deposition of the megabreccia some boulders from the megabreccia are likely to have been remobilized by turbidity currents travelling over the surface. One of these occurs along Fish Creek Wash and is recorded in section 14-1.

Lithofacies A: Thick bedded structureless sandstones



Figure 3-6. Thick bedded, structureless sandstone in outcrop (A). Flutes and groove casts (B and C). Structureless bed with weathered out mudclasts (circled in D). These beds are common within ~1 km of Fish Creek Wash. Structureless sandstone indicates rapid deposition from suspension in high concentration flow (Lowe, 1982).

Amalgamated, Normally Graded Sandstone (Lithofacies B)

Normally graded sandstone beds generally between 50 cm to 2 m with some beds up to 3 m thick are differentiated from Lithofacies A (thick bedded, structureless sandstones) by being thinner bedded and having grain size more rapidly grade up to fine or silt size grains from the base to the top. Beds are often fine grained or coarse grained at their base. Flute and groove casts along with basal mudclasts are common but not observed in all beds. Parallel laminations exist in upper portions of some beds.

Amalgamated beds are differentiated from non-amalgamated beds by thin or non-existent siltstone layer between sandstone beds. Amalgamation is not always constant laterally throughout a bedding interval as some beds pinch out off of the flow axis. From a process perspective, amalgamated, normally graded sandstone beds are differentiated from non-amalgamated beds because a higher degrees of amalgamation indicate deposition more proximal to the channel axis. The beds commonly show Bouma A and B divisions with less common C divisions (ripple cross laminae) as higher energy in axial positions hinders settling of fine grains.

Lithofacies B: Amalgamated, Normally Graded Sandstone

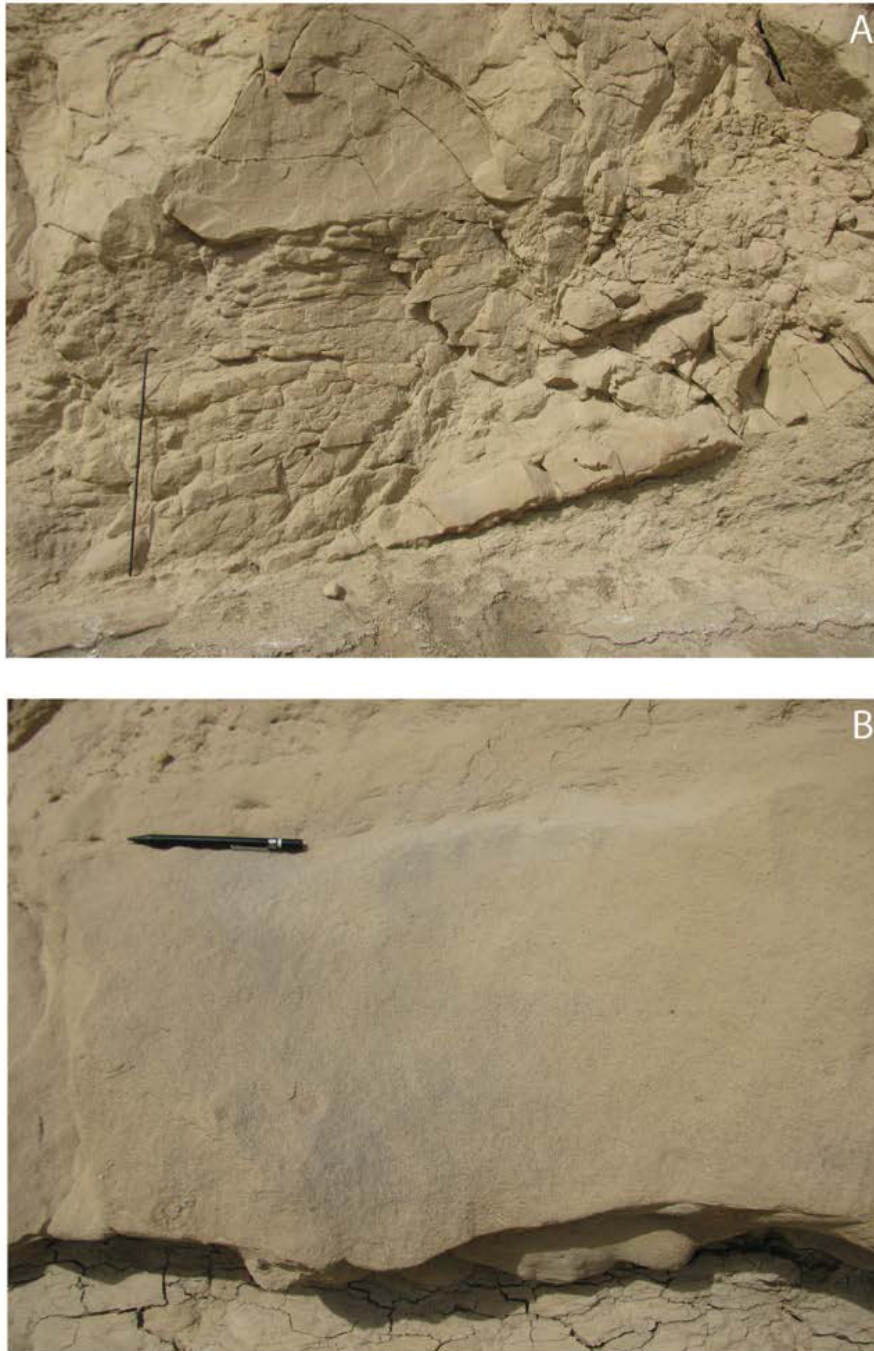


Figure 3-7. Amalgamated beds in outcrop (A). Bedding planes are often difficult to distinguish but tops of beds are recognized by being finer grained than bottoms. (B) shows irregular base of amalgamated bed. These are interpreted to be deposited within the axis of flow.

Non-Amalgamated, Normally Graded Sandstone (Lithofacies C)

Non-amalgamated, normally graded sandstones are generally between 20 cm and 1 m in thickness and exhibit similar features to Lithofacies C with the exception that silty mudstone or claystone intervals are present between sandstone beds. Figure 3-7 shows characteristics of this lithofacies. Some beds show grading from coarse sand through silt although it is often difficult to determine if silt sedimentation represents Bouma D and E divisions or hemipelagic sedimentation. Preservation of these fine grained intervals indicates that these are likely to be off axis deposits in areas where energy is low enough for preservation of fine material. Commonly found with non-amalgamated, normally graded beds are medium or fine sandstone beds with common faint laminations. Due to their frequent occurrence with non-amalgamated, normally graded beds, non-graded beds are included within this lithofacies. These beds are interpreted to have been deposited by waning, decelerative turbidity currents (Talling, 2012).

Lithofacies C: Non-Amalgamated, Normally Graded Sandstone



Figure 3-8. Non-amalgamated sandstone beds ~30 cm thick with heterolithic and silty mudstone units between beds (A). Beds typically have flatter, less scoured bases. Beds outcrop with slightly rounded top due to finer grained portions of beds being more easily eroded (B).

Heterolithic Interbedded Sandstone and Silty Mudstone (Lithofacies D)

This unit consists of sandstones up to 20 cm thick interbedded with silty mudstones occurring as intervals up to a few meters thick in measured sections. Sandstone beds are commonly coarse grained L-Suite beds with ripples toward the top of the bed. Deposition is off axis of main flows resulting in deposition from dilute sediment gravity flows.

Silty Mudstone and Claystone (Lithofacies E)

Silty mudstone and claystone intervals make up fine grained intervals between sandstone beds. Structures are often difficult to determine due to their small scale and heavy weathering. These beds are either deposited by dilute turbidity currents or hemipelagic sedimentation (Talling, 2012).

Outcrop examples and characteristics of these lithofacies are shown in Figure 3-9.

Lithofacies D: Heterolithic Interbedded Sandstone and Silty Mudstone



Lithofacies E: Silty Mudstone



Figure 3-9. Heterolithic interbedded sandstone and mudstone and silty mudstone intervals are interpreted to be deposited by dilute turbidity currents off-axis of main flow or by hemipelagic sedimentation (Talling, 2012). Intervals of these units are often thin in central outcrops within the Wind Caves Member and increase in thickness laterally and also up section.

Facies Variation

Variation of facies can be shown throughout the outcrop extent of the Wind Caves Member. The three longest sections measured, sections 13-9, 14-1, and 14-2, show vertical and lateral facies variation along a ~2 km NW to SE transect. Relative proportions of each of the five lithofacies were calculated for each of the three sections. Deposition of sandstones of Colorado River origin were of primary interest for this study and as a result facies proportions were calculated from the first bed in each outcrop characterized as C-Suite sandstone.

24% of Section 14-1 is comprised of thick bedded, structureless sandstone (LF A) with 41.8% of the sandstone beds in outcrop being amalgamated, normally graded sandstone (LF B). Sections 13-9 and 14-2 outcropping to the NW and SE of Fish Creek Wash did not contain LF A but did contain 22.3% LF B in section 13-9 and 32.3% LF B in section 14-2. Dominant lithofacies for section 13-9 were non-amalgamated normally graded sandstone (LF C) comprising 29.3% and heterolithic, interbedded sandstone and silty mudstone (LF D) making up 36.6%. Section 14-2 contained 25.2% LF C and 11% LF D. Each of the outcrops were measured to have about 10% silty mudstone as discrete layers between non amalgamated sandstones.

Average sandstone bed thicknesses were calculated for 12 outcrop sections containing C-Suite sandstone beds. Average sandstone bed thicknesses range from individual vertical sections ranged from 36.0 cm to 295.0 cm. Sandstone bed thicknesses were greatest in the area around Fish Creek Wash and thinned to the NW and SE. Section

13-15 had the thinnest sandstone bed average (36.0 cm) while section 13-4 had the greatest average (295.0 cm) and was located in Fish Creek Wash.

The lack of structureless and thick bedded sandstones as well as the increase in non-amalgamated sandstones to the NW and SE of Fish Creek Wash indicate off-axis positions of main flow in which fine grained sediment preservation was higher. Thick bedded structureless sandstones and amalgamated normally graded sandstones in section 14-1 indicate that the present day Fish Creek Wash approximates the main flow axis of the turbidite system.

Architectural Elements

Deposits in the Wind Caves Member vary from thick bedded amalgamated sandstones in the lower 50 m and within the central ~2 km of the Wind Caves outcrop belt to thinner bedded sandstones with abundant heterolithics higher in the section and toward the outer ~1 km of the outcrop extent. The lithofacies described above are similar to the basin-floor and lower slope deposits of Plink-Bjorklund et al. (2001) from Splitsbergen and of Carvajal and Steel (2006) from the Laramide Washakie Basin. In these studies, proximal turbidite deposits occur as thick bedded sheet sands and channels on the lowermost slope and basin floor. Thinner bedded sandstones with less amalgamation, increased heterolithics and silty mudstone can be deposited further into the basin as fringe deposits and off axis of the main channels. However, these thinner bedded sandstones, especially discontinuous units within increased muddy successions also occur characteristically as lower or even middle slope channels, i.e. in a more proximal environment than the fans themselves. It is common that muddy deposits come

to overlie more sandy deposits as muddy slopes prograde over the basin floor deposits in most deepwater turbidite basins, including the cases cited above. The reason why the slope deposits are so muddy is that deepwater slopes are primarily bypass zones for turbidite flows feeding sandy basin floor fans (Plink-Bjorklund et al., 2001). Stacking patterns in this study show a gradual transition from axial amalgamated sandstone channel deposits to non-amalgamated lobe and channel deposits higher in the section as the basin became filled with sediment. The characteristics of each architectural element will be described below.

Fan complex: Basin Floor Channels Feeding Thick Sheet Sandstone Fan Lobes

Thick bedded sheet sandstones occur over ~2 km around Fish Creek Wash. Internal geometry of individual sandbodies is difficult to determine from outcrop due to tilting and erosion. Outcrop B in Figure 3-10 shows thick bedded sheet-like sandstones and amalgamated sandstones. These beds are sometimes incised into ~1 m by channelized sandstone beds pinching out over tens of meters. Beds are generally amalgamated with 1-30 cm thick silty mudstone and heterolithics between bedding. Outcrop B, measured along Fish Creek Wash, gives a look at bedding geometry of the thick bedded sandstones approximately along depositional strike. Good lateral exposure is offered in this section, as evidenced by a 7 m thick bed with aligned mudclasts within the first meter maintaining this thickness over ~100 m of exposure. Beds above this are ~1-2 m thick showing a high degree of amalgamation with the degree of amalgamation decreasing over the ~100 m of the exposure. The zone of amalgamation is interpreted to be the main axis of flow with non-amalgamated sandstone beds deposited further off axis

of the main channel. Thick bedded, structureless sandstones and amalgamated normally graded sandstones are strongly associated with base of slope and basin floor channels and sheet sandstones (Plink-Bjorklund et al., 2001; Pyles and Slatt, 2007). This sheet-like nature of sandstone bedding is displayed in Outcrop C (Figure 3-11). This outcrop shows a small channel scouring into the sheet-like sandstones. The channels generally ride above and feed the sheetlike lobes. This association is interpreted as a fan complex centered along the Fish Creek area.

Figure 3-10. Outcrop B shows thick bedded structureless and normally graded sandstones exposed along Fish Creek Wash. On the left side of the picture sandstone beds are highly amalgamated with decreasing amalgamation to the right. The zone of amalgamation is interpreted to be the channel axis with amalgamation decreasing off axis. The measured section is taken from the right hand portion of the photo.

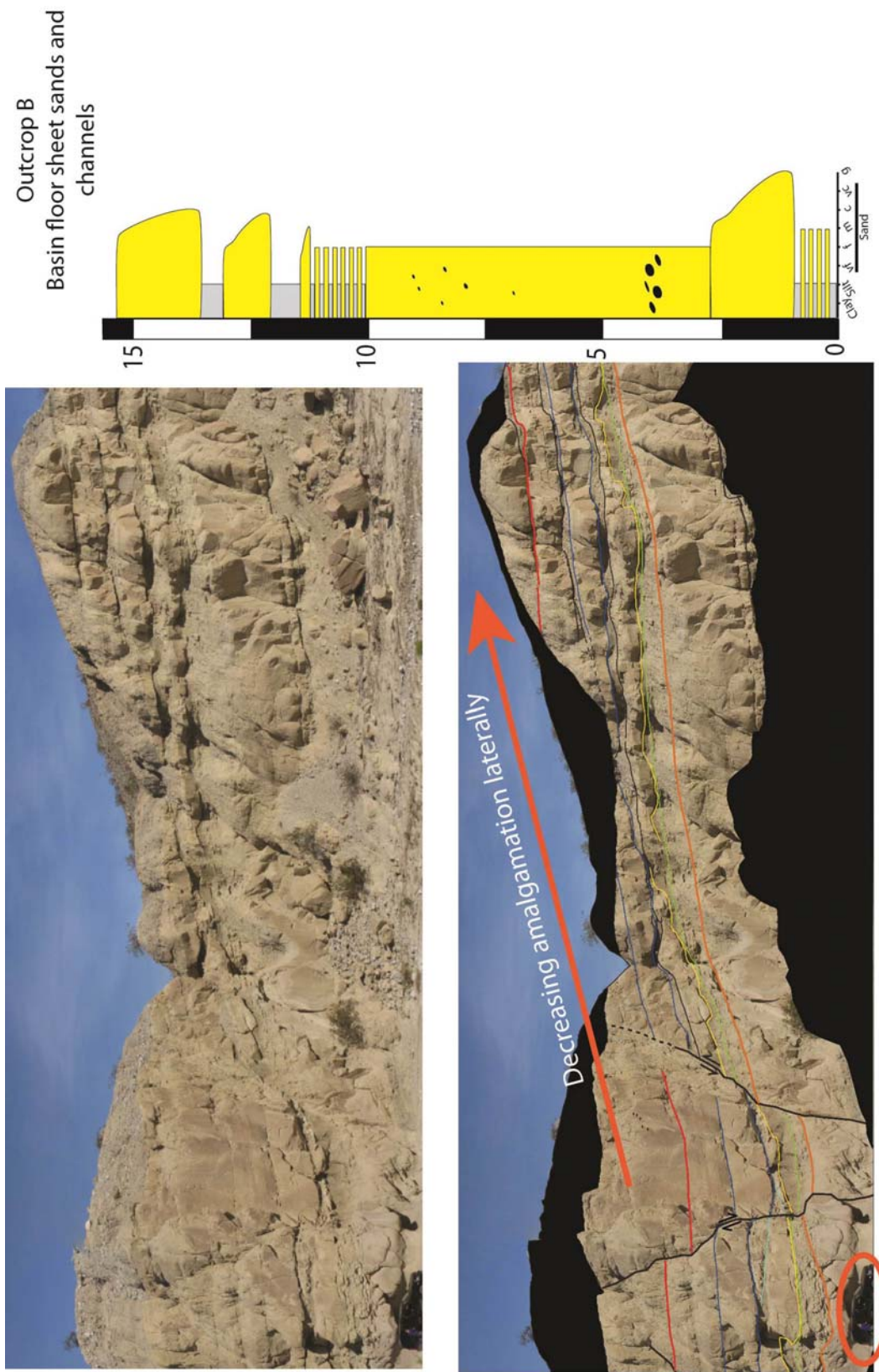


Figure 3-11. Outcrop C shows bedding geometry for thick bedded structureless and amalgamated normally graded sandstones along Fish Creek Wash. Early deposition of C-Suite sand turbidites is characterized by thick bedded sheet sands and channels in outcrop. These beds are interpreted to have been deposited in a basin floor setting with possible confinement which acted to pond turbidity currents.

Outcrop C
Basin floor sheet sands and
channels



Slope deposits: Slope Channeled Sandstone Beds and Lobes Within a Low Net/Gross Succession

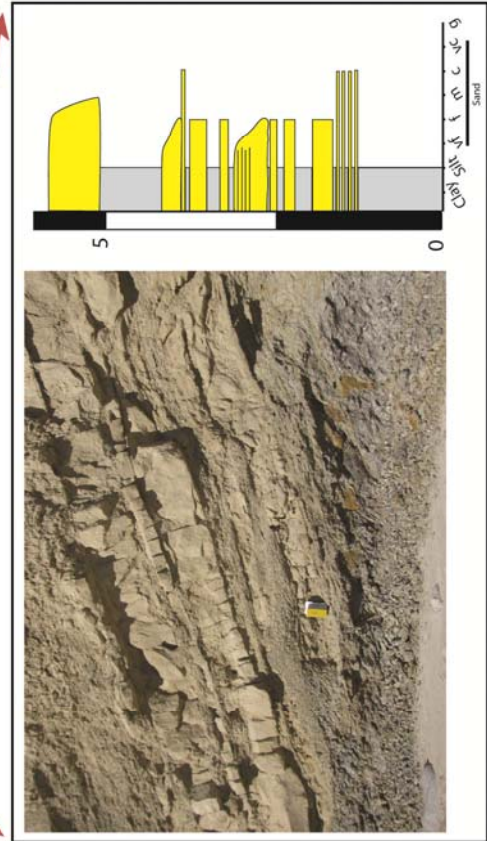
Stratigraphically higher in the Wind Caves succession and also occurring towards the margins of the Wind Caves Member outcrop belt are deposits interpreted as characteristic of the lower to middle slope, shown in Outcrops D and E in Figures 3-12 and 3-13. These include confined sandstone beds or units ~100 m wide interpreted to have deposited in slope chutes or channels and unconfined sandstone beds or units ~500-1000 m wide deposited in slope lobes. The best example of a slope chute or channel is shown in Figure 3-13 and occurred on a vertical outcrop ~30 m in height which could not be measured. Examination of exposed bed bases, fallen blocks, and photopanel showed that individual beds were 0.3 to 1.0 m thick and showed grading from medium to fine sandstone with a lateral bed extent of ~100 m. Scour marks and flute casts were common on bed bottoms. The outcrop measured in section 13-9 and shown in Figure 3-12 best exposes a lobe deposit in the upper Wind Caves Member. This section contained abundant heterolithics and silty mudstone between sandstone beds which were ~0.45 m thick on average, consisting of graded to non-graded with medium to fine sandstone and flat bases. Some thin L-Suite sandstone beds (~10 cm) within units interpreted as lobes were used as marker beds to determine lateral extent. These beds weathered to a reddish brown color forming which was easily recognized on Google Earth satellite imagery. These beds capped more erodible C-Suite sandstone and mudstone beds and could be traced laterally ~750 km. Winker (1987) notes that biotite within L-Suite sandstones

likely weathers to form iron cement giving a reddish color and increasing resistance to erosion.

The above association is interpreted as muddy slope deposits with bypassing turbidite channels and slope lobes associated with the terminating channels. The fact that this muddy association overlies the axial fan complex and is in turn overlain by the thicker Mud Hills unit, is consistent with the above interpretation of a generally progradational muddy slope leading down to a sandier basin floor. Figure 3-13 shows discontinuous sandstone beds interpreted to be slope channels within the Mud Hills. The Mud Hills is interpreted to have been deposited in a middle to upper slope setting with channelization supporting sand bypass to the basin floor.

Figure 3-12. Outcrop D shows thinner bedded, normally graded sandstones with common silty mudstone and heterolithic interbedded sandstone and mudstone between sandstone beds which is common higher in the Wind Caves Member section. These are interpreted to be deposited off axis of main flow as preservation of mudstones is high. Some areas show scour into bedding below (Outcrop E in Figure 3-13) in a confined setting. These confined sandstone beds are interpreted as slope chutes or confined lobes. As the Colorado River delta prograded into the basin, the local depositional environment changed from basin floor to a slope setting.

Outcrop D
Slope Lobes



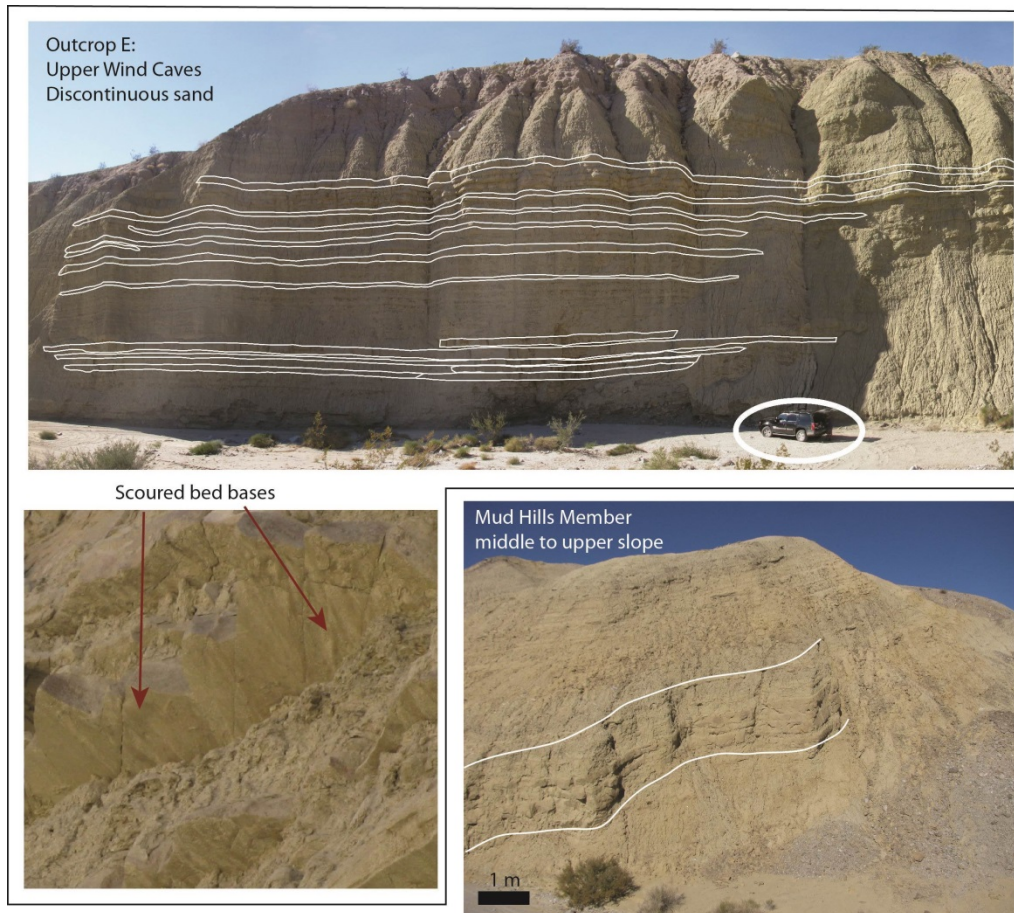


Figure 3-13. Outcrop E shows discontinuous sandstones beds within the upper Wind Caves unit. These beds often have scoured bases. These are interpreted to be lower slope channels feeding slope lobes as well as basin floor fans. Similar confined sandstone beds are found stratigraphically higher within the middle to upper slope deposits found within the Mud Hills.

DISCUSSION

The Wind Caves Member contains the first preserved sediment sourced from a large fluvial system (Pliocene Colorado River) deposited into the Gulf of California (Winker, 1987; Dorsey et al., 2007, 2011). Evidence for this can be seen on the hand sample scale by a change from immature sandstones with angular grains and abundant biotite to quartz-rich, finer grained sandstones deposited as thick bedded sandstones

within the Wind Caves Member. Observed just before the appearance of the first Colorado River-sourced sandstone is a silty mudstone unit that can be correlated over the extent of Wind Caves outcrops. This fine-grained unit could be the result of local depositional systems being essentially blocked by rapid deposition of Colorado River-sourced sediment up depositional dip.

An overall change from thick bedded amalgamated sandstones to thin bedded sandstones with abundant mud rich intervals is a characteristic vertical trend within the Wind Caves Member and are shown through the vertical section correlation in Figure 3-14. Outcrops of the Wind Caves Member expose stratigraphy characteristic of deposition on the basin floor (basin floor thick bedded sheets and channeled sandstones of the lower Wind Caves) and lower to middle slope (thinner bedded, less amalgamated sandstones of the upper Wind Caves) (Plink-Bjorklund et al. 2001; Pyles and Slatt, 2008). The facies change occurring upsection from deposits characteristic of basin floor to lower and middle slope is what would be expected for a basin being rapidly filled by a prograding delta fed by a large-scale delta and fluvial system.

Factors complicating construction of a depositional model for the area are the limited lateral extent of outcrops due to faulting, tilting, and erosion. Vertical measured sections taken over ~5 km of the Wind Caves Member outcrop belt allow for reconstruction of how this system evolved through time, although time equivalent units up depositional dip are eroded and units down depositional dip are buried in the subsurface. Grouping of different bedding characteristics into lithofacies allows for comparison to other studies in order for a depositional model to be created.

Winker's (1987,1995) early study of the Mio-Pliocene stratigraphic succession reported the Wind Caves Member to have been a small submarine fan ponded in a mini basin. This conclusion is consistent with its location currently between two steep sided basement exposures (Vallecito Mountains to the NW and Fish Creek Mountains to the SE) along with the underlying alluvial fans (Late Miocene Elephant Trees Formation) and two successive mass wasting events giving evidence that gradients were likely very steep in the Miocene to early Pliocene. As turbidity currents were focused into this area, confinement would act to channelize flows, creating an environment where the majority of fine-grained material would be scoured away by incoming currents. This mud would be transported as dilute turbidity currents to areas outside of the local confinement. Confinement could either be the result of tectonic control on basin geometry or could have been influenced by deposition of previous units, as the surface of this unit at times pokes through into the lowest L-Suite sandstones of the Wind Caves Member. In section 14-1, sandstone beds abruptly thin at the top of the section into heterolithic interbedded sandstones and silty mudstones.

Winker (1987) interpreted the up section sandstone bed thinning and increase in mudstone to be indicative of a retrogradational stacking package going from proximal to distal turbidite deposits. This conflicts with the overall progradational stacking pattern of Colorado River-sourced sandstones in the basin. This study proposed a lower to middle slope environment for deposition of the thinner bedded sandstones of the upper Wind Caves Member.

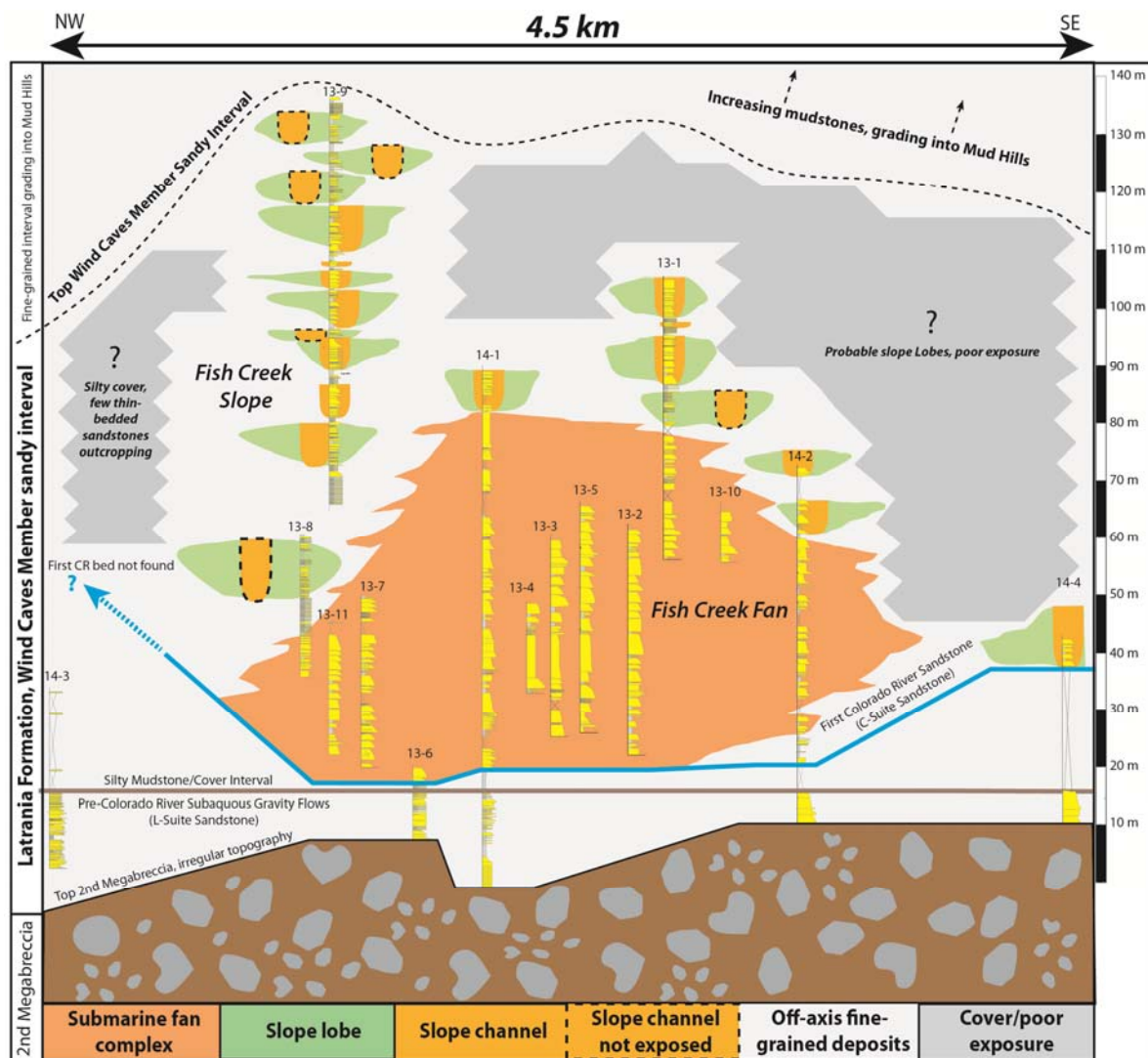


Figure 3-14. Measured section correlation of vertical sections taken along the Wind Caves Member outcrop belt. Central sandstone beds are often thick bedded and amalgamated and likely deposited in a basin floor setting. Bedding thickness decreases off axis of the thick bedded sheet sandstones and channels. Going up section, bedding also becomes thinner with increased silty mudstone and heterolithic interbedded sandstones and mudstones. Depositional environment changed from a confined basin floor setting to a slope setting with more lateral accommodation. This fan and slope outcrop well around the Fish Creek Wash area and as a result are termed the Fish Creek Fan and Fish Creek Slope in this diagram.

Transition from Basin Floor to Slope Deposition

The thickness of the sandstone beds, high degree of amalgamation, and evidence of rapid deposition from suspension in outcrops within ~1 km of Fish Creek Wash suggest that turbidite ponding may have occurred in a confined basin setting in this area, much like Winker (1987) proposed. However, the thinner bedded, laterally persistent sandstones of the upper Wind Caves which were cited as evidence for turbidite deposition in a distal fan setting are accompanied by discontinuous sandstones presently forming cliffs in areas dominated by mudstones. Slope environments are areas of sandstone bypass as most of the sand accumulates in the basin floor fan (Beaubouef et al., 1999). The discontinuous sandstones in the upper Wind Caves are interpreted as channels which feed the more laterally continuous sandstones which are interpreted as slope lobes. These channels acted as conduits for bypass of sand to a topographically lower location. While the upper Wind Caves Member is interpreted as to have been deposited in a lower slope environment, the 400 m thick Mud Hills Member of the Deguynos Formation comprises the majority of the slope. This muddy unit contains confined sand intervals which likely fed a lower slope unit with similar characteristics as the upper Wind Caves. The genetic linkage between lithostratigraphic units is shown in Figure 3-15.

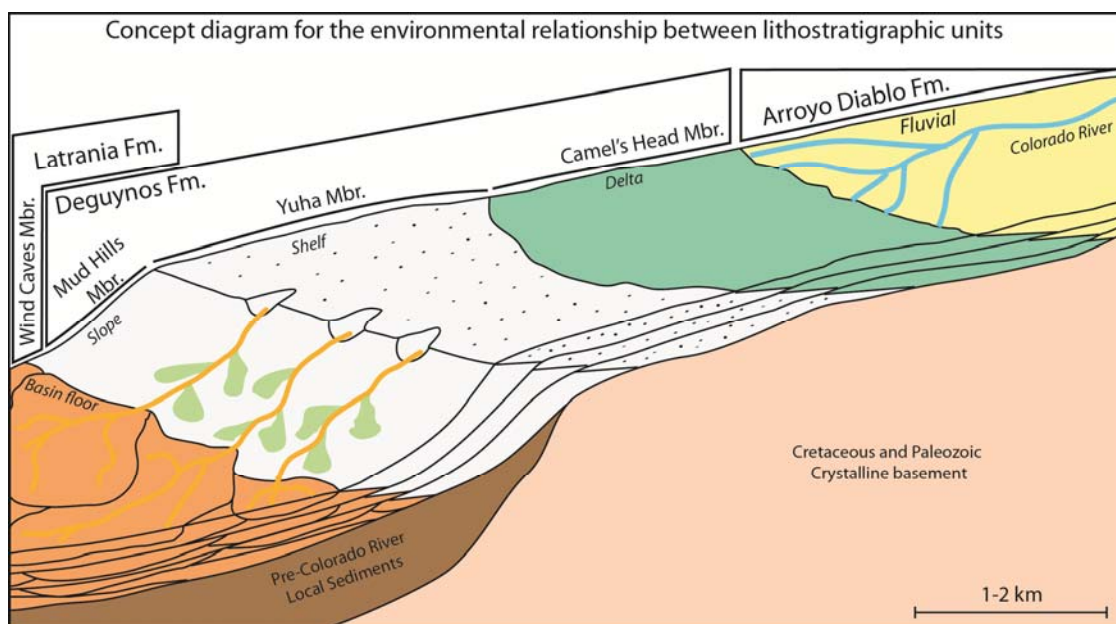


Figure 3-15. Schematic representation of how lithostratigraphic units are genetically related. As the Colorado delta prograded, slope deposits downlapped on to basin floor deposits. This is evidenced by the facies changes observed going up section in the Wind Caves Member. Continued progradation deposited middle to upper slope, shelf, delta, and fluvial units into the basin.

CONCLUSIONS

Deposition of turbidites by the Colorado River and Delta into a deepwater setting in the Gulf of California is denoted by the influx of mature sandstone deposited initially as thick bedded, amalgamated sandstones transitioning to thinner bedded sandstones with lateral extents of 50 m to ~1 km. The discontinuous sandstones were interpreted as slope channels which fed slope lobes and were conduits for sand bypassed to the basin floor. This transition from a basin floor to lower/middle slope environment fits well with the overall progradational sequence observed in the basin.

The three longest vertical sections contained between 45 m and 71 m of section measured through the C-Suite sandstone interval of the Wind Caves Member. In these

sections sandstone bed thicknesses varied from 45.6 cm in section 13-9 in the NW to 104.3 cm in section 14-1 in the central Wind Caves Member outcrop belt to 86.3 cm in section 14-2 to the SE. Smaller sections measured between each of the three larger ones also followed this trend of thickening sandstone beds toward the central outcrop belt. Thick bedded, structureless sandstones (LF A) and amalgamated, normally graded sandstones (LF B) are associated with basin floor sheet sandstones and channels make up ~66% of section 14-1 compared to 22.3% of section 13-9 and 32.3% of 14-2. Combining this with paleocurrent data showing flow radiating from SW to SE gives evidence that sediment originated at the mouth of a single input (Pliocene Colorado River delta) depositing a fan as flow spread outwards. With continued progradation of the system, channeled lower to middle slope deposits of the upper Wind Caves Member came to overly the lower Wind Caves basin floor fan.

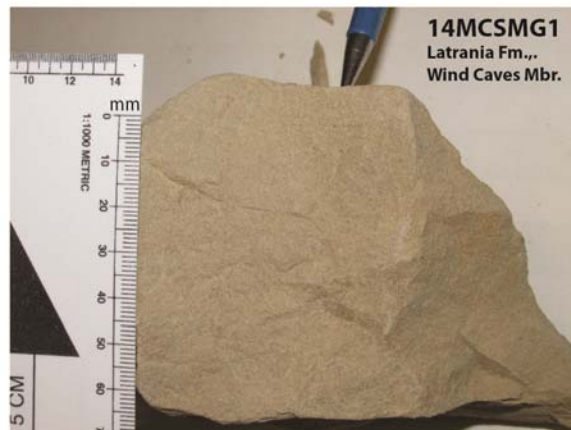
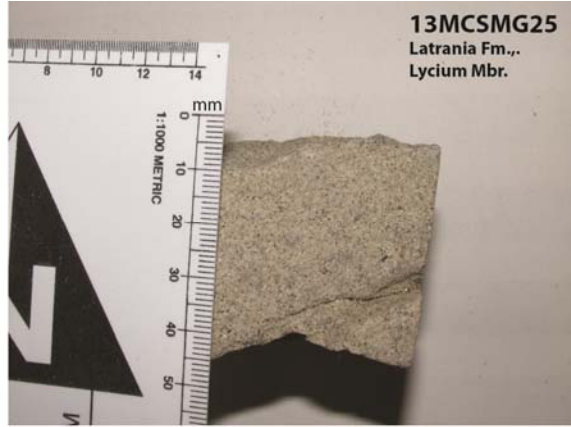
Appendix A: Sample Location Table

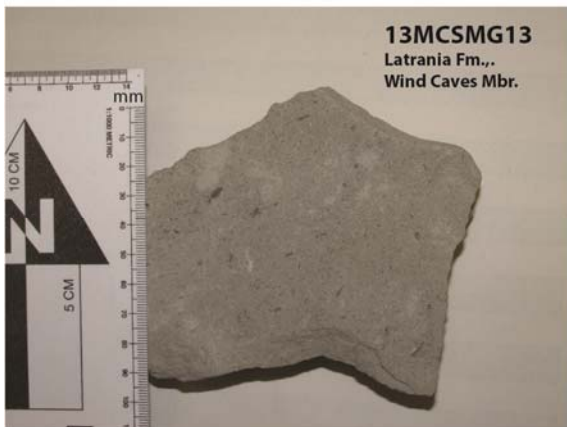
Location	Sample	Formation	Member	Depositional Age	Sst Type	Latitude	Longitude
Gulf of CA	CR05	Modern Delta		Holocene	C-Suite*	32.235300°	-115.055300°
Fish Creek Wash	13MCSMG31	Arroyo Diablo		~4.0-3.5 Ma	C-Suite	32.963591°	-116.188330°
Fish Creek Wash	13MCSMG30	Olla		~4.0-3.5 Ma	L-Suite	32.963579°	-116.187827°
Fish Creek Wash	13MCSMG29	Arroyo Diablo		~4.0 Ma	C-Suite	32.967286°	-116.172791°
Fish Creek Wash	13MCSMG22	Arroyo Diablo		~4.2 Ma	C-Suite	32.972186°	-116.167556°
Fish Creek Wash	13MCSMG21	Deguyunos	Yuhia	~4.8 Ma	C-Suite	32.980295°	-116.144973°
Fish Creek Wash	13MCSMG9	Deguyunos	Rhythmites	~5.0 Ma	C-Suite	32.985333°	-116.127330°
Fish Creek Wash	13MCSMG8	Deguyunos	Rhythmites	~5.0 Ma	C-Suite	32.986610°	-116.126878°
Fish Creek Wash	13MCSMG6	Deguyunos	Mud Hills	~5.1 Ma	L-Suite	32.992846°	-116.132490°
Fish Creek Wash	13MCSMG12	Latrania	Wind Caves	5.3-5.2 Ma	C-Suite	32.992585°	-116.129934°
Fish Creek Wash	13MCSMG13	Latrania	Wind Caves	5.3-5.2 Ma	C-Suite	32.992387°	-116.127399°
Fish Creek Wash	13MCSMG15	Latrania	Wind Caves	5.3-5.2 Ma	C-Suite	32.990199°	-116.116472°
Fish Creek Wash	14MCSMG1	Latrania	Wind Caves	~5.3 Ma	C-Suite	32.992570°	-116.123962°
Fish Creek Wash	14MCSMG3	Latrania	Wind Caves	~5.3 Ma	L-Suite	32.992570°	-116.123962°
Fish Creek Wash	13MCSMG25	Latrania	Lycium	~5.4 Ma	L-Suite	32.995348°	-116.116163°
Fish Creek Wash	12MCSMG4	Latrania	Lycium	~6.2 Ma	L-Suite	33.000762°	-116.115232°
Fish Creek Wash	12MCSMG3	Elephant Trees		~6.5 Ma	L-Suite	33.001510°	-116.115128°
Fish Creek Wash	12MCSMG1	Elephant Trees		~8.0 Ma	L-Suite	33.014097°	-116.112005°
Canyonlands, UT	z07CP51	Navajo SS		L. Jurassic	-	38.5669°	-109.7918°
Canyonlands, UT	z07CP55	Cutler		L. Permian	-	38.4631°	-109.7713°
Canyonlands, UT	z07CP56	Cutler		L. Permian	-	38.4621°	-109.7923°
Canyonlands, UT	z07CP57	Moenkopi		M. Triassic	-	38.456°	-109.811°
Canyonlands, UT	z07CP58	Chimle		U. Triassic	-	38.4533°	-109.8152°
Canyonlands, UT	z07CP59	Wingate		U. Triassic-L. Jurassic	-	38.449°	-109.8188°
Canyonlands, UT	z07CP61	Kayenta		U. Triassic	-	38.4473°	-109.8193°
Canyonlands, UT	z07CP62	Navajo SS		L. Jurassic	-	38.4452°	-109.8214°
Canyonlands, UT	z08CP71	White Rim SS		M. Permian	-	38.4005°	-109.7937°
Canyonlands, UT	z08CP72	Moenkopi		M. Triassic	-	38.2644°	-109.8667°

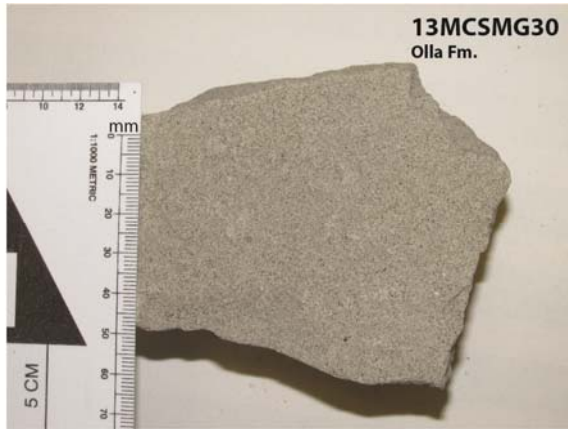
*Received as mineral separate

**Processed by Markella Hoffman at the University of Kansas, 2009

Appendix B: Sample Photographs







Not pictured: CR05
Modern Colorado River Delta
Sent as zircon mineral separate

Appendix C: U-Pb Data Table

12MCSMG1					207/ 235		206/ 238		206/ 207		
	[U] ppm	U/Th	207/235	206/ 238	Age Ma	2 σ err	Age (Ma)	2 σ err	Age (Ma)	2 σ err	% Disc
33	718	2.50	0.08050	0.01120	78.6	2.8	71.8	1.1	293	49	8.7
54	591	2.37	0.07690	0.01120	75.2	2.2	71.8	1.3	227	37	4.5
111	710	2.37	0.07600	0.01152	74.4	1.8	73.8	1.3	159	25	0.8
52	555	2.08	0.07570	0.01152	74.0	1.4	73.8	0.8	140	22	0.2
99	663	2.62	0.07580	0.01156	74.2	1.3	74.1	0.8	121	19	0.2
34	640	2.18	0.08340	0.01177	81.3	2.7	75.4	1.7	272	60	7.3
46	326.6	1.58	0.08530	0.01197	83.1	2.3	76.7	1.3	287	47	7.7
38	99	1.56	0.08130	0.01207	79.2	4.9	77.3	2.3	277	69	2.4
74	406	1.36	0.08020	0.01223	78.3	1.6	78.4	1.2	156	25	0.1
49	2160	6.60	0.08490	0.01293	82.7	1.9	82.8	1.4	117	31	0.1
57	500	9.00	0.08700	0.01308	84.6	2.3	84.0	1.7	193	32	0.7
79	1050	3.40	0.09610	0.01370	93.1	2.1	87.7	1.5	224	24	5.8
69	734	1.90	0.09290	0.01388	90.2	1.5	88.9	0.9	176	21	1.5
65	880	2.60	0.09150	0.01394	88.9	2.4	89.2	2.2	132	23	0.3
22	143	1.78	0.09580	0.01407	92.8	2.7	90.0	1.5	268	40	3.0
48	678	3.50	0.10000	0.01415	96.8	2.0	90.6	1.1	290	42	6.4
80	570	2.17	0.09380	0.01415	91.0	2.6	90.9	1.9	161	28	0.1
76	474	1.20	0.09300	0.01422	90.3	1.7	91.0	1.0	148	28	0.8
118	286	1.59	0.09850	0.01425	95.2	3.2	91.2	1.4	290	56	4.2
41	574	2.10	0.09850	0.01433	95.4	1.7	91.7	1.2	197	22	3.9
29	852	3.35	0.09590	0.01438	92.9	1.8	92.0	1.3	158	23	1.0
50	280	1.86	0.09950	0.01440	96.3	2.2	92.1	1.4	247	39	4.4
100	1042	1.55	0.09710	0.01451	94.1	2.0	92.8	1.8	144	14	1.4
107	362	1.51	0.09510	0.01452	92.2	2.1	92.9	2.1	140	32	0.8
102	541	1.84	0.09860	0.01452	95.4	1.7	93.0	1.1	184	24	2.5
71	427.1	2.68	0.09620	0.01455	93.6	2.1	93.1	1.0	146	30	0.5
45	433	2.00	0.09510	0.01457	92.2	1.9	93.2	1.3	126	20	1.1
78	521	2.18	0.09770	0.01459	94.6	2.0	93.4	1.3	166	24	1.3
72	564	2.68	0.09530	0.01461	92.4	1.8	93.5	1.7	123	20	1.2
28	800	2.07	0.09920	0.01466	96.0	1.8	93.8	1.1	161	18	2.3
68	194	1.47	0.09720	0.01470	94.1	2.4	94.0	1.8	210	35	0.1
73	478	2.66	0.09770	0.01471	94.6	1.8	94.1	1.1	149	26	0.5
53	485	2.50	0.10690	0.01486	103.1	2.7	95.1	1.4	279	48	7.8
1	621	1.52	0.10150	0.01489	98.2	2.2	95.3	1.6	153	24	3.0
16	376	2.20	0.09910	0.01490	95.9	1.7	95.3	1.1	135	19	0.6
96	90.7	1.72	0.10200	0.01491	99.0	11.0	95.4	3.6	263	91	3.6

12MCSMG1					207/ 235		206/ 238		206/ 207		
	[U] ppm	U/Th	207/235	206/ 238	Age Ma	2σ err	Age (Ma)	2σ err	Age (Ma)	2σ err	% Disc
60	454	11.64	0.10300	0.01493	99.5	5.2	95.5	1.3	233	59	4.0
62	413	1.63	0.09680	0.01493	93.8	1.8	95.6	1.1	126	22	1.9
112	128.8	1.22	0.09920	0.01495	96.0	3.5	95.6	2.0	266	47	0.4
36	484	2.15	0.10050	0.01495	97.2	1.3	95.7	1.1	174	20	1.5
103	117.2	1.48	0.10990	0.01506	105.7	4.5	96.4	1.9	429	77	8.8
93	309	1.88	0.10220	0.01510	99.0	2.0	96.6	1.2	158	26	2.4
94	477	3.22	0.10040	0.01511	97.1	1.9	96.7	1.2	171	23	0.4
109	180	1.27	0.10650	0.01517	102.7	3.2	97.0	1.6	326	52	5.6
9	72.6	1.52	0.10640	0.01520	102.5	7.8	97.2	3.0	430	120	5.2
105	290	1.56	0.10490	0.01519	101.6	2.5	97.2	1.9	212	30	4.3
20	145.9	1.60	0.10340	0.01520	99.8	3.7	97.3	2.4	227	38	2.5
6	554	4.97	0.10560	0.01528	101.9	2.7	97.7	2.0	216	24	4.1
8	553	2.30	0.10130	0.01529	98.0	2.1	97.8	1.5	168	26	0.2
39	392	3.54	0.10520	0.01531	101.5	1.7	98.0	1.2	208	23	3.4
114	511	2.36	0.10480	0.01534	101.2	2.5	98.2	2.3	186	25	3.0
116	136.1	1.89	0.10760	0.01535	103.7	4.4	98.2	2.3	294	55	5.3
86	444	1.93	0.10690	0.01538	103.1	1.8	98.4	1.4	215	25	4.6
11	106	1.39	0.11220	0.01543	107.8	4.5	98.7	2.2	326	58	8.4
14	301	1.87	0.10250	0.01552	99.0	2.4	99.2	1.7	153	25	0.2
18	282	2.19	0.10230	0.01551	98.9	2.8	99.2	1.8	153	29	0.3
12	227	2.00	0.10630	0.01552	102.5	2.5	99.3	1.2	201	28	3.1
89	115.7	1.16	0.11340	0.01553	109.4	3.7	99.4	2.0	391	43	9.1
55	488	1.41	0.10250	0.01564	99.1	2.1	100.0	1.1	129	23	0.9
97	494	2.20	0.10190	0.01568	98.5	1.9	100.3	1.2	154	32	1.8
4	270	1.73	0.10600	0.01577	102.2	2.0	100.9	1.2	215	35	1.3
5	170	2.33	0.10860	0.01578	104.6	3.3	101.0	1.3	279	41	3.4
40	275	2.84	0.10740	0.01579	103.5	2.5	101.0	1.6	203	36	2.4
64	214	1.49	0.10360	0.01581	100.1	2.6	101.1	1.7	158	30	1.0
26	166	1.18	0.11410	0.01591	109.6	4.5	101.7	1.6	293	63	7.2
25	545	1.46	0.11200	0.01603	107.7	2.8	102.5	1.7	225	33	4.8
7	324	2.31	0.10870	0.01605	104.8	1.8	102.7	1.1	188	26	2.0
67	164.1	2.20	0.10830	0.01610	104.3	2.7	103.0	1.6	231	41	1.2
49	568	1.83	0.10700	0.01619	103.2	2.5	103.5	1.4	118	37	0.3
61	379	1.72	0.11510	0.01641	110.6	2.8	104.9	1.3	236	37	5.2
23	430	3.05	0.11460	0.01657	110.1	2.4	105.9	1.2	195	23	3.8
84	427	2.47	0.11410	0.01664	109.7	2.5	106.4	1.4	173	30	3.0

12MCSMG1					207/ 235		206/ 238		206/ 207		
	[U] ppm	U/Th	207/235	206/ 238	Age Ma	2σ err	Age (Ma)	2σ err	Age (Ma)	2σ err	% Disc
90	447	3.22	0.12070	0.01670	115.6	3.8	106.7	2.3	299	34	7.7
83	277.2	1.22	0.11410	0.01672	109.6	3.7	106.9	1.7	213	44	2.5
17	505	3.34	0.11170	0.01679	107.4	2.3	107.3	2.0	177	23	0.1
32	217	1.27	0.11480	0.01691	110.2	3.6	108.1	2.1	170	33	1.9
13	172	1.47	0.11390	0.01695	109.4	3.4	108.3	1.6	187	33	1.0
24	243	2.19	0.11660	0.01707	111.9	3.9	109.1	2.6	205	36	2.5
82	177	1.67	0.11570	0.01712	111.1	3.9	109.4	2.0	277	58	1.5
119	108.3	1.15	0.12260	0.01721	118.6	4.7	110.0	2.3	360	54	7.3
120	331	1.34	0.11500	0.01742	110.5	2.5	111.3	1.8	150	26	0.7
104	302	1.28	0.11870	0.01752	113.9	2.2	112.0	1.4	224	32	1.7
106	229	1.13	0.14020	0.02050	133.1	2.9	130.8	2.1	234	27	1.7
63	757	3.97	0.28840	0.03966	257.2	2.9	250.7	2.3	318	18	2.5
75	67.4	1.10	1.90300	0.17980	1081.9	6.4	1065.6	9.9	1121	12	4.9
113	39.5	0.78	2.85500	0.23560	1369.0	10.0	1364.0	14.0	1361	16	0.2
95	676	149.00	4.06300	0.28530	1646.5	7.3	1620.0	14.0	1668	9	2.9
101	540	47.10	3.85700	0.26610	1605.2	7.8	1521.0	14.0	1701	5	10.6

12MCSMG3					207/ 235		206/ 238		206/ 207		
#	[U] ppm	U/Th	207/ 235	206/ 238	Age Ma	2 σ err	Age (Ma)	2 σ err	Age (Ma)	2 σ err	% Disc
67	1134	2.48	0.07070	0.01129	69.4	1.5	72.4	1.3	188.0	26	-4.3
98	171.6	2.44	0.07710	0.01257	75.4	3.0	80.6	2.2	251.0	66	-6.9
104	115.7	2.03	0.09140	0.01343	88.7	4.2	86.0	3.0	327.0	44	3.0
121	5.6	2.33	0.09220	0.01371	89.5	1.9	87.7	1.5	157.0	20	2.0
75	542	2.64	0.08940	0.01375	86.9	2.0	88.0	1.2	167.0	33	-1.3
46	378	2.78	0.09160	0.01376	89.0	2.7	88.1	1.7	206.0	40	1.0
40	639	1.05	0.09260	0.01387	89.9	2.1	88.8	1.7	166.0	24	1.2
43	325	1.61	0.09540	0.01404	92.5	2.6	89.9	1.7	247.0	39	2.8
72	495	2.74	0.09480	0.01411	92.2	2.3	90.3	1.6	182.0	32	2.1
19	436	1.57	0.09500	0.01417	92.1	1.9	90.7	1.2	175.0	28	1.5
61	1360	21.70	0.09540	0.01428	92.5	1.8	91.4	1.2	135.0	19	1.2
74	291	2.25	0.09600	0.01429	93.4	2.7	91.4	1.7	211.0	36	2.1
115	449	8.50	0.09620	0.01436	93.2	2.2	91.9	1.8	203.0	35	1.4
29	248	2.28	0.09420	0.01442	91.3	2.6	92.3	1.8	168.0	37	-1.1
96	520	2.89	0.09370	0.01448	90.9	2.8	92.7	1.5	131.0	24	-2.0
69	639	2.28	0.09690	0.01453	93.9	3.0	93.0	2.0	166.0	27	1.0
102	308	2.78	0.09670	0.01453	93.7	2.7	93.0	1.7	228.0	40	0.7
3	318	1.92	0.09540	0.01456	92.5	2.4	93.2	1.5	145.0	34	-0.8
39	204	2.91	0.09810	0.01460	94.9	3.6	93.4	2.0	264.0	46	1.6
119	7.2	1.92	0.09800	0.01459	94.9	3.1	93.4	1.7	220.0	37	1.6
106	257	1.81	0.09740	0.01461	94.3	2.5	93.5	1.7	214.0	31	0.8
90	571	3.05	0.09570	0.01459	92.7	2.1	93.6	1.5	166.0	28	-1.0
4	771	3.12	0.09510	0.01466	92.2	2.1	93.8	1.0	140.0	28	-1.7
17	690	2.66	0.09730	0.01472	94.3	2.1	94.2	1.4	153.0	29	0.1
114	520.1	2.47	0.09730	0.01475	94.2	1.9	94.5	1.1	134.0	23	-0.3
28	286	1.81	0.09940	0.01485	96.2	2.4	95.0	1.6	229.0	44	1.2
62	325	1.86	0.10160	0.01485	98.2	2.7	95.0	1.5	188.0	21	3.3
27	266	1.35	0.09920	0.01486	95.9	3.9	95.1	2.2	265.0	53	0.8
57	417	1.47	0.09790	0.01486	94.8	2.5	95.1	1.7	183.0	39	-0.3
93	395	2.21	0.09870	0.01486	95.5	2.5	95.1	2.0	190.0	30	0.4
30	382	2.57	0.09780	0.01487	95.0	2.2	95.2	1.3	207.0	33	-0.2
38	391	4.97	0.09660	0.01489	93.6	2.2	95.2	1.7	168.0	28	-1.7
7	77	2.40	0.09500	0.01490	91.9	4.7	95.3	2.7	309.0	68	-3.7
112	404	2.07	0.09600	0.01491	93.0	2.6	95.4	2.0	111.0	30	-2.6
11	243	1.64	0.09710	0.01492	94.0	3.2	95.5	1.6	192.0	31	-1.6

12MCSMG3					207/ 235		206/ 238		206/ 207		
#	[U] ppm	U/Th	207/ 235	206/ 238	Age Ma	2σ err	Age (Ma)	2σ err	Age (Ma)	2σ err	% Disc
111	303	2.18	0.09930	0.01492	96.1	2.2	95.5	1.7	205.0	35	0.6
101	203	3.02	0.10070	0.01494	97.4	3.3	95.6	2.0	241.0	35	1.8
71	569	1.90	0.10830	0.01499	104.3	2.4	95.9	2.0	324.0	38	8.1
41	550	4.26	0.10090	0.01502	97.6	2.3	96.1	1.5	171.0	26	1.5
76	394	3.24	0.09910	0.01502	95.9	2.8	96.1	1.5	215.0	34	-0.2
54	332	1.47	0.10170	0.01506	98.3	2.6	96.4	1.8	178.0	29	1.9
83	207.8	1.66	0.10500	0.01507	101.3	4.0	96.4	2.3	265.0	46	4.8
59	244	2.86	0.10300	0.01513	99.4	3.9	96.8	2.0	267.0	47	2.6
66	421	2.20	0.10140	0.01515	98.0	2.8	96.9	1.5	209.0	47	1.1
87	373	2.19	0.10290	0.01515	99.4	2.0	96.9	1.4	172.0	24	2.5
81	564	3.83	0.10590	0.01516	102.2	2.7	97.0	1.0	220.0	29	5.1
64	660	3.50	0.10220	0.01516	98.8	2.2	97.0	1.9	225.0	40	1.8
16	210	2.63	0.10150	0.01518	98.0	3.2	97.1	2.1	276.0	44	0.9
24	336	3.61	0.09950	0.01518	96.2	2.4	97.1	1.5	138.0	23	-0.9
78	424.3	1.09	0.09930	0.01517	96.1	1.8	97.1	1.3	152.0	28	-1.0
9	258	2.18	0.09960	0.01522	96.3	3.1	97.4	1.7	218.0	41	-1.1
53	404	2.03	0.10360	0.01523	100.0	2.4	97.4	1.8	229.0	38	2.6
42	309	2.60	0.09960	0.01525	96.4	2.4	97.5	2.0	183.0	38	-1.1
55	279	2.11	0.10030	0.01525	97.0	3.5	97.5	1.3	209.0	33	-0.5
49	441	2.30	0.10330	0.01525	100.1	2.3	97.6	1.3	192.0	28	2.5
100	91	2.15	0.10180	0.01526	98.2	5.8	97.6	3.0	423.0	98	0.6
91	229	3.16	0.10100	0.01527	97.6	3.2	97.7	1.7	255.0	42	-0.1
23	285	2.84	0.09920	0.01530	96.0	2.7	97.9	1.5	186.0	36	-2.0
52	664	4.08	0.10240	0.01534	99.0	2.0	98.1	1.1	156.0	21	0.9
73	175	2.85	0.10060	0.01531	97.2	3.5	98.2	2.4	183.0	39	-1.0
77	518	2.13	0.10070	0.01534	97.4	2.0	98.2	1.6	145.0	25	-0.8
95	324	2.52	0.10140	0.01536	98.0	2.1	98.2	1.5	210.0	36	-0.2
48	284	3.25	0.10580	0.01538	102.5	3.6	98.4	2.6	253.0	60	4.0
15	867	2.16	0.10270	0.01541	99.2	1.6	98.6	1.1	167.0	20	0.6
108	479	7.10	0.10040	0.01541	97.1	2.3	98.6	1.3	160.0	26	-1.5
32	272	1.74	0.09950	0.01543	96.3	2.5	98.7	1.8	162.0	27	-2.5
36	428	1.51	0.11390	0.01542	109.4	2.7	98.7	2.3	308.0	48	9.8
37	168	2.58	0.10140	0.01543	98.0	3.1	98.7	2.3	205.0	40	-0.7
85	371	2.71	0.10390	0.01543	100.3	2.5	98.7	1.3	210.0	30	1.6
120	5.9	3.54	0.10630	0.01545	102.6	2.0	98.8	1.5	198.0	25	3.7
5	478	1.67	0.10950	0.01545	105.5	3.5	98.9	2.4	247.0	37	6.3

12MCSMG3					207/ 235		206/ 238		206/ 207		
#	[U] ppm	U/Th	207/ 235	206/ 238	Age Ma	2σ err	Age (Ma)	2σ err	Age (Ma)	2σ err	% Disc
35	38.4	2.73	0.10200	0.01547	98.2	6.8	99.0	2.8	426.0	70	-0.8
70	405	2.05	0.10350	0.01547	100.0	2.4	99.0	1.3	154.0	25	1.0
50	574	3.17	0.10400	0.01549	100.4	2.0	99.1	1.3	164.0	29	1.3
26	359	3.79	0.10570	0.01551	101.9	3.1	99.2	1.6	290.0	39	2.6
105	365	1.62	0.09770	0.01551	94.6	3.9	99.2	1.7	117.0	28	-4.9
79	347	4.30	0.10180	0.01552	98.4	2.3	99.3	1.3	141.0	27	-0.9
80	281	2.12	0.10450	0.01556	100.8	2.9	99.5	1.6	183.0	34	1.3
14	546	1.20	0.10220	0.01556	99.0	1.9	99.6	1.0	146.0	23	-0.6
51	120	2.97	0.10320	0.01559	100.2	5.5	99.7	3.4	403.0	92	0.5
88	330	7.60	0.10370	0.01561	100.0	3.7	99.9	2.4	211.0	38	0.1
117	1450	6.03	0.10380	0.01562	100.3	1.7	99.9	1.9	143.0	28	0.4
2	298.2	2.25	0.10220	0.01563	98.7	4.4	100.0	1.9	200.0	47	-1.3
82	250	4.59	0.10430	0.01565	100.6	4.4	100.1	2.9	239.0	42	0.5
22	671	2.55	0.10490	0.01567	101.2	1.9	100.2	1.1	170.0	30	1.0
89	609	2.33	0.10550	0.01568	102.1	2.5	100.3	2.0	171.0	22	1.8
12	301	1.68	0.10530	0.01570	101.6	2.2	100.4	1.5	193.0	30	1.2
47	256	2.33	0.10520	0.01570	101.5	3.0	100.4	1.7	181.0	26	1.1
31	394	4.07	0.10610	0.01581	102.3	2.9	101.1	1.6	189.0	30	1.2
118	450	3.06	0.10340	0.01580	99.9	2.4	101.1	1.8	130.0	28	-1.2
45	266	2.63	0.10290	0.01585	99.4	3.4	101.3	2.1	210.0	38	-1.9
113	2440	5.91	0.10560	0.01584	101.9	2.1	101.3	1.8	145.0	26	0.6
86	255	2.76	0.10450	0.01585	100.9	6.9	101.4	3.0	250.0	110	-0.5
8	265	1.56	0.10290	0.01587	99.3	3.0	101.5	1.6	149.0	33	-2.2
94	281	1.50	0.10860	0.01592	104.6	3.1	101.8	2.2	294.0	42	2.7
110	344	4.18	0.10850	0.01591	104.9	3.5	101.8	2.1	223.0	41	3.0
13	187	2.31	0.10180	0.01594	98.3	4.0	101.9	2.0	200.0	44	-3.7
33	540	3.84	0.10630	0.01594	102.5	2.5	101.9	1.3	174.0	18	0.6
92	553	2.42	0.10650	0.01596	102.7	2.0	102.1	1.2	185.0	29	0.6
10	371	1.83	0.10130	0.01597	97.9	2.8	102.2	1.6	97.0	29	-4.4
58	546	1.69	0.10470	0.01598	101.0	2.3	102.2	1.9	164.0	26	-1.2
25	194	1.98	0.10960	0.01600	105.4	4.7	102.3	2.1	264.0	51	2.9
56	950	2.07	0.10680	0.01611	103.0	1.8	103.0	1.7	123.0	15	0.0
116	296	1.66	0.10840	0.01610	105.0	2.8	103.0	2.6	188.0	42	1.9
68	368	3.08	0.10920	0.01619	105.2	2.4	103.6	1.6	196.0	31	1.5
99	740	3.04	0.10510	0.01620	101.4	2.0	103.6	1.3	150.0	23	-2.2
21	531	1.72	0.10820	0.01626	104.3	2.7	104.0	2.3	162.0	26	0.3

12MCSMG3					207/ 235		206/ 238		206/ 207		
#	[U ppm	U/Th	207/ 235	206/ 238	Age Ma	2σ err	Age (Ma)	2σ err	Age (Ma)	2σ err	% Disc
97	291	3.65	0.11280	0.01649	108.4	2.9	105.4	1.7	242.0	33	2.8
103	670	2.70	0.10780	0.01650	103.9	2.1	105.5	1.9	146.0	30	-1.5
6	387	1.63	0.11030	0.01668	106.1	2.6	106.6	1.6	150.0	28	-0.5
84	423	2.50	0.11090	0.01672	107.1	2.5	106.9	1.6	180.0	27	0.2
20	206	1.61	0.15950	0.02330	150.2	3.5	148.4	2.1	252.0	32	1.2
65	198.6	1.98	0.17950	0.02647	167.5	4.1	168.4	3.7	213.0	33	-0.5
18	186	2.10	0.18700	0.02766	173.9	4.8	175.8	4.2	223.0	37	-1.1

12MCSMG4					207/ 235		206/ 238		206/ 207		
#	[U] ppm	U/Th	207/ 235	206/ 238	Age Ma	2σ err	Age (Ma)	2σ err	Age (Ma)	2σ err	% Disc
84	835	2.71	0.08920	0.01258	86.7	1.4	80.6	0.8	242.0	19	7.0
58	1570	4.31	0.08800	0.01274	85.6	1.3	81.6	1.1	173.0	19	4.7
117	860	2.00	0.08730	0.01297	85.0	1.8	83.1	1.4	141.0	23	2.2
42	219	3.88	0.08640	0.01311	84.1	1.9	83.9	1.3	115.0	23	0.2
35	1017	5.99	0.08872	0.01317	86.3	0.8	84.3	0.8	144.0	14	2.3
56	1120	28.00	0.08700	0.01318	84.7	1.0	84.4	0.6	118.0	16	0.4
109	661	1.65	0.09010	0.01323	87.6	1.0	84.8	0.8	149.0	18	3.2
13	535.1	1.80	0.08740	0.01328	85.1	1.3	85.0	1.0	96.0	19	0.1
61	779	10.40	0.08720	0.01329	84.9	1.1	85.1	1.0	96.0	13	-0.3
3	1039	3.68	0.08830	0.01336	85.9	0.8	85.6	0.7	101.0	13	0.4
107	970	4.28	0.09000	0.01339	87.5	1.0	85.8	0.7	129.0	13	2.0
22	108.1	3.26	0.09280	0.01340	90.0	3.0	85.8	1.2	224.0	34	4.7
116	1031	6.30	0.08958	0.01341	87.1	0.9	85.8	0.6	128.0	11	1.4
62	1370	51.00	0.08950	0.01342	87.2	1.0	85.9	0.9	126.0	13	1.5
15	625	4.63	0.08880	0.01344	86.4	0.9	86.1	0.7	120.0	14	0.4
98	905	3.14	0.08970	0.01345	87.2	1.1	86.1	0.6	132.0	18	1.3
67	577	10.74	0.08880	0.01347	86.4	1.0	86.2	0.6	96.0	15	0.2
79	636	2.73	0.09230	0.01349	89.6	2.2	86.4	1.0	206.0	43	3.6
60	703	4.03	0.08940	0.01355	87.1	1.1	86.8	0.7	111.0	16	0.4
104	96.6	3.20	0.09310	0.01355	90.4	2.7	86.8	1.7	212.0	35	4.0
49	240	2.23	0.09160	0.01357	89.0	1.6	86.9	1.1	188.0	30	2.4
25	626	10.56	0.08950	0.01357	87.1	1.1	86.9	0.9	110.0	16	0.2
16	325	5.63	0.08910	0.01359	86.6	1.6	87.0	1.0	130.0	19	-0.5
32	746	2.56	0.09130	0.01360	88.7	1.1	87.1	0.7	136.0	15	1.8
31	333	2.40	0.09530	0.01361	92.4	2.2	87.1	1.4	234.0	43	5.7
83	1269	2.29	0.09160	0.01365	89.0	1.0	87.4	0.8	134.0	13	1.8
24	291	8.04	0.09400	0.01369	91.2	1.5	87.7	1.0	204.0	34	3.9
111	490	1.76	0.09480	0.01371	92.0	1.5	87.8	1.3	235.0	26	4.6
4	300	4.54	0.09010	0.01375	87.6	1.4	88.0	0.8	127.0	20	-0.5
114	149.8	3.51	0.09390	0.01373	91.0	2.5	88.1	1.3	206.0	31	3.2
38	362	2.74	0.09890	0.01378	95.7	2.6	88.2	1.1	282.0	43	7.8
53	382	3.67	0.09500	0.01376	92.1	1.9	88.2	0.9	230.0	29	4.2
28	167.1	1.98	0.09240	0.01383	89.7	1.8	88.5	1.0	171.0	29	1.3
93	367	2.72	0.09250	0.01383	89.8	1.1	88.5	0.9	146.0	18	1.4
26	190	2.39	0.09070	0.01385	88.1	2.0	88.6	1.4	133.0	29	-0.6
122	243.6	4.10	0.09580	0.01385	92.9	1.8	88.6	1.1	210.0	30	4.6

12MCSMG4					207/ 235		206/ 238		206/ 207		
#	[U] ppm	U/Th	207/ 235	206/ 238	Age Ma	2σ err	Age (Ma)	2σ err	Age (Ma)	2σ err	% Disc
102	195.4	3.31	0.09700	0.01389	94.0	1.9	88.9	1.0	234.0	21	5.4
11	376.2	3.50	0.09300	0.01389	90.5	1.2	89.0	0.8	163.0	22	1.7
44	907	10.50	0.09190	0.01390	89.2	1.2	89.0	1.1	105.0	11	0.2
59	1040	8.40	0.09230	0.01395	89.6	0.7	89.3	0.7	106.0	11	0.4
10	940	2.70	0.10100	0.01398	97.7	1.3	89.5	1.1	318.0	20	8.4
87	1820	4.74	0.09290	0.01399	90.2	1.0	89.6	0.7	122.0	16	0.7
40	436	5.09	0.09220	0.01400	89.6	1.2	89.6	0.7	125.0	21	0.0
112	593	13.00	0.09440	0.01400	91.6	1.4	89.6	1.1	154.0	21	2.2
57	601	2.82	0.09310	0.01401	90.3	1.7	89.7	1.0	144.0	30	0.7
103	944	3.71	0.09410	0.01401	91.3	1.1	89.7	0.6	127.0	16	1.8
51	842	4.04	0.09330	0.01407	90.6	1.0	90.1	0.7	113.0	13	0.6
1	1890	18.20	0.09360	0.01413	90.8	1.0	90.4	1.0	115.0	15	0.5
43	208	3.27	0.09290	0.01414	90.2	1.9	90.5	0.9	159.0	29	-0.3
95	657	3.00	0.09870	0.01417	95.6	1.5	90.7	0.9	225.0	26	5.1
100	830	4.64	0.09750	0.01418	94.4	1.8	90.7	1.1	185.0	32	3.9
72	662	2.42	0.09380	0.01417	91.1	1.2	90.7	0.9	112.0	16	0.4
106	262.8	2.04	0.09460	0.01419	91.8	1.5	90.8	0.9	165.0	23	1.1
105	329	3.75	0.09570	0.01421	92.7	2.1	91.0	1.1	177.0	32	1.8
63	364	1.84	0.09200	0.01423	89.4	1.3	91.1	0.8	120.0	22	-1.9
2	374	3.10	0.09400	0.01424	91.2	1.4	91.2	0.8	131.0	22	0.1
70	391	3.37	0.09420	0.01424	91.4	1.2	91.2	0.7	129.0	19	0.3
71	1480	2.54	0.09560	0.01427	92.6	1.5	91.3	1.1	159.0	15	1.4
7	268	3.11	0.09410	0.01427	91.2	1.7	91.4	0.9	138.0	18	-0.2
34	328	3.17	0.09490	0.01427	92.1	1.3	91.4	0.8	124.0	16	0.8
45	620	1.01	0.09570	0.01430	92.8	1.2	91.5	0.8	134.0	18	1.4
46	860	9.30	0.09420	0.01430	91.4	1.4	91.5	0.8	83.0	15	-0.1
50	534	6.17	0.09380	0.01430	91.0	1.2	91.6	1.0	94.0	13	-0.6
82	340	3.34	0.09640	0.01432	93.4	1.3	91.7	0.8	157.0	20	1.9
123	700	2.16	0.09430	0.01434	91.5	1.9	91.8	1.1	153.0	26	-0.3
74	884	2.63	0.10040	0.01437	97.1	2.0	92.0	1.1	234.0	35	5.3
68	382	2.15	0.09560	0.01438	92.7	1.3	92.0	0.8	129.0	18	0.7
89	251.6	2.02	0.09960	0.01438	96.4	1.9	92.0	0.9	212.0	26	4.5
65	955	1.07	0.09545	0.01439	92.6	0.9	92.1	0.7	115.0	11	0.5
27	244.4	1.97	0.09500	0.01441	92.2	1.5	92.2	0.9	120.0	16	0.0
85	169.4	2.42	0.09770	0.01440	94.6	1.8	92.2	1.1	162.0	23	2.5
124	333	5.91	0.10510	0.01441	101.4	2.6	92.2	1.0	336.0	49	9.1

12MCSMG4					207/ 235		206/ 238		206/ 207		
#	[U] ppm	U/Th	207/ 235	206/ 238	Age Ma	2σ err	Age (Ma)	2σ err	Age (Ma)	2σ err	% Disc
37	514	1.85	0.09560	0.01446	92.7	1.3	92.5	0.9	140.0	20	0.2
79	427	2.05	0.09810	0.01450	95.0	2.5	92.8	1.5	140.0	18	2.3
21	1556	5.74	0.09470	0.01455	91.8	2.2	93.1	2.0	97.0	21	-1.4
120	265	2.85	0.10160	0.01464	98.2	3.0	93.7	1.0	222.0	43	4.6
6	489	1.62	0.09620	0.01468	93.2	1.0	94.0	0.9	117.0	19	-0.8
12	630	12.70	0.09860	0.01474	95.5	1.6	94.3	1.0	140.0	15	1.3
69	542	1.81	0.09870	0.01485	95.5	1.4	95.0	0.7	120.0	16	0.5
48	1020	2.79	0.09880	0.01492	95.7	1.1	95.5	0.8	116.0	11	0.2
75	346	2.97	0.10580	0.01500	102.1	2.2	96.0	1.0	242.0	33	6.0
96	404	2.53	0.09970	0.01505	96.5	1.7	96.3	1.0	131.0	20	0.2
8	420	3.60	0.10190	0.01539	98.5	2.4	98.5	2.3	124.0	33	0.0
1	429	6.60	0.10290	0.01564	99.4	2.8	100.1	1.2	132.0	41	-0.7
108	225	1.77	0.10370	0.01565	100.2	3.2	100.1	2.1	142.0	40	0.1
87	297	1.91	0.10420	0.01566	100.6	2.5	100.2	1.4	117.0	26	0.4
74	520	2.62	0.10960	0.01603	105.6	2.4	102.5	1.4	158.0	28	2.9
18	195.8	2.82	0.10720	0.01605	103.3	5.7	102.7	2.2	236.0	87	0.6
76	144.5	1.41	0.16290	0.02438	153.2	2.7	155.3	1.8	146.0	24	-1.4
108	114.1	2.04	0.15900	0.02442	150.5	3.8	155.5	2.5	138.0	29	-3.3
52	403	2.06	0.16860	0.02460	158.1	2.4	156.7	1.3	189.0	24	0.9
92	317	1.58	3.87900	0.27180	1609.1	4.3	1550.1	7.9	1690.2	5	8.3

13MCSMG25					207/ 235		206/ 238		206/ 207		
#	[U] ppm	U/Th	207/ 235	206/ 238	Age Ma	2 σ err	Age (Ma)	2 σ err	Age (Ma)	2 σ err	% Disc
10	575	2.53	0.08660	0.01292	84.7	2.5	82.8	1.3	213.0	35	2.2
62	195	3.05	0.08940	0.01320	87.7	3.4	84.5	1.8	231.0	35	3.6
61	316	1.48	0.09350	0.01342	90.7	3.2	85.9	1.6	262.0	44	5.3
57	590	3.65	0.09010	0.01348	87.5	2.3	86.3	1.6	213.0	29	1.4
58	533	2.25	0.09240	0.01349	89.7	2.4	86.4	1.5	208.0	36	3.7
59	186	5.39	0.08740	0.01351	85.0	3.3	86.5	1.9	268.0	57	-1.8
41	542	14.10	0.09230	0.01357	89.6	3.0	86.9	1.4	310.0	53	3.0
63	302	1.99	0.09150	0.01373	88.9	2.7	87.9	1.5	225.0	35	1.1
13	467	2.88	0.08980	0.01384	87.3	2.4	88.6	1.5	203.0	39	-1.5
33	142	2.69	0.09060	0.01395	87.9	3.9	89.3	2.1	254.0	45	-1.6
29	387	1.56	0.09440	0.01406	91.6	2.2	90.0	1.4	173.0	32	1.7
37	352	1.61	0.09810	0.01436	95.0	2.7	91.9	1.3	195.0	30	3.3
110	1380	33.21	0.09590	0.01440	93.0	1.7	92.2	1.0	120.0	23	0.9
21	170	1.75	0.09530	0.01440	92.3	2.8	92.2	1.8	244.0	43	0.1
64	1253	3.58	0.09500	0.01441	92.1	2.8	92.2	1.4	149.0	40	-0.1
102	448	1.68	0.10040	0.01445	97.1	2.5	92.5	1.7	230.0	32	4.7
60	127	1.26	0.09670	0.01454	93.7	3.4	93.0	2.2	238.0	49	0.7
7	247	1.66	0.09740	0.01454	94.3	2.9	93.1	1.5	231.0	39	1.3
96	302	2.33	0.10030	0.01457	96.9	4.6	93.3	1.7	235.0	53	3.7
42	750	16.00	0.09610	0.01459	93.1	2.8	93.4	1.6	170.0	35	-0.3
19	261	1.44	0.09770	0.01462	94.6	2.7	93.6	1.7	162.0	28	1.1
45	446	1.70	0.09670	0.01468	93.6	2.5	93.9	1.3	179.0	27	-0.3
114	240	2.90	0.09760	0.01467	94.4	3.6	93.9	1.9	217.0	43	0.5
46	629	6.70	0.09900	0.01474	95.9	1.6	94.3	1.1	159.0	23	1.7
5	308	1.46	0.09770	0.01475	94.6	2.2	94.4	1.6	217.0	31	0.2
9	238	2.75	0.09920	0.01478	96.0	3.0	94.6	2.0	226.0	35	1.5
74	193	1.73	0.10230	0.01480	98.8	5.4	94.7	2.0	265.0	57	4.1
93	180	1.69	0.10210	0.01482	99.2	4.4	94.8	2.3	300.0	55	4.4
80	497	2.23	0.10130	0.01482	98.0	2.8	94.9	1.4	221.0	46	3.2
103	407	1.92	0.09980	0.01483	96.9	2.6	94.9	1.2	198.0	34	2.1
22	464	3.11	0.10060	0.01486	97.3	2.2	95.1	1.6	175.0	35	2.3
47	350.3	2.00	0.09900	0.01486	95.8	2.5	95.1	1.4	217.0	31	0.7
11	901	6.26	0.09820	0.01492	95.0	2.1	95.4	1.2	168.0	26	-0.4
17	720	5.59	0.10360	0.01492	100.0	3.6	95.5	1.6	266.0	47	4.5
67	265	2.12	0.09920	0.01494	96.0	2.7	95.6	1.7	217.0	36	0.4
99	351	1.42	0.09910	0.01495	95.9	2.6	95.6	1.6	189.0	30	0.3

13MCSMG25					207/ 235		206/ 238		206/ 207		
#	[U] ppm	U/Th	207/ 235	206/ 238	Age Ma	2σ err	Age (Ma)	2σ err	Age (Ma)	2σ err	% Disc
27	195	1.94	0.09650	0.01497	93.4	3.5	95.8	1.8	193.0	36	-2.6
34	101	2.99	0.10400	0.01497	100.2	4.4	95.8	2.5	365.0	58	4.4
113	492	2.13	0.09460	0.01497	91.7	2.3	95.8	1.7	111.0	28	-4.5
3	452	2.71	0.09810	0.01504	95.0	2.4	96.2	1.1	148.0	28	-1.3
84	571	2.87	0.09810	0.01503	95.0	2.1	96.2	1.2	158.0	32	-1.3
98	1770	2.52	0.10030	0.01505	97.0	1.7	96.3	1.4	136.0	21	0.7
100	315	1.92	0.10340	0.01507	99.8	3.2	96.4	1.3	279.0	46	3.4
95	434	2.82	0.10330	0.01508	99.8	3.5	96.5	2.1	304.0	62	3.3
71	720	2.18	0.10180	0.01511	98.4	2.2	96.7	1.5	207.0	36	1.7
25	424	2.05	0.09810	0.01516	95.3	2.1	97.0	1.2	175.0	39	-1.8
70	284	2.29	0.10280	0.01516	99.2	2.9	97.0	2.1	251.0	48	2.2
124	8.8	2.52	0.10170	0.01517	98.2	2.7	97.0	1.7	225.0	42	1.2
68	371	3.41	0.10240	0.01520	98.8	4.0	97.3	2.0	284.0	52	1.5
91	458	1.20	0.10070	0.01521	97.4	2.5	97.3	1.4	137.0	26	0.1
86	416	2.75	0.09990	0.01523	96.6	3.5	97.4	1.4	149.0	36	-0.8
123	8.2	1.52	0.10360	0.01523	100.0	3.6	97.4	1.8	249.0	35	2.6
72	205	2.26	0.10150	0.01524	98.5	3.0	97.5	2.1	201.0	35	1.0
106	225	2.19	0.10200	0.01524	98.5	3.2	97.5	1.6	242.0	37	1.0
111	155	2.11	0.09790	0.01525	94.7	4.3	97.5	2.7	321.0	73	-3.0
8	239	2.88	0.10190	0.01526	98.4	3.1	97.6	1.8	232.0	38	0.8
35	416	2.05	0.10040	0.01525	97.1	2.9	97.6	1.6	164.0	29	-0.5
1	161.6	1.68	0.09880	0.01527	95.5	5.1	97.7	3.6	219.0	49	-2.3
53	354	6.24	0.10220	0.01527	98.8	2.7	97.7	1.6	201.0	29	1.1
118	11	4.11	0.09730	0.01528	94.2	3.5	97.7	1.8	233.0	53	-3.7
122	8.8	2.23	0.10300	0.01529	99.5	3.4	97.8	1.7	200.0	35	1.7
49	408	4.76	0.10160	0.01531	98.2	4.9	97.9	2.6	214.0	45	0.3
87	142.6	1.82	0.10490	0.01531	101.2	4.6	97.9	2.4	339.0	64	3.3
92	498	2.85	0.10380	0.01533	100.2	2.6	98.1	1.7	206.0	33	2.1
48	161	2.37	0.10270	0.01535	99.1	3.8	98.2	2.0	308.0	64	0.9
79	720	2.06	0.10020	0.01538	97.3	2.4	98.4	1.5	162.0	23	-1.1
90	276	1.75	0.09810	0.01539	95.0	3.8	98.5	1.9	205.0	46	-3.7
119	9.2	1.33	0.10190	0.01540	98.5	3.4	98.5	1.7	237.0	79	0.0
20	123	2.51	0.10530	0.01542	102.1	3.6	98.6	2.0	294.0	42	3.4
50	269	2.82	0.10430	0.01546	100.7	2.8	98.9	1.8	224.0	39	1.8
36	139	3.36	0.10800	0.01549	104.0	5.0	99.1	2.2	319.0	56	4.7
2	315	1.95	0.10530	0.01554	101.6	3.1	99.4	1.7	256.0	33	2.2

13MCSMG25					207/ 235		206/ 238		206/ 207		
#	[U] ppm	U/Th	207/ 235	206/ 238	Age Ma	2σ err	Age (Ma)	2σ err	Age (Ma)	2σ err	% Disc
78	120.5	2.60	0.09810	0.01555	94.9	4.0	99.4	2.5	296	76	-4.7
112	668	2.87	0.10320	0.01554	99.7	1.7	99.4	1.5	142	19	0.3
31	685	3.70	0.10640	0.01556	102.7	2.4	99.5	1.6	225	30	3.1
23	98.6	1.34	0.10200	0.01559	99.0	4.7	99.7	2.6	393	78	-0.7
40	166.6	2.20	0.10300	0.01559	99.4	3.2	99.7	2.0	224	42	-0.3
109	780	2.36	0.10300	0.01563	99.5	2.3	99.9	1.5	155	23	-0.4
38	1090	5.20	0.10580	0.01566	102.1	2.3	100.1	1.5	165	26	2.0
94	206	1.00	0.10220	0.01566	98.7	3.7	100.1	2.1	224	41	-1.4
117	12	2.25	0.10640	0.01574	103.0	4.1	100.7	2.4	232	46	2.2
15	601	1.59	0.10310	0.01578	99.6	2.1	100.9	1.2	123	25	-1.3
105	890	3.19	0.10290	0.01583	99.8	2.2	101.3	1.4	124	22	-1.5
44	330	2.12	0.10920	0.01587	105.2	2.7	101.5	1.8	224	40	3.5
121	11	8.00	0.10240	0.01590	99.0	2.5	101.7	1.5	122	21	-2.7
16	456	1.31	0.10540	0.01606	101.7	2.2	102.7	1.4	173	31	-1.0
69	430	2.38	0.10570	0.01606	101.9	3.2	102.7	2.5	152	32	-0.8
75	163	2.98	0.10950	0.01611	105.4	4.2	103.0	2.2	297	48	2.3
51	352	1.63	0.10940	0.01614	105.3	2.8	103.2	1.3	231	37	2.0
97	201.1	2.36	0.10810	0.01617	104.1	3.7	103.4	2.0	189	33	0.7
28	287	2.03	0.11020	0.01618	106.1	4.1	103.5	2.6	234	47	2.5
12	562	2.81	0.11500	0.01624	110.4	6.0	103.8	2.8	259	74	6.0
32	213	1.91	0.10990	0.01624	105.8	3.7	103.9	2.1	273	42	1.8
108	240	4.95	0.10610	0.01631	102.3	3.5	104.3	2.1	170	45	-2.0
43	448	2.13	0.10930	0.01632	105.6	2.1	104.4	1.4	144	18	1.1
76	880	3.89	0.10500	0.01634	101.4	3.6	104.5	2.7	145	40	-3.1
55	351	2.55	0.10790	0.01642	104.0	3.2	105.0	1.3	183	36	-1.0
52	443	1.51	0.10750	0.01652	103.6	2.5	105.6	1.6	152	31	-1.9
54	285	2.01	0.11260	0.01712	108.2	3.8	109.4	2.4	168	34	-1.1
56	173	2.72	0.11600	0.01765	111.3	4.5	112.8	2.3	275	52	-1.3
39	249	1.91	0.16630	0.02433	156.0	3.8	155.0	2.6	196	31	0.6
89	147	2.02	0.17310	0.02434	162.6	5.3	155.0	3.2	311	46	4.7
116	16	1.77	0.18280	0.02448	170.0	6.9	155.9	3.3	398	59	8.3
107	242	1.51	0.17010	0.02478	160.4	3.8	157.8	2.4	246	33	1.6
26	111.6	1.95	0.16680	0.02488	156.4	5.0	158.4	3.0	238	43	-1.3
85	113.2	1.47	0.16560	0.02500	156.2	5.9	159.2	4.1	231	49	-1.9
14	66.4	2.33	0.16810	0.02518	157.4	6.8	160.3	3.4	377	86	-1.8
66	201.1	1.26	0.17220	0.02529	161.2	3.8	161.0	2.5	236	29	0.1

88	121	1.85	0.17340	0.02533	161.9	6.8	161.3	2.9	310	55	0.4
4	610	145.00	0.17430	0.02566	163.1	3.5	163.3	2.5	181	22	-0.1
73	197	1.53	0.18070	0.02567	169.3	4.1	163.4	3.6	235	43	3.5
82	198	3.14	0.17290	0.02585	161.8	4.3	164.5	2.8	210	35	-1.7
83	163	3.36	0.18150	0.02595	169.1	5.5	165.1	2.9	277	46	2.4
24	282	1.34	0.17980	0.02649	167.7	3.8	168.5	2.4	228	33	-0.5
30	79.4	0.73	0.19410	0.02671	179.6	8.1	169.9	5.5	401	50	5.4
18	423	1.46	0.20700	0.03070	191.1	9.4	195.0	7.0	227	30	-2.0
77	257	3.09	0.23190	0.03362	211.6	4.3	213.2	3.1	236	28	-0.8
101	379	2.32	0.26050	0.03705	234.8	7.0	234.5	4.6	275	34	0.1
65	283	34.37	0.77400	0.09470	582.8	5.8	583.1	6.1	593	19	-0.1
4	23.1	0.82	1.86000	0.17180	1073.0	39.0	1022.0	41.0	1191	67	14.2
18	399	4.04	2.83700	0.23260	1365.0	12.0	1348.0	15.0	1412	14	4.5
101	433.8	21.30	3.81000	0.26560	1593.0	24.0	1518.0	27.0	1720	21	11.7

14MCSMG3					207/ 235		206/ 238		206/ 207		
#	[U] ppm	U/Th	207/ 235	206/ 238	Age Ma	2σ err	Age (Ma)	2σ err	Age (Ma)	2σ err	% Disc
36	163.5	1.62	0.08430	0.01255	82.1	4.7	80.4	2.4	190	120	2.1
37	230.7	3.23	0.09300	0.01355	90.1	4.8	86.8	2.2	130	97	3.7
5	1550	21.30	0.09040	0.01378	87.9	2.8	88.2	2.5	69	70	0.3
41	790	7.30	0.09420	0.01388	91.4	2.2	88.9	1.7	109	50	2.7
3	469	1.86	0.09580	0.01448	92.8	2.6	92.7	1.6	105	75	0.1
32	225	3.33	0.10000	0.01456	96.6	3.5	93.2	1.9	222	89	3.5
8	716	2.73	0.09740	0.01461	94.4	2.2	93.5	1.6	106	44	1.0
12	800	11.40	0.09730	0.01467	94.5	1.8	93.9	1.4	106	45	0.6
9	464	1.94	0.10000	0.01469	96.7	2.2	94.0	1.4	163	53	2.8
20	1740	46.40	0.10000	0.01474	96.7	2.6	94.3	2.1	173	52	2.5
33	398	9.20	0.09580	0.01473	92.8	3.3	94.3	2.0	74	69	1.6
6	395	2.01	0.09930	0.01481	96.1	3.0	94.8	2.1	124	62	1.4
10	920	4.78	0.09880	0.01481	95.6	2.3	94.8	1.4	104	51	0.8
42	234	4.71	0.09770	0.01481	94.6	3.1	94.8	1.9	92	77	0.2
45	82.6	2.23	0.10710	0.01487	103.0	7.6	95.1	4.0	250	170	7.7
23	1310	4.58	0.09890	0.01495	95.7	3.4	95.7	2.9	90	66	0.0
11	397	5.60	0.09790	0.01498	94.8	2.3	95.8	1.8	84	60	1.1
14	174.2	2.93	0.10200	0.01498	98.4	4.1	95.8	1.8	158	89	2.6
1	288	3.60	0.10030	0.01512	96.9	3.4	96.7	1.9	117	74	0.2
19	210	1.95	0.09940	0.01511	96.1	4.1	96.7	2.4	100	94	0.6
35	860	14.70	0.10310	0.01513	99.6	4.9	96.8	4.9	150	110	2.8
27	301	2.95	0.09970	0.01516	96.4	2.5	97.0	2.1	143	59	0.6
28	590	2.58	0.10120	0.01526	97.8	2.8	97.6	2.1	128	57	0.2
4	204	2.51	0.10140	0.01532	98.0	3.6	98.0	2.2	145	84	0.0
7	1770	3.20	0.09890	0.01534	95.7	3.1	98.1	3.3	61	77	2.5
44	464	1.98	0.10460	0.01536	100.9	2.7	98.3	1.9	159	61	2.6
2	214	2.24	0.10360	0.01541	99.9	3.9	98.6	2.5	170	81	1.3
50	385	2.25	0.10450	0.01553	100.8	3.0	99.3	2.2	126	64	1.5
17	900	3.58	0.10820	0.01556	104.2	2.5	99.6	1.6	201	51	4.4
24	92.9	2.69	0.10170	0.01572	98.1	4.9	100.6	2.9	90	100	2.5
21	347	2.04	0.10550	0.01580	101.7	3.0	101.0	1.8	111	64	0.7
30	1360	2.78	0.10380	0.01601	100.3	1.7	102.4	2.1	87	40	2.1
29	549	2.79	0.10220	0.01606	98.7	2.6	102.7	2.6	83	61	4.1
22	179	2.76	0.10830	0.01621	104.2	3.7	103.6	2.8	124	87	0.6
34	191	2.20	0.10770	0.01621	103.7	3.7	103.6	2.6	94	82	0.1
31	377	3.01	0.11250	0.01695	108.2	2.5	108.6	2.0	134	54	0.4

14MCSMG3					207/ 235		206/ 238		206/ 207		
#	[U] ppm	U/Th	207/ 235	206/ 238	Age Ma	2σ err	Age (Ma)	2σ err	Age (Ma)	2σ err	% Disc
49	299	2.78	0.11710	0.01805	112.3	4.1	115.3	3.1	77	70	2.7
7	350	1.18	0.12860	0.01877	122.8	4.0	119.9	3.0	210	110	2.4
5	214	1.43	0.16090	0.02318	151.4	5.7	147.7	4.3	240	110	2.4
23	432	1.44	0.15860	0.02344	149.4	3.8	149.4	3.5	207	68	0.0
13	97	2.20	0.16350	0.02433	153.4	6.2	154.9	3.5	190	98	1.0
15	230	1.60	0.16480	0.02434	154.8	3.2	155.0	2.4	134	48	0.1
46	89.8	1.94	0.17020	0.02494	159.1	7.3	158.8	3.8	160	99	0.2
40	127.6	1.54	0.18140	0.02570	169.1	5.5	163.6	3.4	202	85	3.3
25	175	3.14	0.16940	0.02573	159.4	5.0	163.7	3.8	112	79	2.7
18	120	1.92	0.17860	0.02616	166.5	6.1	166.5	3.6	174	82	0.0
38	199	1.48	0.17710	0.02642	165.9	4.1	168.5	3.6	141	62	1.6
43	148	2.40	0.18360	0.02658	170.9	5.0	169.0	4.4	179	71	1.1
39	121	1.71	0.17850	0.02674	166.5	5.2	170.1	3.2	126	79	2.2
48	231	1.36	0.18470	0.02688	171.9	5.3	171.0	2.9	193	72	0.5
26	400	3.56	0.22090	0.03232	202.5	4.4	205.0	3.0	180	56	1.2
35	156	1.75	0.57300	0.07610	459.0	13.0	472.0	17.0	364	90	2.8
47	75.4	0.91	2.23600	0.18730	1191.0	14.0	1106.0	20.0	1310	45	15.6

14MCSMG1					207/ 235		206/ 238		206/ 207		
#	[U] ppm	U/Th	207/ 235	206/ 238	Age Ma	2σ err	Age (Ma)	2σ err	Age (Ma)	2σ err	% Disc
27	105.5	0.69	0.02290	0.00321	22.9	2.0	20.7	1.0	280	200	9.7
54	268.4	0.75	0.02320	0.00352	23.3	1.5	22.7	0.7	120	140	2.7
22	568	0.70	0.02500	0.00377	25.0	2.0	24.3	0.8	30	130	2.9
53	320	1.06	0.02930	0.00388	29.3	1.6	24.9	0.8	350	120	92.9
49	210	0.74	0.02790	0.00410	27.9	2.1	26.4	1.1	150	160	5.4
45	307	1.53	0.02800	0.00425	28.0	2.2	27.4	1.0	100	140	2.3
42	60.2	0.62	0.04080	0.00455	40.2	7.4	29.3	2.0	460	310	93.6
25	464	0.78	0.03470	0.00456	34.6	1.4	29.3	0.5	397	90	92.6
36	225	1.51	0.03380	0.00465	33.7	2.3	29.9	1.1	340	150	91.2
14	316	1.84	0.03340	0.00468	33.4	2.0	30.1	1.1	290	130	9.9
48	185	0.49	0.03450	0.00478	34.4	2.5	30.8	1.1	220	160	86.0
5	62.7	0.89	0.03960	0.00490	39.2	6.3	31.5	2.2	340	280	90.7
30	653	0.45	0.03360	0.00499	33.6	1.2	32.1	0.9	118	70	4.6
56	247	1.90	0.03590	0.00530	35.7	2.0	34.1	1.2	150	110	4.5
19	250	0.51	0.03810	0.00546	37.9	1.7	35.1	1.0	210	110	7.4
33	204	0.75	0.06480	0.00952	64.1	2.8	61.1	1.3	190	90	4.7
3	62.6	0.32	0.07050	0.01007	68.9	5.0	64.6	2.4	240	150	6.2
58	267	0.36	0.22080	0.03087	202.4	4.5	196.0	3.0	271	58	3.2
38	202	0.96	0.23950	0.03364	218.5	5.5	213.3	3.9	308	76	2.4
31	307	1.48	0.44900	0.05790	376.4	7.6	362.5	7.2	425	55	3.7
13	218	2.43	0.44520	0.05891	373.5	6.0	369.6	5.6	406	44	1.0
32	115.2	0.68	0.73800	0.08900	560.4	7.8	549.7	6.7	597	40	1.9
1	29.7	1.86	1.54900	0.15670	950.0	17.0	940.0	18.0	963	61	2.4
15	105	1.44	1.64500	0.16500	988.3	7.9	984.0	13.0	1030	28	4.5
29	7.8	0.93	1.60500	0.15420	966.0	31.0	924.0	32.0	1058	95	12.7
39	88.5	0.95	1.71600	0.16450	1013.0	13.0	982.0	15.0	1084	45	9.4
46	37.4	0.98	1.78100	0.17060	1032.0	29.0	1014.0	35.0	1109	46	8.6
47	73	1.49	2.02100	0.18580	1122.0	10.0	1098.0	13.0	1151	32	4.6
37	112	1.42	2.72200	0.22670	1334.0	17.0	1317.0	24.0	1358	36	3.0
8	65.2	1.15	3.21000	0.25770	1461.0	17.0	1477.0	28.0	1414	24	4.5
21	64.2	0.64	3.18700	0.25660	1457.0	10.0	1472.0	19.0	1431	36	2.9
28	261	1.50	2.85000	0.22810	1363.0	31.0	1322.0	52.0	1431	31	7.6
4	385	1.94	3.06400	0.24560	1423.1	8.2	1416.0	11.0	1432	21	1.1
57	45.1	1.93	3.23200	0.25870	1464.0	12.0	1483.0	19.0	1440	32	3.0
50	60.1	1.01	3.24800	0.25760	1467.0	14.0	1477.0	23.0	1451	35	1.8
9	20.18	1.18	3.13100	0.24900	1441.0	19.0	1432.0	36.0	1452	57	1.4

14MCSMG3					207/ 235		206/ 238		206/ 207		
#	[U ppm]	U/Th	207/ 235	206/ 238	Age Ma	2σ err	Age (Ma)	2σ err	Age (Ma)	2σ err	% Disc
35	302	1.41	3.40400	0.26070	1503.0	18.0	1496.0	17.0	1537	41	2.7
24	86	1.68	4.52400	0.31160	1739.0	18.0	1746.0	39.0	1662	29	5.1
43	109	1.60	4.12900	0.29190	1664.0	11.0	1650.0	20.0	1674	20	1.4
60	177.7	2.23	3.77400	0.26710	1588.0	8.3	1526.0	16.0	1674	22	8.8
16	987	4.17	3.03000	0.21400	1412.0	26.0	1248.0	38.0	1684	17	25.9
34	45.1	0.57	4.25400	0.29830	1685.0	12.0	1682.0	20.0	1684	23	0.1
10	73.6	1.16	4.15100	0.29010	1665.0	12.0	1642.0	18.0	1685	24	2.6
7	185	0.87	4.29000	0.30300	1692.0	20.0	1710.0	40.0	1690	21	1.2
40	195	1.61	4.17200	0.29400	1670.0	7.3	1661.0	14.0	1695	13	2.0
59	191	1.54	4.36700	0.30730	1705.6	7.9	1727.0	16.0	1696	21	1.8
23	50.1	0.49	4.55600	0.31350	1740.0	16.0	1757.0	29.0	1712	29	2.6
44	70.5	0.85	3.79400	0.26140	1591.0	20.0	1496.0	29.0	1714	30	12.7
26	831	1.63	3.82200	0.26070	1596.0	14.0	1493.0	24.0	1726	24	13.5
11	189	2.21	4.33200	0.29840	1698.5	9.9	1683.0	17.0	1728	20	2.6
51	457	1.98	4.41100	0.30200	1715.0	13.0	1700.0	27.0	1732	19	1.8
41	116	1.29	5.55300	0.32810	1910.0	14.0	1834.0	28.0	1999	25	8.3
18	23.9	0.40	6.12000	0.27690	1994.0	50.0	1574.0	42.0	2470	69	36.3

13MCSMG15					207/ 235		206/ 238		206/ 207		
#	[U] ppm	U/Th	207/ 235	206/ 238	Age Ma	2σ err	Age (Ma)	2σ err	Age (Ma)	2σ err	% Disc
23	1624	0.45	0.00468	0.00072	4.7	0.3	4.6	0.1	404.0	74	2.7
104	163.5	0.67	0.01170	0.00151	11.8	1.7	9.7	0.7	1030.0	140	99.1
29	103.5	1.01	0.01610	0.00179	16.1	3.5	11.6	0.9	1440.0	230	99.2
60	630	1.09	0.01700	0.00266	17.1	1.2	17.1	0.5	400.0	110	-0.1
48	771	0.85	0.02030	0.00289	20.4	1.1	18.6	0.5	372.0	89	8.7
41	115.4	0.49	0.02330	0.00345	23.3	3.1	22.2	1.3	850.0	150	4.7
8	343	1.63	0.02590	0.00384	25.9	1.8	24.7	0.8	424.0	71	4.5
32	222	0.86	0.02760	0.00394	27.6	2.5	25.4	0.9	567.0	87	8.1
88	424	1.20	0.02750	0.00406	27.5	1.7	26.1	0.8	451.0	84	5.1
37	125.3	0.78	0.02740	0.00419	27.4	2.6	26.9	1.5	570.0	120	1.8
107	218.8	0.82	0.03300	0.00423	32.9	2.5	27.2	0.9	601.0	90	95.5
92	159	0.93	0.03310	0.00451	33.0	3.4	29.0	1.3	680.0	130	95.7
3	205.3	0.79	0.03010	0.00464	30.1	2.4	29.8	1.1	420.0	89	1.0
2	360	2.48	0.03130	0.00479	31.3	2.9	30.8	1.1	510.0	170	1.6
6	76.2	0.69	0.03250	0.00491	32.3	3.5	31.5	1.7	610.0	120	2.5
111	124.1	1.25	0.03650	0.00491	37.2	3.0	31.6	1.7	770.0	120	95.9
40	230	0.81	0.03420	0.00500	34.1	2.7	32.2	0.9	480.0	100	5.7
127	4.3	0.64	0.03410	0.00512	34.0	2.2	32.9	1.4	375.0	58	3.2
11	73.7	0.79	0.03690	0.00523	36.6	3.7	33.6	1.7	800.0	120	8.2
99	157.8	0.49	0.03510	0.00523	35.3	2.6	33.6	1.3	570.0	110	4.8
61	95.3	0.42	0.03820	0.00531	37.9	4.0	34.1	1.6	710.0	160	95.2
72	83.5	0.70	0.03890	0.00556	38.6	3.8	35.7	1.9	730.0	130	7.5
113	178	0.69	0.04000	0.00560	39.7	2.8	36.0	1.4	487.0	80	9.3
34	122.9	1.01	0.03460	0.00570	34.5	2.1	36.6	1.4	309.0	66	-6.1
89	123	0.51	0.04360	0.00583	43.2	4.9	37.5	1.8	525.0	96	92.9
51	650	0.82	0.03610	0.00588	36.3	2.1	37.8	1.0	283.0	55	-4.1
42	87	0.72	0.05270	0.00597	51.8	6.3	38.4	1.7	1030.0	220	96.3
78	185	1.09	0.04510	0.00630	44.7	3.4	40.5	1.5	620.0	100	9.4
110	54.8	0.54	0.06930	0.01039	67.7	6.9	66.6	2.8	660.0	100	1.6
46	138	0.90	0.08050	0.01205	78.4	4.5	77.5	1.8	369.0	78	1.1
102	217.2	1.72	0.08110	0.01215	79.5	3.2	77.8	1.5	307.0	51	2.1
68	50.8	0.52	0.08750	0.01242	84.6	7.8	79.6	3.2	691.0	96	5.9
79	133.3	0.68	0.10340	0.01529	99.6	5.8	97.8	2.1	481.0	81	1.8
82	227	1.10	0.10170	0.01570	98.2	3.1	100.4	2.0	231.0	45	-2.2
117	325	0.71	0.17710	0.02543	165.4	3.8	162.2	2.4	251.0	40	1.9
36	110.6	0.82	0.17920	0.02589	168.5	5.9	164.8	2.6	328.0	48	2.2

13MCSMG15					207/ 235		206/ 238		206/ 207		
#	[U] ppm	U/Th	207/ 235	206/ 238	Age Ma	2σ err	Age (Ma)	2σ err	Age (Ma)	2σ err	% Disc
57	450	1.15	0.18530	0.02698	172.5	3.0	171.6	2.1	212.0	26	0.5
70	82.9	0.94	0.18500	0.02739	173.0	8.9	174.2	4.4	294.0	45	-0.7
55	170.3	1.17	0.23720	0.03352	216.6	6.0	212.5	2.2	302.0	33	1.9
80	126.8	2.16	0.28020	0.03901	250.4	6.8	246.6	5.4	326.0	39	1.5
35	428	1.89	0.45870	0.06200	384.4	6.7	388.0	6.8	376.0	24	-0.9
96	194	0.75	0.48450	0.06470	400.7	6.8	404.1	5.8	398.0	29	-0.8
50	182	1.46	0.55020	0.07242	444.9	5.6	450.7	5.3	442.0	18	-1.3
93	266	0.83	0.58000	0.07571	464.2	5.4	470.4	5.1	426.0	24	-1.3
39	109	3.80	0.57200	0.07750	460.0	11.0	480.9	7.7	365.0	43	-4.5
12	42.2	0.69	0.69700	0.09020	539.0	15.0	557.5	8.9	470.0	48	-3.4
4	366	1.01	0.77000	0.09353	579.5	6.4	576.3	5.9	571.0	23	0.6
118	202.8	1.36	0.81900	0.09870	610.0	8.7	607.0	10.0	630.0	31	0.5
30	124	0.75	1.10400	0.12040	755.0	11.0	732.0	12.0	831.0	31	3.0
7	168.5	0.55	1.42400	0.14830	899.5	9.0	891.4	7.4	916.0	20	2.7
76	11.39	1.42	1.48000	0.15440	924.0	29.0	929.0	28.0	977.0	46	4.9
121	97	0.88	1.62300	0.15830	978.0	14.0	947.0	21.0	1008.0	25	6.1
94	479.7	60.00	1.84700	0.18230	1062.1	6.6	1079.4	9.3	1014.0	12	-6.4
71	75.7	0.92	1.82400	0.17930	1055.0	13.0	1063.0	13.0	1025.0	21	-3.7
20	109.9	1.68	1.85300	0.17950	1064.0	8.1	1064.4	9.2	1062.0	18	-0.2
84	121.2	1.55	1.73100	0.16750	1021.2	9.5	998.0	13.0	1066.0	23	6.4
81	43.1	1.70	1.91100	0.18400	1087.0	15.0	1088.0	16.0	1067.0	26	-2.0
31	76.1	0.56	1.82800	0.17700	1054.0	11.0	1050.0	12.0	1070.0	23	1.9
90	83.3	1.62	1.90700	0.18410	1084.0	13.0	1089.0	12.0	1089.0	22	0.0
45	156.8	1.96	1.82100	0.17450	1054.0	14.0	1036.0	21.0	1095.0	15	5.4
112	14.8	0.78	2.05000	0.18670	1139.0	40.0	1103.0	35.0	1136.0	53	2.9
115	456	2.47	2.11500	0.19400	1153.4	5.6	1142.8	7.2	1171.7	9	2.5
109	303	1.09	2.17100	0.19530	1171.4	8.3	1151.0	11.0	1190.0	13	3.3
119	137	3.21	2.20300	0.19930	1183.8	9.1	1172.5	9.6	1190.0	19	1.5
128	140	2.26	2.41700	0.21290	1248.0	12.0	1244.0	14.0	1242.0	25	-0.2
95	188	2.21	2.48400	0.21820	1267.7	8.7	1272.5	9.8	1249.0	15	-1.9
53	94	1.40	2.71600	0.23040	1332.0	10.0	1336.0	11.0	1319.0	18	-1.3
114	30	1.50	2.74700	0.22880	1339.0	16.0	1327.0	23.0	1366.0	27	2.9
13	32.7	1.44	2.87600	0.23520	1373.0	17.0	1361.0	20.0	1374.0	25	0.9
49	51.3	0.90	2.87900	0.23680	1375.0	13.0	1370.0	16.0	1374.0	24	0.3
1	56.3	0.79	2.85300	0.23380	1370.0	12.0	1354.0	15.0	1390.0	25	2.6
24	125.4	1.05	2.81700	0.23050	1359.4	9.1	1337.0	15.0	1391.0	11	3.9

13MCSMG15					207/ 235		206/ 238		206/ 207		
#	[U] ppm	U/Th	207/ 235	206/ 238	Age Ma	2σ err	Age (Ma)	2σ err	Age (Ma)	2σ err	% Disc
91	156.8	1.84	2.91600	0.23940	1385.0	16.0	1383.0	20.0	1393.0	25	0.7
62	137.2	1.93	3.09600	0.25230	1431.1	8.2	1452.0	12.0	1407.2	8	-3.2
17	880	0.78	2.41500	0.19680	1245.0	27.0	1156.0	40.0	1414.9	8	18.3
47	52	1.08	2.95800	0.23910	1395.0	20.0	1382.0	22.0	1420.0	27	2.7
15	170.1	1.42	3.06600	0.24870	1423.7	7.7	1431.0	12.0	1421.0	11	-0.7
16	159	2.50	3.08800	0.25110	1431.5	8.9	1444.0	13.0	1424.0	14	-1.4
75	61.9	0.70	3.15700	0.25210	1446.0	12.0	1449.0	17.0	1437.0	19	-0.8
67	75	1.63	3.11700	0.24850	1436.0	12.0	1433.0	17.0	1438.0	16	0.3
19	102.4	0.87	3.08600	0.24690	1428.6	9.6	1422.0	15.0	1444.0	12	1.5
33	268	2.31	3.30100	0.26390	1482.0	11.0	1509.0	20.0	1445.0	11	-4.4
59	20.4	0.88	3.31100	0.26550	1489.0	23.0	1517.0	36.0	1448.0	33	-4.8
91	170.8	1.19	2.88700	0.23150	1378.0	14.0	1343.0	14.0	1448.0	19	7.3
64	379	1.77	3.11000	0.24620	1437.0	11.0	1419.0	16.0	1452.0	11	2.3
120	160	1.28	3.01400	0.23890	1413.0	12.0	1381.0	20.0	1452.0	21	4.9
105	73.2	1.09	3.15900	0.25040	1447.0	13.0	1440.0	20.0	1460.0	18	1.4
63	218	0.67	3.30600	0.26070	1482.1	7.1	1493.0	13.0	1471.0	10	-1.5
108	31.7	0.67	2.94600	0.23240	1396.0	19.0	1347.0	24.0	1478.0	28	8.9
116	116	1.06	3.53600	0.26790	1536.0	16.0	1530.0	16.0	1531.0	24	0.1
14	177.7	4.66	3.23000	0.23540	1463.0	15.0	1362.0	23.0	1604.0	13	15.1
77	91	1.67	3.93700	0.28600	1621.0	14.0	1624.0	21.0	1628.0	16	0.2
9	81.6	0.91	4.12800	0.30050	1659.0	12.0	1696.0	19.0	1631.0	11	-4.0
22	73.8	0.46	3.96800	0.28230	1626.8	9.8	1602.0	17.0	1663.0	13	3.7
26	62.7	0.99	4.22400	0.30040	1677.0	11.0	1693.0	15.0	1683.0	14	-0.6
5	47.3	1.13	4.32100	0.30320	1696.0	13.0	1707.0	20.0	1691.0	20	-0.9
54	250.8	2.98	4.10100	0.28580	1653.0	15.0	1620.0	29.0	1696.9	10	4.5
126	170	1.89	4.29500	0.30040	1694.2	9.4	1693.0	17.0	1698.7	8	0.3
28	108.9	1.36	4.24400	0.29640	1683.2	8.9	1673.0	14.0	1700.0	13	1.6
103	120	1.31	4.32000	0.30150	1696.0	14.0	1698.0	25.0	1708.0	12	0.6
98	165	1.34	4.16300	0.28790	1666.0	11.0	1631.0	21.0	1710.0	14	4.6
73	680	1.86	4.37000	0.29990	1705.0	23.0	1690.0	45.0	1720.0	12	1.7
66	178.9	0.81	4.48300	0.30820	1728.1	9.7	1731.0	13.0	1730.0	10	-0.1
87	179	0.77	4.54200	0.31040	1738.3	7.5	1742.0	15.0	1733.5	8	-0.5
123	170	1.05	4.59600	0.31200	1749.5	8.8	1750.0	21.0	1746.4	7	-0.2
10	151	2.31	4.35300	0.29550	1702.9	8.7	1669.0	13.0	1747.0	11	4.5
44	501	6.00	4.98200	0.33550	1816.0	11.0	1865.0	19.0	1758.0	10	-6.1
56	321	1.81	4.58200	0.30290	1745.0	11.0	1705.0	20.0	1791.7	7	4.8

13MCSMG15					207/ 235		206/ 238		206/ 207		
#	[U] ppm	U/Th	207/ 235	206/ 238	Age Ma	2σ err	Age (Ma)	2σ err	Age (Ma)	2σ err	% Disc
74	25.6	3.74	4.86200	0.32340	1800.0	15.0	1805.0	32.0	1801.0	24	-0.2
27	36.45	0.71	5.00000	0.32410	1817.0	19.0	1809.0	28.0	1825.0	20	0.9
52	31.1	0.74	5.88200	0.36070	1957.0	14.0	1985.0	27.0	1925.0	18	-3.1

13MCSMG13					207/ 235		206/ 238		206/ 207		
#	[U] ppm	U/Th	207/ 235	206/ 238	Age Ma	2σ err	Age (Ma)	2σ err	Age (Ma)	2σ err	% Disc
56	177	1.00	0.00500	0.00071	5.0	1.1	4.6	0.4	1200.0	160	8.6
13	200	0.99	0.00970	0.00080	9.8	1.4	5.1	0.4	1770.0	190	99.7
101	133.2	0.55	0.01850	0.00205	18.5	2.2	13.2	0.9	1230.0	140	98.9
31	349	0.49	0.01570	0.00229	15.8	1.7	14.7	0.8	550.0	130	6.8
79	243	0.39	0.01850	0.00257	18.6	1.7	16.6	0.7	640.0	93	97.4
14	129.2	0.65	0.02000	0.00278	20.0	2.3	17.9	0.9	650.0	140	97.2
58	278	1.65	0.02120	0.00324	21.2	2.0	20.8	0.9	500.0	120	1.7
111	190	0.50	0.02460	0.00357	24.9	2.1	23.0	0.9	550.0	100	7.8
98	400.2	1.55	0.03010	0.00372	30.1	2.2	24.0	0.8	609.0	78	96.1
3	178.3	0.61	0.02670	0.00414	26.8	1.6	26.6	1.0	500.0	100	0.7
23	100.8	1.05	0.02940	0.00414	29.3	3.3	26.6	1.5	640.0	130	9.2
17	713	1.08	0.02650	0.00424	26.6	1.2	27.3	1.0	202.0	39	-2.6
95	258.3	0.61	0.02990	0.00433	29.9	2.7	27.9	1.6	380.0	110	6.7
48	299	1.73	0.02790	0.00458	28.0	1.6	29.4	0.8	266.0	42	-5.1
90	181.2	0.78	0.03450	0.00467	34.4	3.0	30.0	1.1	510.0	110	94.1
16	147	0.87	0.03710	0.00472	36.9	3.2	30.4	1.3	680.0	120	95.5
49	383	0.89	0.03170	0.00477	31.6	2.5	30.7	1.0	398.0	85	2.8
50	387	0.99	0.03170	0.00478	31.7	1.8	30.7	0.8	273.0	68	3.1
99	299	0.92	0.03410	0.00480	34.0	2.1	30.8	1.1	395.0	95	9.4
114	82.7	0.41	0.03310	0.00481	32.9	3.4	30.9	1.5	520.0	95	6.1
120	444	0.98	0.03220	0.00487	32.1	1.2	31.3	0.8	264.0	48	2.4
8	124	0.47	0.03660	0.00492	36.4	3.1	31.6	1.4	680.0	120	95.4
54	74.8	0.80	0.03530	0.00494	35.1	4.0	31.8	1.5	800.0	120	9.4
24	192	0.84	0.03300	0.00512	32.9	2.3	32.9	1.2	356.0	83	0.0
35	677	1.56	0.03530	0.00513	35.2	1.3	33.0	0.7	276.0	37	6.2
63	192	0.52	0.04360	0.00525	43.7	2.7	33.7	1.3	730.0	110	95.4
27	139.6	0.91	0.04310	0.00531	42.7	3.9	34.2	1.4	670.0	110	94.9
46	259	0.47	0.03570	0.00539	35.9	1.8	34.7	1.1	267.0	72	3.3
4	1340	1.52	0.03560	0.00555	35.5	1.6	35.7	0.8	285.0	82	-0.5
60	410	1.07	0.04410	0.00622	43.8	2.0	40.0	1.1	409.0	92	8.7
77	257.2	0.72	0.04780	0.00750	47.4	2.1	48.2	1.2	236.0	46	-1.7
25	159	1.00	0.06950	0.00990	68.1	4.8	63.5	3.0	390.0	100	6.8
55	468.6	1.00	0.07410	0.01144	72.5	2.3	73.3	1.5	213.0	40	-1.1
84	120.9	1.01	0.08010	0.01192	78.1	4.5	76.4	2.6	366.0	66	2.2
57	285	0.79	0.07930	0.01205	77.4	2.9	77.2	1.5	243.0	40	0.3
39	79.8	0.45	0.15740	0.02211	147.9	8.1	141.0	3.7	406.0	54	4.7

13MCSMG13					207/ 235		206/ 238		206/ 207		
#	[U] ppm	U/Th	207/ 235	206/ 238	Age Ma	2σ err	Age (Ma)	2σ err	Age (Ma)	2σ err	% Disc
87	342	1.16	0.23890	0.03366	217.5	3.7	213.4	4.0	257.0	31	1.9
102	88.3	0.53	0.28200	0.03927	252.0	11.0	248.3	5.9	405.0	62	1.5
9	17.7	1.21	0.31100	0.04160	272.0	24.0	263.0	16.0	590.0	120	3.3
110	101	1.04	0.42700	0.05770	360.5	9.9	361.5	8.0	385.0	39	-0.3
124	203	3.06	0.42880	0.05824	362.9	7.0	364.9	6.0	353.0	25	-0.6
115	183.4	1.30	0.59900	0.07230	476.0	12.0	450.0	11.0	596.0	28	5.5
100	501	6.44	0.60520	0.07722	480.3	5.0	479.5	5.0	502.0	16	0.2
89	135	0.91	0.69300	0.08760	534.1	8.8	541.1	9.4	537.0	26	-1.3
83	214	1.59	0.82500	0.09860	611.8	6.7	606.2	8.0	632.0	19	0.9
117	110.5	0.75	0.86700	0.10250	633.3	9.8	629.0	12.0	666.0	26	0.7
67	65.3	1.38	1.32100	0.14320	854.0	11.0	863.0	13.0	853.0	23	-1.2
11	28.18	1.53	1.63700	0.16430	985.0	15.0	980.0	19.0	1003.0	29	2.3
15	264	2.81	1.74600	0.17260	1025.0	15.0	1027.0	22.0	1017.0	35	-1.0
93	162.9	1.52	1.62600	0.16140	980.0	7.5	964.0	11.0	1018.0	14	5.3
52	71.1	1.61	1.75200	0.17160	1027.0	11.0	1022.0	12.0	1041.0	22	1.8
30	776	3.99	1.64900	0.16100	988.8	6.8	962.0	11.0	1046.0	11	8.0
51	86.3	1.24	1.73400	0.17030	1020.3	9.4	1015.0	11.0	1049.0	20	3.2
28	225	1.34	1.67300	0.16030	998.0	9.2	958.0	11.0	1052.0	15	8.9
70	105.9	0.69	1.75000	0.16970	1026.0	10.0	1010.0	11.0	1054.0	18	4.2
74	156.4	0.56	1.80700	0.17430	1047.3	8.1	1035.0	13.0	1066.0	15	2.9
2	101.9	1.26	1.74900	0.16930	1027.0	10.0	1008.0	12.0	1072.0	15	6.0
72	46.4	1.70	1.69500	0.16440	1005.0	22.0	981.0	24.0	1080.0	50	9.2
92	176	0.86	1.77500	0.16990	1035.8	8.4	1012.0	11.0	1083.0	13	6.6
68	107	0.77	1.86700	0.17550	1069.0	11.0	1042.0	20.0	1120.0	21	7.0
20	268	0.82	1.83000	0.17270	1055.0	16.0	1027.0	20.0	1136.0	21	9.6
66	157	1.60	2.03600	0.18990	1127.3	9.1	1123.0	14.0	1150.0	16	2.3
96	105	2.83	2.05100	0.18640	1137.0	13.0	1107.0	19.0	1200.0	26	7.8
21	35.1	2.10	2.25600	0.19800	1197.0	13.0	1164.0	18.0	1232.0	27	5.5
42	41.7	1.47	2.12600	0.17770	1156.0	16.0	1054.0	18.0	1351.0	24	22.0
59	98	1.09	2.64000	0.22000	1313.0	11.0	1284.0	16.0	1364.0	18	5.9
5	50.4	0.63	2.80100	0.23020	1354.0	15.0	1338.0	19.0	1390.0	17	3.7
25	166.7	5.15	2.36100	0.18970	1230.0	15.0	1123.0	18.0	1395.0	16	19.5
44	198	0.91	2.90500	0.23900	1382.0	10.0	1381.0	15.0	1396.0	10	1.1
112	75	0.69	3.09700	0.24960	1431.3	8.5	1436.0	12.0	1426.0	16	-0.7
37	111.8	1.42	3.05800	0.24650	1421.7	7.9	1420.0	16.0	1432.0	15	0.8
34	50.9	0.77	3.09000	0.24730	1431.0	10.0	1424.0	17.0	1439.0	16	1.0

13MCSMG13					207/ 235		206/ 238		206/ 207		
#	[U] ppm	U/Th	207/ 235	206/ 238	Age Ma	2σ err	Age (Ma)	2σ err	Age (Ma)	2σ err	% Disc
1	533	2.14	2.93900	0.23490	1392.9	9.8	1360.0	17.0	1441.8	6	5.7
47	109.7	0.54	3.09500	0.24580	1430.7	9.9	1417.0	19.0	1442.0	15	1.7
71	200.8	1.60	2.70000	0.21440	1328.0	13.0	1252.0	17.0	1442.0	19	13.2
107	85.2	0.80	3.04100	0.24490	1419.0	12.0	1412.0	16.0	1442.0	12	2.1
38	154	2.74	2.60300	0.20920	1301.0	12.0	1224.0	32.0	1446.0	10	15.4
121	37.3	1.30	2.93500	0.23660	1392.0	14.0	1368.0	20.0	1448.0	25	5.5
88	164.6	1.07	2.95800	0.23420	1398.0	12.0	1356.0	15.0	1451.0	13	6.5
76	211	1.59	3.00300	0.23830	1408.0	8.7	1378.0	16.0	1452.0	12	5.1
91	920	1.93	1.94000	0.15400	1068.0	66.0	914.0	85.0	1454.0	13	37.1
103	282	5.90	3.09400	0.24470	1435.0	20.0	1415.0	21.0	1455.0	22	2.7
10	174.7	2.66	2.83800	0.22610	1366.3	7.8	1314.0	13.0	1457.0	12	9.8
106	79.3	1.09	2.99500	0.23760	1407.0	10.0	1374.0	17.0	1461.0	16	6.0
123	122.5	1.32	3.29100	0.26070	1479.0	10.0	1493.0	19.0	1478.0	17	-1.0
12	257	2.09	3.11500	0.24400	1436.0	13.0	1407.0	19.0	1489.0	14	5.5
116	78.1	1.44	3.61300	0.26660	1554.0	13.0	1523.0	15.0	1620.0	16	6.0
41	571	154.50	3.87400	0.27610	1608.0	8.1	1571.0	17.0	1650.0	10	4.8
19	148.9	1.12	4.18200	0.29470	1669.0	11.0	1664.0	25.0	1658.0	14	-0.4
73	528	3.28	3.59500	0.25610	1548.7	5.0	1469.8	9.1	1658.1	7	11.4
12	49.7	1.39	4.67000	0.32800	1760.0	27.0	1828.0	39.0	1662.0	30	-10.0
94	58.4	0.94	4.11900	0.29080	1659.0	14.0	1645.0	22.0	1664.0	15	1.1
45	98	0.81	4.24800	0.30230	1682.0	13.0	1702.0	21.0	1666.0	13	-2.2
6	44.23	0.83	3.56800	0.25320	1541.0	16.0	1454.0	24.0	1670.0	18	12.9
119	51.2	0.60	3.99000	0.28570	1631.0	16.0	1619.0	23.0	1670.0	16	3.1
53	83	0.95	4.16300	0.29490	1665.0	14.0	1666.0	20.0	1671.0	14	0.3
29	387	2.36	4.21700	0.29480	1676.7	9.9	1665.0	19.0	1679.7	9	0.9
62	42.2	1.13	4.21000	0.29560	1674.0	22.0	1669.0	28.0	1681.0	28	0.7
65	81.8	0.90	4.23200	0.29640	1679.4	9.9	1673.0	15.0	1682.0	15	0.5
82	372	3.06	4.27700	0.29920	1688.0	12.0	1687.0	22.0	1682.6	9	-0.3
32	782	4.75	3.90300	0.27210	1613.8	9.0	1551.0	17.0	1697.1	6	8.6
64	48.8	0.68	4.21000	0.28550	1673.0	20.0	1618.0	31.0	1723.0	17	6.1
61	90.3	3.29	3.84300	0.26030	1601.0	16.0	1491.0	27.0	1744.0	22	14.5
122	736	0.93	2.84000	0.19200	1344.0	68.0	1127.0	94.0	1758.2	7	35.9
78	100.6	1.66	4.28400	0.28720	1689.0	16.0	1627.0	29.0	1762.0	14	7.7
40	286	1.24	3.99000	0.27020	1630.0	29.0	1540.0	41.0	1768.0	11	12.9
26	421	4.39	4.33400	0.28360	1699.0	12.0	1609.0	21.0	1810.0	11	11.1
18	44.7	0.85	5.32900	0.33060	1872.0	14.0	1840.0	28.0	1921.0	19	4.2

13MCSMG13					207/ 235		206/ 238		206/ 207		
#	[U] ppm	U/Th	207/ 235	206/ 238	Age Ma	2σ err	Age (Ma)	2σ err	Age (Ma)	2σ err	% Disc
7	314	3.63	5.39300	0.32860	1883.4	7.8	1831.0	17.0	1943.7	6	5.8
69	51.9	1.45	6.70000	0.34390	2072.0	15.0	1905.0	29.0	2230.0	20	14.6
33	275	0.52	14.21000	0.53000	2764.0	10.0	2741.0	27.0	2773.0	11	1.2

13MCSMG12					207/ 235		206/ 238		206/ 207		
#	[U] ppm	U/Th	207/ 235	206/ 238	Age Ma	2σ err	Age (Ma)	2σ err	Age (Ma)	2σ err	% Disc
105	910	0.89	0.00431	0.00067	4.4	0.2	4.3	0.1	271	66	1.8
96	74.9	0.48	0.01900	0.00234	19.3	1.4	15.1	0.6	651	90	97.7
68	117	1.01	0.02610	0.00357	26.2	1.5	23.0	0.8	392	79	94.1
121	220	1.22	0.02472	0.00365	24.8	1.0	23.5	0.4	299	52	5.4
31	650	0.96	0.02379	0.00365	23.9	0.5	23.5	0.4	115	22	1.6
18	440	0.53	0.02552	0.00370	25.7	0.7	23.8	0.4	283	45	7.3
41	425	0.94	0.02760	0.00401	27.6	1.0	25.8	0.3	239	59	6.6
7	137	1.06	0.02830	0.00412	28.3	1.1	26.5	0.5	340	63	6.3
100	166	0.48	0.03060	0.00461	30.6	1.1	29.7	0.5	216	41	3.0
49	66.55	1.10	0.03620	0.00462	35.2	2.6	29.7	0.7	570	100	94.8
119	215.3	0.66	0.03120	0.00474	31.2	0.9	30.5	0.5	210	34	2.2
91	255.6	0.52	0.05060	0.00732	50.1	1.5	47.0	0.6	256	55	6.2
44	294	1.12	0.06270	0.00942	61.7	1.7	60.4	0.7	199	46	2.1
39	180.6	2.07	0.08060	0.01179	78.6	2.1	75.6	1.7	242	40	3.8
6	1570	2.32	0.09117	0.01344	88.6	0.9	86.1	1.0	148	17	2.9
54	255.3	1.72	0.10580	0.01596	102.1	1.6	102.1	1.0	138	17	0.0
23	181.1	0.84	0.16900	0.02382	158.5	3.0	151.7	1.6	260	28	4.3
29	508	1.70	0.24750	0.03203	224.5	2.3	203.6	3.1	432	24	9.3
115	91.5	0.41	0.24720	0.03460	224.1	4.1	219.2	2.7	263	31	2.2
10	479	1.57	0.25200	0.03478	228.2	3.2	220.4	3.5	274	14	3.4
94	138.5	1.02	0.25960	0.03660	234.3	2.8	231.7	2.3	259	23	1.1
86	205	1.88	0.37010	0.05090	320.1	2.9	320.1	2.6	317	13	0.0
89	162	2.74	0.41880	0.05730	355.6	3.2	359.2	3.6	343	16	1.0
122	330	6.20	0.47400	0.06217	393.9	2.8	388.8	2.8	420	9	1.3
125	214	4.21	0.49140	0.06359	405.8	5.0	397.4	3.8	441	16	2.1
12	84.2	0.48	0.49890	0.06409	410.8	4.6	400.4	3.2	460	20	2.5
48	35.9	1.53	0.52400	0.06460	427.1	7.8	403.7	6.9	544	30	5.5
65	171	1.44	0.58950	0.07529	470.3	4.8	467.9	5.6	503	11	0.5
72	37.4	2.53	0.74100	0.09075	562.7	7.2	559.9	5.4	589	23	0.5
108	103.7	1.53	0.81400	0.09421	604.3	8.3	580.3	5.2	683	34	4.0
59	73.58	0.73	0.78900	0.09430	590.5	6.2	580.9	5.7	632	13	1.6
25	97.5	0.71	0.84090	0.09937	620.1	3.6	610.7	4.3	641	10	1.5
125	187	7.10	1.10300	0.11390	755.0	10.0	695.1	7.5	932	25	7.9
62	134.9	0.40	1.37700	0.14320	878.0	10.0	862.9	7.7	915	17	5.7
58	69.1	1.47	1.53500	0.15190	944.2	7.2	911.6	7.5	1025	11	11.1
14	69.9	1.93	1.69400	0.16430	1006.0	12.0	980.0	14.0	1047	16	6.4

13MCSMG12					207/ 235		206/ 238		206/ 207		
#	[U] ppm	U/Th	207/ 235	206/ 238	Age Ma	2σ err	Age (Ma)	2σ err	Age (Ma)	2σ err	% Disc
90	318.7	2.48	1.72740	0.16800	1018.7	3.7	1001.5	6.0	1054	5	5.0
77	349	1.70	1.81660	0.17748	1051.4	3.3	1053.1	5.4	1057	5	0.4
24	107.4	0.82	1.85600	0.17880	1066.2	6.1	1060.5	6.7	1078	9	1.6
85	300	6.72	1.72200	0.16420	1016.4	6.1	980.3	8.1	1106	9	11.3
47	149.2	1.61	1.92900	0.18170	1090.9	4.5	1076.2	5.5	1117	6	3.7
123	195	2.14	2.03300	0.18830	1126.2	6.0	1112.0	10.0	1142	7	2.6
104	283	3.10	2.06600	0.19080	1137.3	7.8	1126.0	14.0	1161	7	3.0
70	481	2.46	2.19700	0.18460	1180.0	13.0	1092.0	12.0	1341	20	18.6
92	189	1.57	2.45900	0.20350	1259.1	9.7	1196.0	15.0	1382	7	13.5
36	166	2.36	2.49200	0.20440	1269.4	5.4	1198.9	9.6	1388	8	13.6
75	45.5	1.45	2.58700	0.21300	1297.5	7.9	1246.0	11.0	1391	10	10.4
74	140.5	1.26	2.89900	0.23540	1382.0	5.3	1362.6	7.9	1416	7	3.8
51	203.1	2.16	2.95700	0.23770	1397.5	4.4	1374.0	11.0	1429	9	3.8
22	232.9	1.04	2.82500	0.22590	1361.6	9.5	1313.0	14.0	1431	9	8.3
46	93.6	1.09	2.90700	0.23310	1383.0	11.0	1350.0	19.0	1431	6	5.7
19	452	1.86	2.72800	0.21930	1335.9	4.5	1278.0	8.5	1436	4	11.0
55	313.4	2.84	2.57100	0.20710	1292.0	7.2	1213.0	10.0	1439	8	15.7
95	118	1.52	3.14800	0.25160	1444.8	7.2	1446.0	11.0	1440	6	0.4
13	128	1.08	3.14600	0.24980	1443.8	5.3	1437.0	11.0	1450	6	0.9
60	454	1.42	2.92200	0.23220	1387.4	5.8	1346.0	12.0	1454	7	7.4
102	196	0.84	2.07000	0.16150	1141.0	28.0	969.0	40.0	1477	12	34.4
73	309	1.27	2.80800	0.21950	1357.0	10.0	1279.0	17.0	1486	12	13.9
57	82.2	1.47	3.00500	0.23400	1408.4	7.2	1355.0	11.0	1493	7	9.2
40	68	0.45	2.75000	0.21100	1341.0	16.0	1234.0	15.0	1511	33	18.3
117	1.724	- 589.00	3.62000	0.27120	1552.0	38.0	1545.0	50.0	1531	54	0.9
124	320	1.49	3.41000	0.25320	1504.0	19.0	1455.0	20.0	1570	22	7.3
35	82.6	0.86	3.41700	0.24740	1508.0	5.5	1424.9	9.2	1629	8	12.5
98	153.5	2.74	3.92100	0.27490	1616.0	14.0	1565.0	25.0	1669	17	6.2
107	41.2	0.59	4.03500	0.28540	1641.7	6.3	1618.5	9.2	1670	8	3.1
64	255	1.15	3.90500	0.27700	1614.5	5.1	1576.0	9.0	1670	5	5.7
11	473	0.94	3.77400	0.26640	1586.7	7.7	1522.0	13.0	1671	4	8.9
32	125.6	1.20	4.24000	0.30070	1683.1	6.7	1695.0	11.0	1680	6	0.9
4	61.1	0.97	3.99400	0.28290	1633.7	8.3	1606.0	15.0	1682	9	4.5
97	205.2	1.27	3.62600	0.25400	1555.0	11.0	1459.0	21.0	1686	13	13.5
82	237	1.79	4.08200	0.28610	1650.1	7.2	1622.0	13.0	1688	6	3.9
120	127.4	1.43	3.97200	0.27720	1629.0	6.3	1577.0	11.0	1691	5	6.7

13MCSMG12					207/ 235		206/ 238		206/ 207		
#	[U] ppm	U/Th	207/ 235	206/ 238	Age Ma	2σ err	Age (Ma)	2σ err	Age (Ma)	2σ err	% Disc
8	351	2.15	3.39500	0.23870	1502.0	13.0	1379.0	19.0	1692	5	18.5
26	151	0.97	4.08200	0.28570	1650.3	6.7	1620.0	10.0	1692	7	4.3
5	177.3	2.27	4.54000	0.31770	1738.1	7.0	1778.0	19.0	1695	6	4.9
34	250.5	2.93	4.00700	0.28150	1635.1	8.4	1598.0	16.0	1697	9	5.8
2	262	2.12	3.89300	0.27270	1612.2	4.4	1554.6	9.9	1697	6	8.4
114	89	0.83	4.02800	0.27920	1639.5	6.9	1587.0	12.0	1701	7	6.7
1	164	0.97	4.20300	0.29250	1674.3	6.6	1653.8	9.7	1704	7	2.9
83	146.2	2.29	4.03600	0.27950	1641.0	6.6	1589.0	13.0	1713	6	7.3
78	135.6	1.20	3.84500	0.26560	1601.8	9.3	1518.0	16.0	1719	8	11.7
53	110	1.50	4.24100	0.29090	1681.6	5.7	1646.0	11.0	1730	6	4.8
87	368	1.87	2.67000	0.18400	1296.0	58.0	1080.0	75.0	1731	8	37.6
80	182.9	2.35	4.13200	0.28050	1660.4	5.7	1594.0	11.0	1746	5	8.7
76	256	7.36	3.80700	0.25720	1596.1	8.8	1475.0	17.0	1762	7	16.3
17	701	2.39	3.80100	0.25330	1592.7	6.3	1455.0	10.0	1774	10	18.0
113	581	7.76	3.45000	0.23300	1517.0	37.0	1349.0	57.0	1778	18	24.1
28	624	2.83	4.07200	0.27110	1647.0	14.0	1548.0	19.0	1783	10	13.2
30	255	2.91	3.84000	0.24730	1598.0	28.0	1422.0	45.0	1851	6	23.2
67	447	59.20	2.85000	0.17900	1359.0	43.0	1058.0	65.0	1858	16	43.1
110	143	1.20	4.97600	0.31530	1816.0	5.7	1769.0	15.0	1871	10	5.5
84	582	9.42	5.16600	0.31760	1846.2	9.7	1778.0	19.0	1923	5	7.6
106	1.667	-99.00	6.90000	0.37400	2104.0	42.0	2048.0	56.0	2156	75	5.0
66	15.32	20.40	5.67000	0.26410	1927.0	16.0	1511.0	18.0	2418	28	37.5
63	262	0.53	10.65000	0.43040	2492.3	9.1	2307.0	18.0	2651	4	13.0
71	116.4	27.40	11.93400	0.48030	2599.7	5.8	2528.0	13.0	2662	5	5.0
45	91.5	1.19	11.93000	0.46830	2598.4	8.0	2475.0	19.0	2696	5	8.2

13MCSMG6					207/ 235		206/ 238		206/ 207		
#	[U] ppm	U/Th	207/ 235	206/ 238	Age Ma	2σ err	Age (Ma)	2σ err	Age (Ma)	2σ err	% Disc
65	474	3.35	0.06160	0.00979	60.7	1.4	62.8	1.1	228.0	27	-3.5
107	360	2.23	0.06860	0.01087	67.2	3.7	69.7	2.6	291.0	69	-3.7
112	980	1.95	0.06970	0.01138	68.4	1.5	73.0	1.2	135.0	20	-6.7
71	702	3.32	0.08690	0.01303	84.6	1.5	83.5	1.1	173.0	24	1.3
33	201	3.01	0.09040	0.01339	87.8	2.8	85.7	1.6	258.0	41	2.4
17	716	2.67	0.08710	0.01354	84.8	1.6	86.7	1.2	118.0	17	-2.2
46	428	1.63	0.09070	0.01358	88.1	2.2	87.0	1.5	148.0	23	1.2
43	378	1.59	0.09100	0.01371	88.4	2.1	87.7	1.4	204.0	33	0.8
34	509	17.80	0.09450	0.01378	91.7	1.7	88.2	1.8	236.0	34	3.8
25	271	2.38	0.09240	0.01386	89.9	2.2	88.8	1.3	216.0	32	1.2
26	699	3.31	0.09220	0.01388	89.5	1.6	88.8	0.9	143.0	22	0.7
36	507	1.70	0.09150	0.01403	89.2	1.8	89.8	1.4	147.0	22	-0.7
93	154	2.49	0.09600	0.01405	93.0	4.2	89.9	2.6	240.0	47	3.3
45	648	3.65	0.09200	0.01410	89.3	2.6	90.3	1.8	113.0	38	-1.1
8	183	2.79	0.09710	0.01413	94.0	2.9	90.5	1.7	271.0	35	3.7
9	289	3.68	0.09360	0.01418	91.1	2.8	90.8	3.1	264.0	51	0.3
87	448	2.14	0.09480	0.01421	91.9	2.1	90.9	1.6	189.0	27	1.1
18	104	3.50	0.09210	0.01423	89.3	4.0	91.1	2.4	360.0	59	-2.0
31	111	3.17	0.09790	0.01428	94.6	4.4	91.4	2.2	340.0	64	3.4
42	272	3.57	0.09560	0.01438	92.7	2.3	92.0	1.5	164.0	28	0.8
13	138	2.23	0.09310	0.01448	90.3	2.9	92.6	2.2	219.0	48	-2.5
37	215	2.81	0.09850	0.01449	95.3	3.1	92.7	2.1	228.0	40	2.7
11	359	2.39	0.09710	0.01450	94.0	2.7	92.8	1.4	197.0	31	1.3
53	660	6.10	0.09660	0.01452	93.6	1.9	93.0	1.4	167.0	28	0.6
57	426	3.72	0.09610	0.01463	93.2	2.3	93.6	1.3	131.0	22	-0.4
117	12	3.34	0.09520	0.01466	92.1	5.7	93.8	2.5	258.0	58	-1.8
100	222	1.61	0.09720	0.01472	94.1	2.7	94.2	1.5	158.0	27	-0.1
84	67.1	2.95	0.09850	0.01476	95.8	4.8	94.4	2.7	348.0	57	1.5
94	73.5	2.23	0.10240	0.01475	98.6	7.1	94.4	2.9	460.0	84	4.3
106	163	3.66	0.09560	0.01476	93.1	3.4	94.4	2.1	245.0	50	-1.4
120	8.2	2.27	0.10050	0.01475	97.1	4.2	94.4	2.0	259.0	54	2.8
23	357	2.28	0.09710	0.01480	94.3	1.8	94.7	1.0	136.0	22	-0.4
29	127.4	2.67	0.09530	0.01480	92.3	3.7	94.7	1.9	215.0	34	-2.6
72	439	2.07	0.10000	0.01480	96.8	2.0	94.7	1.3	189.0	35	2.2
76	359	7.00	0.10100	0.01480	97.6	2.9	94.7	1.7	225.0	37	3.0
86	193	3.46	0.10370	0.01482	100.1	3.3	94.8	1.9	247.0	38	5.3

13MCSMG6					207/ 235		206/ 238		206/ 207		
#	[U] ppm	U/Th	207/ 235	206/ 238	Age Ma	2σ err	Age (Ma)	2σ err	Age (Ma)	2σ err	% Disc
39	246	3.76	0.10000	0.01484	97.1	3.4	94.9	1.9	257.0	47	2.3
3	122.7	2.55	0.09800	0.01489	94.8	3.6	95.3	2.0	238.0	43	-0.5
48	183.4	2.98	0.10120	0.01491	97.7	4.4	95.4	2.3	229.0	41	2.4
5	170	2.90	0.10340	0.01494	99.8	3.5	95.6	2.0	332.0	53	4.2
20	186	2.80	0.09880	0.01495	95.6	3.2	95.7	1.7	255.0	45	-0.1
114	388	5.97	0.09740	0.01495	94.6	2.1	95.7	1.1	137.0	25	-1.2
55	272	1.96	0.09760	0.01497	94.5	2.3	95.8	1.3	148.0	28	-1.4
15	756	2.54	0.09720	0.01501	94.2	2.1	96.0	1.7	114.0	15	-1.9
32	465	1.48	0.09950	0.01501	96.3	2.0	96.1	1.3	152.0	28	0.2
77	256	2.16	0.10190	0.01501	98.5	2.8	96.1	1.6	251.0	47	2.4
62	503	1.39	0.09780	0.01507	94.7	2.2	96.4	1.1	138.0	23	-1.8
108	773	2.05	0.10200	0.01509	98.6	1.8	96.5	2.3	209.0	40	2.1
49	357	1.84	0.10120	0.01511	97.8	3.9	96.7	2.0	199.0	53	1.1
90	500	2.21	0.10200	0.01512	98.6	2.6	96.7	1.7	214.0	32	1.9
41	131.2	2.90	0.09940	0.01515	96.1	3.2	96.9	2.0	212.0	41	-0.8
88	258	1.90	0.09790	0.01518	94.7	2.8	97.1	1.6	176.0	32	-2.5
67	776	6.85	0.10180	0.01521	98.4	2.9	97.3	1.8	146.0	31	1.1
101	290.2	1.85	0.10130	0.01526	97.9	2.3	97.6	1.2	168.0	24	0.3
109	191	4.90	0.09980	0.01525	96.5	3.0	97.6	2.0	214.0	39	-1.1
79	173	4.24	0.10100	0.01527	97.6	4.7	97.7	3.9	186.0	42	-0.1
105	679	2.70	0.10080	0.01528	97.4	1.7	97.7	1.5	153.0	25	-0.3
1	193	6.53	0.09980	0.01529	96.5	2.7	97.8	1.5	192.0	38	-1.3
30	182	2.46	0.10110	0.01532	97.7	3.5	98.0	1.8	176.0	37	-0.3
27	88	2.49	0.09970	0.01540	96.2	6.0	98.5	2.8	311.0	68	-2.4
51	146.1	3.09	0.09940	0.01540	96.1	3.2	98.5	1.8	249.0	47	-2.5
10	581	1.79	0.10670	0.01544	102.9	2.9	98.8	2.6	202.0	32	4.0
16	579	2.67	0.10180	0.01547	98.4	1.9	98.9	1.4	176.0	22	-0.5
50	439	2.25	0.10420	0.01550	100.8	1.9	99.1	1.2	174.0	24	1.7
74	306	1.86	0.10480	0.01552	100.9	4.7	99.2	1.6	297.0	92	1.7
6	151.5	2.75	0.10370	0.01552	100.1	2.6	99.3	2.1	280.0	36	0.8
58	104	2.70	0.09840	0.01552	95.2	3.6	99.3	2.2	233.0	47	-4.3
47	152	1.40	0.10220	0.01560	98.7	3.2	99.8	1.8	217.0	34	-1.1
52	180	2.29	0.10390	0.01561	100.7	3.8	99.9	1.6	220.0	44	0.8
102	669	6.40	0.10440	0.01566	100.7	2.0	100.2	1.5	194.0	27	0.5
12	180	2.15	0.09840	0.01570	95.2	3.7	100.4	2.7	194.0	47	-5.5
59	110	1.75	0.10590	0.01570	101.9	5.2	100.4	3.0	382.0	86	1.5

13MCSMG6					207/ 235		206/ 238		206/ 207		
#	[U] ppm	U/Th	207/ 235	206/ 238	Age Ma	2σ err	Age (Ma)	2σ err	Age (Ma)	2σ err	% Disc
73	435	2.80	0.10870	0.01573	104.8	2.5	100.6	1.3	243.0	39	4.0
97	357	4.78	0.10400	0.01573	100.7	2.1	100.6	1.6	188.0	35	0.1
63	501	2.08	0.10520	0.01574	101.6	2.0	100.7	1.0	177.0	25	0.9
28	281	1.55	0.10430	0.01586	100.7	2.7	101.4	1.5	189.0	31	-0.7
44	153	2.97	0.10960	0.01602	105.5	4.1	102.4	3.1	366.0	54	2.9
113	520	4.52	0.10840	0.01604	104.3	4.1	102.6	2.4	230.0	47	1.6
75	409	3.16	0.11120	0.01607	107.0	2.6	102.8	2.1	229.0	31	3.9
80	987	2.25	0.11030	0.01642	106.4	1.7	105.0	1.4	149.0	20	1.3
81	1016	15.60	0.10850	0.01654	104.5	4.3	105.7	3.9	149.0	42	-1.1
82	370	3.18	0.11270	0.01664	108.3	4.5	106.3	2.2	182.0	36	1.8
111	321	2.67	0.11050	0.01672	107.2	3.0	106.9	2.5	194.0	39	0.3
68	582	3.78	0.10860	0.01689	104.6	2.8	108.0	2.8	158.0	44	-3.3
116	790	2.97	0.11890	0.01703	114.0	2.7	108.9	2.1	284.0	25	4.5
7	80.2	2.89	0.15130	0.02229	142.9	8.1	142.1	4.6	262.0	59	0.6
83	158.9	4.25	0.14950	0.02236	141.3	4.7	143.0	2.9	226.0	50	-1.2
67	120.4	2.51	0.14570	0.02254	137.9	7.5	143.7	3.8	215.0	57	-4.2
91	198.2	1.44	0.15630	0.02281	147.3	3.3	145.4	2.0	233.0	30	1.3
38	279	1.49	0.15940	0.02351	150.5	3.5	149.8	1.6	191.0	28	0.5
110	161.2	1.45	0.17880	0.02385	166.8	5.7	151.9	2.7	377.0	51	8.9
19	272	2.37	0.16140	0.02403	151.8	3.2	153.1	2.1	213.0	30	-0.9
69	145.1	2.11	0.16150	0.02464	151.9	3.8	156.9	2.7	192.0	31	-3.3
96	175.6	1.54	0.16900	0.02466	158.4	5.4	157.0	3.0	200.0	47	0.9
40	227	4.24	0.17370	0.02488	162.5	3.6	158.4	2.8	233.0	28	2.5
78	131	1.81	0.17050	0.02507	159.7	5.0	159.6	2.6	253.0	36	0.1
61	124	2.26	0.17500	0.02510	163.5	4.7	159.8	2.6	262.0	39	2.3
92	76.1	1.55	0.18360	0.02525	171.6	6.8	160.8	4.0	412.0	48	6.3
85	158	2.08	0.17570	0.02543	164.2	4.0	161.8	2.2	221.0	37	1.5
4	239	1.68	0.17130	0.02544	160.9	4.8	161.9	3.5	227.0	40	-0.6
35	111.2	2.44	0.17310	0.02573	161.8	5.2	163.8	3.1	193.0	33	-1.2
64	139.2	1.43	0.18560	0.02612	172.6	8.1	166.2	3.8	348.0	42	3.7
119	9.9	1.52	0.17790	0.02617	166.0	4.9	166.5	3.5	259.0	38	-0.3
22	97.9	1.67	0.17450	0.02629	163.0	7.2	167.3	3.8	272.0	63	-2.6
24	166	2.79	0.17170	0.02632	160.8	3.3	167.5	1.9	196.0	32	-4.2
66	169	1.54	0.18240	0.02640	169.9	4.1	168.0	2.6	250.0	37	1.1
118	13	1.31	0.18000	0.02643	169.7	9.4	168.2	4.7	276.0	65	0.9
89	109	1.71	0.17730	0.02645	165.6	3.7	168.3	3.3	182.0	27	-1.6

13MCSMG6					207/ 235		206/ 238		206/ 207		
#	[U ppm	U/Th	207/ 235	206/ 238	Age Ma	2σ err	Age (Ma)	2σ err	Age (Ma)	2σ err	% Disc
81	92	1.75	0.19580	0.02671	181.4	7.9	171.2	6.2	329.0	84	5.6
21	820	2.13	0.18480	0.02733	172.1	3.8	173.8	2.8	161.0	19	-1.0
56	290	1.62	0.19460	0.02855	180.4	4.2	181.4	3.1	191.0	33	-0.6
68	108.5	1.01	0.20200	0.03038	186.4	9.9	192.9	5.7	139.0	53	-3.5
103	133.5	2.68	0.21520	0.03126	197.7	4.7	198.4	3.2	292.0	39	-0.4
104	71.5	0.71	1.21500	0.12700	807.0	14.0	770.0	18.0	917.0	23	4.6
70	284	0.99	1.89000	0.18120	1077.4	7.1	1073.3	8.3	1080.5	10	0.7
54	115.3	1.22	1.81800	0.16870	1052.7	8.9	1005.0	11.0	1148.0	19	12.5
95	83	1.70	2.35100	0.19690	1225.0	29.0	1158.0	33.0	1350.0	33	14.2

13MCSMG8					207/ 235		206/ 238		206/ 207		
#	[U] ppm	U/Th	207/ 235	206/ 238	Age Ma	2 σ err	Age (Ma)	2 σ err	Age (Ma)	2 σ err	% Disc
73	253	1.01	0.00380	0.00060	3.8	1.1	3.8	0.3	990.0	330	-1.1
105	152	1.22	0.00470	0.00061	4.8	1.2	3.9	0.5	1310.0	250	99.7
233	2	1.02	0.00900	0.00061	9.1	2.3	3.9	0.6	7.1	370	99.8
28	1.4	1.01	0.00540	0.00064	5.5	1.5	4.1	0.5	5.9	280	99.8
228	1.3	0.91	0.00430	0.00067	4.4	1.3	4.3	0.5	18.0	270	99.7
239	0.63	0.90	0.00442	0.00069	4.5	0.5	4.4	0.2	17.0	130	1.3
59	1053	0.47	0.00545	0.00069	5.5	0.5	4.5	0.2	590.0	140	99.2
26	2090	3.30	0.02120	0.00312	21.3	0.6	20.1	0.4	182.0	30	5.8
106	107.4	0.95	0.02420	0.00317	24.2	2.4	20.4	1.2	810.0	130	97.5
215	1.9	1.27	0.02115	0.00339	21.2	0.9	21.8	0.5	13.0	54	-2.8
79	296.7	0.90	0.02210	0.00352	22.2	1.3	22.7	0.7	349.0	83	-2.1
27	3.5	1.12	0.02860	0.00365	28.6	2.5	23.5	0.9	6.3	84	96.3
221	1.7	0.46	0.02440	0.00368	24.4	1.3	23.7	0.7	75.0	54	3.0
29	109	1.29	0.02870	0.00377	28.7	5.1	24.2	1.7	660.0	130	96.3
3	86.2	0.71	0.02870	0.00396	28.6	3.0	25.5	1.5	680.0	100	96.3
72	199	0.89	0.02810	0.00403	28.1	1.9	25.9	0.9	479.0	83	7.8
12	189	0.98	0.02760	0.00407	27.6	2.1	26.2	1.0	449.0	76	5.1
55	193	1.03	0.03080	0.00417	30.8	2.4	26.8	0.9	466.0	87	94.2
216	2.8	0.95	0.02730	0.00424	27.3	1.6	27.3	1.0	25.0	65	0.0
229	6.1	1.76	0.03510	0.00425	34.9	3.3	27.3	1.3	15.0	100	96.3
20	616	0.77	0.02840	0.00425	28.4	1.6	27.3	0.8	372.0	75	3.8
238	4.2	1.62	0.03150	0.00444	31.4	2.0	28.6	1.0	9.4	110	8.9
99	727	1.37	0.02890	0.00447	28.9	1.1	28.8	0.8	185.0	53	0.5
34	272	0.69	0.03630	0.00452	36.2	2.7	29.1	0.9	760.0	120	96.2
107	244	1.53	0.02950	0.00453	29.5	1.8	29.1	0.7	272.0	67	1.3
14	124.4	0.50	0.02860	0.00460	28.5	3.1	29.6	1.2	410.0	99	-3.9
8	688	0.86	0.03140	0.00476	31.3	1.1	30.6	0.6	278.0	59	2.2
222	2.5	0.52	0.03190	0.00486	31.9	2.0	31.2	1.0	38.0	77	2.1
28	135.3	0.72	0.02950	0.00496	29.5	2.1	31.9	1.6	328.0	81	-8.1
44	161.8	0.40	0.03520	0.00537	35.4	2.6	34.5	1.1	498.0	96	2.5
21	2.9	0.72	0.03480	0.00540	34.7	1.2	34.8	0.9	81.0	49	-0.1
118	199.7	0.44	0.04410	0.00558	43.8	5.2	35.8	1.9	520.0	160	93.1
37	245	1.48	0.04390	0.00632	43.5	3.2	40.6	1.3	510.0	110	6.7
112	252	0.54	0.04480	0.00650	44.5	2.5	41.8	1.1	301.0	49	6.1
10	208	1.61	0.07960	0.01210	77.7	2.6	77.6	1.5	215.0	47	0.1
26	6.4	1.32	0.08090	0.01217	78.9	2.2	78.0	1.5	21.0	38	1.1

13MCSMG8					207/ 235		206/ 238		206/ 207		
#	[U] ppm	U/Th	207/ 235	206/ 238	Age Ma	2σ err	Age (Ma)	2σ err	Age (Ma)	2σ err	% Disc
2	397	1.41	0.08550	0.01333	83.5	2.1	85.4	1.5	183.0	36	-2.3
27	582	1.06	0.09430	0.01406	91.5	1.6	90.0	1.1	190.0	30	1.6
78	401	1.60	0.09500	0.01449	92.4	2.7	92.7	1.1	152.0	23	-0.3
41	165	0.50	0.09940	0.01459	96.1	3.9	93.4	2.1	370.0	69	2.8
11	335	1.76	0.10370	0.01494	100.4	2.6	95.6	1.6	223.0	31	4.8
53	561	1.87	0.10080	0.01514	97.5	2.0	96.9	1.1	167.0	29	0.6
81	108.7	0.51	0.10920	0.01606	105.1	4.2	102.7	2.1	306.0	51	2.3
83	338	0.92	0.11080	0.01636	106.6	3.5	105.1	2.8	214.0	38	1.4
32	87.2	0.92	0.16300	0.02310	154.0	6.2	147.2	4.6	315.0	45	4.4
87	95	0.91	0.16590	0.02483	155.4	8.5	158.1	4.6	285.0	66	-1.7
21	158.5	0.75	0.16900	0.02502	158.4	4.6	159.3	2.7	170.0	31	-0.6
29	22	1.13	0.24200	0.03390	220.0	13.0	214.9	6.8	5.9	81	2.3
64	422	2.51	0.26010	0.03572	234.6	4.0	226.3	3.1	314.0	34	3.5
4	204.4	1.25	0.29610	0.04158	263.1	5.7	262.6	3.8	265.0	31	0.2
52	333	1.47	0.30430	0.04159	269.5	5.1	262.7	3.3	351.0	31	2.5
97	680	1.23	0.29600	0.04214	263.2	4.7	266.1	5.4	266.0	31	-1.1
113	550	9.15	0.32740	0.04560	287.5	3.1	287.5	2.9	296.0	22	0.0
24	30	1.79	0.48210	0.06030	399.2	6.1	377.2	6.5	8.1	17	5.5
19	378	0.68	0.49300	0.06045	406.4	7.5	378.3	5.3	554.0	36	6.9
58	100.7	1.10	0.46700	0.06121	389.0	8.0	382.9	6.0	445.0	32	1.6
93	341	3.35	0.49200	0.06150	405.8	7.5	384.4	7.8	541.0	26	5.3
100	536	0.95	0.47500	0.06184	394.5	4.3	386.8	4.2	440.0	21	2.0
86	211	2.56	0.48160	0.06348	399.6	5.2	396.7	4.5	405.0	25	0.7
31	313	2.45	0.50270	0.06489	413.3	5.0	405.3	4.2	462.0	17	1.9
71	322	0.96	0.53180	0.06610	432.8	4.8	412.8	6.1	549.0	24	4.6
60	201	0.87	0.51480	0.06652	421.2	6.6	415.2	4.7	446.0	20	1.4
43	246	0.95	0.52380	0.06730	427.5	5.4	419.9	4.8	495.0	25	1.8
51	130	1.80	0.57800	0.06767	463.9	7.4	422.1	5.9	662.0	25	9.0
98	127	1.62	0.50300	0.06803	414.5	7.0	424.2	6.0	401.0	30	-2.3
210	34	0.85	0.59300	0.07417	475.0	9.5	461.2	5.7	7.4	34	2.9
88	90.4	0.84	0.64500	0.08070	504.0	17.0	500.3	9.1	520.0	51	0.7
88	161	1.81	0.72800	0.08880	555.0	12.0	548.0	14.0	536.0	28	1.3
38	95.5	1.17	0.70600	0.08880	545.0	10.0	548.7	7.0	552.0	31	-0.7
23	40	1.22	0.75100	0.09100	568.3	7.4	561.1	6.6	2.4	22	1.3
230	40	0.81	0.77900	0.09230	584.5	9.5	569.2	7.5	8.5	28	2.6
122	159	1.37	0.83000	0.09430	613.0	12.0	581.0	14.0	748.0	47	5.2

13MCSMG8					207/ 235		206/ 238		206/ 207		
#	[U] ppm	U/Th	207/ 235	206/ 238	Age Ma	2σ err	Age (Ma)	2σ err	Age (Ma)	2σ err	% Disc
24	129.8	0.93	0.80100	0.09750	596.6	8.5	599.5	8.6	568.0	22	-0.5
77	327	1.15	0.80510	0.09787	599.4	5.5	601.9	5.5	591.0	13	-0.4
13	35.7	1.16	0.87900	0.10450	639.0	13.0	640.6	9.9	679.0	33	-0.3
68	31.6	1.56	1.50600	0.15500	931.0	13.0	928.0	14.0	938.0	32	1.1
57	31.1	1.58	1.59500	0.15820	968.0	16.0	946.0	15.0	1030.0	31	8.2
109	31.5	0.71	1.71000	0.16460	1010.0	18.0	982.0	20.0	1078.0	38	8.9
36	72.5	1.47	1.66400	0.16080	995.0	13.0	964.0	17.0	1083.0	25	11.0
5	6.7	2.23	1.64700	0.16420	989.0	31.0	979.0	29.0	1092.0	60	10.3
89	182.5	1.24	2.00300	0.18690	1116.0	8.1	1104.0	12.0	1126.0	14	2.0
17	154	1.06	2.08700	0.19300	1144.8	8.5	1137.3	9.5	1145.0	14	0.7
92	128.5	1.35	2.07300	0.19030	1139.0	10.0	1123.0	13.0	1168.0	19	3.9
80	70	0.67	2.21400	0.19900	1186.0	12.0	1170.0	13.0	1198.0	23	2.3
123	176.9	0.80	2.17400	0.19670	1174.0	9.9	1158.0	11.0	1198.0	17	3.3
25	95	2.10	2.06700	0.18640	1137.0	11.0	1102.0	15.0	15.0	20	9.4
66	70.1	0.83	2.66300	0.23000	1317.0	10.0	1334.0	15.0	1288.0	18	-3.6
220	110	1.28	1.64900	0.14200	989.0	12.0	856.0	17.0	210.0	9	33.8
120	124	1.32	2.77800	0.23220	1349.0	10.0	1348.0	17.0	1360.5	10	0.9
122	41.5	1.52	2.40500	0.20360	1243.0	25.0	1194.0	26.0	1366.0	38	12.6
110	218	1.68	2.48600	0.20560	1270.0	15.0	1205.0	24.0	1387.0	21	13.1
108	51	0.62	3.00200	0.24620	1410.0	12.0	1419.0	15.0	1392.0	17	-1.9
22	95	0.74	2.59000	0.20970	1296.0	20.0	1227.0	17.0	2.7	20	12.4
40	326	1.05	2.95700	0.24050	1397.2	8.6	1391.0	17.0	1414.0	12	1.6
63	133	1.45	3.09400	0.24940	1430.4	9.9	1438.0	16.0	1416.0	12	-1.6
7	424	0.57	2.57200	0.20670	1294.0	11.0	1211.0	18.0	1421.0	10	14.8
212	92	0.50	3.11000	0.25040	1435.7	9.8	1440.0	12.0	3.5	14	-0.2
65	34.92	0.62	2.51900	0.19920	1276.0	19.0	1171.0	19.0	1456.0	33	19.6
232	90	0.74	2.74000	0.21570	1341.6	9.1	1259.0	11.0	8.2	13	14.4
67	111.4	1.33	2.57100	0.20160	1288.0	26.0	1184.0	23.0	1481.0	31	20.1
104	78	0.76	3.26300	0.25530	1470.0	23.0	1465.0	30.0	1490.0	18	1.7
18	137	1.45	3.29900	0.25510	1480.4	9.2	1464.0	18.0	1496.0	13	2.1
16	93.9	0.95	3.39700	0.26180	1503.2	7.7	1499.0	12.0	1510.0	11	0.7
82	111.8	1.79	3.35000	0.26020	1490.0	33.0	1490.0	43.0	1516.0	32	1.7
103	271	0.57	2.56000	0.19390	1288.0	21.0	1142.0	30.0	1544.0	13	26.0
240	100	1.32	2.75600	0.20850	1342.0	25.0	1220.0	32.0	1.1	32	21.4
15	169.8	1.13	2.33700	0.17330	1223.0	15.0	1030.0	15.0	1577.0	22	34.7
42	298	2.06	2.88800	0.21030	1378.0	12.0	1230.0	17.0	1625.0	13	24.3

13MCSMG8					207/ 235		206/ 238		206/ 207		
#	[U] ppm	U/Th	207/ 235	206/ 238	Age Ma	2σ err	Age (Ma)	2σ err	Age (Ma)	2σ err	% Disc
94	119.7	0.74	3.86900	0.28090	1607.8	9.0	1596.0	15.0	1628.0	11	2.0
49	73	1.18	4.17700	0.29760	1668.0	13.0	1679.0	18.0	1642.0	12	-2.3
236	100	0.67	3.95300	0.28130	1624.0	10.0	1598.0	15.0	7.9	12	4.3
50	208	1.22	4.09700	0.28970	1653.0	10.0	1640.0	16.0	1670.4	10	1.8
116	55.5	1.14	4.22300	0.29690	1679.0	10.0	1675.0	18.0	1689.0	14	0.8
101	96.5	1.43	4.28300	0.29910	1689.0	10.0	1686.0	16.0	1690.0	15	0.2
25	117	1.71	3.79000	0.26200	1588.0	25.0	1505.0	56.0	1692.0	46	11.1
91	317	1.20	3.96200	0.27580	1626.2	6.2	1570.0	11.0	1695.0	10	7.4
96	1190	1.04	4.46200	0.31160	1728.0	12.0	1748.0	24.0	1696.4	6	-3.0
114	100	0.79	3.78000	0.26490	1587.0	16.0	1514.0	33.0	1699.0	15	10.9
46	410	0.75	4.17500	0.29090	1669.0	14.0	1646.0	22.0	1701.0	16	3.2
224	110	0.70	4.13300	0.28770	1660.4	9.2	1630.0	16.0	17.0	12	4.3
69	260	1.31	4.26700	0.29690	1686.3	8.8	1678.0	15.0	1706.9	7	1.7
1	147	0.82	4.44600	0.30740	1720.4	8.0	1728.0	18.0	1707.0	14	-1.2
225	110	1.16	3.78500	0.26250	1588.0	15.0	1502.0	25.0	6.5	14	12.1
48	111.3	1.83	4.27400	0.29620	1689.8	7.5	1672.0	12.0	1710.0	12	2.2
226	110	0.67	3.92300	0.27160	1622.0	12.0	1548.0	20.0	1.8	16	9.6
70	153	1.14	4.29300	0.29710	1691.5	7.9	1677.0	18.0	1716.3	9	2.3
61	120	0.62	4.32300	0.30040	1698.3	8.5	1693.0	16.0	1720.0	12	1.6
237	110	16.50	4.19100	0.28900	1672.1	7.0	1636.0	16.0	13.0	12	5.0
35	187	11.70	4.17400	0.28840	1668.2	8.4	1633.0	11.0	1729.7	9	5.6
85	192	1.13	4.65500	0.31790	1758.6	9.1	1779.0	17.0	1735.3	7	-2.5
39	142.1	0.81	4.47900	0.30830	1728.9	9.8	1732.0	19.0	1736.6	10	0.3
23	526	1.04	4.24000	0.28480	1680.0	21.0	1614.0	37.0	1743.0	16	7.4
22	441	2.82	2.87000	0.19540	1379.0	32.0	1149.0	44.0	1763.0	13	34.8
211	120	1.62	3.94500	0.26520	1621.0	15.0	1519.0	22.0	7.3	15	13.9
231	110	1.70	4.10700	0.27720	1655.1	9.8	1577.0	16.0	9.6	12	10.7
124	336	1.18	5.77000	0.36290	1942.0	10.0	1996.0	22.0	1873.0	12	-6.6
47	186.4	5.90	5.37600	0.33880	1881.7	8.7	1880.0	16.0	1890.3	8	0.5
213	110	0.30	4.96200	0.27840	1812.0	17.0	1583.0	26.0	2.7	20	24.1
111	142.9	0.83	10.57200	0.46380	2485.8	7.1	2456.0	16.0	2508.2	6	2.1
121	272	1.29	11.31000	0.46350	2551.0	17.0	2454.0	32.0	2626.0	11	6.5
30	196	0.78	11.65800	0.47230	2577.0	7.7	2496.0	20.0	2643.1	8	5.6

13MCSMG9					207/ 235		206/ 238		206/ 207		
#	[U] ppm	U/Th	207/ 235	206/ 238	Age Ma	2σ err	Age (Ma)	2σ err	Age (Ma)	2σ err	% Disc
4	830	0.50	0.00527	0.00065	5.3	0.5	4.2	0.1	620.0	130	99.3
36	1379	0.93	0.00704	0.00074	7.1	0.4	4.7	0.1	935.0	77	99.5
86	413	0.99	0.01700	0.00077	17.0	3.9	5.0	0.3	1920.0	340	99.7
19	266.2	1.22	0.01664	0.00239	16.8	0.7	15.4	0.3	329.0	45	8.0
57	764	1.44	0.02377	0.00367	23.9	0.5	23.6	0.3	116.0	22	1.1
103	2020	0.63	0.02491	0.00375	25.0	0.5	24.2	0.3	140.0	28	3.3
93	606	0.56	0.03150	0.00429	31.5	1.5	27.6	0.7	373.0	75	92.6
124	215	0.67	0.02795	0.00429	28.0	0.9	27.6	0.6	246.0	38	1.3
5	483.5	1.05	0.02888	0.00437	28.9	0.7	28.1	0.4	152.0	28	2.8
21	605	0.83	0.03096	0.00466	31.0	0.6	30.0	0.4	168.0	29	3.2
101	79.9	0.94	0.04350	0.00478	43.1	3.9	30.8	0.9	850.0	140	96.4
121	73.4	0.83	0.03420	0.00499	34.1	2.8	32.1	1.4	388.0	72	5.9
10	295	0.38	0.04640	0.00528	46.5	2.9	34.0	0.6	780.0	89	95.6
15	258	2.49	0.03540	0.00537	35.4	1.0	34.5	0.5	213.0	45	2.5
43	455	0.84	0.03910	0.00564	39.0	1.1	36.3	0.6	277.0	67	7.0
60	614	0.76	0.03860	0.00587	38.5	1.4	37.7	0.6	178.0	39	2.0
34	383	1.26	0.05750	0.00874	56.8	1.2	56.1	0.6	158.0	28	1.2
92	85	0.75	0.06270	0.00977	61.7	2.7	62.7	1.3	183.0	36	-1.6
127	38.47	1.06	0.07680	0.01086	75.0	5.6	69.6	2.8	254.0	83	7.2
13	240.4	1.86	0.08090	0.01123	78.9	2.7	72.0	1.2	299.0	34	8.7
104	109.5	0.58	0.08230	0.01202	80.3	3.6	77.0	1.3	321.0	68	4.1
68	307	1.18	0.09090	0.01325	88.3	2.0	84.9	1.5	206.0	32	3.9
39	107.5	0.63	0.17080	0.02335	160.0	4.2	149.3	2.7	303.0	29	6.7
28	167.6	0.57	0.22880	0.03254	209.2	3.0	206.4	2.0	277.0	21	1.3
53	347	0.78	0.28900	0.04011	257.7	3.4	253.5	2.4	296.0	26	1.6
14	178	1.85	0.40270	0.05301	343.4	6.1	332.9	4.8	427.0	31	3.1
66	426.5	2.55	0.44530	0.05686	373.9	5.5	356.5	5.9	481.0	17	4.7
105	550	1.46	0.44230	0.05905	371.8	3.2	369.8	3.3	387.4	10	0.5
7	103	1.13	0.46680	0.06109	388.8	4.5	382.2	3.1	441.0	18	1.7
90	438	1.19	0.50160	0.06410	412.7	5.3	400.4	7.7	471.0	19	3.0
37	295.8	1.07	0.49820	0.06570	410.4	3.2	410.2	2.9	420.0	12	0.0
42	329	1.84	0.50320	0.06601	413.7	3.9	412.1	3.7	441.0	11	0.4
18	307	1.03	0.51320	0.06750	420.5	4.4	421.1	3.5	431.0	18	-0.1
123	102.6	1.19	0.57940	0.07324	463.8	5.7	455.6	4.9	496.0	22	1.8
3	368	1.18	0.60700	0.07370	482.3	4.7	458.4	4.2	576.0	18	5.0
102	170.1	1.09	0.68100	0.08131	528.0	3.6	503.9	4.7	620.0	15	4.6

13MCSMG9					207/ 235		206/ 238		206/ 207		
#	[U] ppm	U/Th	207/ 235	206/ 238	Age Ma	2σ err	Age (Ma)	2σ err	Age (Ma)	2σ err	% Disc
22	264	7.30	0.73900	0.08500	558.0	20.0	526.0	15.0	758.0	62	5.7
44	77.7	0.47	0.71800	0.08740	549.4	7.3	540.2	8.2	592.0	31	1.7
74	460	1.77	0.82990	0.09104	613.4	5.0	561.7	3.9	833.0	14	8.4
95	219.5	0.49	0.75690	0.09253	572.6	3.6	570.5	3.7	566.0	13	0.4
113	227	3.48	0.79270	0.09520	592.5	5.5	586.2	6.4	624.0	17	1.1
78	305	1.57	0.93400	0.10690	669.3	5.6	654.6	6.4	716.5	9	2.2
9	42.3	3.55	1.00300	0.11620	705.9	8.2	708.8	6.1	717.0	21	-0.4
79	11.26	0.26	1.56700	0.15970	958.0	17.0	955.0	15.0	958.0	36	0.3
65	94.2	0.74	1.63200	0.16250	982.5	6.6	970.5	6.7	1018.0	12	4.7
38	117.4	2.32	1.52300	0.15140	939.4	4.8	908.9	7.3	1025.0	11	11.3
49	111.9	1.09	1.70600	0.16900	1010.4	9.0	1006.3	8.6	1026.0	13	1.9
110	44.7	1.36	1.65600	0.16160	990.0	19.0	966.0	12.0	1032.0	41	6.4
100	130.9	1.90	1.67500	0.16410	998.8	5.0	979.4	7.4	1039.9	9	5.8
106	147.4	1.98	2.09100	0.19410	1145.8	4.0	1143.6	6.6	1152.2	7	0.7
48	63	2.29	2.17700	0.19920	1175.0	13.0	1171.0	11.0	1182.0	23	0.9
46	85.5	1.31	2.11500	0.19210	1153.3	8.5	1133.8	8.5	1183.0	15	4.2
98	66.8	1.13	2.13100	0.19260	1158.6	5.8	1135.5	8.9	1198.4	9	5.2
29	331	1.44	2.61700	0.22020	1305.3	4.6	1282.9	8.9	1346.6	5	4.7
73	65.7	0.65	2.73700	0.22930	1338.3	5.3	1330.5	9.4	1362.3	8	2.3
87	45.9	1.20	2.79200	0.23090	1353.0	10.0	1339.0	16.0	1371.0	16	2.3
112	20.87	1.09	2.34900	0.19180	1221.0	25.0	1131.0	13.0	1392.0	53	18.8
75	152	1.27	2.96500	0.24140	1398.5	8.8	1394.0	11.0	1420.0	13	1.8
16	159.1	1.64	2.91400	0.23440	1385.0	7.3	1357.0	12.0	1426.3	9	4.9
122	89.5	0.69	3.02100	0.24330	1414.4	8.8	1404.0	13.0	1427.0	15	1.6
40	228.9	1.61	3.01600	0.24240	1411.4	5.3	1399.2	8.2	1428.8	6	2.1
82	108	0.91	3.05800	0.24590	1421.9	6.9	1417.1	9.9	1444.0	11	1.9
120	94	0.80	3.00300	0.23800	1408.1	9.9	1376.0	17.0	1452.0	11	5.2
70	37.19	0.53	2.28200	0.18130	1206.0	11.0	1074.0	17.0	1461.0	20	26.5
96	275	1.42	2.26600	0.17500	1201.0	11.0	1040.0	15.0	1500.7	8	30.7
6	263.5	1.31	3.19800	0.24630	1456.1	7.2	1419.0	13.0	1509.9	6	6.0
108	164.6	2.70	3.73900	0.27800	1578.0	17.0	1580.0	33.0	1567.0	19	-0.8
83	194.1	1.56	3.43200	0.25480	1512.1	4.7	1463.3	8.9	1581.2	6	7.5
32	264.1	3.63	3.25500	0.23980	1469.0	19.0	1385.0	26.0	1583.5	9	12.5
114	99.6	1.16	2.85000	0.20600	1362.0	40.0	1203.0	57.0	1652.4	8	27.2
35	133.4	1.41	3.92700	0.27630	1619.0	7.9	1572.0	16.0	1679.0	9	6.4
85	94.5	1.14	4.66800	0.32710	1761.4	5.1	1824.0	12.0	1683.9	6	-8.3

13MCSMG9					207/ 235		206/ 238		206/ 207		
#	[U] ppm	U/Th	207/ 235	206/ 238	Age Ma	2σ err	Age (Ma)	2σ err	Age (Ma)	2σ err	% Disc
11	471	1.52	2.69000	0.18720	1309.0	41.0	1102.0	52.0	1687.0	12	34.7
50	192	1.42	4.31700	0.29870	1694.0	15.0	1684.0	23.0	1690.9	7	0.4
76	58	40.70	3.39700	0.23470	1503.0	11.0	1359.0	16.0	1707.0	17	20.4
69	167.5	0.52	4.17400	0.29010	1668.6	5.9	1643.0	11.0	1711.0	5	4.0
58	137.4	1.92	4.32400	0.29860	1697.7	9.9	1684.0	19.0	1713.0	11	1.7
99	314	0.78	4.30600	0.29580	1694.3	6.3	1670.0	13.0	1715.1	8	2.6
54	751	2.66	3.96700	0.27130	1627.3	4.7	1547.5	8.2	1732.6	6	10.7
59	357	1.34	4.19800	0.28610	1673.2	6.5	1622.0	13.0	1736.2	6	6.6
118	334	1.16	4.18700	0.28640	1670.0	14.0	1623.0	28.0	1736.8	8	6.6
55	245	1.37	4.16300	0.28250	1666.6	7.1	1604.0	15.0	1742.6	6	8.0
80	486	1.95	3.84300	0.25990	1602.0	10.0	1489.0	20.0	1752.7	6	15.0
25	216	1.96	4.21000	0.28500	1672.0	23.0	1615.0	39.0	1753.0	8	7.9
17	126.1	0.61	4.59500	0.30810	1748.1	5.2	1731.0	11.0	1771.4	5	2.3
88	229	1.00	4.31000	0.27590	1690.0	25.0	1570.0	12.0	1850.0	47	15.1
116	275	1.33	3.25900	0.20700	1471.0	11.0	1212.0	21.0	1869.0	14	35.2
24	171	1.18	4.76000	0.30200	1769.0	32.0	1698.0	56.0	1891.0	17	10.2
84	54.3	9.10	5.02500	0.31140	1823.0	9.2	1747.0	15.0	1899.0	9	8.0
89	172.8	0.95	6.03600	0.34850	1980.8	5.3	1927.0	12.0	2032.0	10	5.2
115	100.2	0.89	5.18000	0.27910	1849.0	11.0	1586.0	17.0	2155.0	8	26.4
30	172	1.20	7.77000	0.32950	2203.0	15.0	1835.0	25.0	2566.9	6	28.5
31	42.2	1.47	15.10600	0.52020	2821.7	5.6	2699.0	16.0	2912.4	5	7.3

13MCSMG21					207/ 235		206/ 238		206/ 207		
#	[U] ppm	U/Th	207/ 235	206/ 238	Age Ma	2σ err	Age (Ma)	2σ err	Age (Ma)	2σ err	% Disc
2125	0.51	0.98	0.00603	0.00065	6.1	0.7	4.2	0.2	950.0	140	99.6
288	192	0.91	0.00785	0.00070	7.9	1.0	4.5	0.2	1260.0	170	99.6
282	551	0.94	0.01700	0.00263	17.1	0.8	16.9	0.3	170.0	44	1.0
2108	99.4	0.73	0.03980	0.00311	39.6	1.9	20.0	0.6	1491.0	58	98.7
239	64.8	0.72	0.02720	0.00359	27.2	2.8	23.1	1.0	440.0	100	94.8
256	519	0.91	0.02688	0.00403	26.9	0.6	25.9	0.3	169.0	27	3.8
2123	2.1	1.43	0.03260	0.00431	32.5	1.4	27.7	0.5	457.0	80	93.9
2105	295	0.70	0.02862	0.00434	28.7	0.9	27.9	0.4	213.0	40	2.7
279	349	0.82	0.02955	0.00434	29.6	0.7	27.9	0.3	210.0	27	5.5
228	149.3	1.07	0.03140	0.00458	31.4	1.5	29.5	0.6	410.0	130	6.2
2100	287.6	2.64	0.02900	0.00460	29.0	0.7	29.6	0.4	113.0	28	-2.0
253	142.9	0.74	0.03200	0.00462	32.0	1.9	29.7	0.8	333.0	73	7.1
28	364	0.96	0.03340	0.00504	33.4	1.5	32.4	0.6	227.0	62	3.0
2122	2.5	0.84	0.03930	0.00513	39.0	3.4	33.0	0.8	750.0	140	95.6
295	205	0.74	0.03410	0.00516	34.2	1.4	33.2	0.5	283.0	54	3.0
223	542	0.80	0.03440	0.00519	34.3	0.9	33.4	0.4	169.0	38	2.8
2102	250.8	0.46	0.04160	0.00549	41.4	1.5	35.3	0.6	405.0	55	91.3
2120	320	1.60	0.04920	0.00737	48.7	1.3	47.3	0.5	198.0	37	2.9
236	240	1.65	0.05340	0.00798	52.8	1.6	51.2	0.7	175.0	38	3.0
255	510	0.80	0.07950	0.01145	77.7	1.3	73.4	0.7	214.0	33	5.5
271	247	1.41	0.09460	0.01407	91.8	1.7	90.1	1.0	178.0	27	1.9
2118	465	0.90	0.09300	0.01419	90.2	1.3	90.8	0.7	111.0	15	-0.7
243	128	0.33	0.09670	0.01504	93.7	2.4	96.2	2.1	128.0	29	-2.7
2107	301	1.80	0.10070	0.01513	97.4	1.5	96.8	1.0	129.0	23	0.6
246	74.5	0.51	0.21610	0.02980	198.4	5.3	189.3	2.0	323.0	47	4.6
24	285	0.97	0.23170	0.03337	211.5	3.0	211.6	2.4	209.0	18	0.0
226	291	0.79	0.27820	0.03570	249.2	2.3	226.1	1.6	474.0	19	9.3
229	195	0.78	0.40320	0.05467	343.9	2.7	343.1	2.8	340.0	14	0.2
2119	253	1.55	0.44250	0.05915	372.3	3.3	370.5	2.9	391.0	11	0.5
2126	18	8.93	0.48810	0.06283	403.9	3.3	392.8	2.8	459.0	16	2.7
290	310	0.70	0.48690	0.06368	402.7	3.2	398.0	2.9	427.0	12	1.2
22	186.3	1.02	0.61800	0.07380	487.9	9.2	458.9	7.7	634.0	26	5.9
283	35.7	0.94	0.67500	0.07750	523.0	15.0	480.9	8.7	694.0	49	8.0
258	469	2.97	0.66240	0.08278	516.0	3.2	512.7	3.8	534.0	9	0.6
283	76.7	1.48	0.72200	0.08690	552.7	8.9	537.4	7.7	631.0	29	2.8
218	253	1.59	0.73410	0.08786	558.9	3.5	542.9	3.7	622.1	10	2.9

13MCSMG21					207/ 235		206/ 238		206/ 207		
#	[U] ppm	U/Th	207/ 235	206/ 238	Age Ma	2σ err	Age (Ma)	2σ err	Age (Ma)	2σ err	% Disc
240	163	0.63	0.75710	0.09111	572.7	5.1	562.1	4.4	604.3	9	1.9
273	51.7	0.96	0.83800	0.09330	617.0	17.0	576.8	7.8	768.0	48	6.5
219	159	2.18	0.78650	0.09383	588.9	5.2	578.1	3.8	633.0	14	1.8
273	158.2	1.17	0.83800	0.10070	617.0	12.0	618.0	19.0	661.0	30	-0.2
2112	200.3	0.72	0.97140	0.10905	689.1	4.6	667.2	4.7	762.5	8	3.2
234	549	11.10	1.38000	0.13560	880.3	6.1	819.6	9.0	1009.0	7	6.9
289	64.5	1.91	1.42000	0.14610	896.9	8.2	879.2	7.7	935.0	17	6.0
2121	209.4	2.26	1.53300	0.15800	944.0	11.0	945.0	11.0	951.0	12	0.6
225	74.7	3.23	1.49100	0.15193	926.2	6.8	911.7	5.4	961.0	11	5.1
2121	334.6	3.69	1.44400	0.14620	907.0	8.0	879.8	8.7	980.0	11	10.2
274	37.5	1.44	1.71800	0.16830	1014.8	8.5	1003.0	12.0	1045.0	17	4.0
250	251.2	0.75	1.58000	0.15430	961.7	7.2	925.0	8.8	1045.5	7	11.5
292	174.7	1.24	1.68100	0.16270	1001.4	4.6	971.8	6.1	1063.2	10	8.6
2103	104.6	2.02	1.76600	0.16870	1033.5	6.1	1006.0	8.8	1086.1	8	7.4
27	444	1.47	1.82000	0.17280	1052.6	3.5	1027.3	5.5	1102.6	5	6.8
210	30.4	0.79	1.75100	0.16720	1029.0	11.0	997.0	11.0	1103.0	15	9.6
2113	104.4	1.22	1.81600	0.17140	1050.9	7.7	1020.0	12.0	1135.0	13	10.1
259	79	0.93	1.95100	0.18130	1098.6	6.8	1076.0	10.0	1149.0	12	6.4
280	51.2	0.78	2.01800	0.18790	1121.1	6.9	1109.9	7.6	1150.0	14	3.5
230	50.5	1.85	1.95800	0.18110	1100.8	7.2	1073.0	7.2	1156.4	9	7.2
277	94	0.88	1.92900	0.17680	1091.7	6.9	1050.6	7.4	1162.4	9	9.6
212	316	1.95	2.03800	0.18780	1128.6	4.0	1109.1	5.5	1163.7	6	4.7
227	1060	11.00	1.79700	0.16620	1044.0	12.0	991.0	15.0	1167.2	8	15.1
254	130.5	0.82	2.10100	0.19020	1149.4	4.3	1122.3	7.7	1191.7	7	5.8
264	53.24	1.74	2.03200	0.18280	1126.0	11.0	1082.0	16.0	1197.0	23	9.6
257	98	0.55	2.21800	0.19860	1186.5	6.2	1167.8	7.7	1219.9	6	4.3
264	69	1.86	1.93600	0.17400	1093.0	10.0	1034.0	14.0	1220.6	8	15.3
270	35.2	0.85	2.03100	0.18020	1125.5	9.1	1068.0	14.0	1232.0	12	13.3
235	62.5	0.53	2.70000	0.22540	1330.0	6.3	1310.1	8.4	1356.0	10	3.4
248	101.9	0.77	2.79300	0.23000	1353.0	11.0	1334.0	16.0	1379.3	9	3.3
221	89.4	1.67	2.80000	0.23040	1355.9	4.9	1336.4	7.0	1389.5	7	3.8
2111	200	1.54	2.15700	0.17690	1162.0	25.0	1048.0	33.0	1391.9	5	24.7
2114	104.1	1.54	2.85200	0.23240	1369.0	5.1	1346.9	6.4	1400.6	7	3.8
2110	1905	1.65	2.20100	0.18010	1182.0	11.0	1067.0	15.0	1406.8	5	24.2
224	94.3	0.72	2.88600	0.23300	1378.2	5.7	1350.3	8.4	1433.8	7	5.8
262	275	0.89	2.83500	0.22690	1364.7	5.3	1318.3	8.9	1436.7	5	8.2

13MCSMG21					207/ 235		206/ 238		206/ 207		
#	[U] ppm	U/Th	207/ 235	206/ 238	Age Ma	2σ err	Age (Ma)	2σ err	Age (Ma)	2σ err	% Disc
217	127.4	1.04	2.83300	0.22630	1363.9	6.1	1315.0	11.0	1441.3	7	8.8
213	109	0.86	2.94200	0.23510	1392.5	4.9	1362.1	7.7	1442.1	6	5.5
293	248	1.18	2.93300	0.23440	1390.3	4.5	1357.6	5.9	1446.4	5	6.1
241	427	1.10	2.95100	0.23330	1394.4	9.6	1351.0	17.0	1463.3	5	7.7
214	216	3.23	2.85900	0.22650	1371.0	10.0	1316.0	18.0	1464.8	9	10.2
25	263	0.74	2.98500	0.23570	1403.0	8.8	1364.0	12.0	1466.5	7	7.0
286	160.4	1.39	3.11300	0.24300	1435.8	5.0	1402.1	7.4	1483.5	5	5.5
276	163	0.80	2.65600	0.20760	1316.1	7.0	1215.7	8.7	1489.4	8	18.4
232	161	1.78	3.27500	0.25350	1475.1	3.3	1456.5	5.8	1501.7	4	3.0
29	70	0.68	3.60000	0.26140	1549.0	7.1	1497.0	12.0	1622.5	8	7.7
2124	60	0.74	3.59000	0.26060	1546.0	13.0	1492.0	22.0	1624.8	6	8.2
281	63.5	0.79	3.59200	0.25990	1547.3	7.0	1489.0	12.0	1625.2	9	8.4
261	190	1.65	3.84500	0.27270	1602.0	5.4	1554.0	10.0	1662.8	6	6.5
251	201	1.62	3.93000	0.27460	1619.6	5.3	1564.2	9.0	1681.7	5	7.0
249	278	1.28	3.98800	0.27870	1631.3	7.2	1586.0	12.0	1688.1	6	6.0
222	621	2.23	2.14000	0.14840	1163.0	40.0	907.0	48.0	1691.1	7	46.4
263	237.8	1.00	3.72700	0.25970	1578.0	11.0	1488.0	15.0	1697.6	6	12.3
231	216	1.13	4.13300	0.28890	1660.7	5.1	1636.0	7.9	1700.0	8	3.8
220	145.1	1.33	3.32000	0.23170	1485.0	10.0	1343.0	14.0	1700.7	7	21.0
278	145.9	0.50	3.84300	0.26570	1603.0	12.0	1522.0	21.0	1702.8	6	10.6
2106	381	3.17	4.03400	0.27940	1640.7	5.7	1588.5	8.4	1706.4	6	6.9
2117	356	1.24	3.84200	0.26450	1600.0	11.0	1512.0	21.0	1718.8	5	12.0
233	57	1.11	4.15400	0.28300	1665.7	7.7	1606.0	11.0	1731.1	10	7.2
211	349	1.18	4.34900	0.29810	1702.4	6.5	1681.0	15.0	1731.4	6	2.9
244	182.2	2.06	3.98300	0.27160	1631.1	5.4	1548.9	7.7	1732.0	5	10.6
284	47.2	1.95	3.92500	0.26730	1618.4	7.0	1529.0	12.0	1738.1	9	12.0
2116	324	3.83	4.10400	0.27980	1654.3	8.7	1590.0	11.0	1738.3	7	8.5
296	625	1.99	2.96200	0.20110	1397.7	5.7	1181.0	7.4	1745.6	5	32.3
252	431	6.20	4.33300	0.29310	1699.0	11.0	1660.0	20.0	1756.7	5	5.5
266	364	3.05	4.39600	0.29610	1711.1	8.4	1674.0	15.0	1762.6	4	5.0
268	61.6	1.21	4.24800	0.28340	1683.1	7.4	1610.0	10.0	1770.9	8	9.1
285	109.9	1.17	4.02900	0.26720	1637.0	18.0	1525.0	29.0	1786.7	8	14.6
267	240	2.14	4.57400	0.30090	1744.5	3.7	1695.8	7.8	1800.6	4	5.8
260	1870	1.90	3.49000	0.22700	1515.0	44.0	1315.0	65.0	1806.1	4	27.2
287	21.68	0.97	4.62900	0.29830	1755.1	9.2	1683.0	16.0	1835.0	15	8.3
247	163	1.09	4.85500	0.31250	1794.1	5.7	1753.0	11.0	1841.1	5	4.8

13MCSMG21					207/ 235		206/ 238		206/ 207		
#	[U] ppm	U/Th	207/ 235	206/ 238	Age Ma	2σ err	Age (Ma)	2σ err	Age (Ma)	2σ err	% Disc
2115	349	1.22	5.40700	0.31560	1886.4	6.5	1768.0	11.0	2017.4	5	12.4
291	95.6	0.78	6.08000	0.32320	1988.0	17.0	1804.0	42.0	2172.0	14	16.9
214	147	1.47	9.57600	0.41880	2394.7	9.0	2255.0	21.0	2501.1	9	9.8
238	59.5	0.47	11.77500	0.46690	2586.1	7.8	2469.0	17.0	2674.0	4	7.7
216	107.1	0.72	12.17200	0.47790	2617.5	4.9	2518.0	13.0	2698.2	4	6.7
269	21.4	0.99	11.32700	0.43630	2549.9	7.7	2336.0	18.0	2727.7	8	14.4

13MCSMG22					207/ 235		206/ 238		206/ 207		
#	[U] ppm	U/Th	207/ 235	206/ 238	Age Ma	2σ err	Age (Ma)	2σ err	Age (Ma)	2σ err	% Disc
210	409	0.90	0.00737	0.00078	7.5	1.0	5.0	0.3	1220.0	160	99.6
239	2.2	0.41	0.02630	0.00383	26.3	1.5	24.6	0.6	9.8	75	6.4
4	72.5	0.76	0.02460	0.00389	24.6	1.9	25.0	0.7	358.0	66	-1.6
46	95	1.17	0.03100	0.00401	31.0	1.9	25.8	0.7	605.0	89	95.7
112	596	1.71	0.02625	0.00403	26.3	0.7	25.9	0.4	186.0	32	1.4
25	132	0.69	0.03190	0.00409	31.8	3.8	26.3	0.8	610.0	180	95.7
252	3.6	0.91	0.03510	0.00419	35.0	2.4	26.9	1.0	8.1	94	96.1
9	135.6	0.74	0.03010	0.00438	30.1	1.4	28.1	0.6	280.0	49	6.5
19	115.3	0.75	0.03200	0.00440	32.2	1.7	28.3	0.7	477.0	75	94.1
212	2.8	0.95	0.02940	0.00444	29.4	2.1	28.5	0.8	474.0	95	3.0
61	35.1	0.91	0.03290	0.00459	32.8	2.2	29.5	1.3	489.0	69	94.0
218	3.6	0.79	0.03220	0.00491	32.1	2.5	31.6	1.2	469.0	83	1.6
24	338	1.52	0.03397	0.00492	33.9	0.8	31.6	0.5	236.0	31	6.7
85	167	1.39	0.03060	0.00502	30.6	1.2	32.3	0.6	178.0	46	-5.4
18	117.7	0.51	0.03330	0.00503	33.2	1.3	32.4	0.7	236.0	49	2.6
27	167	0.70	0.03360	0.00511	33.5	2.3	32.8	0.9	481.0	84	2.0
91	150.8	0.62	0.03560	0.00524	35.5	1.2	33.7	0.7	286.0	41	5.2
47	859	1.53	0.03466	0.00525	34.6	0.6	33.8	0.4	136.0	22	2.3
222	2.8	2.50	0.03577	0.00548	35.7	0.8	35.2	0.6	15.0	23	1.3
54	314	1.00	0.04850	0.00625	48.0	3.0	40.2	0.8	550.0	110	92.7
84	416.9	1.39	0.04388	0.00642	43.6	0.9	41.3	0.5	200.0	25	5.4
68	75.8	1.24	0.04440	0.00648	44.1	2.3	41.6	1.0	373.0	79	5.7
126	291	2.21	0.04530	0.00691	45.0	1.2	44.4	0.6	174.0	34	1.3
257	4	1.54	0.04920	0.00716	48.7	1.9	46.0	0.9	17.0	53	5.6
17	152	1.18	0.07590	0.01130	74.2	1.9	72.4	0.9	202.0	33	2.4
24	243	1.12	0.07790	0.01191	76.0	3.6	76.3	2.1	278.0	59	-0.4
122	482	1.12	0.08330	0.01218	81.2	1.4	78.0	0.7	188.0	22	3.9
226	7	1.09	0.08760	0.01313	85.2	3.3	84.1	2.0	19.0	35	1.3
228	8.6	2.60	0.09020	0.01337	87.6	3.3	85.6	1.8	5.5	39	2.3
107	272	1.05	0.09190	0.01376	89.3	1.7	88.1	0.9	158.0	23	1.3
229	10	16.20	0.09280	0.01381	90.1	2.2	88.4	1.5	6.3	37	1.9
90	883	0.68	0.09187	0.01381	89.2	0.8	88.4	0.7	98.0	12	0.9
95	252	2.11	0.09100	0.01396	88.4	1.7	89.4	1.0	122.0	18	-1.1
245	8.8	3.86	0.09410	0.01401	91.2	3.3	89.7	2.1	3.2	37	1.6
251	7.5	1.22	0.09210	0.01411	89.4	3.1	90.3	1.8	13.0	35	-1.0
6	231	1.17	0.11230	0.01495	107.7	5.7	95.6	1.2	375.0	83	74.5

13MCSMG22					207/ 235		206/ 238		206/ 207		
#	[U] ppm	U/Th	207/ 235	206/ 238	Age Ma	2σ err	Age (Ma)	2σ err	Age (Ma)	2σ err	% Disc
103	400	0.93	0.12030	0.01575	115.2	4.0	100.7	1.2	405.0	75	75.1
80	225	1.64	0.16050	0.02286	151.0	3.1	145.7	1.5	247.0	36	3.5
21	276	1.88	0.15740	0.02301	148.3	4.4	146.7	3.6	209.0	31	1.1
31	270	1.19	0.16590	0.02333	155.8	2.5	148.7	1.2	257.0	30	4.6
22	370	0.67	0.17660	0.02572	165.1	2.0	163.7	1.5	166.0	12	0.8
238	12	1.18	0.18040	0.02632	168.4	1.8	167.5	1.9	40.0	15	0.5
243	22	0.44	0.32450	0.04430	285.1	5.4	279.4	3.8	55.0	31	2.0
113	56.4	1.39	0.53500	0.06978	434.5	6.6	434.8	4.6	460.0	25	-0.1
37	175	3.50	0.66800	0.07510	518.0	14.0	466.9	9.9	733.0	35	9.9
240	37	1.05	0.60200	0.07580	479.2	8.7	470.8	6.8	2.1	36	1.8
66	202.8	2.36	0.70090	0.08636	539.1	4.6	533.9	4.0	563.0	16	1.0
254	71	1.08	1.54400	0.15540	947.7	8.7	931.0	13.0	0.8	21	8.1
69	126	1.40	1.79900	0.17320	1044.6	6.5	1030.5	6.2	1087.0	12	5.2
16	185	1.45	1.84100	0.17500	1059.9	6.1	1039.7	9.3	1096.1	7	5.1
259	75	1.42	1.75100	0.16730	1027.1	8.9	997.0	13.0	6.7	16	9.9
231	73	2.09	1.74200	0.16250	1025.0	10.0	970.0	12.0	1.5	18	14.5
75	151	3.14	2.01900	0.18760	1122.5	5.8	1108.5	8.7	1144.5	9	3.1
106	284	4.11	2.00500	0.18520	1117.0	6.6	1095.0	9.2	1158.0	13	5.4
88	134.4	0.97	2.03900	0.18210	1127.7	9.9	1078.0	14.0	1225.0	11	12.0
121	154.9	2.12	2.31800	0.20670	1217.7	4.2	1211.0	6.5	1230.6	7	1.6
15	50.2	1.43	2.20000	0.18970	1178.0	16.0	1119.0	21.0	1299.0	13	13.9
74	109.5	1.53	2.62600	0.22430	1307.7	5.8	1304.0	10.0	1318.7	7	1.1
7	171.7	1.51	2.51700	0.21280	1276.6	6.9	1244.0	11.0	1333.1	8	6.7
221	97	1.11	2.60600	0.21350	1301.7	9.7	1247.0	15.0	12.0	11	10.6
256	100	2.13	2.62400	0.21650	1307.0	11.0	1263.0	19.0	2.5	20	10.0
244	110	1.72	2.83800	0.23130	1366.0	15.0	1340.0	28.0	19.0	19	4.6
39	239	1.24	2.77000	0.22440	1347.2	4.6	1305.0	10.0	1414.4	7	7.7
1	178	0.79	3.05200	0.24810	1421.2	5.2	1428.3	8.4	1414.5	8	-1.0
249	95	1.08	3.00200	0.24220	1407.7	7.8	1398.0	12.0	21.0	11	1.6
86	187	1.35	2.93100	0.23500	1389.7	6.7	1360.0	11.0	1433.7	7	5.1
118	78	0.82	3.00200	0.24060	1408.0	15.0	1389.0	23.0	1436.0	11	3.3
216	96	3.11	2.93100	0.23420	1391.0	12.0	1356.0	15.0	1437.0	11	5.6
33	66.8	0.88	2.94400	0.23630	1393.0	6.6	1367.0	13.0	1438.0	8	4.9
99	52	1.27	2.97500	0.23540	1401.0	6.9	1364.0	11.0	1441.6	9	5.4
105	140.1	0.89	2.81100	0.22230	1359.1	6.1	1294.0	11.0	1451.9	9	10.9
92	194	1.07	3.12700	0.24790	1440.0	7.0	1427.7	9.6	1457.1	8	2.0

13MCSMG22					207/ 235		206/ 238		206/ 207		
#	[U] ppm	U/Th	207/ 235	206/ 238	Age Ma	2σ err	Age (Ma)	2σ err	Age (Ma)	2σ err	% Disc
242	100	1.85	2.91900	0.22970	1386.0	11.0	1333.0	19.0	4.5	17	9.4
26	88.6	0.89	3.19400	0.24710	1455.5	4.9	1423.2	7.8	1499.8	7	5.1
81	182.8	0.60	2.94300	0.22650	1394.0	15.0	1316.0	10.0	1508.0	38	12.7
30	478	60.10	3.66000	0.26900	1562.0	11.0	1535.0	13.0	1610.0	12	4.7
100	61.8	0.81	3.46800	0.25160	1519.0	11.0	1446.0	17.0	1615.2	8	10.5
114	136.8	2.41	3.65800	0.26140	1562.0	14.0	1503.0	25.0	1640.6	9	8.4
116	79.9	0.81	4.02000	0.28360	1637.9	5.8	1609.0	10.0	1674.4	7	3.9
5	220	1.85	4.04200	0.28560	1643.2	6.4	1619.0	14.0	1676.6	6	3.4
125	514	2.98	2.91000	0.20400	1352.0	59.0	1186.0	76.0	1679.0	12	29.4
248	110	1.79	3.97200	0.28170	1627.8	9.0	1600.0	16.0	4.6	12	4.9
258	110	0.91	3.74800	0.26460	1581.0	11.0	1513.0	23.0	7.6	14	10.4
102	163	1.40	3.94100	0.27450	1621.9	5.1	1563.0	10.0	1689.7	4	7.5
41	293.6	0.97	4.01100	0.28190	1636.4	4.1	1600.7	9.7	1695.6	6	5.6
50	336.8	2.97	4.01600	0.28070	1637.4	5.7	1595.0	14.0	1696.8	7	6.0
35	480	1.00	2.58000	0.17800	1286.0	38.0	1062.0	52.0	1708.0	10	37.8
247	110	0.88	3.90700	0.27220	1616.7	9.1	1552.0	20.0	19.0	10	9.3
44	880	1.79	4.32600	0.30130	1698.0	6.5	1697.0	14.0	1712.4	6	0.9
58	202	2.59	4.09000	0.28090	1650.0	21.0	1594.0	36.0	1718.6	7	7.3
213	130	1.03	3.81000	0.26210	1593.0	18.0	1500.0	28.0	1720.0	24	12.8
22	123.8	2.20	2.98400	0.20710	1404.0	14.0	1213.0	22.0	1721.0	18	29.5
227	170	8.40	4.69000	0.31800	1758.0	32.0	1784.0	58.0	7.9	8	-2.9
40	104.4	2.32	4.16000	0.28500	1666.0	5.1	1616.5	9.0	1740.4	5	7.1
77	201.5	1.13	4.04500	0.27320	1643.0	11.0	1557.0	18.0	1756.8	10	11.4
110	693	10.90	4.40000	0.29600	1707.0	35.0	1669.0	58.0	1759.1	9	5.1
34	208	2.14	4.51700	0.30530	1733.8	6.1	1717.3	9.8	1762.0	6	2.5
28	324	1.44	4.53600	0.30490	1736.9	8.9	1718.0	19.0	1767.0	11	2.8
23	164	0.66	3.49600	0.23460	1524.0	17.0	1358.0	33.0	1778.0	19	23.6
43	90.8	2.11	4.62600	0.30430	1753.6	6.7	1712.0	11.0	1808.0	8	5.3
30	274.9	1.24	4.19300	0.27240	1672.0	15.0	1553.0	21.0	1822.0	14	14.8
55	121.2	1.88	5.07000	0.31080	1830.5	9.4	1744.0	19.0	1929.8	9	9.6
230	140	1.26	5.80000	0.33120	1946.0	21.0	1848.0	33.0	0.7	26	10.2
217	170	0.83	13.82000	0.53100	2735.0	16.0	2743.0	42.0	2719.0	15	-0.9
29	377	1.45	12.62000	0.48950	2652.4	8.2	2568.0	21.0	2724.6	6	5.7
28	26.1	0.95	13.14000	0.49990	2687.0	17.0	2616.0	22.0	2743.0	15	4.6

13MCSMG29					207/ 235		206/ 238		206/ 207		
#	[U] ppm	U/Th	207/ 235	206/ 238	Age Ma	2σ err	Age (Ma)	2σ err	Age (Ma)	2σ err	% Disc
246	351	0.52	0.02630	0.00382	26.4	1.5	24.6	0.7	371.0	68	6.9
229	114.9	0.65	0.02730	0.00438	27.3	2.7	28.1	1.1	500.0	120	-2.9
2112	401	0.82	0.02920	0.00450	29.2	1.8	28.9	0.8	219.0	40	1.0
220	85	0.50	0.03480	0.00459	34.6	3.6	29.5	1.8	650.0	120	95.5
278	141	0.64	0.03830	0.00482	37.9	5.3	31.0	1.6	760.0	170	95.9
2128	2.9	0.82	0.03160	0.00484	31.5	1.8	31.2	1.0	334.0	64	1.1
214	240	0.48	0.03310	0.00489	33.0	2.0	31.4	1.0	463.0	83	4.8
222	271	0.65	0.03410	0.00506	34.0	2.0	32.5	1.1	422.0	76	4.4
22	135.8	1.15	0.03730	0.00518	37.2	2.9	33.3	1.3	660.0	130	95.0
219	800	0.90	0.03720	0.00554	37.1	1.8	35.6	1.1	252.0	49	4.0
295	301	0.57	0.04190	0.00556	41.7	2.8	35.8	1.1	600.0	97	94.0
236	125	0.86	0.03940	0.00572	39.2	3.0	36.8	1.5	570.0	110	6.1
282	169	0.57	0.04850	0.00589	47.9	3.9	37.9	1.5	820.0	110	95.4
228	260	0.79	0.03950	0.00609	39.3	2.4	39.1	1.4	328.0	68	0.5
297	306	1.14	0.04360	0.00636	43.3	2.6	40.9	1.3	271.0	53	5.5
210	124.6	0.39	0.04210	0.00649	41.8	2.9	41.7	1.7	409.0	77	0.2
279	127	0.99	0.04770	0.00673	47.2	4.0	43.3	2.2	520.0	110	8.3
243	611	1.09	0.05200	0.00736	51.4	2.7	47.3	1.0	349.0	98	8.0
249	302	0.76	0.05050	0.00757	50.0	2.4	48.6	1.2	281.0	44	2.8
213	14.82	1.21	0.07700	0.01120	74.0	15.0	71.8	4.8	990.0	180	3.0
261	128	1.75	0.09290	0.01482	90.8	5.3	94.8	3.1	307.0	64	-4.4
2110	352	0.81	0.09720	0.01498	94.6	3.1	95.9	2.1	231.0	43	-1.4
238	134	1.02	0.10640	0.01522	102.5	4.2	97.4	2.4	337.0	61	5.0
2109	118	1.95	0.10820	0.01525	104.1	4.6	97.9	2.2	403.0	53	6.0
277	355	1.20	0.10220	0.01560	98.8	2.7	99.8	1.7	169.0	31	-1.0
224	71.2	3.12	0.11180	0.01612	107.0	8.0	103.1	2.9	480.0	80	3.6
283	1040	11.30	0.10730	0.01612	103.8	2.4	103.1	2.0	162.0	22	0.7
21	163	2.81	0.10140	0.01626	97.9	4.4	104.0	2.8	173.0	44	-6.2
28	415.8	1.88	0.10950	0.01642	105.5	2.7	105.0	1.5	186.0	31	0.5
227	160.3	0.78	0.10960	0.01699	105.4	3.9	108.6	2.6	205.0	39	-3.0
262	247	0.68	0.16280	0.02382	154.2	4.7	151.7	2.5	203.0	36	1.6
250	159	1.05	0.16310	0.02451	153.2	4.5	156.1	3.1	185.0	30	-1.9
242	494	0.71	0.17370	0.02537	162.5	3.5	161.5	2.3	187.0	29	0.6
267	193	0.63	0.17640	0.02578	164.8	4.6	164.1	2.5	242.0	38	0.4
2114	158	0.53	0.19240	0.02693	178.5	4.6	171.3	3.4	289.0	39	4.0
221	513	1.27	0.25170	0.03614	228.3	3.3	228.9	2.3	203.0	24	-0.3

13MCSMG29					207/ 235		206/ 238		206/ 207		
#	[U] ppm	U/Th	207/ 235	206/ 238	Age Ma	2σ err	Age (Ma)	2σ err	Age (Ma)	2σ err	% Disc
273	146.4	1.08	0.30130	0.04137	267.0	7.3	261.3	3.6	329.0	35	2.1
218	178	0.68	0.32350	0.04296	284.3	6.0	271.1	4.6	368.0	32	4.6
2118	362	0.92	0.48140	0.06327	398.8	5.7	395.4	4.4	425.0	24	0.9
2124	495	7.63	0.51040	0.06329	418.5	6.7	395.6	5.1	553.0	38	5.5
211	250	1.47	0.47900	0.06500	397.0	7.3	405.9	6.4	388.0	21	-2.2
257	241	0.98	0.50620	0.06623	415.5	6.6	413.4	4.2	431.0	28	0.5
230	252.4	1.41	0.54000	0.06634	438.0	6.7	414.0	4.6	568.0	34	5.5
274	219	1.03	0.54400	0.06995	440.6	7.8	435.8	6.0	477.0	32	1.1
235	191	1.32	0.55300	0.07054	446.4	7.5	439.4	5.2	453.0	25	1.6
226	54.3	0.78	0.81200	0.09620	603.0	19.0	592.2	9.2	651.0	67	1.8
232	99.6	1.09	0.81600	0.09700	605.0	10.0	596.6	8.7	628.0	34	1.4
241	75.5	0.58	0.87300	0.10360	636.0	12.0	635.3	9.4	627.0	30	0.1
266	170	1.57	1.67700	0.17230	999.4	9.1	1025.0	11.0	958.0	15	-7.0
260	96.3	1.38	1.61900	0.16190	978.0	10.0	967.0	11.0	1006.0	19	3.9
294	63.8	2.49	1.71200	0.16990	1013.0	13.0	1011.0	16.0	1040.0	24	2.8
286	63.6	1.34	2.10900	0.19730	1150.0	12.0	1161.0	13.0	1145.0	24	-1.4
289	17.85	1.03	1.87600	0.17190	1068.0	24.0	1022.0	21.0	1184.0	40	13.7
233	19.27	2.01	2.08000	0.18450	1130.0	39.0	1091.0	25.0	1258.0	94	13.3
270	112.2	1.72	2.55000	0.22330	1286.8	9.5	1299.0	11.0	1273.0	15	-2.0
271	119.5	1.55	2.76800	0.23750	1347.0	11.0	1373.0	26.0	1307.0	31	-5.0
26	72.4	1.39	3.05200	0.25620	1420.0	13.0	1470.0	18.0	1350.0	15	-8.9
296	103.5	0.82	2.71800	0.22470	1333.0	10.0	1307.0	16.0	1395.0	17	6.3
288	38.5	0.94	3.13300	0.25440	1438.0	21.0	1461.0	27.0	1397.0	26	-4.6
265	46.3	1.00	2.99800	0.23990	1406.0	16.0	1386.0	21.0	1399.0	18	0.9
254	202	1.19	2.88300	0.23640	1377.1	8.1	1368.0	13.0	1403.0	13	2.5
2111	35.2	1.14	3.24500	0.26520	1466.0	16.0	1519.0	27.0	1403.0	24	-8.3
2125	84.1	0.95	3.05300	0.25390	1421.5	9.8	1458.0	13.0	1409.0	14	-3.5
2107	50.8	0.79	3.40400	0.27110	1504.0	18.0	1546.0	23.0	1437.0	26	-7.6
2119	147.1	0.89	3.22200	0.25740	1461.8	8.6	1478.0	13.0	1454.0	12	-1.7
251	226	1.41	3.64400	0.27610	1558.9	7.1	1572.0	14.0	1525.0	10	-3.1
225	66	0.67	4.41400	0.31300	1714.0	13.0	1755.0	22.0	1650.0	14	-6.4
2115	25.5	0.83	3.77500	0.27030	1585.0	19.0	1551.0	31.0	1656.0	34	6.3
240	327	1.57	4.13900	0.29310	1662.6	8.6	1657.0	14.0	1658.0	12	0.1
284	279	1.85	4.05400	0.28920	1644.3	9.6	1637.0	16.0	1666.9	8	1.8
275	410	3.60	4.08200	0.28770	1650.3	9.2	1630.0	17.0	1668.0	10	2.3
223	98.9	0.64	4.54300	0.31800	1738.0	13.0	1783.0	22.0	1681.0	16	-6.1

13MCSMG29					207/ 235		206/ 238		206/ 207		
#	[U ppm	U/Th	207/ 235	206/ 238	Age Ma	2σ err	Age (Ma)	2σ err	Age (Ma)	2σ err	% Disc
263	177	0.69	4.18000	0.29090	1669.7	6.4	1646.0	12.0	1692.4	7	2.7
2122	211	1.85	4.17300	0.29430	1668.2	7.4	1665.0	12.0	1701.0	11	2.1
231	136	0.64	4.45300	0.30790	1721.0	12.0	1730.0	14.0	1704.0	11	-1.5
23	580	12.19	4.18100	0.29260	1671.0	10.0	1654.0	20.0	1710.0	16	3.3
258	270	1.51	4.43400	0.30950	1718.3	7.9	1738.0	16.0	1710.4	7	-1.6
276	712	2.68	4.51500	0.31070	1734.2	5.7	1744.0	12.0	1717.9	6	-1.5
298	300	1.24	4.57600	0.31650	1744.0	10.0	1772.0	18.0	1722.5	8	-2.9
25	345	0.52	4.24700	0.29020	1684.2	9.3	1642.0	16.0	1722.6	9	4.7
252	83.4	0.85	4.40400	0.30210	1712.0	11.0	1706.0	22.0	1731.0	14	1.4
216	170	2.14	4.61400	0.31700	1751.3	9.0	1775.0	18.0	1732.9	9	-2.4
24	324	1.59	4.28300	0.29370	1694.0	11.0	1660.0	18.0	1740.2	9	4.6
253	220	1.23	4.69000	0.31750	1764.9	9.0	1777.0	19.0	1760.0	11	-1.0
2126	221	1.52	4.66000	0.31370	1759.7	8.9	1758.0	16.0	1771.0	12	0.7
272	157	1.84	5.00500	0.33370	1822.0	11.0	1856.0	11.0	1778.0	10	-4.4
212	32.5	0.65	4.52000	0.24390	1733.0	27.0	1407.0	30.0	2231.0	40	36.9
293	96.8	0.64	13.05000	0.52610	2682.0	11.0	2724.0	29.0	2662.0	10	-2.3
2106	33.2	0.39	11.95000	0.47610	2602.0	12.0	2510.0	29.0	2684.0	12	6.5

13MCSMG30					207/ 235		206/ 238		206/ 207		
#	[U] ppm	U/Th	207/ 235	206/ 238	Age Ma	2σ err	Age (Ma)	2σ err	Age (Ma)	2σ err	% Disc
84	256	1.24	0.09280	0.01326	89.9	4.3	84.9	2.4	367.0	57	5.6
85	211	1.39	0.09190	0.01372	89.7	5.2	87.8	2.3	375.0	79	2.1
3	751	6.14	0.09760	0.01432	94.5	2.2	91.7	1.2	241.0	36	3.0
60	158	1.46	0.10200	0.01440	98.4	4.6	92.2	2.2	371.0	66	6.3
80	502	1.54	0.09680	0.01452	93.8	3.0	92.9	1.8	230.0	46	1.0
52	366	1.84	0.10170	0.01486	98.2	3.2	95.1	2.1	235.0	42	3.2
100	355	1.54	0.10710	0.01495	103.2	4.4	95.7	1.7	386.0	66	7.3
43	311	1.02	0.10020	0.01500	96.8	3.4	95.9	1.9	230.0	37	0.9
71	127	1.23	0.10150	0.01514	98.0	5.0	96.9	2.8	309.0	48	1.1
46	108	1.54	0.11060	0.01516	107.2	6.1	97.0	3.3	467.0	80	9.5
19	790	32.50	0.09970	0.01518	96.4	2.5	97.1	1.4	139.0	23	-0.7
73	382	3.58	0.10210	0.01520	98.6	2.7	97.3	1.8	182.0	42	1.3
108	309	2.19	0.10450	0.01520	100.8	2.9	97.3	1.8	252.0	41	3.5
48	197	3.83	0.10080	0.01524	97.3	4.7	97.5	2.8	282.0	53	-0.2
30	371	2.71	0.10310	0.01528	99.5	2.6	97.8	1.7	215.0	35	1.7
50	235	1.52	0.09900	0.01534	95.7	3.4	98.1	2.3	194.0	41	-2.5
1	278	1.56	0.10160	0.01560	98.6	3.6	99.8	2.3	236.0	35	-1.2
24	298	1.44	0.10270	0.01564	99.2	3.4	100.0	2.2	190.0	48	-0.8
49	119.1	1.11	0.10300	0.01567	99.3	4.7	100.2	2.3	305.0	47	-0.9
68	92	1.12	0.10280	0.01567	99.0	6.7	100.2	4.2	353.0	67	-1.2
5	53.6	1.42	0.09580	0.01576	92.6	6.4	100.8	3.5	370.0	92	-8.9
69	213	1.13	0.10650	0.01578	102.6	4.0	100.9	2.4	234.0	43	1.7
8	130	2.07	0.10420	0.01582	100.4	4.6	101.2	2.5	300.0	51	-0.8
14	407	1.93	0.10650	0.01588	102.7	3.5	101.5	2.3	229.0	49	1.2
21	910	1.89	0.11230	0.01590	107.9	4.0	101.7	2.5	259.0	64	5.7
34	237.4	0.98	0.10850	0.01592	104.5	3.3	101.8	2.0	271.0	42	2.6
58	120	1.27	0.10980	0.01595	105.6	4.7	102.0	2.4	301.0	46	3.4
90	549	1.92	0.10150	0.01597	98.1	2.6	102.2	1.6	160.0	30	-4.2
36	800	2.30	0.11480	0.01654	110.3	3.0	105.8	2.1	249.0	36	4.1
74	1160	53.00	0.11410	0.01683	109.7	2.2	107.6	2.1	174.0	29	1.9
96	927	0.84	0.11020	0.01683	106.1	2.3	107.6	1.8	134.0	25	-1.4
28	46.5	3.34	0.11810	0.01698	112.7	8.8	108.5	4.7	660.0	100	3.7
47	232	1.84	0.11250	0.01715	108.1	3.8	109.6	2.4	224.0	44	-1.4
51	71.4	2.45	0.11730	0.01751	112.4	7.0	111.9	5.3	400.0	100	0.4
16	344	3.27	0.12890	0.01836	122.8	5.7	117.2	5.0	263.0	40	4.6
63	934	13.30	0.13260	0.01932	126.4	4.6	123.3	3.9	199.0	31	2.5

13MCSMG30					207/ 235		206/ 238		206/ 207		
#	[U] ppm	U/Th	207/ 235	206/ 238	Age Ma	2σ err	Age (Ma)	2σ err	Age (Ma)	2σ err	% Disc
27	545	2.62	0.12880	0.01943	122.9	4.2	124.0	3.4	155.0	23	-0.9
105	303	18.00	0.14340	0.02080	136.0	4.0	132.7	2.4	281.0	41	2.4
61	178	4.17	0.15100	0.02291	142.3	7.5	146.0	6.0	220.0	44	-2.6
23	368	1.43	0.16250	0.02374	152.8	4.9	151.3	3.5	177.0	51	1.0
86	308	1.58	0.15980	0.02390	150.4	4.8	152.2	3.9	246.0	41	-1.2
26	276	1.37	0.16220	0.02398	153.1	3.7	152.8	2.3	181.0	27	0.2
82	394	1.65	0.16230	0.02439	152.6	4.0	155.3	2.2	189.0	36	-1.8
110	238	1.59	0.16510	0.02439	155.0	4.7	155.3	2.7	256.0	40	-0.2
81	330.3	1.18	0.16940	0.02455	159.4	4.8	156.4	3.0	247.0	43	1.9
31	185	1.94	0.16850	0.02483	157.9	4.6	158.1	2.9	225.0	36	-0.1
37	683	31.00	0.16610	0.02491	156.8	6.4	158.6	3.9	171.0	24	-1.1
56	167.6	1.66	0.17180	0.02493	160.8	4.6	158.7	3.1	241.0	36	1.3
62	280	1.22	0.16750	0.02488	157.1	4.8	158.8	2.8	233.0	35	-1.1
89	114.4	1.79	0.17090	0.02551	160.8	8.1	162.4	3.5	352.0	51	-1.0
101	104.6	1.73	0.17980	0.02552	167.5	6.7	162.5	3.7	350.0	53	3.0
65	219	1.43	0.17530	0.02576	163.9	4.3	164.0	2.6	220.0	34	-0.1
42	127	2.72	0.17760	0.02587	165.7	5.8	164.6	3.7	276.0	44	0.7
45	271	3.49	0.17340	0.02594	162.2	3.6	165.1	2.3	181.0	27	-1.8
12	224	11.85	0.17950	0.02595	167.4	6.8	165.2	4.0	187.0	36	1.3
20	215	1.45	0.17800	0.02596	166.9	4.8	165.2	2.8	232.0	31	1.0
78	155	1.73	0.17840	0.02597	166.4	6.0	165.2	3.6	314.0	49	0.7
38	104.7	1.59	0.18000	0.02599	167.7	7.3	165.4	3.7	310.0	52	1.4
103	117.8	1.53	0.17460	0.02610	163.0	7.2	166.1	3.8	270.0	50	-1.9
54	476	9.90	0.17670	0.02612	165.1	4.4	166.2	2.7	177.0	34	-0.7
7	155.8	1.60	0.17580	0.02620	164.3	4.3	166.7	3.1	240.0	46	-1.5
97	187	1.68	0.19570	0.02626	180.9	8.1	167.1	3.5	356.0	61	7.6
102	324	4.15	0.17810	0.02626	166.3	4.9	167.1	4.0	239.0	46	-0.5
10	224	1.16	0.18020	0.02630	168.1	4.1	167.3	3.0	216.0	34	0.5
32	178	1.46	0.17890	0.02644	166.9	4.6	168.2	3.4	244.0	37	-0.8
39	191	1.61	0.16980	0.02644	159.0	5.6	168.2	4.0	170.0	33	-5.8
11	110.2	1.38	0.17900	0.02645	166.9	5.8	168.3	3.3	234.0	37	-0.8
66	118.2	1.86	0.17730	0.02646	166.3	5.3	168.3	3.1	222.0	36	-1.2
76	487	6.08	0.18140	0.02672	169.1	3.3	170.0	2.0	188.0	28	-0.5
88	179	3.78	0.17530	0.02678	163.7	6.3	170.3	3.8	262.0	52	-4.0
33	180	1.17	0.18860	0.02681	175.2	4.5	170.5	3.1	267.0	31	2.7
79	155	1.90	0.17450	0.02691	164.1	7.2	171.2	4.9	224.0	49	-4.3

13MCSMG30					207/ 235		206/ 238		206/ 207		
#	[U] ppm	U/Th	207/ 235	206/ 238	Age Ma	2σ err	Age (Ma)	2σ err	Age (Ma)	2σ err	% Disc
17	298	1.55	0.18930	0.02698	175.9	4.1	171.6	2.7	230.0	36	2.4
99	204.4	1.46	0.17680	0.02707	165.9	5.1	172.2	2.9	235.0	45	-3.8
77	180	1.37	0.18250	0.02719	169.9	6.1	172.9	3.2	257.0	45	-1.8
41	364	1.41	0.18200	0.02727	170.2	3.6	173.5	2.7	192.0	30	-1.9
9	119	1.85	0.19930	0.02730	184.1	7.5	173.6	4.5	346.0	53	5.7
29	174	1.72	0.19350	0.02735	179.2	6.7	173.9	3.4	286.0	47	3.0
55	174	2.73	0.18090	0.02768	168.6	5.5	176.0	4.6	193.0	37	-4.4
91	977	7.87	0.18660	0.02779	173.6	5.1	176.7	3.0	183.0	28	-1.8
83	967	1.76	0.20190	0.02904	187.1	3.3	184.5	2.3	220.0	24	1.4
107	289.1	1.16	0.20650	0.03020	190.5	4.1	191.8	3.1	209.0	33	-0.7
63	271.7	1.45	0.29300	0.03982	260.7	8.5	251.7	4.9	316.0	55	3.5
106	506	1.45	0.29810	0.04011	264.7	5.1	253.5	2.6	357.0	40	4.2
75	248	0.52	0.29930	0.04069	265.6	5.5	257.1	3.5	323.0	31	3.2
40	116	1.00	0.30380	0.04224	269.0	7.6	266.7	5.3	319.0	35	0.9
67	109.2	0.94	0.63000	0.07600	495.0	11.0	472.3	9.2	569.0	30	4.6
64	128.9	1.40	2.01400	0.19090	1120.0	13.0	1126.0	28.0	1113.0	26	-1.2
92	21.7	1.69	2.61000	0.23800	1315.0	55.0	1375.0	59.0	1188.0	73	-15.7
57	344	1.00	2.91900	0.23640	1387.3	7.6	1368.0	12.0	1416.7	9	3.4
104	206	1.04	2.95400	0.23690	1395.0	10.0	1370.0	18.0	1438.0	16	4.7
12	241	1.76	3.04800	0.24070	1419.0	21.0	1390.0	35.0	1445.0	24	3.8
13	1076	9.20	2.55200	0.18410	1286.0	18.0	1089.0	26.0	1638.0	12	33.5
25	761	194.00	3.73100	0.26340	1577.0	11.0	1507.0	20.0	1661.7	8	9.3
93	217	1.67	4.12200	0.29460	1662.0	12.0	1664.0	20.0	1689.9	9	1.5
22	143	1.44	4.03200	0.28200	1640.0	13.0	1601.0	15.0	1696.0	15	5.6
70	71.9	1.49	4.68000	0.32370	1768.0	16.0	1807.0	46.0	1702.0	13	-6.2
72	50.9	1.08	2.84200	0.18540	1365.0	21.0	1096.0	28.0	1811.0	24	39.5
94	159	1.38	4.56000	0.22910	1746.0	20.0	1329.0	35.0	2333.0	16	43.0

13MCSMG31					207/ 235		206/ 238		206/ 207		
#	[U] ppm	U/Th	207/ 235	206/ 238	Age Ma	2σ err	Age (Ma)	2σ err	Age (Ma)	2σ err	% Disc
366	289	0.93	0.01560	0.00260	15.7	1.6	16.7	0.5	690.0	210	-6.6
34	377	1.61	0.02390	0.00327	23.9	1.3	21.0	0.5	491.0	78	95.7
32	315.8	0.61	0.02900	0.00432	29.0	1.7	27.8	0.8	362.0	64	4.1
3106	695	1.41	0.03150	0.00448	31.5	1.9	28.8	0.8	236.0	28	8.4
3127	3.1	3.25	0.02962	0.00453	29.6	1.0	29.2	0.6	226.0	37	1.6
367	509	0.93	0.03000	0.00453	30.0	1.3	29.2	0.8	260.0	52	2.8
388	378	1.45	0.02910	0.00460	29.1	1.6	29.6	0.7	372.0	77	-1.6
340	744	1.01	0.04390	0.00484	43.5	2.3	31.2	0.7	700.0	110	95.6
374	92	0.76	0.03700	0.00496	36.7	3.3	31.9	1.5	730.0	140	95.6
3110	110.2	0.63	0.03350	0.00499	33.4	3.1	32.1	2.7	476.0	84	3.9
332	619	1.49	0.03490	0.00499	34.8	1.3	32.1	0.6	294.0	45	7.7
387	746	4.80	0.03330	0.00509	33.3	1.1	32.7	0.6	188.0	42	1.7
379	166.9	0.72	0.03100	0.00511	31.0	2.2	32.9	1.0	369.0	79	-6.1
359	252	0.83	0.04060	0.00518	40.4	2.6	33.3	1.1	585.0	90	94.3
322	1375	2.98	0.03700	0.00579	36.9	1.4	37.2	1.0	112.0	35	-0.8
354	269	0.79	0.07310	0.01069	71.6	3.0	68.6	1.5	314.0	62	4.2
311	99.5	0.84	0.07890	0.01199	76.8	5.4	76.8	2.1	327.0	92	0.0
3117	491	1.25	0.09210	0.01373	89.4	2.3	87.9	1.4	195.0	37	1.7
357	266	3.01	0.09330	0.01383	90.5	2.9	88.5	1.4	247.0	42	2.2
344	284.2	1.15	0.09480	0.01391	91.9	3.5	89.0	1.9	242.0	44	3.2
313	250	2.11	0.09790	0.01431	95.1	3.0	91.6	1.8	269.0	42	3.7
352	279	1.57	0.09640	0.01468	93.4	3.0	93.9	1.8	206.0	44	-0.5
349	247	2.54	0.09910	0.01480	96.3	3.4	94.7	1.6	247.0	60	1.7
399	453	2.16	0.09970	0.01479	96.4	2.3	94.7	1.6	221.0	34	1.8
323	330	1.91	0.11130	0.01507	106.7	6.6	96.4	1.9	354.0	77	9.7
338	117	3.95	0.10500	0.01516	101.1	5.6	97.0	2.7	428.0	82	4.1
3111	168	0.76	0.09960	0.01536	96.2	4.2	98.3	2.0	192.0	41	-2.2
3100	396	8.70	0.10670	0.01556	102.9	2.6	99.5	1.8	197.0	30	3.3
341	505	1.24	0.10830	0.01577	104.4	2.5	100.9	1.6	217.0	34	3.4
3114	66.1	0.67	0.15700	0.02195	147.7	8.0	140.0	5.0	520.0	63	5.2
321	322.9	0.84	0.16760	0.02433	157.7	3.2	155.0	2.3	231.0	35	1.7
375	190	1.19	0.17230	0.02522	161.3	3.8	160.6	3.1	229.0	37	0.4
37	151	0.56	0.20430	0.02907	188.5	4.9	184.7	2.5	302.0	39	2.0
348	161	0.79	0.22710	0.03290	207.5	5.4	208.7	3.3	231.0	30	-0.6
3101	310	1.17	0.24270	0.03352	220.5	5.2	212.5	3.5	341.0	38	3.6
362	122	0.92	0.24370	0.03412	221.1	6.5	216.3	3.9	306.0	34	2.2

13MCSMG31					207/ 235		206/ 238		206/ 207		
#	[U] ppm	U/Th	207/ 235	206/ 238	Age Ma	2σ err	Age (Ma)	2σ err	Age (Ma)	2σ err	% Disc
36	136.2	0.96	0.26480	0.03729	238.3	6.5	236.0	4.1	269.0	39	1.0
3116	728	0.55	0.26510	0.03730	238.5	5.6	236.1	2.8	271.0	39	1.0
370	240	0.97	0.28530	0.03957	255.3	5.1	250.2	2.9	304.0	33	2.0
317	115.6	0.57	0.32750	0.04488	287.2	7.1	283.0	3.5	313.0	33	1.5
3126	21	1.76	0.34750	0.04769	303.3	4.2	300.3	3.6	316.0	18	1.0
394	308	1.32	0.42640	0.05429	361.5	5.6	340.8	5.6	495.0	38	5.7
350	234	1.85	0.41970	0.05589	355.5	6.3	350.5	5.3	419.0	22	1.4
33	357.7	41.70	0.47550	0.06165	394.8	5.6	385.6	4.5	463.0	27	2.3
3123	130.2	8.20	0.67700	0.07870	523.0	15.0	488.0	10.0	695.0	43	6.7
380	40.1	0.72	0.69300	0.08290	534.0	12.0	514.0	11.0	623.0	40	3.7
38	46.6	1.07	0.76800	0.09340	580.0	13.0	575.0	12.0	595.0	33	0.9
376	87	1.04	0.86000	0.09770	630.0	12.0	601.0	11.0	757.0	39	4.6
315	59	2.19	1.48800	0.15190	926.0	12.0	911.0	12.0	965.0	27	5.6
392	71.8	1.70	1.59900	0.16270	968.0	15.0	971.0	15.0	986.0	25	1.5
3115	263.1	2.20	1.63800	0.16010	986.9	9.3	957.0	14.0	1061.0	12	9.8
31	24.7	1.88	2.01400	0.18960	1120.0	15.0	1119.0	17.0	1127.0	29	0.7
3103	81	1.12	1.87400	0.17500	1071.0	13.0	1040.0	13.0	1147.0	18	9.3
386	192	1.48	2.27600	0.20320	1204.5	7.3	1192.0	11.0	1225.0	12	2.7
35	42.1	0.98	2.41900	0.21120	1252.0	11.0	1235.0	13.0	1289.0	19	4.2
339	366.2	0.68	2.74200	0.22580	1339.4	9.1	1312.0	12.0	1393.0	11	5.8
371	137.3	1.26	2.72100	0.21970	1334.5	9.5	1280.0	17.0	1405.0	14	8.9
3108	1185	0.91	1.90300	0.15380	1081.7	7.9	922.0	11.0	1414.9	8	34.8
327	237	0.79	2.87400	0.23370	1374.8	7.8	1354.0	15.0	1415.0	11	4.3
384	241	1.38	2.95100	0.23980	1394.0	10.0	1385.0	19.0	1423.0	13	2.7
316	171.6	1.76	2.96600	0.24080	1399.5	6.6	1394.0	13.0	1426.0	11	2.2
363	179	0.90	3.04400	0.24640	1418.0	10.0	1420.0	16.0	1427.0	13	0.5
337	26.64	0.63	2.67700	0.21420	1325.0	16.0	1251.0	17.0	1432.0	27	12.6
318	245	1.63	3.01200	0.24320	1410.2	7.5	1403.0	13.0	1435.0	10	2.2
3113	153.1	1.47	3.26000	0.26340	1473.9	8.8	1507.0	13.0	1435.0	11	-5.0
328	380	1.15	2.83700	0.22420	1365.0	10.0	1304.0	17.0	1447.0	13	9.9
335	36.6	0.53	2.54500	0.20310	1284.0	17.0	1191.0	23.0	1450.0	18	17.9
372	153	1.20	2.95400	0.23690	1395.4	9.5	1371.0	14.0	1451.8	9	5.6
347	86.7	1.20	2.93300	0.23310	1389.0	11.0	1351.0	16.0	1459.0	14	7.4
391	280	1.26	3.05200	0.23890	1422.4	9.3	1381.0	14.0	1474.3	10	6.3
361	46.3	1.05	3.65000	0.26520	1562.0	14.0	1520.0	27.0	1598.0	22	4.9
312	63.8	0.76	3.68100	0.26540	1566.0	11.0	1517.0	18.0	1632.0	14	7.0

13MCSMG31					207/ 235		206/ 238		206/ 207		
#	[U] ppm	U/Th	207/ 235	206/ 238	Age Ma	2σ err	Age (Ma)	2σ err	Age (Ma)	2σ err	% Disc
3121	118	0.87	4.21300	0.29880	1675.8	8.6	1685.0	18.0	1664.0	12	-1.3
358	182	1.17	3.99700	0.28080	1634.2	8.3	1595.0	17.0	1667.0	12	4.3
3102	32.5	0.73	4.20000	0.29830	1674.0	19.0	1681.0	34.0	1670.0	17	-0.7
343	217	1.32	4.18400	0.29310	1670.5	7.4	1657.0	12.0	1675.0	10	1.1
3125	110	0.79	3.64400	0.25880	1560.0	10.0	1484.0	19.0	1676.0	13	11.5
3109	47.8	0.71	4.11500	0.28990	1656.0	16.0	1640.0	27.0	1682.0	16	2.5
346	37.4	0.39	4.19000	0.29330	1673.0	11.0	1658.0	20.0	1688.0	18	1.8
345	311	1.17	4.24800	0.29670	1683.0	6.4	1675.0	11.0	1690.5	9	0.9
3107	157.7	0.92	3.81200	0.26770	1596.2	9.5	1529.0	15.0	1693.7	10	9.7
3105	217	1.23	3.96000	0.27590	1625.4	8.9	1571.0	14.0	1700.0	11	7.6
3120	74.5	0.85	3.94400	0.27280	1622.0	12.0	1554.0	27.0	1701.0	15	8.6
353	125	1.24	4.27800	0.29730	1689.0	16.0	1677.0	26.0	1705.0	12	1.6
356	85.3	2.24	3.58900	0.24760	1545.0	20.0	1426.0	29.0	1705.0	16	16.4
3112	115	1.39	4.24400	0.29580	1682.0	15.0	1670.0	24.0	1706.0	15	2.1
390	54.8	1.78	3.91000	0.27280	1614.0	24.0	1554.0	36.0	1712.0	15	9.2
373	51.8	1.67	4.28300	0.29240	1690.0	12.0	1653.0	25.0	1714.0	13	3.6
398	135	0.85	4.07700	0.28260	1648.9	9.8	1604.0	15.0	1715.0	10	6.5
3124	341	6.32	3.09000	0.21490	1429.0	15.0	1255.0	21.0	1716.6	10	26.9
3104	284	1.60	3.65100	0.25140	1560.1	9.4	1445.0	16.0	1726.0	12	16.3
39	399	3.77	4.51800	0.31030	1733.8	7.7	1742.0	16.0	1729.2	7	-0.7
395	720	9.50	4.41900	0.30450	1714.0	12.0	1713.0	22.0	1734.0	6	1.2
377	60.5	0.55	4.07800	0.28070	1649.0	14.0	1595.0	19.0	1735.0	18	8.1
381	147	1.75	4.16100	0.28520	1665.7	7.8	1617.0	15.0	1738.7	9	7.0
326	410	1.11	2.48300	0.16870	1266.7	8.8	1005.0	12.0	1746.0	11	42.4
364	174	1.40	4.56600	0.30830	1742.3	9.4	1732.0	18.0	1751.1	9	1.1
329	315	1.26	4.34200	0.29080	1700.9	8.7	1645.0	18.0	1769.0	8	7.0
324	167.6	0.70	3.87900	0.26140	1609.0	11.0	1497.0	15.0	1771.8	10	15.5
382	260.8	3.69	4.33000	0.29000	1698.8	8.1	1642.0	18.0	1779.2	9	7.7
393	75.7	0.65	5.25600	0.32720	1863.0	13.0	1825.0	16.0	1899.0	18	3.9
389	15.89	1.28	9.71000	0.42600	2406.0	18.0	2293.0	35.0	2513.0	21	8.8
396	53.7	0.91	11.91000	0.48730	2596.9	9.1	2558.0	21.0	2637.6	9	3.0
360	302	1.03	12.61000	0.50090	2650.4	9.2	2617.0	26.0	2675.8	6	2.2
3128	170	3.04	12.77900	0.49400	2663.1	7.0	2588.0	19.0	2734.8	5	5.4
365	44.5	2.11	13.49000	0.50890	2713.9	9.5	2655.0	27.0	2760.0	13	3.8
314	55.7	0.75	13.58000	0.51220	2723.0	11.0	2668.0	24.0	2774.0	7	3.8

CR05					207/ 235		206/ 238		206/ 207		
#	[U] ppm	U/Th	207/ 235	206/ 238	Age Ma	2σ err	Age (Ma)	2σ err	Age (Ma)	2σ err	% Disc
220	40.9	0.26	0.01890	0.00255	18.7	6.9	16.4	2.1	50	530	67.2
101	226	0.53	0.02160	0.00309	21.6	2.4	19.9	0.8	170	200	7.8
28	245	0.54	0.02800	0.00416	28.0	2.4	26.8	1.0	110	180	4.3
271	46.3	0.61	0.03820	0.00495	37.8	6.4	31.8	2.8	360	350	91.2
58	104.4	0.69	0.04300	0.00547	42.6	4.1	35.2	1.6	380	200	90.7
12	301	0.99	0.06550	0.00958	64.4	2.2	61.4	1.5	176	70	4.7
224	93	0.92	0.06510	0.01000	63.9	3.5	64.1	2.3	110	100	0.3
227	154	1.59	0.08150	0.01185	79.4	4.3	75.9	1.9	190	110	4.4
150	440	1.01	0.09070	0.01382	88.1	2.7	88.5	2.1	133	68	0.5
139	376	2.29	0.09300	0.01415	90.6	2.5	90.6	1.3	84	65	0.0
178	570	1.97	0.10800	0.01466	104.0	3.7	93.8	1.6	324	74	9.8
164	113.6	0.52	0.11330	0.01581	108.8	3.7	101.1	2.9	243	83	7.1
225	205	1.24	0.10590	0.01588	102.0	3.5	101.5	1.9	147	81	0.5
26	318	2.39	0.14080	0.01943	134.8	4.1	124.0	2.9	273	58	8.0
126	123.1	0.33	0.14860	0.02201	140.4	4.9	140.3	3.0	141	77	0.1
182	379.2	0.86	0.15390	0.02218	145.3	3.7	141.4	3.1	181	54	2.7
241	99	0.52	0.15840	0.02263	149.0	6.2	144.3	3.4	206	94	3.2
157	410	0.31	0.15850	0.02268	149.3	3.1	144.5	2.2	224	48	3.2
43	57	0.41	0.16400	0.02319	153.0	10.0	147.8	4.5	230	130	3.4
63	75	0.39	0.16570	0.02373	156.5	6.1	151.2	4.1	250	100	3.4
21	502	0.82	0.16670	0.02385	156.5	2.8	151.9	2.1	208	47	2.9
269	615	1.06	0.16180	0.02385	152.1	3.2	152.0	2.9	152	40	0.1
85	141	0.94	0.16810	0.02415	157.5	4.6	154.3	3.9	259	68	2.0
256	230	0.77	0.17790	0.02464	166.1	4.1	156.9	2.4	270	73	5.5
151	512	0.83	0.16890	0.02489	158.4	2.8	158.5	2.0	173	44	0.1
24	292	0.53	0.18400	0.02601	171.3	3.6	165.5	2.6	207	57	3.4
119	531	3.21	0.17820	0.02622	166.4	2.6	166.8	2.8	177	37	0.2
221	480	0.25	0.18350	0.02622	171.0	2.7	166.8	2.0	221	43	2.5
170	291	0.71	0.18530	0.02730	172.5	3.6	173.6	3.3	182	47	0.6
183	295	1.92	0.20400	0.02850	188.4	4.5	181.2	3.4	259	50	3.8
84	84.4	0.73	0.20990	0.02965	193.1	6.5	188.4	3.5	260	87	2.4
131	502	1.83	0.21640	0.03035	198.7	5.5	192.7	4.3	220	41	3.0
159	151.2	2.15	0.24650	0.03427	223.5	5.4	217.2	3.3	272	75	2.8
54	1480	2.95	0.24290	0.03442	221.1	2.9	218.1	2.6	237	30	1.4
23	304	0.99	0.27710	0.03685	248.1	4.7	233.3	4.2	357	37	6.0
238	203	0.70	0.27530	0.03728	246.6	6.0	235.9	3.8	386	65	4.3

CR05					207/ 235		206/ 238		206/ 207		
#	[U] ppm	U/Th	207/ 235	206/ 238	Age Ma	2σ err	Age (Ma)	2σ err	Age (Ma)	2σ err	% Disc
279	384	0.77	0.28640	0.03969	255.7	3.5	250.9	3.2	271	40	1.9
106	299	0.52	0.36120	0.04993	312.9	5.3	314.0	5.9	296	35	0.4
136	300	2.40	0.37440	0.05074	322.8	4.0	319.0	3.6	333	35	1.2
195	169.3	2.44	0.38120	0.05177	327.6	5.9	325.3	3.5	347	48	0.7
291	273.3	0.67	0.38510	0.05226	330.6	4.2	328.3	4.4	338	38	0.7
22	171.1	1.24	0.39090	0.05280	334.8	5.2	331.7	3.8	337	43	0.9
40	175.7	3.39	0.41490	0.05574	352.0	6.0	349.6	5.2	371	40	0.7
219	40.4	0.67	0.43500	0.05770	365.0	11.0	361.8	8.1	379	87	0.9
15	544	3.58	0.45400	0.05867	379.0	15.0	367.5	5.6	420	71	3.0
142	133.1	0.69	0.45300	0.06010	378.7	7.5	376.1	7.3	402	53	0.7
76	153	1.10	0.45200	0.06027	378.2	8.5	377.2	5.0	399	56	0.3
190	581	5.83	0.45170	0.06067	378.3	3.1	379.7	3.5	363	22	0.4
108	201	0.34	0.48470	0.06214	401.0	4.8	388.6	4.3	447	34	3.1
113	377	6.70	0.51100	0.06313	418.4	6.8	394.6	4.6	538	47	5.7
298	121	1.21	0.47600	0.06320	395.7	6.7	394.9	7.4	402	53	0.2
231	313	2.55	0.48140	0.06328	398.9	4.6	395.5	5.8	439	27	0.9
36	181	1.89	0.47960	0.06351	398.2	6.5	396.9	4.9	417	43	0.3
141	241	1.24	0.49520	0.06360	408.2	5.7	397.4	6.2	482	37	2.6
278	394	0.48	0.50030	0.06417	411.7	4.8	400.9	5.0	442	31	2.6
53	430	1.63	0.48990	0.06504	405.2	4.5	406.2	4.1	388	30	0.2
94	308	5.10	0.50300	0.06580	413.0	7.2	410.6	7.5	441	32	0.6
252	138	0.57	0.51700	0.06629	422.3	6.9	413.7	4.2	460	47	2.0
306	257.9	1.18	0.51270	0.06644	420.1	4.9	414.7	5.4	442	33	1.3
262	60.6	0.66	0.50900	0.06750	417.0	8.9	420.7	9.3	386	73	0.9
111	132	1.09	0.53550	0.06890	435.1	6.2	429.2	6.6	418	48	1.4
124	215	2.26	0.52100	0.06910	425.3	7.6	430.3	8.4	452	37	1.2
211	483	15.81	0.52540	0.06915	428.6	4.1	431.0	3.0	423	23	0.6
194	179.3	0.97	0.52990	0.06944	432.2	5.9	432.7	5.3	433	40	0.1
110	229	0.71	0.55470	0.07057	447.7	6.3	439.6	5.4	456	34	1.8
4	92.8	0.99	0.55600	0.07090	449.5	8.3	441.5	9.2	466	50	1.8
75	103.2	0.88	0.56300	0.07193	452.6	7.9	447.7	5.9	481	47	1.1
166	488	0.89	0.64200	0.07420	502.9	8.2	461.0	10.0	712	34	8.3
50	210	91.20	0.59360	0.07430	472.9	6.3	461.7	6.7	525	41	2.4
260	244	0.75	0.61920	0.07551	489.1	6.0	469.2	5.5	561	39	4.1
77	73.6	1.46	0.66700	0.08090	519.0	11.0	501.7	8.0	578	67	3.3
1	154	1.23	0.65200	0.08307	510.2	6.4	514.3	5.8	517	35	0.8

CR05					207/ 235		206/ 238		206/ 207		
#	[U] ppm	U/Th	207/ 235	206/ 238	Age Ma	2σ err	Age (Ma)	2σ err	Age (Ma)	2σ err	% Disc
230	28.7	0.86	0.68400	0.08360	528.0	12.0	518.0	11.0	617	79	1.9
97	309	0.95	0.72700	0.08610	556.1	6.9	532.5	6.3	636	40	4.2
127	55.1	1.44	0.72500	0.08660	554.0	11.0	536.0	10.0	645	59	3.2
114	19.42	0.65	0.71400	0.08660	547.0	20.0	537.0	12.0	540	110	1.8
145a	83.9	1.40	0.71500	0.08690	549.4	8.0	537.2	7.6	602	46	2.2
35	61.7	0.62	0.79300	0.08720	592.0	12.0	539.0	15.0	834	65	9.0
46	108	1.08	0.73200	0.08880	557.0	12.0	548.0	13.0	611	52	1.6
193	35.8	0.41	0.75900	0.08900	571.0	16.0	549.7	9.5	704	81	3.7
138	155.2	0.89	0.73700	0.09010	562.0	11.0	556.0	12.0	566	41	1.1
44	194	0.70	0.77200	0.09340	580.2	9.0	575.4	9.4	607	38	0.8
258	65.7	0.78	0.82000	0.09460	608.8	9.3	582.6	9.5	694	52	4.3
56	60.3	0.76	0.81700	0.09620	605.0	13.0	592.0	10.0	664	55	2.1
282	202	1.38	0.80800	0.09770	601.1	6.3	600.8	9.1	605	32	0.0
19	212	1.17	0.82300	0.09780	610.3	6.0	601.2	7.0	613	27	1.5
247	343	1.15	0.82290	0.09840	609.4	5.0	605.3	6.0	632	26	0.7
95	394	0.89	0.84130	0.10005	620.3	4.4	615.4	5.3	648	23	0.8
249	109.2	1.18	0.86500	0.10070	631.9	9.0	618.6	7.5	678	42	2.1
129	332	0.52	0.84900	0.10090	624.0	5.9	619.9	7.8	641	28	0.7
213	239.1	1.58	0.87800	0.10110	639.6	9.1	622.0	9.1	714	30	2.8
237	223	1.37	0.84600	0.10180	621.9	7.4	624.8	8.9	619	31	0.5
175	55.8	1.06	0.86900	0.10500	638.0	14.0	645.0	12.0	633	54	1.1
176	245	0.49	0.91500	0.10750	658.9	8.2	658.1	8.2	688	29	0.1
208	204	2.48	1.02300	0.11680	715.0	22.0	711.0	23.0	756	33	0.6
92	72	1.27	1.27400	0.13300	833.0	14.0	805.0	13.0	933	44	3.4
51	182	1.59	1.38000	0.13470	878.0	15.0	814.0	21.0	1053	23	7.3
173	33.8	1.13	1.45300	0.15020	911.0	16.0	902.0	17.0	947	54	4.8
285	47.3	1.61	1.61500	0.16220	976.0	13.0	970.0	14.0	966	43	0.4
90	35.2	0.90	1.56000	0.15840	953.0	13.0	947.0	13.0	980	46	3.4
214	24.7	0.40	1.52900	0.15580	941.0	16.0	933.0	16.0	980	55	4.8
79	273	3.80	1.62300	0.16280	978.7	5.9	972.4	8.0	999	22	2.7
162	104.3	1.16	1.66400	0.16460	994.4	9.4	982.0	13.0	1001	41	1.9
216	160.3	1.29	1.69200	0.16890	1005.8	8.8	1006.1	9.8	1008	24	0.2
307	360	1.41	1.64900	0.16230	988.8	5.5	969.7	6.9	1008	19	3.8
149	42.5	4.86	1.56700	0.15570	957.0	12.0	932.0	22.0	1013	46	8.0
174	28	0.58	1.54500	0.15550	946.0	18.0	932.0	14.0	1014	58	8.1
294	170.3	1.15	1.64700	0.16480	987.9	8.7	983.0	12.0	1014	28	3.1

CR05					207/ 235		206/ 238		206/ 207		
#	[U] ppm	U/Th	207/ 235	206/ 238	Age Ma	2σ err	Age (Ma)	2σ err	Age (Ma)	2σ err	% Disc
296	176	1.75	1.69600	0.16920	1008.4	7.7	1009.0	11.0	1016	24	0.7
41	23.4	0.56	1.76000	0.17270	1030.0	17.0	1027.0	16.0	1018	61	0.9
196	110	1.45	1.71400	0.17100	1013.2	8.9	1017.3	9.6	1021	33	0.4
281	397	67.30	1.68600	0.16570	1004.2	8.2	988.0	11.0	1021	24	3.2
187	46.2	1.35	1.69700	0.16460	1006.0	13.0	982.0	14.0	1029	49	4.6
200	113	0.99	1.75200	0.17390	1027.0	9.9	1033.0	14.0	1035	31	0.2
32	271	1.38	1.45500	0.14330	911.0	13.0	863.0	17.0	1042	31	17.2
301	171	1.84	1.80400	0.17600	1047.0	11.0	1045.0	17.0	1042	23	0.3
13	111.8	2.08	1.78500	0.17380	1040.0	16.0	1033.0	21.0	1047	23	1.3
184	216	1.21	1.71700	0.16570	1015.1	8.7	988.0	13.0	1047	24	5.6
98	22.45	0.64	1.55700	0.15100	950.0	21.0	906.0	22.0	1054	74	14.0
300	114	1.54	1.68700	0.16300	1002.0	11.0	973.0	13.0	1056	33	7.9
246	131	2.06	1.73800	0.16940	1025.3	8.5	1009.0	11.0	1057	26	4.5
2	67	1.28	1.79800	0.17500	1043.0	14.0	1042.0	18.0	1058	38	1.5
71	317.5	0.93	1.82100	0.17770	1052.9	5.8	1054.0	8.7	1061	18	0.7
276	90.5	2.04	1.87300	0.17920	1072.0	11.0	1062.0	16.0	1067	33	0.5
248	53	1.01	1.80700	0.17310	1048.0	11.0	1031.0	11.0	1072	34	3.8
305	28.9	0.78	1.54700	0.14860	947.0	17.0	893.0	16.0	1075	54	16.9
179	90	1.25	1.79100	0.17260	1045.0	11.0	1026.0	12.0	1077	37	4.7
20	279	2.21	1.91900	0.18400	1088.0	5.7	1088.9	7.8	1084	17	0.5
10	141.8	1.99	1.74000	0.16580	1023.1	7.4	989.0	12.0	1089	23	9.2
299	646	2.41	1.86400	0.17660	1068.3	4.7	1048.2	8.8	1094	14	4.2
202	39.5	0.93	1.93900	0.18510	1092.0	15.0	1094.0	21.0	1101	35	0.6
209	120.8	1.70	1.79700	0.17000	1045.1	9.3	1012.0	14.0	1107	27	8.6
132	63.5	32.20	1.89100	0.17660	1076.0	14.0	1048.0	14.0	1112	41	5.8
273	74	0.97	1.85600	0.17810	1064.0	12.0	1056.0	17.0	1121	39	5.8
268	166	1.51	2.01800	0.19170	1122.1	7.6	1130.0	14.0	1126	21	0.4
245	67	1.84	2.01600	0.18870	1119.0	15.0	1114.0	13.0	1134	32	1.8
254	102.5	1.60	2.00200	0.18460	1115.4	8.2	1092.0	11.0	1137	24	4.0
145	92.7	1.75	2.14000	0.19860	1162.0	10.0	1168.0	15.0	1142	29	2.3
140	115.6	1.64	1.95900	0.17940	1100.6	9.5	1063.0	12.0	1143	33	7.0
250	145	0.80	1.96900	0.18300	1104.4	9.4	1083.0	11.0	1143	24	5.2
47	248	11.80	1.99300	0.18480	1111.0	19.0	1093.0	24.0	1151	27	5.0
73	614	5.16	1.73300	0.16030	1018.0	21.0	957.0	30.0	1155	24	17.1
122	79.4	1.49	2.02000	0.18840	1121.0	13.0	1113.0	18.0	1155	27	3.6
102	29.2	1.21	1.83700	0.17010	1060.0	17.0	1012.0	19.0	1163	60	13.0

CR05					207/ 235		206/ 238		206/ 207		
#	[U] ppm	U/Th	207/ 235	206/ 238	Age Ma	2σ err	Age (Ma)	2σ err	Age (Ma)	2σ err	% Disc
167	74	1.06	2.12400	0.19490	1156.0	12.0	1148.0	11.0	1171	33	2.0
143	40.4	1.51	2.07300	0.18800	1138.0	15.0	1110.0	15.0	1176	55	5.6
135	1295	16.12	2.08900	0.18920	1144.8	6.1	1117.0	11.0	1178	12	5.2
172	9.11	0.53	1.89800	0.17060	1078.0	28.0	1014.0	29.0	1180	110	14.1
222	106.8	1.22	2.06000	0.18880	1137.3	8.3	1115.0	11.0	1182	24	5.7
165	182	1.96	2.18400	0.19920	1175.0	11.0	1171.0	17.0	1183	24	1.0
6	70.3	2.04	1.95700	0.17690	1102.0	11.0	1050.0	15.0	1186	29	11.5
7	52.9	2.07	2.14200	0.19330	1163.0	16.0	1139.0	22.0	1187	30	4.0
25	26.7	0.99	1.62600	0.14830	977.0	21.0	891.0	28.0	1187	72	24.9
91	216	1.00	2.00000	0.18180	1115.3	6.7	1077.0	10.0	1188	16	9.3
177	145	0.59	2.02000	0.18640	1121.7	7.9	1101.0	15.0	1188	26	7.3
161	140.5	1.80	2.02000	0.18060	1120.0	26.0	1070.0	31.0	1189	38	10.0
272	76	0.71	2.07000	0.19140	1139.0	18.0	1128.0	23.0	1193	43	5.4
274	104.9	0.73	2.14300	0.19620	1163.6	9.3	1155.0	12.0	1200	28	3.8
37	137	1.90	2.31000	0.20980	1214.9	7.9	1228.0	12.0	1208	24	1.7
185	217	1.22	2.26000	0.20270	1199.5	7.3	1189.9	8.9	1210	18	1.7
59	319	1.28	2.50600	0.22130	1273.5	7.7	1289.0	12.0	1253	19	2.9
18	98	1.66	2.41000	0.21080	1247.0	11.0	1233.0	18.0	1254	30	1.7
14	219	0.90	2.52600	0.21640	1279.1	7.7	1265.0	13.0	1304	22	3.0
147	782	3.10	2.20200	0.19260	1182.4	6.6	1135.0	19.0	1304	28	13.0
292	369	2.42	2.73000	0.23160	1335.7	9.9	1342.0	19.0	1317	19	1.9
64	119.1	1.52	2.80500	0.23680	1356.2	7.9	1370.0	13.0	1339	23	2.3
180	100.1	1.08	2.62400	0.22110	1306.7	9.6	1288.0	18.0	1343	28	4.1
289	144	1.60	1.91500	0.16220	1086.0	18.0	969.0	11.0	1347	59	28.1
283	92.7	1.10	2.72600	0.22590	1335.0	12.0	1313.0	20.0	1360	23	3.5
212	100.2	0.96	2.65300	0.22230	1315.0	10.0	1294.0	14.0	1361	24	4.9
104	24.8	0.57	3.00600	0.25000	1407.0	19.0	1438.0	27.0	1362	51	5.6
52	196	1.19	2.73800	0.22630	1338.2	7.5	1316.0	14.0	1373	18	4.2
100	758	1.05	2.67800	0.22040	1322.9	5.3	1284.0	11.0	1380	14	7.0
266	187	1.69	2.54900	0.21150	1285.4	9.1	1238.0	13.0	1380	24	10.3
144	148	2.05	2.75300	0.22560	1343.4	7.7	1311.4	9.8	1384	18	5.2
156	68	0.46	2.78700	0.22650	1350.0	18.0	1315.0	26.0	1392	39	5.5
228	105	1.21	2.62200	0.21730	1307.0	11.0	1267.0	19.0	1398	31	9.4
87	239	1.75	2.57900	0.21260	1294.0	10.0	1244.0	15.0	1399	15	11.1
280	232	1.34	2.16600	0.17630	1171.6	9.9	1046.0	15.0	1405	42	25.6
160	274	1.46	2.97100	0.23800	1399.9	7.9	1376.0	12.0	1414	19	2.7

CR05					207/ 235		206/ 238		206/ 207		
#	[U] ppm	U/Th	207/ 235	206/ 238	Age Ma	2σ err	Age (Ma)	2σ err	Age (Ma)	2σ err	% Disc
109	125	1.83	2.79700	0.22600	1354.0	11.0	1313.0	17.0	1418	21	7.4
103	33.8	0.93	2.87700	0.23320	1377.0	16.0	1351.0	24.0	1427	41	5.3
128	105.2	1.19	2.89900	0.23330	1381.0	11.0	1352.0	13.0	1432	26	5.6
130	56.5	1.17	3.13900	0.24850	1444.0	11.0	1433.0	19.0	1434	28	0.1
3	265	2.00	3.08300	0.24790	1428.1	8.2	1427.0	20.0	1438	14	0.8
117	70.6	1.89	2.98600	0.24030	1405.0	12.0	1388.0	15.0	1438	31	3.5
197	62.5	1.20	3.06900	0.24720	1424.0	13.0	1424.0	19.0	1442	26	1.2
277	168	0.78	3.01000	0.23830	1411.0	13.0	1377.0	14.0	1448	21	4.9
9	149	0.57	3.23500	0.25630	1466.0	10.0	1470.0	17.0	1449	17	1.4
204	421	0.77	2.88100	0.22930	1376.0	14.0	1330.0	23.0	1453	15	8.5
30	56.6	1.18	3.20600	0.25370	1459.0	11.0	1457.0	18.0	1454	26	0.2
74	340	3.89	2.88100	0.22920	1376.3	8.5	1330.0	16.0	1456	21	8.7
242	111.3	1.14	2.42300	0.19350	1248.0	14.0	1140.0	16.0	1461	29	22.0
169	638	0.84	2.88800	0.22670	1381.0	13.0	1321.0	22.0	1470	21	10.1
158	213	1.33	3.17200	0.24650	1450.0	8.1	1420.0	13.0	1475	18	3.7
259	80	1.72	3.22400	0.25070	1462.0	14.0	1445.0	21.0	1475	32	2.0
286	144.5	1.17	2.94900	0.22770	1393.0	12.0	1322.0	19.0	1482	23	10.8
155	159	0.78	3.38900	0.26500	1501.0	14.0	1515.0	26.0	1495	26	1.3
267	398	1.53	2.97200	0.23140	1400.3	6.2	1342.0	14.0	1502	16	10.7
239	72.8	0.54	3.30500	0.25800	1481.3	9.2	1479.0	15.0	1503	23	1.6
48	288.2	1.93	2.84500	0.22060	1366.0	16.0	1285.0	23.0	1504	27	14.6
39	32.5	1.19	3.20800	0.24650	1456.0	22.0	1420.0	23.0	1525	43	6.9
86	74.8	1.18	3.06200	0.23620	1424.0	12.0	1367.0	17.0	1525	27	10.4
308	126.3	1.08	2.96500	0.22420	1403.0	17.0	1303.0	30.0	1528	37	14.7
149	12.2	0.90	3.14000	0.24000	1441.0	67.0	1383.0	68.0	1540	100	10.2
293	169	1.53	3.48100	0.26150	1527.0	17.0	1497.0	21.0	1565	33	4.3
69	97.1	0.75	3.63000	0.26420	1555.0	11.0	1511.0	16.0	1617	24	6.6
61	81.9	1.21	3.74600	0.27390	1580.7	7.7	1560.0	14.0	1621	23	3.8
236	135.5	1.33	3.66700	0.26630	1563.0	19.0	1521.0	26.0	1623	24	6.3
261	644	4.67	3.94600	0.28480	1620.0	10.0	1615.0	19.0	1625	20	0.6
153	112.1	0.62	3.81800	0.27600	1596.0	8.4	1573.0	17.0	1631	20	3.6
120	291	1.09	3.69000	0.26740	1567.0	22.0	1533.0	38.0	1632	23	6.1
60	119.7	2.58	3.47500	0.24850	1524.0	14.0	1433.0	19.0	1647	25	13.0
264	82.2	0.89	3.94800	0.28060	1622.0	12.0	1597.0	20.0	1647	19	3.0
218	57.3	1.08	3.96900	0.28500	1629.0	13.0	1616.0	19.0	1650	33	2.1
275	45.5	0.76	3.83900	0.27860	1600.0	13.0	1584.0	22.0	1653	34	4.2

CR05					207/ 235		206/ 238		206/ 207		
#	[U] ppm	U/Th	207/ 235	206/ 238	Age Ma	2σ err	Age (Ma)	2σ err	Age (Ma)	2σ err	% Disc
116	60.2	0.45	3.84300	0.27470	1601.0	13.0	1564.0	22.0	1656	29	5.6
288	220	1.25	4.06700	0.28860	1648.0	8.5	1637.0	21.0	1659	22	1.3
229	39.9	0.92	3.85400	0.27650	1605.0	16.0	1577.0	23.0	1662	38	5.1
201	198	0.62	3.95100	0.28300	1626.1	7.7	1606.0	13.0	1668	19	3.7
215	219	2.55	3.55900	0.25430	1542.0	18.0	1459.0	31.0	1671	19	12.7
188	63.1	1.12	4.00300	0.28390	1633.0	13.0	1610.0	22.0	1673	24	3.8
82	345	2.16	3.43000	0.24500	1512.0	30.0	1417.0	52.0	1676	19	15.5
78	92.2	1.07	4.12900	0.29100	1661.0	11.0	1646.0	22.0	1677	21	1.8
5	230	2.05	4.16500	0.29250	1668.1	7.0	1654.0	15.0	1681	18	1.6
34	170	0.84	4.02300	0.28550	1639.4	7.8	1618.0	17.0	1681	22	3.7
121	120.2	1.32	4.25100	0.29920	1683.1	9.1	1687.0	16.0	1681	18	0.4
243	155.4	1.12	4.16000	0.29590	1665.6	8.2	1671.0	18.0	1682	19	0.7
66	63.4	1.20	3.87300	0.27530	1607.0	10.0	1567.0	23.0	1683	29	6.9
133	187	0.97	4.18000	0.29010	1669.0	11.0	1642.0	18.0	1684	20	2.5
186	478	3.01	4.34900	0.30310	1701.9	9.0	1706.0	19.0	1688	14	1.1
198	79	0.61	4.11700	0.28880	1658.0	10.0	1637.0	15.0	1688	26	3.0
290	113	0.92	3.97800	0.28170	1631.0	14.0	1599.0	27.0	1689	30	5.3
192	1160	3.17	4.60000	0.32310	1755.0	20.0	1803.0	35.0	1693	14	6.5
287	47.6	0.53	4.20100	0.29480	1675.0	16.0	1665.0	27.0	1693	31	1.7
80	337	1.48	4.21500	0.29640	1678.0	14.0	1673.0	28.0	1696	23	1.4
105	431	1.70	3.21000	0.22300	1451.0	56.0	1290.0	82.0	1700	18	24.1
265	183	1.20	4.26600	0.29640	1689.0	12.0	1675.0	20.0	1700	17	1.5
27	94	2.37	4.36900	0.30140	1705.6	9.5	1698.0	16.0	1709	19	0.6
263	171	2.57	4.32400	0.29930	1697.2	8.3	1687.0	16.0	1709	15	1.3
70	230	1.06	4.24700	0.29400	1683.8	9.9	1661.0	20.0	1710	22	2.9
191	168.4	1.45	4.28000	0.29460	1691.0	10.0	1664.0	20.0	1711	22	2.7
118	2150	2.86	4.40400	0.30290	1713.0	15.0	1705.0	24.0	1718	12	0.8
83	103.4	0.79	4.23600	0.29420	1682.0	11.0	1662.0	20.0	1725	22	3.7
93	415	1.53	4.24300	0.29280	1681.6	9.0	1655.0	17.0	1725	15	4.1
244	80.4	0.77	4.19500	0.29160	1675.0	13.0	1649.0	21.0	1731	27	4.7
31	388	1.08	4.37000	0.30400	1706.0	30.0	1706.0	51.0	1732	15	1.5
115	695	8.32	4.18000	0.28370	1664.0	24.0	1608.0	37.0	1732	17	7.2
302	305	0.57	4.55800	0.30670	1743.9	9.6	1724.0	18.0	1742	14	1.0
88	155.4	1.45	4.54900	0.30950	1740.4	6.8	1740.0	15.0	1743	17	0.2
16	159	2.52	4.61300	0.31090	1750.9	8.2	1745.0	16.0	1749	17	0.2
72	811	0.99	4.70700	0.31720	1768.0	16.0	1779.0	30.0	1756	14	1.3

CR05					207/ 235		206/ 238		206/ 207		
#	[U] ppm	U/Th	207/ 235	206/ 238	Age Ma	2 σ err	Age (Ma)	2 σ err	Age (Ma)	2 σ err	% Disc
112	83.4	2.49	4.60900	0.30850	1751.0	13.0	1732.0	24.0	1759	26	1.5
199	101	1.70	4.88400	0.33190	1800.0	13.0	1847.0	24.0	1761	18	4.9
303	231.3	1.47	4.41800	0.29570	1715.4	6.7	1670.0	14.0	1761	18	5.2
65	293	1.55	3.09000	0.20760	1432.0	20.0	1215.0	32.0	1763	25	31.1
284	49.4	2.00	4.40800	0.29340	1713.0	13.0	1658.0	18.0	1779	33	6.8
123	44.5	1.21	4.56100	0.30310	1745.0	11.0	1709.0	23.0	1802	27	5.2
89	34.1	0.78	4.40400	0.29210	1714.0	15.0	1652.0	22.0	1805	42	8.5
240	242	1.43	4.65100	0.30800	1758.1	6.1	1731.0	10.0	1810	12	4.4
295	72.2	1.26	4.62200	0.30320	1752.0	13.0	1707.0	24.0	1821	27	6.3
137	329	1.46	4.10400	0.26580	1652.0	19.0	1517.0	48.0	1823	29	16.8
234	52.6	1.13	5.30400	0.34260	1868.9	9.2	1899.0	21.0	1841	23	3.2
11	74.5	0.76	5.21200	0.32840	1854.1	9.1	1830.0	21.0	1875	18	2.4
107	77.9	1.70	5.20800	0.32770	1853.2	9.5	1827.0	15.0	1877	21	2.7
8	99.9	2.27	5.42000	0.34070	1889.0	16.0	1889.0	31.0	1880	17	0.5
255	99	1.99	5.43100	0.33450	1889.2	8.1	1860.0	15.0	1911	18	2.7
207	151.1	7.82	4.48400	0.27400	1727.0	13.0	1563.0	21.0	1944	22	19.6
163	6.57	0.31	4.77000	0.28120	1781.0	32.0	1601.0	47.0	1977	78	19.0
171	48.2	1.97	6.23000	0.36120	2010.7	9.2	1987.0	20.0	2055	23	3.3
232	25.7	0.99	6.40000	0.36070	2032.0	14.0	1984.0	28.0	2104	28	5.7
205	429	2.19	4.63000	0.22470	1752.0	18.0	1306.0	23.0	2342	17	44.2
257	276	1.73	8.97000	0.41380	2334.4	9.1	2232.0	17.0	2412	13	7.5
99	177	1.50	9.51600	0.42690	2388.6	7.7	2291.0	15.0	2474	13	7.4
81	144	0.96	11.67000	0.47000	2574.0	31.0	2488.0	56.0	2666	19	6.7
181	40.7	3.26	11.96000	0.47500	2608.0	27.0	2509.0	60.0	2666	18	5.9
203	22.8	0.75	10.98000	0.42840	2519.0	20.0	2312.0	41.0	2704	28	14.5
253	65.9	0.79	13.31000	0.51580	2702.0	10.0	2680.0	28.0	2704	16	0.9
45	85.8	1.64	12.31000	0.48120	2627.7	9.8	2532.0	24.0	2709	15	6.5
152	146	0.81	13.00000	0.50680	2679.2	6.5	2642.0	18.0	2715	13	2.7
125	42.4	0.59	12.72000	0.49460	2661.0	11.0	2593.0	27.0	2724	17	4.8
154	104.5	0.61	13.09000	0.49720	2685.0	10.0	2601.0	26.0	2757	15	5.7
134	150	1.18	15.77000	0.54890	2861.0	12.0	2819.0	33.0	2881	12	2.2
206	764	2.86	14.62000	0.48400	2793.0	37.0	2549.0	50.0	3012	29	15.4
49	94.2	1.04	24.05000	0.63370	3269.9	9.1	3171.0	27.0	3321	12	4.5

Appendix D: Sample (U-Th)/He Data Table

Sample	Age, Ma	err., Ma	U (ppm)	Th (ppm)	¹⁴⁷ Sm (ppm)	He (nmol/g)	mass (ug)	Ft	ESR
ICP date: 10/16/2013									
z12MCSMG1-104	57.2	4.6	170.4	68.5	0.4	41.9	3.14	0.73	41.94
z12MCSMG1-106	56.0	4.5	177.9	58.1	0.8	43.1	3.82	0.74	45.02
z12MCSMG1-111	39.8	3.2	463.4	80.7	0.4	74.5	2.90	0.72	40.23
z12MCSMG1-13	44.7	3.6	223.6	27.2	0.5	43.5	6.59	0.78	53.08
z12MCSMG1-36	60.8	4.9	577.6	89.5	0.3	148.0	4.29	0.75	45.91
z12MCSMG1-38	49.9	4.0	128.1	63.3	0.4	28.5	3.69	0.74	44.69
z12MCSMG1-6	63.2	5.1	372.8	56.5	0.6	103.2	6.21	0.78	53.10
z12MCSMG1-64	54.4	4.4	197.8	54.1	0.4	48.3	6.10	0.78	53.02
z12MCSMG1-80	70.3	5.6	349.0	81.6	0.2	100.3	2.81	0.72	39.93
z12MCSMG1-99	53.9	4.3	551.6	159.7	0.5	122.0	3.03	0.71	39.16
z12MCSMG4-100	69.2	5.5	323.7	63.4	0.4	106.1	16.76	0.84	72.12
z12MCSMG4-101	63.2	5.1	670.9	53.6	2.0	200.1	23.00	0.86	82.01
z12MCSMG4-18	64.2	5.1	84.4	14.0	0.2	25.8	18.44	0.85	77.02
z12MCSMG4-2	54.7	4.4	441.3	54.2	0.4	102.7	4.98	0.76	48.47
z12MCSMG4-24	60.0	4.8	218.5	17.2	0.3	62.2	28.26	0.86	84.21
z12MCSMG4-4	65.2	5.2	176.1	35.7	0.5	53.4	11.50	0.82	65.57
z12MCSMG4-6	72.6	5.8	317.6	84.8	0.7	101.6	6.74	0.77	49.56
z12MCSMG4-76	61.0	4.9	134.5	24.0	0.3	38.1	12.61	0.82	66.84
z12MCSMG4-73	60.4	4.8	268.3	32.5	0.3	77.2	23.40	0.86	81.97
z13MCSMG21-1	337.6	27.0	8.4	0.5	0.0	11.8	4.20	0.75	44.74
z13MCSMG21-100	28.6	2.3	312.7	204.3	0.7	39.4	3.42	0.71	39.55
z13MCSMG21-24	66.2	5.3	59.6	32.4	0.7	17.7	3.83	0.74	44.18
z13MCSMG21-30	471.1	37.7	26.5	10.6	0.4	59.6	5.83	0.78	53.32
z13MCSMG21-36	66.7	5.3	173.3	82.9	0.8	49.9	3.50	0.72	40.80
z13MCSMG21-47	297.7	23.8	113.4	55.5	1.0	150.2	3.56	0.73	42.23
z13MCSMG21-56	27.1	2.2	380.1	283.0	0.6	48.1	3.77	0.73	44.26
z13MCSMG21-59	77.0	6.2	58.2	26.3	0.8	19.6	3.47	0.73	42.54
z13MCSMG21-64	89.8	7.2	42.4	21.3	1.9	17.1	3.66	0.74	44.73
z13MCSMG21-71	84.6	6.8	126.4	53.9	0.6	48.8	4.64	0.77	49.92
z13MCSMG21-84	113.6	9.1	78.9	27.1	0.9	37.1	2.43	0.71	38.72
z13MCSMG21-88	3.6	0.3	112.4	70.5	15.7	1.7	2.52	0.69	37.37
z13MCSMG21-90	302.3	24.2	131.5	145.3	1.1	198.4	3.19	0.72	42.35
z13MCSMG21-91	982.0	78.6	28.2	15.8	1.1	147.2	8.04	0.80	60.02
z13MCSMG21-93	187.9	15.0	195.6	88.6	1.2	172.0	6.07	0.77	52.11

Sample	Age, Ma	err., Ma	U (ppm)	Th (ppm)	147Sm (ppm)	He (nmol/g)	mass (ug)	Ft	ESR
z13MCSMG21-95	32.2	2.6	86.3	83.6	0.5	14.2	6.11	0.77	52.15
z13MCSMG21-124	146.0	11.7	59.6	52.2	0.6	40.7	2.69	0.71	40.69
z13MCSMG21-4	182.1	14.6	146.1	107.7	0.5	128.3	4.17	0.75	47.97
z13MCSMG21-50	213.1	17.0	174.5	93.9	2.8	171.8	3.89	0.75	46.84
z13MCSMG21-58	374.9	30.0	230.9	57.5	0.7	366.9	2.68	0.72	41.24
z13MCSMG21-60	49.6	4.0	438.8	137.6	1.1	93.0	3.22	0.74	43.67
z13MCSMG21-67	251.7	20.1	103.0	23.3	0.6	109.6	2.89	0.73	42.64
zUTFCT-270	26.1	2.1	302.2	196.6	0.7	36.8	4.41	0.75	46.68
zUTFCT-271	26.3	2.1	363.3	212.8	0.4	44.2	4.40	0.75	47.11

Sample	Age, Ma	err., Ma	U (ppm)	Th (ppm)	147Sm (ppm)	He (nmol/g)	mass (ug)	Ft	ESR
ICP date: 12/23/2013									
z13MCSMG15-118	254.1	20.3	120.6	62.3	1.4	145.8	5.38	0.77	52.07
z13MCSMG15-119	63.8	5.1	366.9	56.1	7.9	97.5	3.57	0.74	44.14
z13MCSMG15-12			0.5	0.3	-0.1	59.9	2.24	0.69	37.66
z13MCSMG15-22	162.8	13.0	56.0	58.6	0.8	45.0	3.50	0.73	43.31
z13MCSMG15-27	237.8	19.0	151.2	69.7	0.8	168.9	5.42	0.77	51.79
z13MCSMG15-28	283.7	22.7	90.2	62.3	1.3	126.8	6.49	0.78	53.01
z13MCSMG15-31	452.1	36.2	35.9	45.6	1.3	92.6	7.18	0.79	57.48
z13MCSMG15-33	179.9	14.4	226.5	124.9	2.2	185.6	3.66	0.74	44.74
z13MCSMG15-39	269.2	21.5	76.7	28.6	0.6	89.8	3.50	0.73	42.39
z13MCSMG15-4	91.2	7.3	278.4	1985.7	173.8	269.9	3.66	0.73	45.48
z13MCSMG15-49	52.5	4.2	30.5	24.1	1.3	8.1	7.95	0.79	57.18
z13MCSMG15-53	64.2	5.1	77.0	40.4	3.6	21.9	3.48	0.73	42.49
z13MCSMG15-56	142.1	11.4	293.0	77.0	0.8	165.9	2.22	0.69	36.33
z13MCSMG15-63	269.6	21.6	160.2	79.4	1.7	193.8	3.30	0.73	43.37
z13MCSMG15-64	70.7	5.7	937.7	253.3	9.0	291.6	5.42	0.76	49.05
z13MCSMG15-70	85.7	6.9	132.1	76.0	1.0	46.8	2.03	0.67	34.59
z13MCSMG15-79	94.2	7.5	101.1	68.0	0.5	46.1	5.34	0.77	51.46
z13MCSMG15-80	206.5	16.5	200.8	84.5	0.8	193.4	6.59	0.78	52.48
z13MCSMG15-84	25.4	2.0	109.9	53.8	1.3	13.6	9.17	0.81	61.74
z13MCSMG15-98	87.9	7.0	136.5	37.3	0.4	53.1	4.79	0.77	49.76
z13MCSMG6-111	64.3	5.1	1063.5	169.2	3.7	297.5	6.10	0.77	51.09
z13MCSMG6-68	60.9	4.9	978.9	217.0	1.9	256.8	5.25	0.76	47.20

Sample	Age, Ma	err., Ma	U (ppm)	Th (ppm)	147Sm (ppm)	He (nmol/g)	mass (ug)	Ft	ESR
z13MCSMG6-69	86.1	6.9	187.7	35.8	0.3	69.8	5.57	0.76	48.46
z13MCSMG6-7	70.6	5.6	190.2	21.6	0.3	61.4	12.79	0.82	66.14
z13MCSMG6-88	76.5	6.1	226.7	31.8	0.7	76.8	7.34	0.79	55.29
z13MCSMG9-100	30.2	2.4	1486.4	423.5	178.5	175.7	1.68	0.68	35.00
z13MCSMG9-105	233.8	18.7	277.5	119.9	2.0	261.7	1.90	0.67	34.16
z13MCSMG9-31	308.7	24.7	33.1	15.0	0.3	41.6	1.65	0.67	34.28
z13MCSMG9-38	340.8	27.3	44.7	15.6	0.2	65.4	2.52	0.72	40.73
z13MCSMG9-40	32.5	2.6	97.5	26.1	0.5	13.4	3.11	0.74	43.59
z13MCSMG9-42	181.6	14.5	236.3	93.3	1.8	172.6	1.88	0.68	34.70
z13MCSMG9-50	51.7	4.1	114.9	38.1	0.6	23.7	1.92	0.68	35.77
z13MCSMG9-54	70.8	5.7	289.8	50.9	0.5	82.0	2.41	0.71	38.64
z13MCSMG9-55	37.0	3.0	262.6	321.7	13.3	46.8	2.45	0.69	37.96
z13MCSMG9-59	57.5	4.6	369.1	147.6	1.1	89.3	2.72	0.71	39.65
z13MCSMG9-66	159.3	12.7	432.5	107.0	16.6	278.3	2.25	0.70	37.70
z13MCSMG9-75	73.9	5.9	97.2	54.8	0.8	30.0	1.96	0.68	35.84
z13MCSMG9-78	258.8	20.7	172.0	53.6	2.9	188.9	2.61	0.72	40.95
zUTFCT-302	36.8	2.9	167.5	83.8	1.2	29.0	7.39	0.78	53.15
zUTFCT-303	36.7	2.9	149.3	78.2	0.5	26.1	7.89	0.79	55.16

Sample	Age, Ma	err., Ma	U (ppm)	Th (ppm)	147Sm (ppm)	He (nmol/g)	mass (ug)	Ft	ESR
ICP date: 1/3/2014									
z13MCSMG12-104	449.6	36.0	197.9	62.1	1.8	355.2	1.68	0.67	33.94
z13MCSMG12-114	434.1	34.7	69.0	55.7	0.7	154.0	6.46	0.78	53.54
z13MCSMG12-122	329.1	26.3	114.8	18.2	0.8	162.3	3.77	0.75	45.74
z13MCSMG12-123	221.4	17.7	118.9	54.5	1.3	110.0	2.45	0.69	36.76
z13MCSMG12-14	346.9	27.8	52.6	17.5	0.4	82.1	4.00	0.76	47.32
z13MCSMG12-36	13.6	1.1	189.4	23.3	0.3	11.3	6.89	0.79	54.67
z13MCSMG12-45	221.7	17.7	63.5	29.8	0.9	61.3	2.70	0.72	40.74
z13MCSMG12-48	319.6	25.6	17.3	14.2	0.2	27.9	5.72	0.77	51.54
z13MCSMG12-57	179.6	14.4	40.2	25.6	0.6	33.4	3.51	0.74	44.47
z13MCSMG12-58	269.9	21.6	33.3	16.4	0.5	42.0	4.75	0.76	49.39
z13MCSMG12-62	190.4	15.2	47.7	60.6	3.9	46.0	2.82	0.72	41.53
z13MCSMG12-71	309.1	24.7	65.1	9.9	0.4	81.4	2.28	0.71	38.70
z13MCSMG12-72	361.5	28.9	37.6	9.5	0.5	60.4	4.44	0.76	47.83
z13MCSMG12-75	111.7	8.9	26.9	21.2	0.9	13.9	2.86	0.72	41.76

Sample	Age, Ma	err., Ma	U (ppm)	Th (ppm)	147Sm (ppm)	He (nmol/g)	mass (ug)	Ft	ESR
z13MCSMG12-82	47.5	3.8	93.8	12.1	0.2	18.0	3.09	0.73	41.06
z13MCSMG12-86	232.9	18.6	60.3	21.5	0.6	63.4	4.66	0.76	48.69
z13MCSMG12-98	52.4	4.2	105.8	21.3	0.3	24.3	5.41	0.77	50.97
z13MCSMG13-1	91.1	7.3	512.7	159.5	3.2	206.7	5.21	0.76	48.38
z13MCSMG13-107	192.4	15.4	64.8	34.3	0.5	55.3	3.75	0.72	41.74
z13MCSMG13-11	590.8	47.3	17.5	13.9	0.9	54.5	7.70	0.79	56.67
z13MCSMG13-110	206.7	16.5	85.9	44.7	0.8	78.2	2.71	0.72	41.15
z13MCSMG13-112	146.3	11.7	147.0	71.1	1.0	91.1	2.58	0.70	38.10
z13MCSMG13-12	42.3	3.4	171.4	60.4	0.6	30.2	3.09	0.71	39.89
z13MCSMG13-18	390.6	31.3	64.7	44.0	0.7	112.4	2.58	0.69	37.62
z13MCSMG13-2	228.6	18.3	53.3	35.1	0.7	62.9	10.54	0.82	65.52
z13MCSMG13-21	264.6	21.2	22.3	12.6	0.6	30.1	11.71	0.82	65.61
z13MCSMG13-25	74.9	6.0	131.0	84.3	0.4	44.4	3.60	0.72	42.35
z13MCSMG13-29	58.4	4.7	383.0	65.1	1.7	92.9	3.38	0.74	43.44
z13MCSMG13-32	78.4	6.3	646.2	105.6	1.9	206.7	3.05	0.73	41.28
z13MCSMG13-33	267.4	21.4	206.7	118.3	2.2	259.7	4.10	0.75	47.86
z13MCSMG13-40	114.4	9.2	196.2	92.7	0.7	101.8	4.02	0.75	46.91
z13MCSMG13-62	180.6	14.4	140.8	83.3	3.8	118.5	4.21	0.75	46.81
z13MCSMG13-69	275.9	22.1	64.7	33.6	0.5	77.4	2.46	0.70	38.89
z13MCSMG13-7	217.6	17.4	186.3	42.4	1.3	182.6	5.56	0.78	53.01
z13MCSMG13-72	343.5	27.5	29.5	14.8	0.4	50.5	9.09	0.81	61.36
z13MCSMG13-77	53.7	4.3	153.4	94.2	0.5	39.8	6.51	0.78	54.20
z13MCSMG13-78	145.8	11.7	177.6	49.7	0.9	118.0	6.35	0.79	54.42
z13MCSMG13-83	320.7	25.7	105.0	49.9	0.4	166.0	8.35	0.80	60.50
z13MCSMG13-84	99.1	7.9	87.2	79.5	0.3	42.9	5.19	0.75	48.10
z13MCSMG13-93	236.1	18.9	92.5	32.9	0.3	96.3	3.79	0.74	44.92
zUTFCT-304	50.5	4.0	130.8	68.2	0.5	32.5	12.30	0.81	63.25
zUTFCT-305	31.5	2.5	133.3	82.6	0.6	20.6	8.15	0.79	57.00

Sample	Age, Ma	err., Ma	U (ppm)	Th (ppm)	147Sm (ppm)	He (nmol/g)	mass (ug)	Ft	ESR
ICP date: 2/20/2014									
z13MCSMG22-102	85.4	6.83	208.2	63.0	0.6	76.5	3.68	0.74	44.43
z13MCSMG22-106	296.1	23.69	105.1	26.4	0.5	143.6	6.65	0.79	55.70
z13MCSMG22-110	68.5	5.48	321.7	78.9	0.5	90.3	2.62	0.72	39.84
z13MCSMG22-114	66.6	5.33	386.2	100.7	1.3	110.2	4.03	0.75	45.30

Sample	Age, Ma	err., Ma	U (ppm)	Th (ppm)	¹⁴⁷ Sm (ppm)	He (nmol/g)	mass (ug)	Ft	ESR
z13MCSMG22-118	201.7	16.14	34.6	22.8	1.0	34.2	7.04	0.78	52.99
z13MCSMG22-126	40.7	3.26	237.6	111.8	0.9	45.4	7.32	0.78	54.07
z13MCSMG22-22	83.9	6.71	305.7	246.9	0.7	121.5	3.86	0.73	44.36
z13MCSMG22-28	367.8	29.43	29.1	17.6	0.2	48.1	2.56	0.71	40.13
z13MCSMG22-55	348.1	27.85	92.3	33.7	0.8	144.4	3.90	0.75	46.23
z13MCSMG22-99	58.5	4.68	44.9	27.5	0.7	11.1	1.93	0.68	35.93
z13MCSMG222-1	54.9	4.39	225.7	30.4	0.5	56.5	12.90	0.82	63.77
z13MCSMG222-12	26.8	2.15	166.9	86.1	0.8	22.4	14.57	0.82	68.14
z13MCSMG222-16	42.8	3.42	93.2	31.3	0.8	17.1	4.16	0.73	43.32
z13MCSMG222-26	73.8	5.90	183.2	118.2	0.8	62.6	4.28	0.74	45.49
z13MCSMG222-3	218.1	17.45	199.3	128.8	7.1	198.7	3.73	0.73	42.45
z13MCSMG222-31	738.6	59.09	40.4	12.1	0.6	147.0	8.39	0.80	59.73
z13MCSMG222-42	410.3	32.82	295.8	99.6	11.4	532.7	4.27	0.73	43.09
z13MCSMG222-45	73.4	5.87	305.3	75.4	1.5	95.7	4.50	0.75	45.17
z13MCSMG222-48	61.4	4.91	137.3	55.9	0.6	38.2	5.05	0.77	49.73
z13MCSMG222-54	364.0	29.12	24.3	14.8	0.5	42.9	4.98	0.77	50.44
z13MCSMG222-56	51.9	4.15	142.6	37.7	0.5	32.1	4.42	0.75	47.07
z13MCSMG222-57	53.7	4.29	281.9	84.2	1.6	64.4	3.85	0.74	43.35
z13MCSMG222-9	357.4	28.59	139.4	59.1	0.4	255.7	16.98	0.84	76.10
z13MCSMG31-53	233.8	18.70	149.6	72.3	2.4	144.8	2.08	0.68	35.48
z13MCSMG8-111	454.5	36.36	94.9	75.1	4.7	199.7	2.31	0.70	39.17
z13MCSMG8-112	38.8	3.10	92.8	92.6	1.7	17.0	2.40	0.71	39.89
z13MCSMG8-117	290.2	23.22	63.8	63.7	0.9	87.4	2.25	0.70	38.49
z13MCSMG8-32	93.2	7.45	65.6	47.5	0.7	25.9	1.89	0.67	34.54
z13MCSMG8-35	172.1	13.77	93.7	38.5	2.8	71.6	3.41	0.74	44.94
z13MCSMG8-39	146.6	11.73	167.2	92.8	1.1	102.8	2.13	0.68	35.87
z13MCSMG8-63	38.3	3.07	122.3	95.0	1.4	22.3	4.54	0.74	46.12
z13MCSMG8-68	137.2	10.98	39.2	16.0	0.5	23.8	3.54	0.74	44.80
z13MCSMG8-7	243.2	19.45	108.1	80.6	13.8	119.4	2.81	0.71	39.43
z13MCSMG8-70	90.6	7.25	87.9	40.3	0.4	35.6	3.64	0.74	45.55
z13MCSMG8-78	60.8	4.87	133.9	41.2	0.2	36.6	5.34	0.77	51.70
z13MCSMG88-25	137.1	10.97	67.3	47.7	0.9	41.6	2.57	0.71	40.08
z13MCSMG88-3	255.1	20.40	100.0	57.2	0.5	121.3	4.88	0.76	50.07
z13MCSMG88-33	3.6	0.29	78.0	42.9	1.6	1.2	2.14	0.69	37.00
z13MCSMG88-36	161.2	12.89	130.7	53.6	1.6	87.8	2.32	0.70	37.74

Sample	Age, Ma	err., Ma	U (ppm)	Th (ppm)	147Sm (ppm)	He (nmol/g)	mass (ug)	Ft	ESR
z13MCSMG88-37	72.7	5.82	805.5	170.4	2.4	247.6	3.31	0.74	44.57
z13MCSMG88-4	322.5	25.80	158.6	47.8	0.9	205.8	2.03	0.68	35.47
zUTFCT-312	32.5	2.60	51.2	30.7	0.3	7.4	2.59	0.72	40.95
zUTFCT-313	26.4	2.11	255.1	114.9	1.0	29.8	4.19	0.74	44.65

Sample	Age, Ma	err., Ma	U (ppm)	Th (ppm)	147Sm (ppm)	He (nmol/g)	mass (ug)	Ft	ESR
ICP date: 3/28/2014									
z13MCSMG29-107	154.7	12.38	112.2	57.3	2.3	82.9	7.78	0.78	54.25
z13MCSMG29-111	607.1	48.57	79.9	40.4	2.5	235.4	6.08	0.77	50.91
z13MCSMG29-115	664.6	53.17	24.2	11.8	1.3	75.1	3.66	0.74	44.72
z13MCSMG29-119	216.5	17.32	81.5	49.0	0.6	78.8	2.61	0.72	40.79
z13MCSMG29-122	139.3	11.14	121.8	93.0	2.3	84.8	6.73	0.78	53.98
z13MCSMG29-125	92.8	7.43	82.9	44.0	0.5	34.9	3.82	0.74	45.35
z13MCSMG29-126	44.6	3.57	203.4	119.4	5.0	42.0	4.82	0.75	47.58
z13MCSMG29-25	114.7	9.17	50.8	26.5	0.4	28.7	9.84	0.81	62.35
z13MCSMG29-4	92.9	7.43	150.7	60.6	0.6	65.2	7.07	0.78	54.61
z13MCSMG29-5	101.8	8.15	217.4	158.4	1.4	109.2	6.37	0.78	53.22
z13MCSMG29-53	61.1	4.89	331.4	55.4	0.6	85.0	3.95	0.75	45.06
z13MCSMG29-58	63.4	5.07	237.4	143.8	0.9	71.1	5.24	0.76	49.95
z13MCSMG29-6	47.2	3.78	190.4	64.4	0.8	37.8	2.89	0.72	41.10
z13MCSMG29-60	289.2	23.13	59.3	30.3	0.5	80.6	4.60	0.76	49.69
z13MCSMG29-70	488.6	39.09	101.6	46.7	1.2	246.5	8.42	0.80	59.50
z13MCSMG29-71	526.5	42.12	114.8	44.2	2.3	284.6	4.93	0.77	50.87
z13MCSMG29-75	63.5	5.08	174.5	52.7	0.8	48.7	5.65	0.76	47.82
z13MCSMG29-76	97.3	7.78	445.9	69.8	0.6	176.5	2.81	0.72	40.89
z13MCSMG29-88	122.1	9.77	83.4	67.6	1.5	46.3	2.24	0.70	39.09
z13MCSMG29-96	145.4	11.63	117.5	100.5	0.8	80.7	3.26	0.72	42.24
z13MCSMG29-98	145.3	11.62	137.8	82.0	0.7	100.2	8.82	0.81	61.79
z13MCSMG31-1	283.1	22.64	44.5	18.7	0.9	57.3	4.15	0.75	46.95
z13MCSMG31-103	283.9	22.71	57.2	29.2	3.1	73.0	3.05	0.73	43.20
z13MCSMG31-105	80.9	6.47	146.6	44.7	0.3	52.8	4.74	0.77	49.85
z13MCSMG31-112	114.3	9.14	135.8	82.9	12.5	76.2	7.85	0.79	56.55
z13MCSMG31-113	703.2	56.26	121.6	65.1	4.8	437.6	7.76	0.80	58.61

Sample	Age, Ma	err., Ma	U (ppm)	Th (ppm)	¹⁴⁷ Sm (ppm)	He (nmol/g)	mass (ug)	Ft	ESR
z13MCSMG31-120	64.3	5.14	88.9	25.5	0.4	25.1	4.19	0.76	48.30
z13MCSMG31-121	87.1	6.97	49.0	23.2	0.3	21.1	11.21	0.82	65.60
z13MCSMG31-125	325.5	26.04	53.3	43.5	0.7	82.3	3.28	0.72	42.39
z13MCSMG31-16	645.3	51.63	169.1	51.0	4.0	471.9	2.89	0.72	39.98
z13MCSMG31-27	979.0	78.32	25.2	11.2	0.1	114.4	3.17	0.72	41.60
z13MCSMG31-39	128.0	10.24	104.6	84.1	1.3	64.8	4.17	0.75	47.02
z13MCSMG31-43	123.2	9.85	152.1	33.5	0.7	86.9	10.10	0.81	61.99
z13MCSMG31-5	578.1	46.25	25.8	23.2	2.2	74.3	3.81	0.73	44.03
z13MCSMG31-53	233.8	18.70	149.6	72.3	2.4	144.8	2.08	0.68	35.48
z13MCSMG31-61	198.2	15.85	52.1	33.4	0.7	50.5	6.06	0.78	53.19
z13MCSMG31-73	74.9	5.99	100.0	25.2	0.6	31.5	3.17	0.73	42.80
z13MCSMG31-81	83.5	6.68	97.0	45.9	0.3	35.8	3.28	0.73	43.59
z13MCSMG31-84	193.9	15.51	337.5	146.8	0.8	280.8	3.09	0.71	40.07
z13MCSMG31-91	260.6	20.85	192.2	58.6	0.7	221.4	4.27	0.75	46.54
z13MCSMG31-92	717.7	57.41	25.2	9.0	0.4	92.7	11.75	0.83	68.05
z13MCSMG31-98	96.5	7.72	64.7	44.0	0.4	29.0	3.86	0.74	44.74
zUTFCT-340	23.2	1.85	267.1	164.2	0.9	27.9	3.45	0.73	43.10
zUTFCT-341	24.0	1.92	200.7	102.4	0.9	21.7	4.53	0.75	45.78

Sample	Age, Ma	err., Ma	U (ppm)	Th (ppm)	¹⁴⁷ Sm (ppm)	He (nmol/g)	mass (ug)	Ft	ESR
ICP date: 4/24/2014									
zCR05-74	24.8	1.49	215.0	53.3	0.4	24.1	7.42	0.79	55.52
zCR05-244	41.3	2.48	185.6	63.3	1.7	32.7	3.14	0.73	42.71
zCR05-263	41.4	2.48	418.5	68.8	1.1	65.5	1.95	0.67	34.03
zCR05-191	52.8	3.17	174.9	52.2	0.4	39.0	2.96	0.73	42.28
zCR05-9	62.2	3.73	122.1	62.9	0.6	32.2	2.47	0.70	38.02
zCR05-277	64.2	3.85	71.1	69.7	0.3	22.3	3.39	0.73	44.27
zCR05-302	82.3	4.94	319.3	183.1	1.1	118.5	3.57	0.73	43.71
zCR05-34	92.4	5.55	202.9	88.1	6.9	79.2	2.32	0.71	39.04
zCR05-228	93.1	5.59	82.0	36.5	0.4	35.7	5.91	0.78	53.70
zCR05-93	102.9	6.17	293.7	86.9	1.0	137.4	8.12	0.78	53.90
zCR05-83	109.3	6.56	53.5	30.4	0.3	29.5	11.33	0.82	66.81
zCR05-133	135.6	8.14	151.2	48.7	0.7	84.3	2.30	0.70	38.20
zCR05-116	136.7	8.20	66.1	44.7	0.6	43.3	5.56	0.76	49.11
zCR05-61	140.6	8.44	110.4	44.0	1.6	65.1	2.32	0.70	38.63
zCR05-160	146.6	8.80	417.7	120.8	1.5	253.3	2.64	0.71	39.45

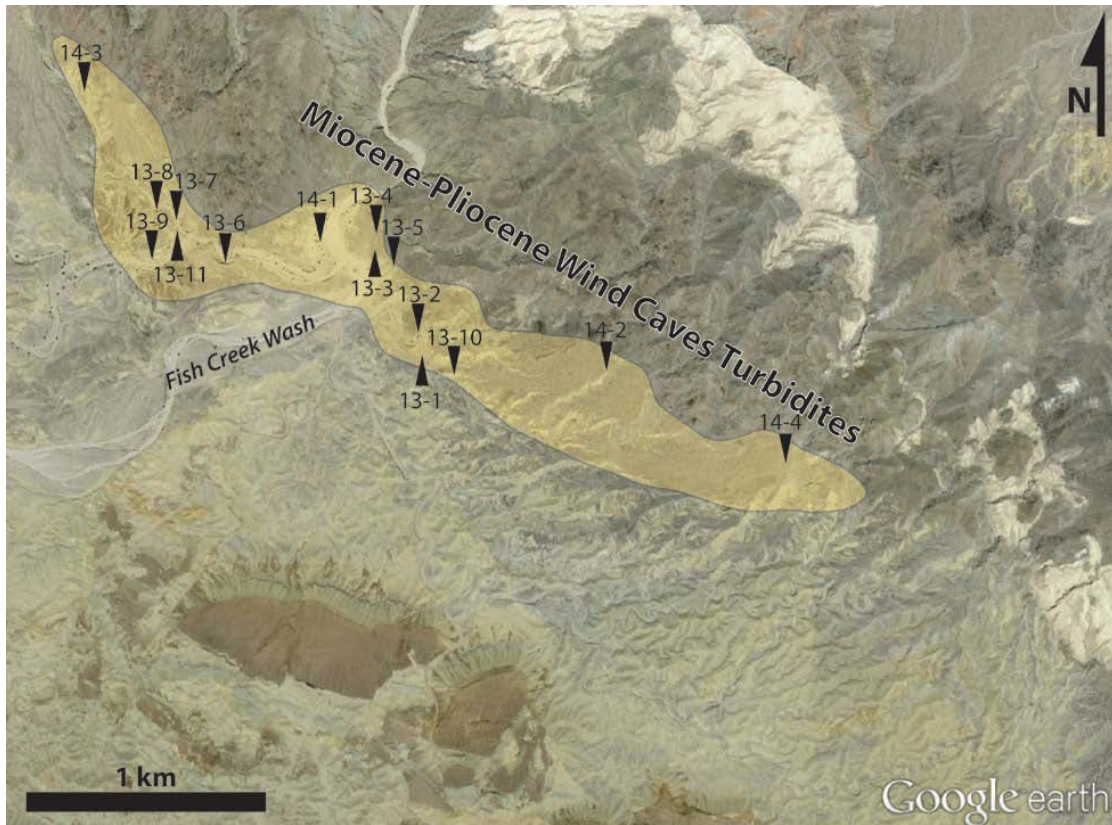
Sample	Age, Ma	err., Ma	U (ppm)	Th (ppm)	147Sm (ppm)	He (nmol/g)	mass (ug)	Ft	ESR
zCR05-264	147.3	8.84	67.5	36.9	0.7	42.1	2.12	0.69	36.80
zCR05-186	164.7	9.88	308.7	119.9	0.8	220.5	3.55	0.73	42.57
zCR05-292	183.4	11.01	177.1	32.4	0.8	135.8	3.33	0.73	42.86
zCR05-5	184.9	11.10	269.8	90.4	1.6	203.0	2.18	0.69	36.70
zCR05-156	186.2	11.17	147.1	78.1	0.9	116.9	2.60	0.70	37.71
zCR05-128	209.8	12.59	171.8	147.4	6.8	157.0	1.55	0.66	34.12
zCR05-198	225.9	13.55	105.1	58.9	2.5	105.5	2.63	0.72	41.06
zCR05-201	235.6	14.14	117.9	42.3	0.9	116.2	2.24	0.70	38.60
zCR05-188	256.7	15.40	41.1	19.1	0.6	48.1	4.10	0.75	46.51
zCR05-100	257.7	15.46	244.5	100.9	3.3	292.1	5.11	0.77	50.88
zCR05-212	258.3	15.50	64.1	36.2	1.5	77.2	3.97	0.75	46.89
zCR05-64	297.7	17.86	36.4	21.0	0.5	48.8	2.72	0.72	41.58
zCR05-218	316.2	18.97	49.7	27.6	0.3	77.4	6.70	0.79	56.45
zCR05-153	328.8	19.73	86.0	67.8	0.9	127.0	2.01	0.69	37.13
zCR05-259	341.7	20.50	41.0	18.7	0.9	61.2	2.50	0.72	40.41
zCR05-286	345.4	20.72	129.6	68.7	2.4	200.0	3.27	0.72	41.37
zCR05-155	362.6	21.75	79.7	53.3	1.8	146.4	7.09	0.79	57.03
zCR05-144	362.9	21.77	76.5	21.1	1.2	126.9	5.26	0.78	51.86
zCR05-239	366.1	21.97	51.7	43.3	0.5	92.8	3.66	0.74	45.56
zCR05-293	386.4	23.18	146.4	46.0	2.2	233.7	2.59	0.70	37.23
zCR05-243	426.1	25.57	132.2	73.1	4.0	257.2	2.98	0.73	42.71
zCR05-229	530.0	31.80	37.2	24.4	0.8	97.4	5.05	0.76	50.12
zCR05-267	587.9	35.28	107.0	44.7	0.5	270.0	2.00	0.70	37.55
zCR05-265	717.0	43.02	57.2	30.3	1.1	184.8	2.46	0.71	39.29
zCR05-112	806.7	48.40	95.5	36.6	2.7	353.9	3.23	0.74	43.61
zUTFCT2-48	27.0	1.62	231.0	126.1	0.6	27.8	3.97	0.73	43.39
zUTFCT2-49	25.7	1.54	195.2	117.6	1.0	24.0	6.24	0.78	52.93

Sample	Age, Ma	err., Ma	U (ppm)	Th (ppm)	147Sm (ppm)	He (nmol/g)	mass (ug)	Ft	ESR
ICP date: 7/15/2014									
z13MCSMG12-1	94.5	7.56	237.5	131.2	2.0	89.1	1.46	0.65	31.97
z13MCSMG13-123	202.9	16.23	141.1	107.4	2.8	132.2	2.64	0.72	41.25
z13MCSMG13-34	63.9	5.11	51.8	39.2	0.9	14.6	2.11	0.69	37.62
z13MCSMG13-47	164.2	13.14	336.2	130.4	8.3	261.0	7.42	0.79	57.36
z13MCSMG13-51	249.2	19.94	105.6	41.0	0.6	115.5	3.10	0.73	43.42

Sample	Age, Ma	err., Ma	U (ppm)	Th (ppm)	¹⁴⁷ Sm (ppm)	He (nmol/g)	mass (ug)	Ft	ESR
z13MCSMG13-52	760.1	60.81	33.8	19.7	0.4	129.5	5.54	0.77	52.51
z13MCSMG13-66	208.5	16.68	86.4	45.6	3.1	87.0	6.29	0.79	55.28
z13MCSMG13-70	465.7	37.26	77.2	60.9	0.6	157.6	1.56	0.67	34.37
z13MCSMG13-92	874.7	69.98	50.5	39.7	0.8	228.2	4.31	0.76	48.73
z13MCSMG15-103	668.1	53.45	195.3	88.3	5.8	538.4	1.60	0.66	33.35
z13MCSMG15-5	94.2	7.53	70.1	35.8	0.6	29.2	3.23	0.73	42.88
z13MCSMG15-77	169.2	13.54	116.0	26.4	0.4	81.8	3.18	0.73	41.55
z13MCSMG31-14	383.5	30.68	64.9	53.2	0.7	118.4	3.08	0.72	42.20
z13MCSMG31-3	106.5	8.52	219.6	8.6	0.9	97.6	4.25	0.76	47.66
z13MCSMG31-52	83.4	6.67	192.7	32.9	0.7	72.9	9.12	0.80	59.69
z13MCSMG31-60	62.7	5.02	360.7	174.0	5.0	102.4	4.93	0.75	46.97
z13MCSMG31-7	187.4	14.99	126.4	124.1	1.1	113.5	2.66	0.71	40.90
z13MCSMG31-8	328.5	26.28	60.9	57.2	1.1	100.9	4.55	0.75	47.55
z13MCSMG31-96	187.3	14.99	28.8	26.8	0.4	26.5	3.48	0.74	45.25
zCR05-125	1283.9	102.71	40.2	46.7	0.3	292.2	3.98	0.75	47.14
zCR05-126	71.8	5.74	40.1	56.7	0.9	14.6	2.83	0.70	39.91
zCR05-13	234.9	18.80	189.3	34.6	1.0	187.5	3.29	0.74	43.43
zCR05-134	1142.1	91.37	66.2	39.1	1.0	372.9	3.44	0.73	43.67
zCR05-140	357.0	28.56	70.4	34.8	0.9	109.2	2.23	0.71	39.02
zCR05-165	461.7	36.93	126.5	50.6	2.0	260.9	3.15	0.73	43.30
zCR05-170	147.1	11.77	261.4	212.3	0.9	179.8	3.20	0.72	42.02
zCR05-171	431.8	34.55	13.8	14.4	0.7	28.0	1.90	0.68	36.56
zCR05-176	143.0	11.44	116.4	79.7	1.0	71.0	1.89	0.68	35.32
zCR05-187	371.4	29.71	33.0	28.8	0.8	61.3	4.27	0.75	47.59
zCR05-20	294.1	23.53	172.3	47.8	0.8	215.1	2.66	0.72	41.48
zCR05-21	168.9	13.51	345.6	247.3	1.6	264.8	3.26	0.71	40.48
zCR05-221	12.4	0.99	16.4	28.4	0.7	1.1	3.38	0.73	44.77
zCR05-237	348.9	27.91	147.9	65.1	1.0	226.0	3.07	0.72	41.00
zCR05-37	446.9	35.76	38.4	16.4	0.4	78.3	3.58	0.74	45.45
zCR05-44	274.2	21.93	76.7	58.6	1.3	93.4	1.94	0.69	36.84
zCR05-49	385.2	30.81	85.5	104.3	3.4	164.2	2.42	0.70	39.49
zCR05-56	252.5	20.20	50.3	49.9	1.7	60.2	2.28	0.70	39.11
zCR05-7	362.6	29.01	117.9	20.7	1.0	186.0	4.02	0.76	46.84
zCR05-94	279.9	22.39	186.4	41.7	1.4	209.0	2.14	0.69	36.64
zUTFCT2-71	42.3	3.38	282.2	154.1	1.0	54.4	4.66	0.75	46.32

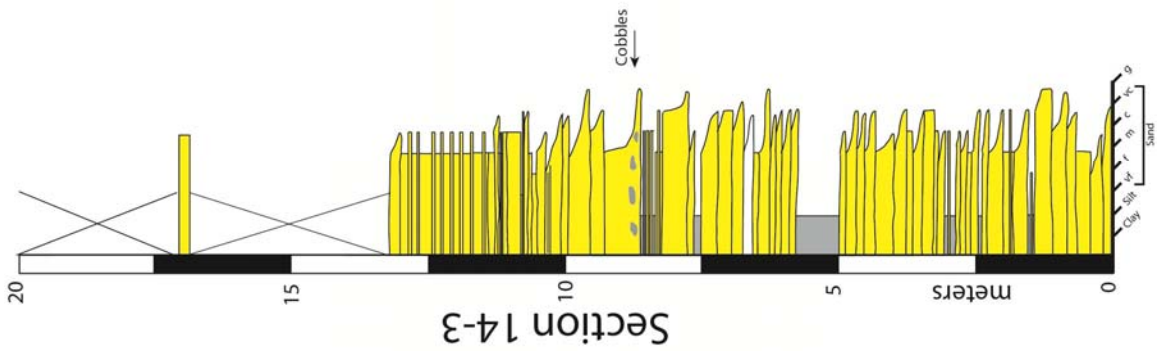
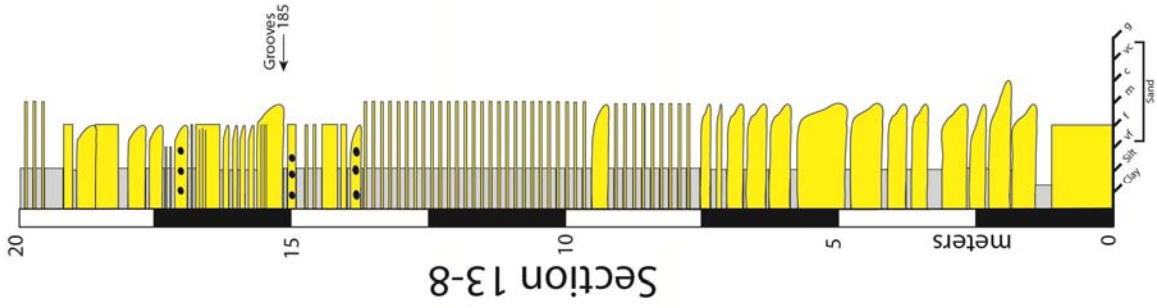
Appendix E: Measured Section Illustrations

Vertical measured sections are listed from NW to SE. An image of the Wind Caves Member outcrop belt is provided below for reference.

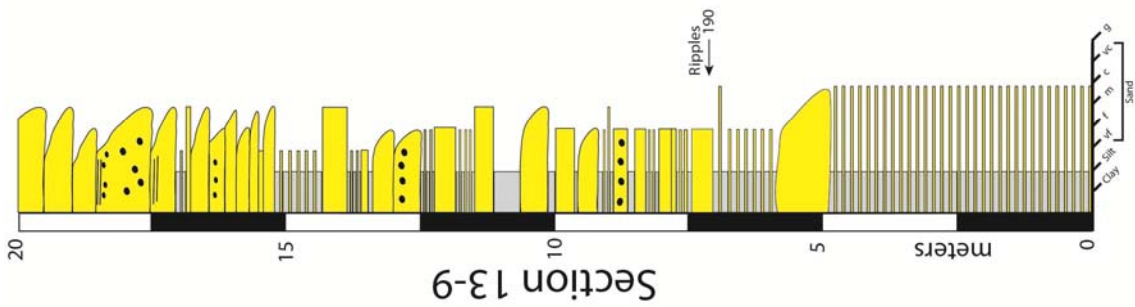
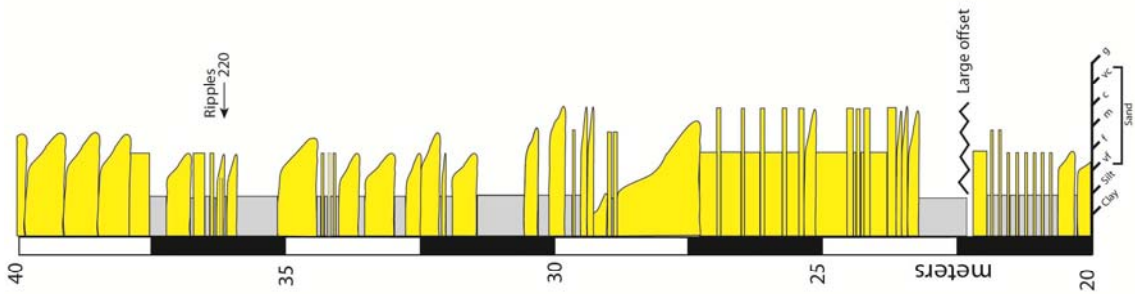
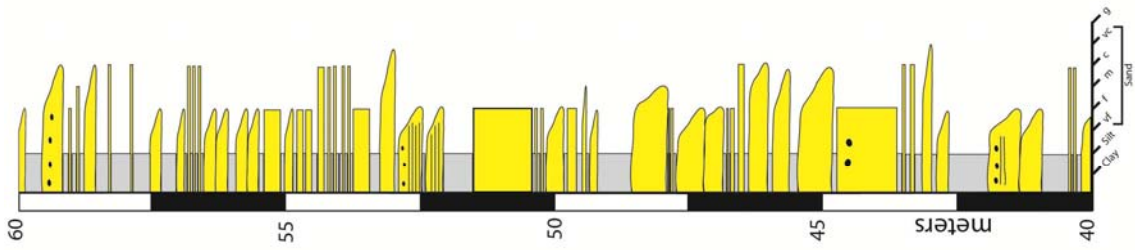
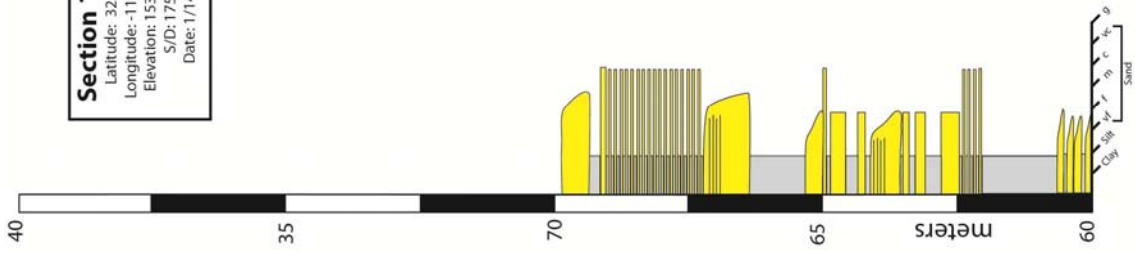


Section 14-3
 Latitude: 33.003866°
 Longitude: -116.134769°
 Elevation: 204 m
 Date: 1/10/2014

Section 13-8
 Latitude: 32.994788°
 Longitude: -116.127633°
 Elevation: 150 m
 S/D: 1257/25°
 Date: 1/15/2013



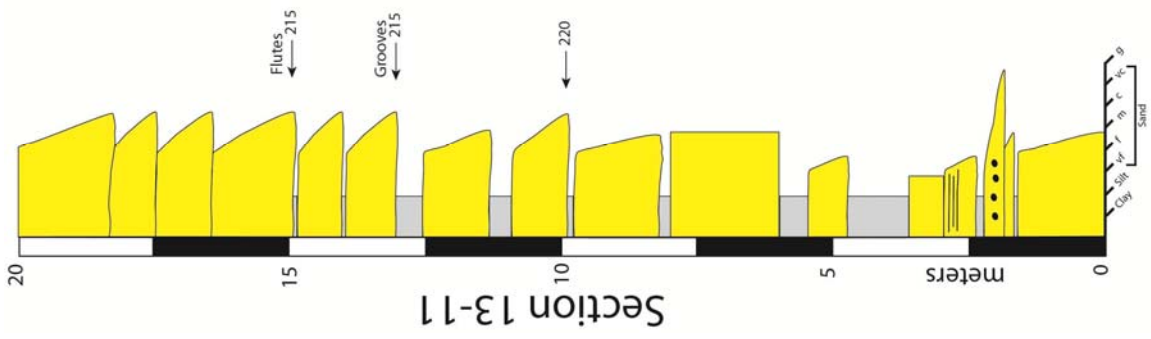
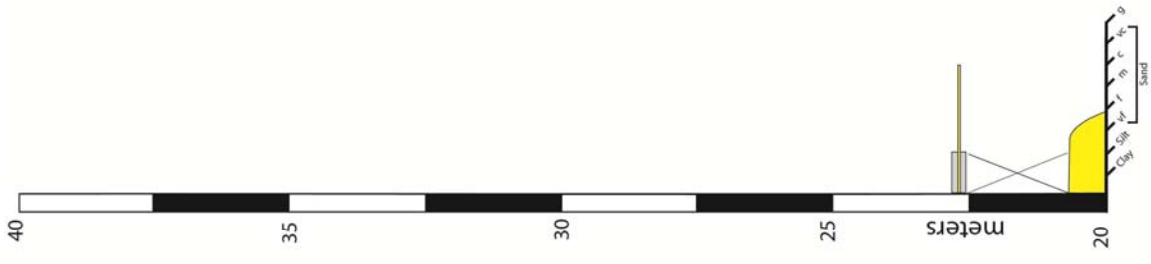
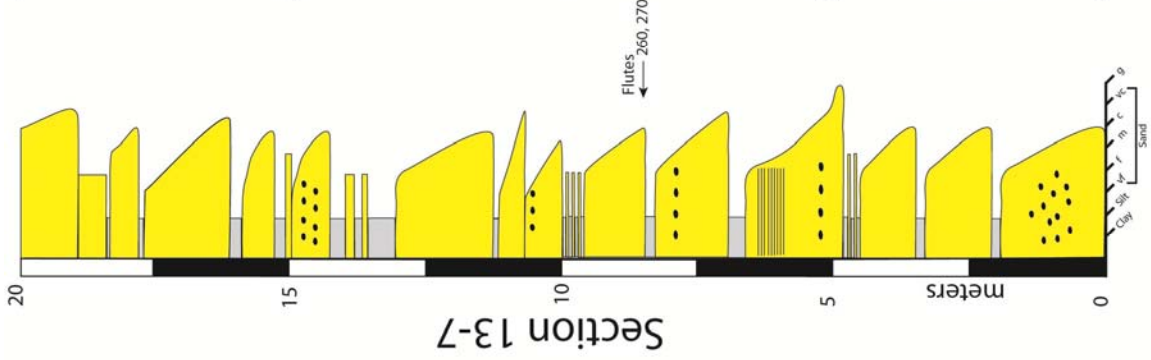
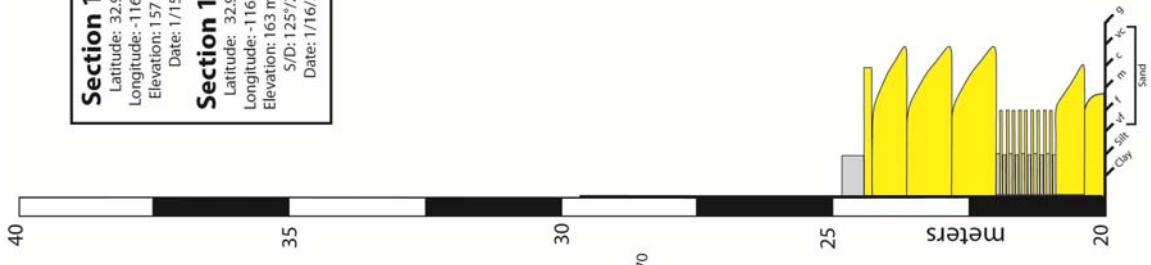
Section 13-9
 Latitude: 32.992612°
 Longitude: -116.127301°
 Elevation: 153 m
 S/D: 175°/20°
 Date: 1/14/2013

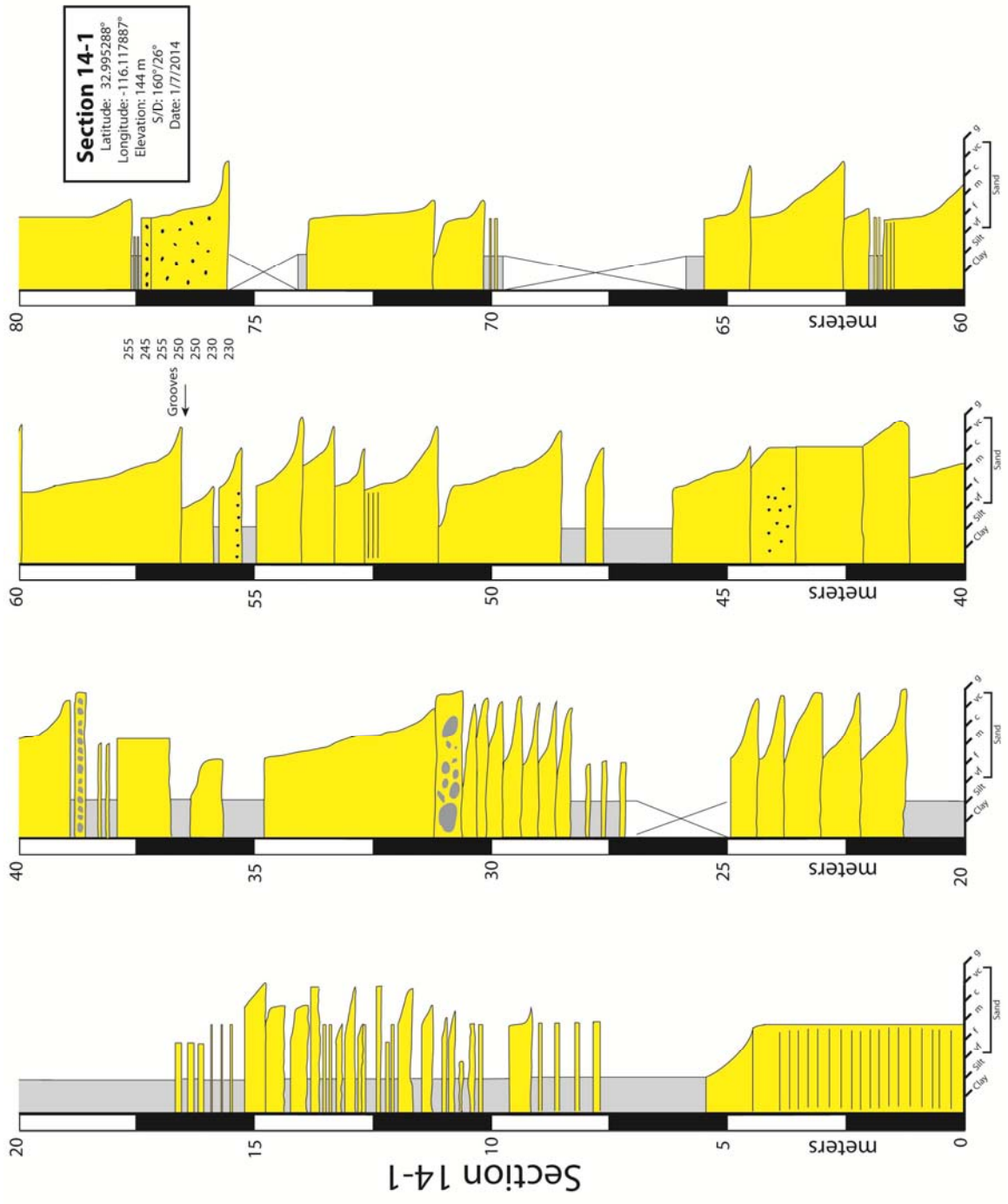


Section 13-9

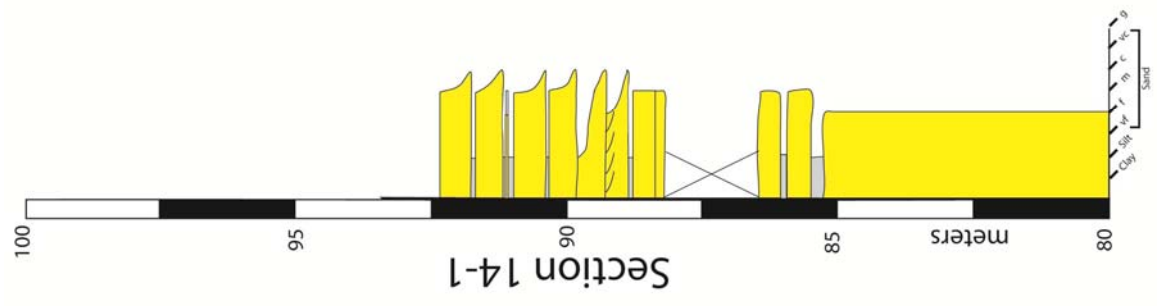
Section 13-11
 Latitude: 32.993626°
 Longitude: -116.126574°
 Elevation: 157 m
 Date: 1/15/2013

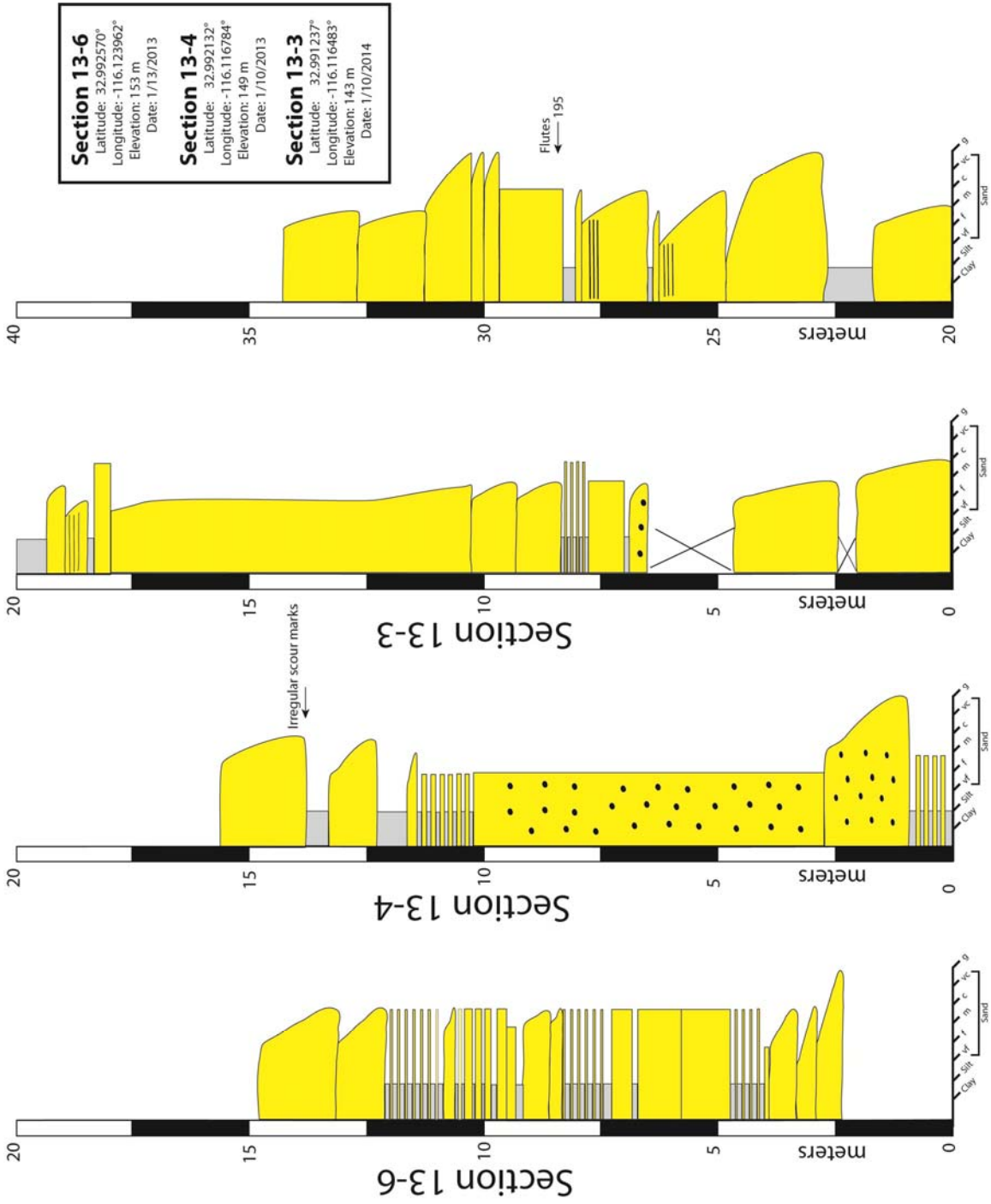
Section 13-7
 Latitude: 32.995715°
 Longitude: -116.127302°
 Elevation: 163 m
 S/D: 125°/25°
 Date: 1/16/2013



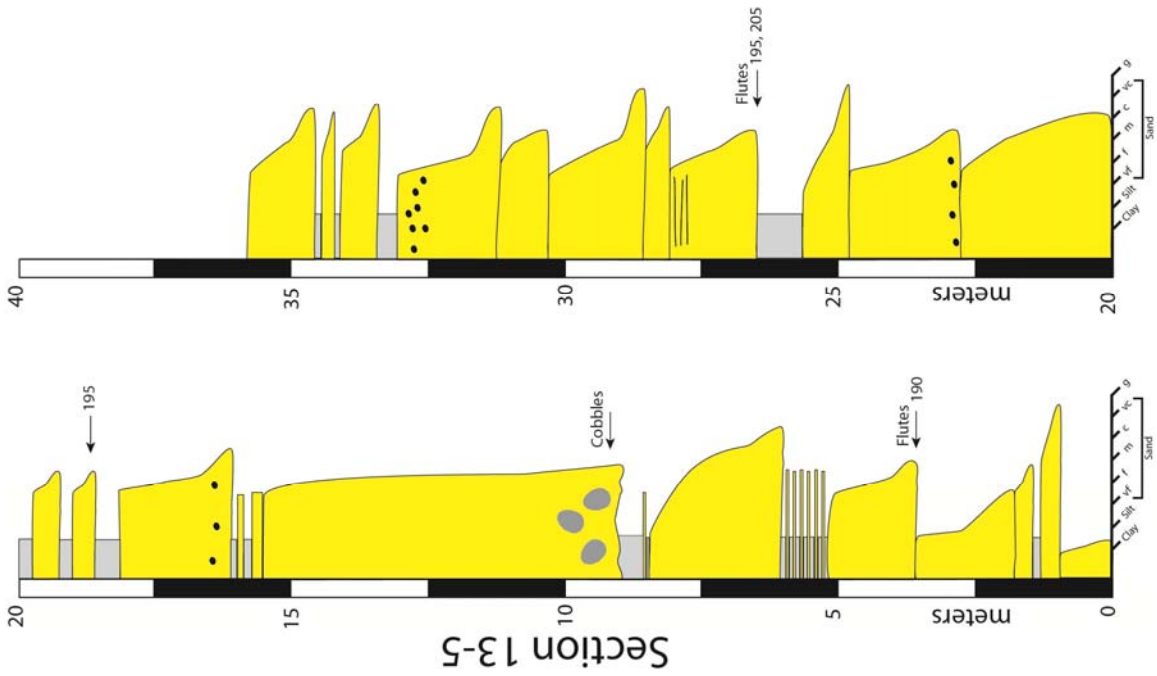


Section 14-1
 Latitude: 32.995288°
 Longitude: -116.117887°
 Elevation: 144 m
 S/D: 160726°
 Date: 1/7/2014

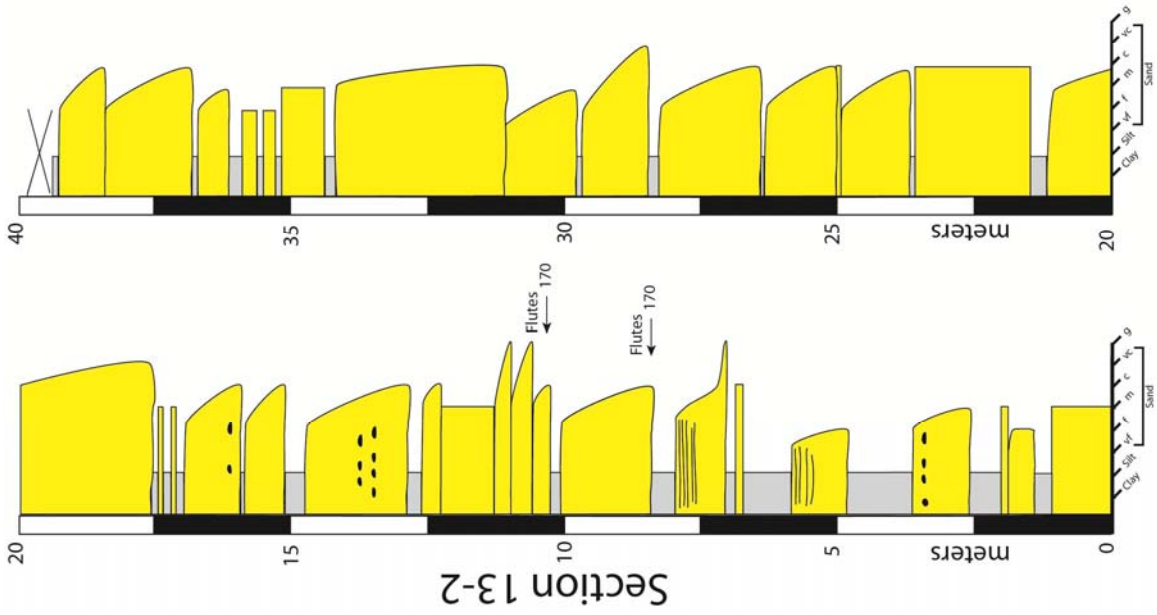




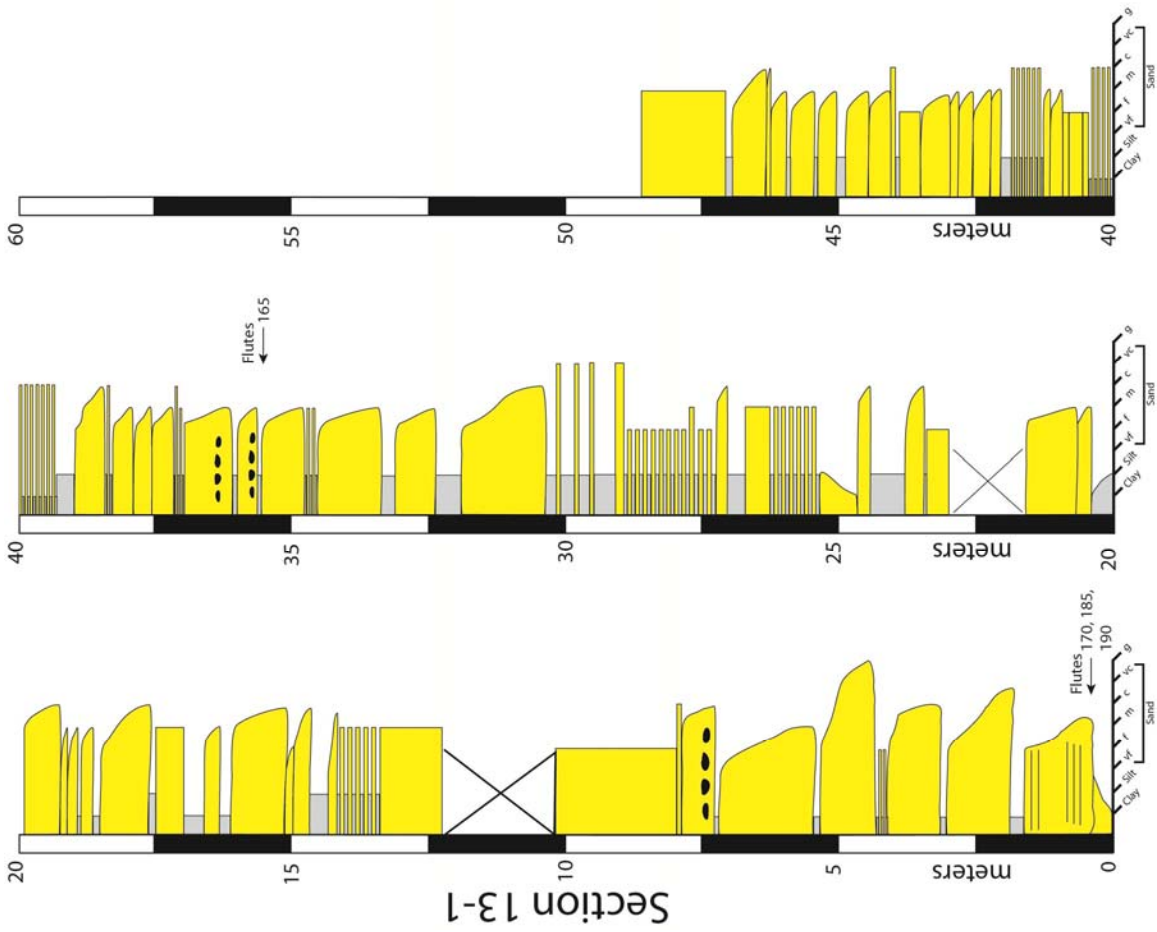
Section 13-5
 Latitude: 32.990284°
 Longitude: -116.115743°
 Elevation: 152 m
 S/D: 140°/20°
 Date: 1/12/2013



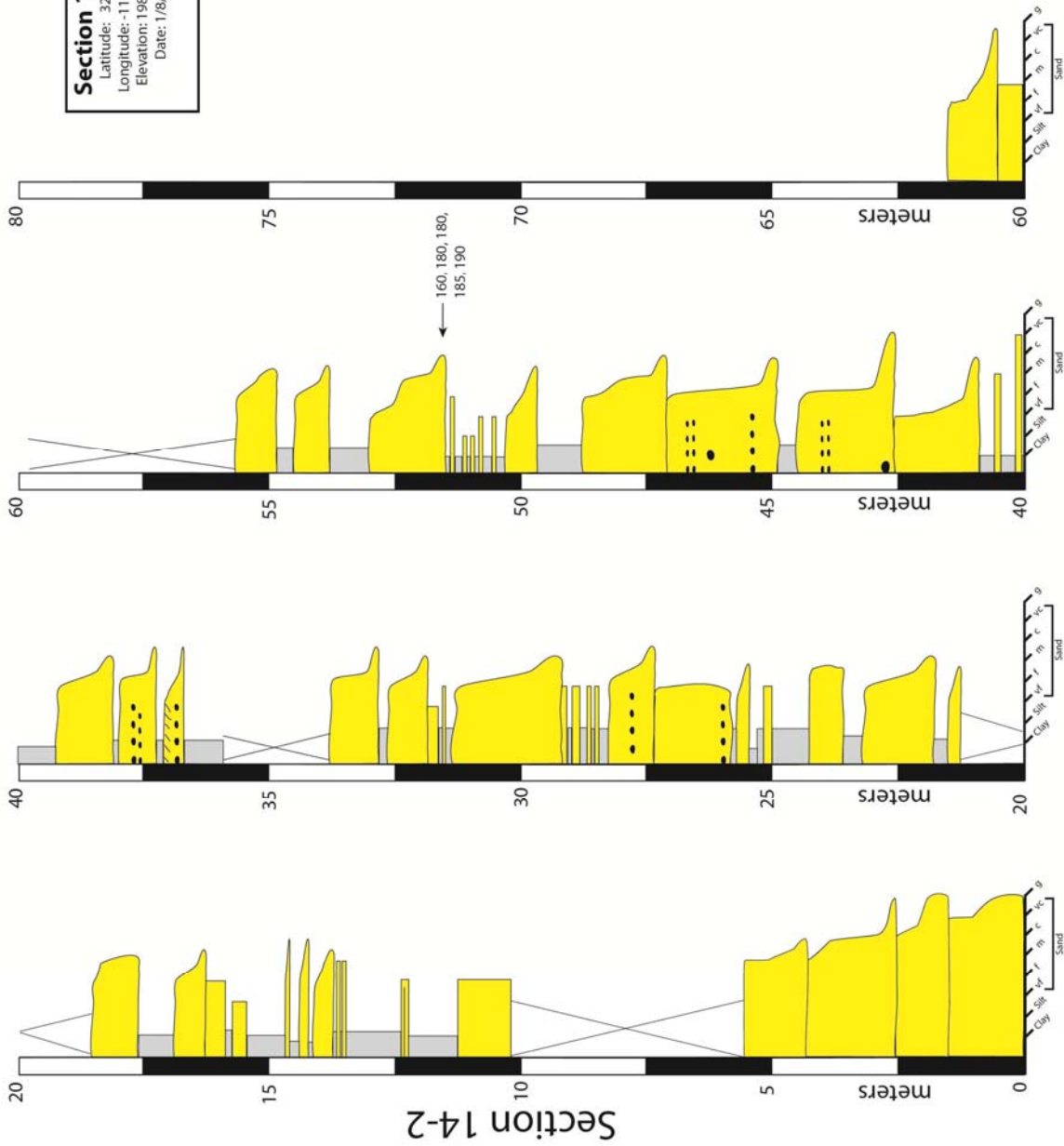
Section 13-2
 Latitude: 32.988589°
 Longitude: -116.114486°
 Elevation: 153 m
 S/D: 120°/20°
 Date: 1/9/2013



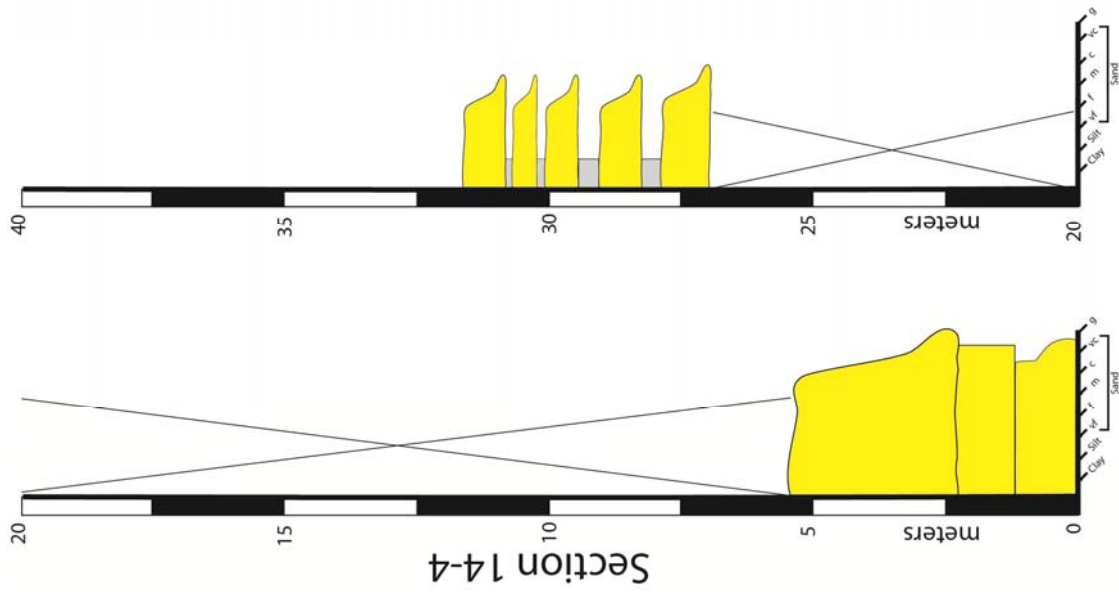
Section 13-1
 Latitude: 32.987612°
 Longitude: -116.114100°
 Elevation: 162 m
 Date: 1/9/2013



Section 14-2
 Latitude: 32.987485°
 Longitude: -116.102596°
 Elevation: 198 m
 Date: 1/8/2014



Section 14-4
 Latitude: 32.982736°
 Longitude: -116.095762°
 Elevation: 225 m
 Date: 1/10/2014



References

- Abbott, P. L., Kerr, D. R., Borron, S. E., Washburn, J. L., and Rightmer, D. A., 2002, Neogene sturzstrom deposits, Split Mountain area, Anza-Borrego Desert State Park, California: *Reviews in Engineering Geology*, v.15, p. 379-400.
- Andrews, E. D., 1991, Sediment transport in the Colorado River basin: in *Colorado River Ecology and Dam Management*, Committee to Review the Glen Canyon Environmental Studies, Water Science and Technology Board, Commission on Geosciences, Environment, and Resources, National Academy of Sciences Press, p. 54–74.
- Axen, G.J., and Fletcher, J.M., 1998, Late Miocene–Pleistocene extensional faulting, northern Gulf of California, Mexico and Salton Trough, California: *International Geology Review*, v. 40, p. 217–244, doi: 10.1080/00206819809465207.
- Axen, G. J., Grove, M., Stockli, D., Lovera, O. M., Rothstein, D. A., Fletcher, J. M., Farley, K., and Abbott, P. L., 2000, Thermal evolution of Monte Blanco dome: Low-angle normal faulting during Gulf of California rifting and late Eocene denudation of the eastern Peninsular Ranges: *Tectonics*, v. 19, p. 197–212.
- Beaubouef, R. T., C. Rossen, F. B. Zelt, M. D. Sullivan, D. C. Mohrig, and D. C. Jennette, 1999, Deep-water sandstones, Brushy Canyon Formation, West Texas: Field Guide, AAPG Hedberg Field Research Conference.
- Bouma, A. H., 1962, *Sedimentology of Some Flysch Deposits: A Graphic Approach to Facies Interpretation*. Elsevier, Amsterdam/New York 168 pp.
- Buising, A. V., 1990. The Bouse formation and bracketing units, southeastern California and western Arizona: Implications for the evolution of the Proto-Gulf of California and the lower Colorado River: *Journal of Geophysical Research* v. 95, p. 20,111-20,132.
- Campbell, I.H., Reiners, P.W., Allen, C.M., Nicolescu, S., and Upadhyay, R., 2005, He-Pb double dating of detrital zircons from the Ganges and Indus Rivers: Implications for sediment recycling and provenance studies: *Earth and Planetary Science Letters*, v. 237, p. 402–432, doi: 10.1016/j.epsl.2005.06.043.
- Carvajal, C. and Steel, R.J., 2006, Thick turbidite successions from supply-dominated shelves during sea-level highstand: *Geology*. 34, 665-9.

- Cather, S.M., Chapin, C.E., and Kelley, S.A., 2012, Diachronous episodes of Cenozoic erosion in southwestern North America and their relationship to surface uplift, paleoclimate, paleodrainage, and paleoaltimetry: *Geosphere*, doi:10.1130/GES00801.1.
- DeCelles, P. G., 2004, Late Jurassic to Eocene evolution of the Cordilleran thrust belt and foreland basin system, western USA: *American Journal of Science*, v. 304, p. 105-168.
- Dickinson, W.R. 2004, Evolution of the North American Cordillera: *Annual Review of Earth and Planetary Sciences*, v. 32, doi:10.1146/annurev.earth.32.101802.120257, p. 13–44.
- Dickinson, W.R., Cather, S.M., and Gehrels, G.E., 2010, Detrital zircon evidence for derivation of arkosic sandstone in the eolian Narbona Pass Member of the Eocene–Oligocene Chuska Sandstone from Precambrian basement rocks in central Arizona, in Fassett, J.E., Zeigler, K.E., and Lueth, V.W., eds., *Four Corners Country: New Mexico Geological Society 61st Annual Field Conference Guidebook*, p. 125–134.
- Dickinson, W.R., and Gehrels, G.E., 2003, U–Pb ages of detrital zircons from Permian and Jurassic eolian sandstones of the Colorado Plateau, USA: *Paleogeographic implications: Sedimentary Geology*, v. 163, p. 29–66, doi: 10.1016/S0037-0738(03)00158-1.
- Dickinson, W., and Gehrels, G., 2010, Insights into North American Paleogeography and Paleotectonics from U–Pb ages of detrital zircons in Mesozoic strata of the Colorado Plateau, USA: *International Journal of Earth Sciences*, v. 99, p. 1247-1265.
- Dickinson, W. R., 2013, Rejection of the lake spillover model for initial incision of the Grand Canyon, and discussion of alternatives: *Geosphere*, v. 9, p. 1–20.
- Dickinson, W. R., and Snyder, W. S., 1978, Plate tectonics of the Laramide orogeny: *Geological Society of America Memoir 151*, p. 355–366.
- Dorsey, R. J., Fluette, A., McDougall, K. A., Housen, B. A., Janecke, S. U., Axen, G. J., and Shirvell, C. R., 2007, Chronology of Miocene–Pliocene deposits at Split Mountain Gorge, southern California: A record of regional tectonics and Colorado River evolution: *Geology*, v. 35, p. 57–60.

- Dorsey, R. J., Housen, B. A., Janecke, S. U., Fanning, C. M., and Spears, A. L. F., 2011, Stratigraphic record of basin development within the San Andreas fault system: Late Cenozoic Fish Creek–Vallecito basin, southern California: Geological Society of America Bulletin, v. 123, p. 771-793.
- Dorsey, R. J., Axen, G. J., Peryam, T. C., and Kairouz, M. E., 2012, Initiation of the southern Elsinore fault at ~1.2 Ma: Evidence from the Fish Creek – Vallecito Basin, southern California: Tectonics, v. 31, TC2006, doi:10.1029/2011TC003009, 21 pp.
- Dumitru, T. A., 1990, Subnormal Cenozoic geothermal gradients in the extinct Sierra Nevada magmatic arc: Consequences of Laramide and Post-Laramide shallow-angle subduction: Journal of Geophysical Research, v. 95, p. 4925-4941.
- Dumitru, T. A., Duddy, I. R., and Green, P. F., 1994, Mesozoic-Cenozoic burial, uplift, and erosion history of the west-central Colorado Plateau, Geology, v. 22, p. 499-502.
- Faulds, J. E., Price, L. M., and Wallace, M. A., 2001, Pre-Colorado paleogeography and extension along the Colorado Plateau-Basin and Range boundary, northwest Arizona, in Young, R.A., and Spamer, E.E., eds., Colorado River Origin and Evolution: Grand Canyon National Park, Grand Canyon Association, p. 93–99.
- Flowers, R.M., and Farley, K.A., 2012, Apatite $4\text{He}/3\text{He}$ and $(\text{U-Th})/\text{He}$ Evidence for an Ancient Grand Canyon: Science, v. 338, p. 1616-1619.
- Foster, D.A. and John, B., 1999 Quantifying tectonic exhumation in an extensional orogeny with thermochronology; examples from the southern Basin and Range province, in Ring, U., Brandon, M.T., Lister, G.S., and Willett, S. D., eds., Exhumations Processes; normal faulting, ductile flow and erosion: Geological Society, London, Special Publications, 154, 343-364.
- Gastil, R. G., Phillips, R. P., and Allison, E. C., 1975, Reconnaissance geology of the State of Baja California: Geological Society of America Memoir 140, 170 pp.
- Gehrels, G. E., and Dickinson, W. R., 1995, Detrital zircon provenance of Cambrian to Triassic miogeoclinal and eugeoclinal strata in Nevada: American Journal of Science, v. 295, p. 18-48.

- Gehrels., G. E., Blakey, R., Karlstrom, K. E., Timmons, J. M., Dickinson, B., and Pecha, M., 2011, Detrital zircon U-Pb geochronology of Paleozoic strata in the Grand Canyon, Arizona: *Lithosphere*, v. 3, p. 183-200.
- Gehrels, G.E., and Pecha, M., 2014, Detrital Zircon U-Pb geochronology and Hf isotope geochemistry of Paleozoic and Triassic passive margin strata of western North America: *Geosphere*, v. 10, p. 49-65, doi:10.1130/GES00889.1
- Grove, M., Lovera, O., and Harrison, M., 2003, Late Cretaceous cooling of the east-central Peninsula Ranges batholith (33N): Relationship to La Posta pluton emplacement, Laramide shallow subduction, and forearc sedimentation, in *Tectonic Evolution of Northwestern Mexico and the Southwestern USA: Geological Society of America Special Paper No. 374*, p. 355–379.
- Hamilton, W. B., and Myers, W. B., 1967, Cenozoic tectonics of the western United States: *Reviews of Geophysics*, v. 4, p. 509-549
- Hoffman, M., 2009, Mio-Pliocene Erosional Exhumation of the Central Colorado Plateau, Eastern Utah: New Insights from Apatite (U-Th)/He Thermochronometry: Unpublished M.S. Thesis, University of Kansas, 176 pp.
- Hoffman, M., Stockli, D. F., Kelley, S. A., Pederson, J., and Lee, J., 2011, Mio-Pliocene erosional exhumation of the central Colorado Plateau, eastern Utah—New insights from apatite (U-Th)/He thermochronometry, in Beard, L.S., Karlstrom, K.E., Young, R.E., and Billingsley, G.H., eds., *CREvolution 2—Origin and Evolution of the Colorado River System*, Workshop Abstracts: U.S. Geological Survey Open-File Report 2011-1210, p. 132–136.
- Howard, C. S., 1947, Suspended sediment in the Colorado River, 1925-1941: U. S. Geological Survey Water Supply Paper 998, 165 pp.
- Hunt, C. B., 1956, Cenozoic geology of the Colorado Plateau: U.S. Geological Survey Professional Paper 279, 99 pp.
- Ingersoll, R. V., Grove, M., Jacobson, C. E., Kimbrough, D. L., and Hoyt, J. F., 2013, Detrital zircons indicate no drainage link between southern California rivers and the Colorado Plateau from mid-Cretaceous through Pliocene: *Geology*, v. 41 p. 311-314.

- Irons, W. V., Hembree, C. H., and Oakland, G. L. 1965. Water resources of the Upper Colorado River Basin. Technical report: Washington, D.C., U.S. Geological Survey Professional Paper 441, 370 pp.
- Johnson, N. M., Officer, C. B., Opdyke, N. D., Woodard, G. D., Zeitler, P. K., and Lindsay, E. H., 1983, Rates of late Cenozoic tectonism in the Vallecito–Fish Creek basin, western Imperial Valley, California: *Geology*, v. 11, p. 664–667.
- Karlstrom, K.E., 23 others, and the CREST Working Group, 2012, Mantle-driven dynamic uplift of the Rocky Mountains and Colorado Plateau and its surface response: Toward a unified hypothesis: *Lithosphere*, v. 4, p. 3–22, doi:10.1130/L150.1., 2012.
- Kerr, D.R., 1984, Early Neogene continental sedimentation in the Vallecito and Fish Creek Mountains, western Salton Trough, California: *Sedimentary Geology*, v. 38, p. 217–246, doi: 10.1016/0037–0738(84)90080–0.
- Kimbrough, D. L., Grove, M., Gehrels, G. E., Mahoney, J. B., Dorsey, R. J., Howard, K. A., House, P. K., Pearthree, P. A., and Flessa, K., 2011, Detrital zircon record of Colorado River integration into the Salton Trough: U.S. Geological Survey Open-File Report 2011–1210, p. 168-174.
- Kimbrough, D. L., Grove, M., Gehrels, G., Dorsey, R. J., Howard, K.A., Lovera, O., Aslan, A., House, P. K., and Pearthree, P. A., in press, Detrital zircon U-Pb provenance record of the Colorado River; Implications for late Cenozoic drainage evolution of the American southwest. *Geosphere*.
- Kluth, C. F., 1986, Plate tectonics of the Ancestral Rocky Mountains: in J. A. Peterson, ed., *Paleotectonics and Sedimentation in the Rocky Mountain Region, United States: American Association of Petroleum Geologists Memoir 41*, p. 353–369.
- Lee, J.P., Stockli, D.F., Kelley, S., and Pederson, J., 2011, Unroofing and incision of the Grand Canyon region as constrained through low-temperature thermochronology, in Beard, L.S., et al., eds., *CREvolution 2— Origin and evolution of the Colorado River system*, workshop abstracts: U.S. Geological Survey Open-File Report 2011–1210, p. 175–179, <http://pubs.usgs.gov/of/2011/1210/>.

- Lowe, D.R., 1982, Sediment gravity flows. 2. Depositional models with special reference to high density turbidity currents: *Journal of Sedimentary Petrology*, v. 52, p. 279–298.
- Lucchitta, I., 1972, Early History of the Colorado River in the Basin and Range Province: *Geological Society of America Bulletin*, v. 83, p. 1933-1948.
- Lucchitta, I., 1989, History of the Grand Canyon and of the Colorado River in Arizona, in Jenney, J.P., and Reynolds, S.J., eds., *Geologic evolution of Arizona*, Arizona Geological Society Digest, p. 701-716.
- Lucchitta, I., McDougall, K., Metzger, D.G., Morgan, P., Smith, G.R., and Chernoff, B., 2001, The Bouse Formation and post-Miocene uplift of the Colorado Plateau, in Young, R.A., and Spamer, E.E., eds., *The Colorado River: Origin and Evolution: Grand Canyon, Arizona*, Grand Canyon Association Monograph 12, p. 173–178.
- McKenzie, D., 1978, Some remarks on the development of sedimentary basins: *Earth and Planetary Science Letters*, v. 40, p. 25–32.
- Meek, N., and Douglass, J., 2001, Lake Overflow: An alternative hypothesis for Grand Canyon incision and development of the Colorado River: in Young, R. A., and Spamer, E. E., eds., *The Colorado River: Origin and Evolution*, Grand Canyon, Arizona: Grand Canyon Association Monograph 12, p. 199-204.
- Merriam, R., and Bandy, O. L., 1965, Source of upper Cenozoic sediments in Colorado Delta region: *Journal of Sedimentary Petrology*, v. 35, p. 911–916.
- Parsons, T., 1995, The Basin and Range Province: in *Continental Rifts: Evolution, Structure and Tectonics*, Olsen, K., ed., Amsterdam, Elsevier, p. 277-324
- Pederson, J. L., Mackley, R. D., and Eddleman, J. L., 2002, Colorado Plateau uplift and erosion evaluated using GIS: *GSA Today*, v. 12, p. 4-10.
- Plink-Bjorklund, P., Mellere, D., and Steel, R. J., 2001, Turbidite variability and architecture of sand-prone, deep-water slopes: Eocene clinofolds in the Central Basin, Spitsbergen: *Journal of Sedimentary Research*, v. 71, p. 895-912.
- Potochnik, A. R., 2001, Paleogeomorphic evolution of the Salt River Region: Implications for Cretaceous-Laramide inheritance for ancestral Colorado River drainage: in Young, R.A., and Spamer, E.E., eds., *Colorado River Origin and Evolution: Grand Canyon, Arizona*: Grand Canyon Association, p. 17–24.

- Pyles, D.R., and R.M. Slatt, 2007, Stratigraphy of the Lewis Shale, Wyoming, USA: Applications to understanding shelf-edge to base-of-slope changes in stratigraphic architecture of prograding basin margins, in T. H. Nilsen, R.D. Shew, G.S. Steffens, J.R.J. Studlick, Atlas of Deepwater Outcrops: AAPG Studies in Geology 56, p. 485-489.
- Rahl, J. M., Reiners, P. W., Campbell, I. H., Nicolescu, S., and Allen, C. M., 2003, Combined single-grain (U-Th)/He and U/Pb dating of detrital zircons from the Navajo Sandstone, Utah: *Geology*, v. 31, p. 761–764.
- Rast, N., 1989, The evolution of the Appalachian chain: in, *Geology of North America. Volume A. Geological Society of America*, p. 323-348.
- Ravnas, R. and Steel, R. J., 1998: Architecture of marine syn-rift basins: *American Association of Petroleum Geologists Bulletin*, v. 82, p. 110-146.
- Ring, U., Brandon, M.T., Willett, S., and Lister, G.S., 1999, Exhumation processes, in Ring, U., et al., eds., *Exhumation processes: Normal faulting, ductile flow, and erosion: Geological Society [London] Special Publication 154*, p. 1–27.
- Reiners, P. W., Campbell, I. H., Nicolescu, S., Allen, C. M., Hourigan, J. K., Garver, J. I., Mattinson, J. M., and Cowan, D. S., 2005, (U-Th)/(He-Pb) double dating of detrital zircons: *American Journal of Science*, v. 305, p. 259-311.
- Shirvell, C. R., Stockli, D. F., Axen, G. J., and Grove, M., 2009, Miocene-Pliocene exhumation along the west Salton detachment fault, southern California, from (U-Th)/He thermochronometry of apatite and zircon: *Tectonics*, v. 28, TC2006, doi:10.1029/2007TC002172, 14 pp.
- Silver, L. T., and Chappell, B., 1988, The Peninsular Ranges batholith: An insight into the evolution of the Cordilleran batholiths of southwestern North America: *Transactions of the Royal Society of Edinburgh Earth Sciences*, v. 79, p. 105-121.
- Spencer, J.E., and Patchett, P.J., 1997, Sr isotope evidence for a lacustrine origin for the Upper Miocene to Pliocene Bouse Formation, lower Colorado River trough, and implications for timing of Colorado Plateau uplift: *Geological Society of America Bulletin*, v. 109, p. 767–778, doi:10.1130/0016-7606(1997)109<0767:SIEFAL>2.3.CO;2.

- Spencer, J.E., and Pearthree, P.A., 2001, Headward erosion versus closed-basin spillover as alternative causes of Neogene capture of the ancestral Colorado River by the Gulf of California, in Young, R.A., and Spamer, E.E., eds., *Colorado River: Origin and Evolution: Grand Canyon, Arizona*, Grand Canyon Association Monograph 12, p. 215–219.
- Talling, P. J., Masson, D. G., Sumner, E. J., and Malgesini, G., 2012, Subaqueous sediment density flows: Depositional processes and deposit types: *Sedimentology*, v. 59, p. 1937-2003.
- Vermeesch, P., 2012. On the visualisation of detrital age distributions: *Chemical Geology*, v.312-313, 190-194, doi: 10.1016/j.chemgeo.2012.04.021
- Weltje, G.J. and Von Eynatten, H., 2004, Quantitative provenance analysis of sediments: review and outlook: *Sedimentary Geology*, v. 171, 1-11.
- Wernicke, B., 1992., Cenozoic extensional tectonics of the U. S. Cordillera., in: Burchfiel, B. C. , Lipman, P. W., and Zoback M. L. , eds., *The Cordilleran Orogen; Conterminous U.S. The Geology of North America*, Geological Society of America, *Decade of North American Geology*, v. G-3, p. 553-581.
- Wernicke, B., Christiansen, R.L., England, P.C., Sonder, L.J., 1987. Tectonomagmatic evolution of Cenozoic extension in the North American Cordillera. In: Coward, M.P., Dewey, J.F., Hancock, P.L. (Eds.), *Continental Extensional Tectonics*. Geol. Soc. Spec. Pub., Boulder, CO, pp. 203– 221.
- Whitmeyer, S.J., and Karlstrom, K.E., 2007, Tectonic model for the Proterozoic growth of North America: *Geosphere*, v. 3, p. 220–259, doi: 10.1130 /GES00055.1.
- Winker, C. D., 1987, Neogene Stratigraphy of the Fish Creek-Vallecito Section, Southern California : Implications for Early History of the Northern Gulf of California and Colorado Delta: Unpublished PhD Dissertation, University of Arizona, Tucson, 494 pp.
- Winker, C. D., and Kidwell, S. M., 1996, Stratigraphy of a marine rift basin: Neogene of the western Salton Trough, California: in Abbott, P.L., and Cooper, J.D., eds., *Field Conference Guidebook and Volume for the American Association of Petroleum Geologists Annual Convention: American Association of Petroleum Geologists: Bakersfield, California*, p. 295–336.

Zoback, M. L., Anderson, R. E., and Thompson, G. A., 1981, Cainozoic evolution of the state of stress and style of tectonism of the Basin and Range province of the western United States: Royal Society of London Philosophical Transactions, v. A300, p. 407-434.

Vita

Michael Cloos was born in Austin, TX in 1989. He graduated from McCallum High School in 2008. In May of 2012, he graduated from Texas Christian University in Fort Worth, Texas with a Bachelor of Science in Geology. He attended the University of Texas at Austin in August of 2012 to pursue a Master of Science in Geological Sciences.

Permanent email address: michael.cloos@utexas.edu

This thesis was typed by the author.